

**DETERMINATION OF CUTTINGS TRANSPORT PROPERTIES OF
GASIFIED DRILLING FLUIDS**

**A THESIS SUBMITTED TO
THE GRADUATE SCHOOL OF NATURAL AND APPLIED SCIENCES
OF
MIDDLE EAST TECHNICAL UNIVERSITY**

BY

REZA ETTEHADI OSGOUEI

**IN PARTIAL FULFILLMENT OF THE REQUIREMENTS
FOR
THE DEGREE OF DOCTOR OF PHILOSOPHY
IN
PETROLEUM AND NATURAL GAS ENGINEERING**

OCTOBER 2010

Approval of the thesis:

**DETERMINATION OF CUTTINGS TRANSPORT PROPERTIES OF
GASIFIED DRILLING FLUIDS**

submitted by **REZA ETTEHADI OSGOUEI** in partial fulfillment of the requirements for the degree of **Doctor of Philosophy in Petroleum and Natural Gas Engineering Department, Middle East Technical University** by,

Prof. Dr. Canan Özgen _____

Dean, Graduate School of **Natural and Applied Sciences**

Prof. Dr. Mahmut Parlaktuna _____

Head of Department, **Petroleum and Natural Gas Engineering**

Prof. Dr. Tanju Mehmetoğlu _____

Supervisor, **Petroleum and Natural Gas Engineering Dept., METU**

Assoc. Prof. Dr. Mehmet Evren Özbayoğlu _____

Co supervisor, **Petroleum Engineering Dept., TULSA UN**

Examining Committee Members:

Prof. Dr. Mahmut Parlaktuna _____

Petroleum and Natural Gas Engineering Dept, METU

Prof. Dr. Tanju Mehmetoğlu _____

Petroleum and Natural Gas Engineering Dept., METU

Prof. Dr. Nurkan Karahanoğlu _____

Geological Engineering Department, METU

Assoc. Prof. Dr. İsmail Hakkı Gücüyener _____

Petroleum and Natural Gas Engineering Dept, METU

Assist. Prof. Dr. Gürşat Altun _____

Petroleum and Natural Gas Engineering Dept, İTÜ

Date: 13.10.2010

I hereby declare that all information in this document has been obtained and presented in accordance with academic rules and ethical conduct. I also declare that, as required by these rules and conduct, I have fully cited and referenced all material and results that are not original to this work.

Name, Last name: Reza Ettehadı Osgouei

Signature:

ABSTRACT

DETERMINATION OF CUTTINGS TRANSPORT PROPERTIES OF GASIFIED DRILLING FLUIDS

Ettehad Osgouei, Reza

Ph.D., Petroleum and Natural Gas Engineering Department

Supervisor: Prof. Dr. Tanju Mehmetoğlu

Co supervisor: Assoc. Prof. Dr. Mehmet Evren Özbayoğlu

October 2010, 236 pages

The studies conducted on hole cleaning have been started with single phase drilling fluids for vertical holes in 1930's, and have reached to multiphase drilling fluids for directional and horizontal wells today. The influence of flow rate and hole inclination on cuttings transport has been well understood, and many studies have been conducted on effective hole cleaning either experimentally or theoretically. However, neither the hydraulic behavior nor the hole cleaning mechanism of gasified drilling fluids has been properly understood.

The aims of this study are to investigate and analyze the hole cleaning performance of gasified drilling fluids in horizontal, directional and vertical wells experimentally, to identify the drilling parameters those have the major influence on cuttings transport, to define the flow pattern types and boundaries as well as to observe the behavior of cuttings in detail by using digital image processing techniques, and to develop a mechanistic model based on the fundamental principles of physics and mathematics with the help of the experimental observations.

A mechanistic model is developed with the help of the obtained experimental data. Developed model is used for estimating optimum flow rates for liquid and gas phases for effective cuttings transport as well as for determining the total pressure losses and void fraction of each phase for a given drilling conditions. The

mechanistic model obtained using the experimental data within the scope of this study will be used to develop the hydraulic program and equipment selection to be used in the field during underbalanced drilling applications.

Keywords: Cuttings transport, Directional drilling, Aerated drilling fluids, underbalanced drilling, Mechanistic model

ÖZ

Gaz-Sıvı Karışımli Sondaj Akışkanlarının Kesinti (kırıntı) Taşıma Özelliklerinin Tayini

Ettehadı Osgouei, Reza

Doktora, Petrol ve Doğal Gaz Mühendisliği Bölümü

Tez Yöneticisi : Prof. Dr. Tanju Mehmetođlu

Ortak Tez Yöneticisi: Doç. Dr. Mehmet Evren Özbayođlu

Ekim 2010, 236 sayfa

Kesinti taşınması ile ilgili çalışmalar, 1930'larda dik kuyular ve tek fazlı akışkanlar ile başlamış, günümüzde yönlü ve yatay sondajlarda iki fazlı akışkanlara kadar uzanmıştır. Kuyu eğiminin ve akışkan debisinin kesinti taşıma performansı üzerinde önemli etkileri olduğu anlaşılmış, etkin kesinti taşınması için gereken uygun akışkan debisi tayini ile ilgili gerek deneysel, gerekse modelleme odaklı birçok önemli çalışma gerçekleştirilmiştir. Ancak, gaz-sıvı karışımli sondaj akışkanlarının gerek hidrolik davranışları, gerekse kesinti taşıma mekanizması ve performansı henüz tam olarak anlaşılamamıştır. Özellikle fazlara ait en uygun debi seçimi konusunda büyük bir belirsizlik mevcuttur.

Bu çalışmanın amacı, sondaj esnasında yatay, yönlü ve dikey kuyularda, gaz-sıvı karışımli akışkanları kesinti taşıma performanslarını deneysel olarak gözlemlemek ve analiz etmek, kesinti taşıma performansı üzerinde birincil derecede etkili sondaj değişkenlerini tespit etmek, dijital görüntü işleme teknikleri yardımıyla kesinti hareketlerinin detaylı incelemesini gerçekleştirmek ve akış örüntülerinin çeşitlerini ve sınırlarını tespit etmek, ve matematik ve fiziğin temel prensiplerine dayanan bir mekanistik model oluşturmaktır.

Elde edilen deneysel veriler ışığında, kesinti taşınması işlemini açıklayan bir mekanistik model oluşturulmuştur. Elde edilen model, etkin kesinti taşıma koşullarını sağlayan en uygun gaz ve sıvı debilerinin tespit edilebilmesi için kullanılıb ve ilgili

sondaj kořullarındaki akıř rnts ve basın kayıpları hesaplanabilmektedir. Bu alıřmadan elde edilen veriler ve deneysel alıřmaların ıřıėında meydana getirilen matematiksel model, dřk basınlı sondaj uygulamalarının hidrolik programlarının hazırlanmasında ve arazide kullanılacak ekipman seiminde nemli lde katkıda bulunacaktır.

Anahtar Kelimeler: Kesinti tařıma, ynl sondaj, hava karıřımlı sondaj sıvıları, Underbalanced sondaj, Mekanistik modeli

To My Wife
VAHDEH

ACKNOWLEDGEMENTS

It has been a great experience working on a subject such as underbalanced drilling. I am grateful to my supervisor Prof. Dr. Tanju Mehmetođlu and my co supervisor Assoc. Dr. Mehmet Evren Özbayođlu for their guidance and sincere support all throughout the research. It has been a pleasure working in such a distinctive research with my co supervisor who has contributed to drilling industry with important findings.

The feeling of a great honor has always been effective for being privileged enough to study at the department of Petroleum and Natural Gas Engineering, Middle East Technical University. It is always a compliment to be thankful to all of the instructors at the department.

Special thanks also should be given to TÜBİTAK (The Scientific and Technological Research Council of Turkey) for funding the project through 108 M 106. Thanks are also due to Middle East Technical University (METU) for partial support of this project.

My wife and my family truly deserve appreciation as they have always been next to me. Their encouragement and support definitely increased the quality of the current study.

Finally the countless friends, administrative staff of our department and the colleagues not mentioned deserves the best regards and appreciation for their invaluable contribution and support towards the realization of this study. Their support has been among one of the most important incentives to perform this work.

A great establishment would have been achieved; in case this study could bring new insights to the drilling industry due to being one of the pioneering works in underbalanced drilling.

TABLE OF CONTENTS

ABSTRACT.....	iv
ÖZ.....	vi
ACKNOWLEDGMENTS.....	ix
TABLE OF CONTENTS.....	x
LIST OF TABLES.....	xiv
LIST OF FIGURE.....	xvi
NOMENCLATURE.....	xxix
CHAPTER	
1. INTRODUCTION.....	1
2. LITERATURE REVIEW.....	5
2-1 Gas-Liquid Two-Phase Flow in Pipe.....	5
2-2 Gas-Liquid Two-Phase Flow in Annuli.....	10
2-3 Flow in Eccentric Annuli and Conformal Mapping.....	19
2-4 Cuttings Transport.....	21
2-4-1 Solid Transport with Drilling Fluid Flow in Pipes.....	21
2-4-2 Solid-Liquid Two-Phase Flow in Wellbores.....	23
2-4-3 Solid Transport with Two-Phase Flow in Pipes.....	36
2-4-4 Solid Transport with Two-Phase Flow in Wellbore.....	38
3. STATEMENT OF THE PROBLEM.....	45
4. SCOPE OF THE STUDY AND APPROCH.....	47
5. EXPERIMENTAL SETUP.....	49
5.1 Experimental Setup.....	49
5-2 Installation of Data Acquisition System.....	58
5-3 Experimental Test Procedure and Data Acquisition.....	60
5-3-1 Two-Phase Gas-Liquid Flow.....	61
5-3-2 Cutting-Liquid Two Phase Flow.....	62
5-3-3 Three Phase Flow (Air-Water-Cutting).....	64
5-4 Sensitivity Analysis of Experimental Data.....	66
5-5 Experimental Data Analysis Procedure.....	67

5.6 Methodology of Image Analysis Technique.....	68
5-6-1 Common Initial Steps for Algorithms.....	68
5-6-2 Liquid Hold up Determination by Using Image Analysis Technique Applied in Gas-Liquid Two Phase Flow.....	69
5-6-3 Cutting Concentration Determination by Using Image Analysis Technique Applied in Cutting- Liquid Two Phase Flow.....	73
5-6-4 Cutting Concentration Determination by Using Image Analysis Technique Applied in Three Phase Flow.....	76
5-6-5 Calculating Cutting Velocity.....	80
5-7 Initial Experiments: Single-Phase Water Flow to Validate the Experimental Setup Along with the Data Acquisition System.....	81
6. THEORY.....	83
6-1 Flow Pattern Identification for Cutting-Liquid and Gas-Liquid Two Phase Flow.....	83
6-1-1 Discriminant Analysis.....	85
6-1-2 Development of Flow Pattern Map by Using Discriminant Analysis Gas-Liquid Two Phase Flow in Horizontal Section.....	85
6-1-3 Development of Flow Pattern Map by Using Discriminant Analysis Cutting-Liquid Two Phase Flow in Horizontal Section....	89
6-2 Dimensional Analysis to Estimate Liquid Hold up and Friction Pressure Loss in Gas-Liquid Two Phase Flow through Horizontal Eccentric Annuli.....	91
6-2-1 Liquid Holdup Prediction.....	91
6-2-2 Friction Pressure Loss Prediction.....	97
6-3 Dimensional Analysis for Cutting-Liquid Two Phase Flow in Horizontal Eccentric Annuli.....	107
6-3-1 Development of Empirical Correlations to Estimate Parameters Measured by Using Image Analysis Technique.....	108
6-3-2 Determination of Friction Factor for Two Phase Cutting and Liquid Flow in Horizontal Eccentric Annuli.....	111
6-4 Mechanistic Models.....	117
6-4-1 Conformal Mapping.....	117

6-4-2 Model Assumptions.....	121
6-4-3 Mechanistic Model for Gas-Liquid Two Phase Homogeneous Flow in Vertical and Inclined Eccentric Annuli.....	121
6-4-4 Solid-Gas-Liquid Three Phase Homogeneous Flow in Horizontal, Vertical and Inclined Eccentric Annuli.....	125
7. RESULTS & DISCUSSIONS.....	133
7-1 Experimental Observations and Sensitivity Analysis.....	133
7-1-1 Cutting-Liquid Two Phase Flow.....	133
7-1-2 Gas-Liquid Two Phase Flow.....	141
7-1-3 Cutting-Gas-Liquid Three Phase Flow.....	146
7-2 Comparison between Mechanistic Models Results and the Experimental Data.....	156
7-2-1 Solid (Cutting)-Liquid Two Phase Flow.....	156
7-2-2 Gas-Liquid Two Phase Flow.....	158
7-2-3 Cutting-Gas-Liquid Three Phase Flow.....	160
8. CONCLUSION.....	169
RECOMMENDATIONS.....	172
REFERENCES.....	173
APPENDICES	
A. Results of Experiments	186
B. Developed Excel Macro to Calculate the Average of Experimental Data.....	196
C. Image Processing Techniques	199
D. Developed Excel Macro to Determine the Flow Pattern.....	201
E. Developed Excel Macro to Estimated Friction Pressure Drop for Flow in Horizontal Annuli by Using Beggs & Brill Method.....	207
F. Developed Matlab Code to Determine Relationship between Liquid and Gas Superficial Reynolds Number and Experimentally Observed Friction Factor for Current Experimental Data by Using Matlab Statistical Tool Box and Applying Robust Regression.....	210
G. Resultant Mix Velocity.....	211
H. Developed Excel Macro to Find Interfacial Friction Factor.....	214

I. Developed Excel Macro to Apply and Verify Developed Mechanistic Model for Gas-Liquid Two Phase Homogeneous Flow in Vertical and Inclined Eccentric Annuli to Experimental Data.....	222
J. Developed Excel Macro to Apply and Verify Developed Mechanistic Model for Cutting-Gas-Liquid Three Phase Homogeneous Flow in Horizontal, Vertical and Inclined Eccentric Annuli to Experimental Data...	226
K. Calculation of Gas, Particle and Liquid Slip Void Fraction into the Three Phase Mixture.....	231
VITA.....	233

LIST OF TABLES

TABLES

Table 5.1 Capacity and Brand Name of Experimental Components.....	58
Table 5.2 The Solid Particle Characteristics.....	58
Table 5.3 Test Matrix for Gas-Liquid Two Phase Flow Tests.....	62
Table 5.4 Test Matrix for Cutting-Liquid Two Phases Flow Tests.....	64
Table 5.5 Test Matrix for Gas-Cutting-Liquid Three Phases Flow Tests.....	66
Table 5.6: Labeling Levels and Intervals.....	71
Table 5.7: Used Levels for Frame Types to Generate Gas and Liquid Mixture.....	71
Table 6.1: Boundary Equation Coefficients.....	89
Table 6.2- Evaluated New Constants for Flow in Annuli (Beggs & Brill)	93
Table 6.3- Evaluated New Constants for Flow in Annuli (Lockhart & Martinelli)..	94
Table 6.4 Equation Coefficients Obtained by Robust Regression.....	102
Table 6.5 New Concentric Annulus Geometry Properties for METU-PETE-CTFL Obtained by Using Conformal Mapping Technique	120
Table 7.1 -Minimum Gas Superficial Velocity for Three Phase Flow in Horizontal Eccentric Annuli $V_{SL}=3$ ft/s, ROP=80 ft/hr.....	166
Table A.1 Two-phase Flow Experimental Data for Horizontal Eccentric Annulus Air-Water Flow without Drill pipe Rotation.....	186
Table A.2 Two-phase Flow Experimental Data for Inclined (15.0° from Horizontal) Eccentric Annulus Air-Water Flow without Drill pipe Rotation.....	187

Table A.3 Two-phase Flow Experimental Data for Inclined (30.0° from Horizontal) Eccentric Annulus Air-Water Flow without Drill pipe Rotation.....	187
Table A.4 Two-phase Flow Experimental Data for Inclined (77.5° from Horizontal) Eccentric Annulus Air-Water Flow without Drill pipe Rotation.....	188
Table A.5 Two-phase Flow Repeated Experimental Data for Inclined (77.5° from Horizontal) Eccentric Annulus Air-Water Flow without Drill pipe Rotation.....	188
Table A.6 Two-phase Flow Experimental Data for Inclined (45.0° from Horizontal) Eccentric Annulus Air-Water Flow without Drill pipe Rotation.....	189
Table A.7 Two-phase Flow Experimental Data for Horizontal Eccentric Annulus Cutting-Water Flow	190
Table A.8 Two-phase Flow Experimental Data for Inclined (77.5° from Horizontal) Eccentric Annulus Cutting-Water Flow.....	191
Table A.9 Two-phase Flow Experimental Data for Inclined (45.0° from Horizontal) Eccentric Annulus Cutting-Water Flow.....	192
Table A.10 Three-phase Flow Experimental Data for Horizontal Eccentric Annulus Cutting-Gas-Water Flow.....	193
Table A.11 Three-phase Flow Experimental Data for Inclined (77.5° from Horizontal) Eccentric Annulus Cutting-Gas-Water Flow.....	194
Table A.12 Three-phase Flow Experimental Data for Inclined (45.0°) Eccentric Annulus Cutting-Gas-Water Flow.....	195

LIST OF FIGURES

FIGURES

Figure 5.1 METU-PETE-CT Flow Loop.....	50
Figure 5.2 Annular Test Section Inlet and Movable Corner.....	51
Figure 5.3 Separation Section and Modified Shale Shaker.....	51
Figure 5.4 Data Logger System (National Instruments NI SCXI-100).....	52
Figure 5.5 Constructed Plat Form for Camera and Annular Test Section.....	52
Figure 5.6 Drill Pipe - Range of Eccentricities.....	53
Figure 5.7 Cutting Injection Tank and Helicoids (Screw) Metal Chip Conveyor	53
Figure 5.8 Centrifugal Pump for the Liquid Phase.....	54
Figure 5.9 Fisher Control Valve and Toshiba Flow Meter.....	54
Figure 5.10-A Air Compressor and Accumulator Tank.....	55
Figure 5.10-B Air Compressor and Accumulator Tank.....	55
Figure 5.11 Air Dryer and Air Pipe Line.....	56
Figure 5.12 Fisher Control Valve and ABB Gas Mass Flow Meter.....	56
Figure 5.13 Schematic of Experimental Setup.....	57
Figure 5.14 Back Panel of Lab View Designed by Researcher.....	59
Figure 5.15 Front Panel of Lab View Designed by Researcher.....	60

Figure 5.16 Finding Annulus.....	69
Figure 5.17 Pixel Intensity Labeling Algorithm.....	69
Figure 5.18 Labeling Using Boundary Algorithm.....	70
Figure 5.19 Partial Intensity Labeling Algorithm.....	71
Figure 5.20 Combination of Partial Intensity Labeling and Labeling Using Boundary Algorithm.....	72
Figure 5.21 Three-Dimensional System to Two-Dimensional Frame.....	73
Figure 5.22 Flow Types (a) Stationary Bed (b) Moving Bed (c) Dispersed.....	73
Figure 5.23 Stable Cutting Algorithm.....	74
Figure 5.24 Moving Cutting Algorithm Applied to Slug Frame	75
Figure 5.25 Moving Cutting Algorithm Applied to Dispersed Frame Type.....	75
Figure 5.26 Flow Patterns (a) Stationary-Bed Flow (b) Dispersed Flow.....	76
Figure 5.27 Stationary Bed Algorithms.....	78
Figure 5.28 Dispersed Algorithms.....	79
Figure 5.29 Pixel Distance Calculators.....	81
Figure 5.30 Comparing Measured and Calculated Single-Phase Friction Pressure Drop in Horizontal Test Section.....	82
Figure 6.1 Flow Patterns for Horizontal (Air-Water) Flow without Drill pipe Rotation.....	84
Figure 6.2 Flow Patterns for Horizontal (Cutting-Water) Flow with or without Drill pipe Rotation a) Flow with Bed Existence (b) Dispersed Flow.....	85

Figure 6.3 Flow Pattern Map for Horizontal Air-Water Flow without Drill Pipe Rotation.....	87
Figure 6.4 Boundaries between Various Flow Patterns Determined by Using Diagonal Quadratic Discriminant Analysis Method.....	88
Figure 6.5 Flow Pattern Map for Horizontal Cutting-Water Flow with Drill Pipe Rotation.....	91
Figure 6.6 Relationships between the Liquid Hold up Values and the Velocity Ratio for Different Geometries.....	92
Figure 6.7 Comparisons between Experimental Liquid Hold up for Flow in Annuli and Estimated Liquid Hold up for Flow in Pipes (Beggs & Brill).	93
Figure 6.8 Comparisons between Experimental Liquid Hold up and Estimated Liquid Hold up for Flow in Annuli (Modified Beggs & Brill)	95
Figure 6.9 Comparisons between Experimental Liquid Hold up and Estimated Liquid Hold up for Flow in Annuli (Modified Lockhart & Martinelli)	95
Figure 6.10 Comparisons between Experimental Data Obtained from Sunthakar Study and Estimated Liquid Hold up for Flow in Annuli (Modified Beggs & Brill).	96
Figure 6.11 Comparisons between Experimental Data Obtained from Sunthakar Study and Estimated Liquid Hold up for Flow in Annuli (Modified Lockhart & Martinelli).....	96
Figure 6.12 Comparisons between Experimental Data Obtained from Current Study and Sunthakar Study and Estimated Liquid Hold up for Flow in Annuli by Using Equation (6.11)	97
Figure 6.13 Comparisons between Experimental Data Obtained from Current Study and Estimated Friction Pressure Drop for Flow in Annuli by Using Beggs & Brill Method.....	98

Figure 6.14 Comparisons between Experimental Data Obtained from Sunthakar Study (2002) and Estimated Friction Pressure Drop for Flow in Annuli by Using Beggs & Brill Method.....	98
Figure 6.15 Relationships between Mixture Friction and Mixture Reynolds Number.....	100
Figure 6.16 Relationships between Liquid and Gas Superficial Reynolds Number and Experimentally Observed Friction Factor for Current Experimental Data.....	102
Figure 6.17 Comparisons between the Friction Factors Calculated by Equation 6.17 Obtained by Applying Robust Regression Analysis and Experimentally Observed Friction Factors.....	102
Figure 6.18 Comparison between Calculated Pressure Gradients by Using Friction Coefficients Obtained by Robust Regression Analysis Method and Measured Pressure Gradients.....	103
Figure 6.19 Comparisons between Experimental Data Obtained from Current Study and Estimated Friction Pressure Drop for Flow in Annuli by Using Modified Beggs & Brill Method.....	104
Figure 6.20 Comparisons between Experimental Data Obtained from Sunthakar Study (2002) and Estimated Friction Pressure Drop for Flow in Annuli by Using Modified Beggs & Brill Method.....	104
Figure 6.21 Relationship between Liquid Dimensionless Pressure Gradient Parameter and Liquid Surface Pressure Gradients.....	106
Figure 6.22 Comparisons between Experimental Data Obtained from Current Study and Estimated Friction Pressure Drop for Flow in Annuli by Using Modified Lockhart-Martinelli Method.....	107

Figure 6.23 Comparisons between Experimental Data Obtained from Sunthakar Study (2002) and Estimated Friction Pressure Drop for Flow in Annuli by Using Modified Lockhart-Martinelli Method.....	107
Figure 6.24 Comparisons between Experimental Data Obtained from Current Study and Estimated Cutting Concentration.....	110
Figure 6.25 Comparisons between Experimental Data Obtained from Current Study and Estimated Moving Cutting Concentration.....	110
Figure 6.26 Comparisons between Experimental Data Obtained from Current Study and Estimated Ratio of Moving Cutting Velocity to Mud Axial Velocity.....	111
Figure 6.27 Comparisons between Experimental Data Obtained from Current Study and Estimated Ratio of Bed Height to Well Diameter.....	111
Figure 6.28 Comparisons between Experimental Data Obtained from Current Study and Estimated Interfacial Friction Factor.....	115
Figure 6.29 Comparisons between Experimental Data Obtained from Current Study and Estimated Friction Factor.....	116
Figure 6.30 Bipolar Coordinate System (Jeng-Tzong Chen, Ming-Hong Tsai, Chein-Shan Liu 2009)	117
Figure 6.31 Mapping of the Eccentric Annulus to a Concentric Annulus (Jeng-Tzong Chen, Ming-Hong Tsai, Chein-Shan Liu 2009)	118
Figure 6.32 Geometry of Eccentric Annulus System (Tosun & Ozgen, 1987).....	119
Figure 6.33 the Applicability Region for Conformal Mapping (Tosun & Ozgen, 1987)	121
Figure 6.34 Free Body Diagram for a Particle of Dispersed Phase (Solid Particle) in Gas and Liquid Homogeneous Mixture.....	126

Figure 7.1 Ratio of Cutting Area Observed inside Wellbore from Image Analysis vs. Fluid Superficial Velocity in Horizontal Test Section ($\theta=0$) for RPM=80 (1/min), ROP=60, 80,100 &120 (ft/hrs)	134
Figure 7.2 Ratio of Cutting Area Observed inside Wellbore from Image Analysis vs. Fluid Superficial Velocity in Horizontal Test Section ($\theta=0$) for ROP=80(ft/hrs) RPM=0, 60, 80, 100 & 120 (1/min).....	134
Figure 7.3 Measured Pressure Drop vs. Water Superficial Velocity in Horizontal Test Section ($\theta=0$) for RPM=80(1/min), ROP=60, 80,100 &120(ft/hrs)	136
Figure 7.4 Measured Pressure Drop vs. Water Superficial Velocity in Nearly Vertical Test Section ($\theta=77.5$) for RPM=80(1/min), ROP=60, 80,100 &120(ft/hrs)	136
Figure 7.5 Measured Pressure Drop vs. Water Superficial Velocity in Inclined Test Section ($\theta=45.0$) for RPM=80(1/min), ROP=80,100 &120(ft/hrs)	137
Figure 7.6 Measured Pressure Drop vs. Water Superficial Velocity in Horizontal Test Section ($\theta=0$) ROP=80(ft/hrs) RPM=0, 60, 80, 100 & 120 (1/min)	137
Figure 7.7 Measured Pressure Drop vs. Water Superficial Velocity in Nearly Vertical Test Section ($\theta=77.5$) ROP=80(ft/hrs), RPM=60, 80, 100 & 120 (1/min)	138
Figure 7.8 Measured Pressure Drop vs. Water Superficial Velocity in Inclined Test Section ($\theta=45.0$) ROP=80(ft/hrs) RPM=0, 80 & 120 (1/min)	138
Figure 7.9 Measured Pressure Drop vs. Water Superficial Velocity in Horizontal ($\theta=0.$), nearly Vertical ($\theta=77.5$) and Inclined ($\theta=45.0$) Test Sections ROP=80(ft/hrs) RPM=80 & 120 (1/min)	139
Figure 7.10 Measured Moving Cutting Velocity vs. Water Superficial Velocity in Horizontal Test Section ($\theta=0$) for RPM=80(1/min), ROP=60, 80,100 &120(ft/hrs)	140

Figure 7.11 Measured Moving Cutting Velocity vs. Water Superficial Velocity in Horizontal Test Section ($\theta=0$) for ROP=80(ft/hrs) RPM=0, 60, 80, 100 & 120 (1/min)	140
Figure 7.12 Measured Liquid Hold up vs. Gas Superficial Velocity in Horizontal Test Section ($\theta=0$) for Different Water Flow Rate.....	141
Figure 7.13 Measured Pressure Drop vs. Gas Superficial Velocity in Horizontal Test Section ($\theta=0$) for Different Water Flow Rate.....	142
Figure 7.14 Measured Pressure Drop vs. Gas Superficial Velocity in Inclined Test Section ($\theta=15.0$) for Different Water Flow Rate.....	143
Figure 7.15 Measured Pressure Drop vs. Gas Superficial Velocity in Nearly Vertical Test Section ($\theta=77.5$) for Different Water Flow Rate.....	144
Figure 7.16 Measured Pressure Drop vs. Gas Superficial Velocity in Inclined Test Section ($\theta=45.0$) for Different Water Flow Rate.....	144
Figure 7.17 Measured Pressure Drop vs. Gas Superficial Velocity in Inclined Test Section ($\theta=30.0$) for Different Water Flow Rate.....	145
Figure 7.18 Measured Pressure Drop vs. Gas Superficial Velocity in Horizontal ($\theta=0.$), nearly Vertical ($\theta=77.5$) and Inclined ($\theta=45.0, 30.0$ & 15.0) Test Sections for $V_{SL}=2.0$ (ft/sec)	145
Figure 7.19 Ratio of Cutting Area Observed Inside Wellbore from Image Analysis vs. Air Superficial Velocity in Horizontal Test Section ($\theta=0$) for $V_{SL}= 2.0$, ROP=100(ft/hrs) RPM=80, 100 & 120 (1/min)	146
Figure7.20 Ratio of Cutting Area Observed inside Wellbore from Image Analysis vs. Air Superficial Velocity in Horizontal Test Section ($\theta=0$) for $V_{SL}= 3.0$, ROP=100(ft/hrs) RPM=80, 100 & 120 (1/min)	147

Figure7.21 Ratio of Cutting Area Observed inside Wellbore from Image Analysis vs. Air Superficial Velocity in Horizontal Test Section ($\theta=0$) for $V_{SL}=2.0$, RPM=100(1/min) ROP=80, 100 & 120 (ft/hrs)	147
Figure7.22 Ratio of Cutting Area Observed inside Wellbore from Image Analysis vs. Air Superficial Velocity in Horizontal Test Section ($\theta=0$) for $V_{SL}=3.0$, RPM=100(1/min) ROP=80, 100 & 120 (ft/hrs)	148
Figure7.23 Ratio of Cutting Area Observed inside Wellbore from Image Analysis vs. Air Superficial Velocity in Horizontal Test Section for Different Liquid Superficial Velocity ROP=80(ft/hrs) RPM=100 (1/min)	148
Figure 7.24 Measured Pressure Drop vs. Gas Superficial Velocity in Horizontal Test Section ($\theta=0$) $V_{SL}=2.0$ (ft/sec), ROP=100(ft/hrs) and RPM=80,100,120 (1/min)	150
Figure 7.25 Measured Pressure Drop vs. Gas Superficial Velocity in Horizontal Test Section ($\theta=0$) $V_{SL}=3.0$ (ft/sec), ROP=100(ft/hrs) and RPM=80,100,120 (1/min)	150
Figure 7.26 Measured Pressure Drop vs. Gas Superficial Velocity in Horizontal Test Section ($\theta=0$) $V_{SL}=4.0$ (ft/sec), ROP=100(ft/hrs) and RPM=80,100,120 (1/min)	151
Figure 7.27 Measured Pressure Drop vs. Gas Superficial Velocity in Horizontal Test Section ($\theta=0$) $V_{SL}=2.0$ (ft/sec), RPM=80 (1/min) and ROP=80,100,120(ft/hrs)	151
Figure 7.28 Measured Pressure Drop vs. Gas Superficial Velocity in Horizontal Test Section ($\theta=0$) $V_{SL}=2.0, 3.0, 4.0, 5.0$ and 6.0 (ft/sec), ROP=80(ft/hrs) and RPM=80, (1/min)	152

Figure 7.29 Measured Pressure Drop vs. Gas Superficial Velocity in Inclined Test Section ($\theta=45.0$) $V_{SL}=2.0$ (ft/sec), ROP=120(ft/hrs) and RPM=80, 120 (1/min)	152
Figure 7.30 Measured Pressure Drop vs. Gas Superficial Velocity in Inclined Test Section ($\theta=45.0$) $V_{SL}=2.0$ (ft/sec), RPM=80 (1/min) and ROP=80,100,120 (ft/hrs)	153
Figure 7.31 Measured Pressure Drop vs. Gas Superficial Velocity in Inclined Test Section ($\theta=45.0$) $V_{SL}=2.0, 3.0, 4.0\&5.0$ (ft/sec), RPM=80 (1/min) and ROP=80 (ft/hrs)	153
Figure 7.32 Measured Pressure Drop vs. Gas Superficial Velocity in Nearly Vertical Test Section ($\theta=77.5$) $V_{SL}=2.0$ (ft/sec), ROP=120(ft/hrs) and RPM=80,100,120(1/min)	154
Figure 7.33 Measured Pressure Drop vs. Gas Superficial Velocity in Nearly Vertical Test Section ($\theta=77.5$) $V_{SL}=3.0$ (ft/sec), RPM=80 (1/min) and ROP=80,100,120(ft/hrs)	154
Figure 7.34 Measured Pressure Drop vs. Gas Superficial Velocity in Nearly Vertical Test Section ($\theta=77.5$) $V_{SL}=2.0, 3.0, 4.0\&5.0$ (ft/sec), RPM=80 (1/min) and ROP=80 (ft/hrs)	155
Figure 7.35 Measured Pressure Drop vs. Gas Superficial Velocity in Nearly Vertical ($\theta=77.5$) and Inclined ($\theta=45.0, 30.0\&15.0$) Test Section for $V_{SL}=2.0$ (ft/sec), RPM=120 (1/min) and ROP=120 (ft/hrs)	156
Figure 7.36 Comparisons between Experimental Data Obtained from Current Study and Estimated Friction Pressure Loss for Horizontal ($\theta=0$) Water-Solid (Cutting) Flow in Annuli with Inner Pipe Rotation by Using Developed Mechanistic Method (Presented in Section 6-4-4)	157

Figure 7.37 Comparisons between Experimental Data Obtained from Current Study and Estimated Total Pressure Loss for Nearly Vertical ($\theta=77.5$) Water-Solid (Cutting) Flow in Annuli with Inner Pipe Rotation by Using Developed Mechanistic Method (Presented in Section 6-4-4)	157
Figure 7.38 Comparisons between Experimental Data Obtained from Current Study and Estimated Total Pressure Loss for Inclined ($\theta=45.0$) Water-Solid (Cutting) Flow in Annuli with Inner Pipe Rotation by Using Developed Mechanistic Method (Presented in Section 6-4-4).....	158
Figure 7.39 Comparisons between Experimental Data Obtained from Current Study and Estimated Total Pressure Loss for Nearly Vertical ($\theta=77.5$) Water-Air Flow in Annuli without Inner Pipe Rotation by Using Developed Mechanistic Method (Presented in Section 6-4-3)	159
Figure 7.40 Comparisons between Experimental Data Obtained from Current Study and Estimated Total Pressure Loss for Inclined ($\theta=45.0$) Water-Air Flow in Annuli without Inner Pipe Rotation by Using Developed Mechanistic Method (Presented in Section 6-4-3).....	159
Figure 7.41 Comparisons between Experimental Data Obtained from Current Study and Estimated Total Pressure Loss for Inclined ($\theta=30.0$) Water-Air Flow in Annuli without Inner Pipe Rotation by Using Developed Mechanistic Method (Presented in Section 6-4-3).....	160
Figure 7.42 Comparisons between Experimental Data Obtained from Current Study and Estimated Total Pressure Loss for Inclined ($\theta=15.0$) Water-Air Flow in Annuli without Inner Pipe Rotation by Using Developed Mechanistic Method (Presented in Section 6-4-3).....	160
Figure 7.43 Ratio of Cutting Area Observed inside Wellbore from Image Analysis and Calculated Cutting Concentration by Mechanistic Model vs. Gas Superficial Velocity for $V_{SL}=2.0$ (ft/sec), $ROP=80$ (ft/hrs), $RPM=80,100$ & 120 (1/min) for	

Horizontal Water-Air and Cutting Three Phases Flow in Eccentric Annuli with Inner Pipe Rotation by Using Developed Mechanistic Method.....161

Figure 7.44 Ratio of Cutting Area Observed inside Wellbore from Image Analysis and Calculated Cutting Concentration by Mechanistic Model vs. Gas Superficial Velocity for $V_{SL}=3.0$ (ft/sec), ROP=120(ft/hrs), RPM=80,100 &120 (1/min) for Horizontal Water-Air and Cutting Three Phases Flow in Eccentric Annuli with Inner Pipe Rotation by Using Developed Mechanistic Method.....162

Figure 7.45 Ratio of Cutting Area Observed inside Wellbore from Image Analysis and Calculated Cutting Concentration by Mechanistic Model vs. Gas Superficial Velocity for $V_{SL}=4.0$ (ft/sec), ROP=120(ft/hrs), RPM=80,100 &120 (1/min) for Horizontal Water-Air and Cutting Three Phases Flow in Eccentric Annuli with Inner Pipe Rotation by Using Developed Mechanistic Method.....162

Figure 7.46 Calculated Cutting Concentration by Mechanistic Model vs. Gas Superficial Velocity for $V_{SL}=2.0$ (ft/sec), ROP=80(ft/hrs), RPM=80 (1/min) in Horizontal ($\theta=0.$), Nearly Vertical ($\theta=77.5$) and Inclined ($\theta=45.0,30.0\&15.0$) Test Sections for Water-Air and Cutting Three Phases Flow in Eccentric Annuli with Inner Pipe Rotation by Using Developed Mechanistic Method 163

Figure 7.47 Measured and Predicted Pressure Drop vs. Gas Superficial Velocity by Mechanistic Model vs. Gas Superficial Velocity for $V_{SL}=2.0$ (ft/sec), ROP=120(ft/hrs), RPM=80,100 &120 (1/min) for Horizontal Water-Air and Cutting Three Phases Flow in Eccentric Annuli with Inner Pipe Rotation by Using Developed Mechanistic Method (presented in section 6-4-4)164

Figure 7.48 Measured and Predicted Pressure Drop vs. Gas Superficial Velocity by Mechanistic Model vs. Gas Superficial Velocity for $V_{SL}=3.0$ (ft/sec), ROP=100(ft/hrs), RPM=80,100 &120 (1/min) for Horizontal Water-Air and Cutting Three Phases Flow in Eccentric Annuli with Inner Pipe Rotation by Using Developed Mechanistic Method (presented in section 6-4-4)164

Figure 7.49 Measured and Predicted Pressure Drop vs. Gas Superficial Velocity by Mechanistic Model vs. Gas Superficial Velocity for $V_{SL}=4.0$ (ft/sec), ROP=120(ft/hrs), RPM=80,100 &120 (1/min) for Horizontal Water-Air and Cutting Three Phases Flow in Eccentric Annuli with Inner Pipe Rotation by Using Developed Mechanistic Method (presented in section 6-4-4)165

Figure 7.50 Measured and Predicted Pressure Drop vs. Gas Superficial Velocity by Mechanistic Model vs. Gas Superficial Velocity for $V_{SL}=6.0$ (ft/sec), ROP=100(ft/hrs), RPM=80&120 (1/min) for Horizontal Water-Air and Cutting Three Phases Flow in Eccentric Annuli with Inner Pipe Rotation by Using Developed Mechanistic Method (presented in section 6-4-4).....165

Figure 7.51 Measured and Predicted Pressure Drop vs. Gas Superficial Velocity by Mechanistic Model vs. Gas Superficial Velocity for $V_{SL}=2.0, 3.0, 4.0$ (ft/sec), ROP=100(ft/hrs), RPM=80 (1/min) for Horizontal Water-Air and Cutting Three Phases Flow in Eccentric Annuli with Inner Pipe Rotation by Using Developed Mechanistic Method (presented in section 6-4-4).....166

Figure 7.52 Measured and Predicted Pressure Drop vs. Gas Superficial Velocity by Mechanistic Model vs. Gas Superficial Velocity for $V_{SL}=2.0, 3.0, 4.0,5.0$ (ft/sec), ROP=80,100,120(ft/hrs), RPM=80,100,120 (1/min) for Nearly Vertical ($\theta=77.5$) Water-Air and Cutting Three Phases Flow in Eccentric Annuli with Inner Pipe Rotation by Using Developed Mechanistic Method167

Figure 7.53 Measured and Predicted Pressure Drop vs. Gas Superficial Velocity by Mechanistic Model vs. Gas Superficial Velocity for $V_{SL}=2.0, 3.0, 4.0,5.0$ (ft/sec), ROP=80,100,120(ft/hrs), RPM=80,100,120 (1/min) for Inclined ($\theta=45.0$) Water-Air and Cutting Three Phases Flow in Eccentric Annuli with Inner Pipe Rotation by Using Developed Mechanistic Method.....167

Figure 7.54 Measured and Predicted Pressure Drop vs. Gas Superficial Velocity by Mechanistic Model vs. Gas Superficial Velocity for $V_{SL}=2.0, 3.0, 4.0,5.0$ (ft/sec), ROP=80,100,120(ft/hrs), RPM=80,100,120 (1/min) for Inclined ($\theta=30.0$) Water-Air

and Cutting Three Phases Flow in Eccentric Annuli with Inner Pipe Rotation by Using Developed Mechanistic Method (presented in section 6-4-4)	168
Figure 7.55 Measured and Predicted Pressure Drop vs. Gas Superficial Velocity by Mechanistic Model vs. Gas Superficial Velocity for $V_{SL}=2.0, 3.0, 4.0, 5.0$ (ft/sec), ROP=80,100,120(ft/hrs), RPM=80,100,120 (1/min) for Nearly Horizontal ($\theta=15.0$) Water-Air and Cutting Three Phases Flow in Eccentric Annuli with Inner Pipe Rotation by Using Developed Mechanistic Method.....	168
Figure D.1 Flowchart for Flow Pattern Identification in an Annular Section.....	201
Figure G.1 Tangential Velocity Profile in the Annuli.....	211

NOMENCLATURE

A_f	:	Area of flow for the fluid in cutting – liquid two phase flow, L^2
A_w	:	Wellbore area, L^2
A_c	:	Stationary Cutting Bed area in two phase liquid-cutting mixture, L^2
C_D	:	Drag Coefficient
C_{Dp}	:	Drag Coefficient
C_c	:	Total Slip void fraction of Solid phase in two phase liquid-cutting mixture
C_{cm}	:	Moving Slip void fraction of Solid phase in two phase liquid- cutting mixture
D_{wh}	:	Wellbore diameter, L
D_{dp}	:	Drill pipe diameter, L
D_h	:	Hydraulic Diameter, L ($D_h = (D_{wh} - D_{dp})$)
D_p	:	Solid Particle Diameter, L
D_B	:	Bit Diameter, L
D_{uph}	:	Hydraulic Diameter of Upper Layer in Cutting Liquid Two Phase Flow, L
D_{loh}	:	Hydraulic Diameter of Lower Layer in Cutting Liquid Two Phase Flow, L
f_F	:	Friction factor between the fluid and moving cutting mixture and annular walls in cutting – liquid two phase flow
f_{Fc}	:	Friction factor between the bed cutting and annular walls in cutting – liquid two phase flow
f_{Fi}	:	Interfacial friction factor in cutting – liquid two phase flow
$F_{C.Lr}$:	Dimensionless Group – 3 (Pseudo Froude Number) in Cutting-Water Two Phase Flow
h	:	Liquid Column Height, L

- H_L : slip void fraction of Liquid in two phase flow (Liquid hold up)
- H_{bed} : Stationary Cutting Bed height in two phase liquid-cutting mixture, L
- $N_{Re_{CW.mix.l}}$: Reynolds Number for solid particle motion in fluid of lower layer in cutting – liquid two phase flow
- $N_{Re_{CW.mix.up}}$: Reynolds Number for solid particle motion in fluid of upper layer in cutting – liquid two phase flow
- N_{Re_p} : Reynolds Number for solid particle motion in fluid
- $N_{Re_{th.mix}}$: Reynolds Number based on the hydraulic diameter of cylinder for liquid, cutting and gas homogenous mixture
- $N_{Re_{SG}}$: Gas superficial Reynolds numbers in two phase liquid and gas flow
- $N_{Re_{SL}}$: Liquid superficial Reynolds numbers in two phase liquid and gas flow
- $N_{Re_{CW.mix}}$: Dimensionless group – 1 (pseudo axial mixture Reynolds number) in cutting-water two phase flow
- $N_{Re_{Gw.mix}}$: Mixture Reynolds number in gas-water two phase flow
- $N_{Re_{ro}}$: Dimensionless group – 2 (pseudo tangential Reynolds number) in cutting-water two phase flow
- N_{Fr} : Froude number in gas-water two phase flow
- Q_S : Solid phase flow rate, L³/t
- Q_L : Liquid phase flow rate, L³/t
- Q_G : Gas phase flow rate, L³/t
- r_{ei} : Drill pipe radius
- r_{eo} : Well bore radius
- r_e^* : Radius ratio
- V_{stm} : Three phase liquid, gas and cutting mixture slip velocity, L/t
- V_{SC} : Solid particle superficial velocity, L/t
- \vec{v}_{sp} : Slip velocity of solid particle, L/t

V_{sm}	:	Two phase liquid and gas mixture resultant velocity, L/t
V_{SL}	:	Liquid superficial velocity, L/t
V_{SG}	:	Gas superficial velocity, L/t
V_Z	:	Mixture axial velocity in cutting – liquid two phase flow, L/t
V_{θ}	:	Tangential velocity, L/t
V_m	:	Mixture axial velocity in gas – liquid two phase flow, L/t
V_{mact}	:	Moving axial cutting velocity in cutting – liquid two phase flow, L/t
X	:	Lockhart & Martinelli (1969) parameter in two phase flow
x, y, z	:	Rectangular coordinate axes
ρ_{fm}	:	Fluid and moving cutting mixture density which flow in upper layer in two layer model, m/L^3
u_{fm}	:	Fluid and moving cutting mixture resultant velocity in the upper layer in two layer model, L/t
u_{cm}	:	average resultant velocity of the cuttings bed in the lower layer in two layer model in cutting – liquid two phase flow, L/t

Greek Letters

ε	:	Cutting (solid) bed porosity
η, ζ, z :		Bipolar coordinates
ϵ	:	Eccentricity ratio
μ_L	:	Liquid viscosity, $m/ (L t)$
μ_G	:	Gas viscosity, $m/ (L t)$
μ_m	:	Non slip mixture viscosity in air-water two phase flow, $m/ (L t)$
μ_{fm}	:	Two phase liquid and cutting homogeneous mixture viscosity in upper layer in cutting – liquid two phase flow, $m/ (L t)$
μ_{cm}	:	Two phase liquid and cutting homogeneous mixture viscosity in lower layer in cutting – liquid two phase flow, $m/ (L t)$
$\mu_{C.Lmix}$:	Non slip mixture viscosity in cutting-water two phase flow, $m/ (L t)$

- μ_{dmix} : Fluid and moving cutting mixture viscosity in dispersed cutting – liquid two phases, m/ (L t)
- μ_{stm} : Three phase liquid, gas and cutting mixture viscosity, m/ (L t)
- μ_{sm} : Slip mixture viscosity of two phase liquid and, m/ (L t)
- ρ_L : Liquid density, m/L³
- ρ_C : Cutting density, m/L³
- ρ_G : Gas density, m/L³
- ρ_m : Non slip mixture density in air-water two phase flow, m/L³
- ρ_{cm} : Two phase liquid and cutting homogeneous mixture density in lower layer in cutting – liquid two phase flow, m/L³
- ρ_{dm} : Fluid and moving cutting mixture density in dispersed cutting – liquid two phase flow, m/L³
- ρ_{mix} : Non slip mixture density in cutting-water two phase flow, m/L³
- ρ_{stm} : Three phase liquid, gas and cutting mixture density, m/L³
- ρ_{sm} : Slip mixture density of two phase liquid and, m/L³
- σ : Liquid kinetic viscosity m/ (L t)
- λ_L : Non slip void fraction of Liquid in two phase flow
- φ_{avg} : Relative density of two phase flow in liquid and gas homogeneous mixture
- \emptyset_{avL} : Slip void fraction of Liquid phase in two phase liquid and gas homogeneous mixture
- \emptyset_{avG} : Slip void fraction of Gas phase in two phase liquid and gas homogeneous mixture
- \emptyset_{Lt} : Slip void fraction of Liquid phase in three phase liquid, gas and cutting homogeneous mixture
- \emptyset_{avp} : Slip void fraction of Solid phase in three phase liquid, gas and cutting homogeneous mixture
- \emptyset_{Gt} : Slip void fraction of Gas phase in three phase liquid, gas and cutting homogeneous mixture

ω : Drill pipe angular velocity, L/t

CHAPTER I

INTRODUCTION

In depleted reservoirs, production is provided by secondary production techniques. In order to apply these methods, it is necessary to drill new wells. In conventional drilling operations, the hydrostatic pressure of drilling fluid is more than the pore pressure in the formation rock. However, in low-pressure reservoirs or depleted reservoirs, conventional drilling methods should cause to reduced or total absence of fluid flow up the annulus, and that cause pollution in the reservoir. The aerated drilling fluids have major advantage of controlling mud effective density, which influences the borehole pressure. Thus, the aerated fluids can be used to explore and exploit low-pressure reservoir and meet the requirements of underbalanced and/or balanced drilling. Generally, underbalanced drilling operation is applied with drilling fluid which consists of gas-liquid mixture, and by using this type of fluids, reservoir pollution is largely or completely eliminated.

The aerated fluids have a potential to increase rate of penetration, minimize formation damage, minimize lost circulation, reduce drill pipe sticking and therefore, assist in improving the productivity. Recently, the technology of drilling using aerated fluids has reached even in the area of offshore drilling. The use of compressible drilling fluids in offshore technology has found applications in old depleted reservoirs and in the new fields with special drilling problems.

However, the drilling performed with gas-liquid mixture, calculating the pressure losses and the performance of cutting transportation is more difficult than single-phase fluid due to the characteristics of multi-phase fluid flow. In case configured drilling is directional or horizontal, these types of calculations are becoming more difficult depending on the slope of the wells. Both hydraulic behavior and mechanism of cutting transportation of the drilling fluids formed by

gas-liquid mixture are not fully understood yet, especially there is a large uncertainty in selection of most appropriate flow regarding two phases.

It is, therefore, necessary to understand better the hydraulics of aerated mudflows in order to calculate accurately desired bottom hole pressure and optimal flow rates for drilling. In the past, experiments have been conducted by few researchers in small-scale annuli to study the flow characteristics of both Newtonian and non-Newtonian fluids. Due to non-linear relationships between flow rate, pipe size and pressure drop, it is difficult to apply their results to conventional drilling operations. Therefore, this research will be focused on the study of the flow of aerated drilling fluids through large-scale horizontal and inclined wellbores.

The main objective of the present study is to better understand the hydraulics and characteristics of the two-phase and three phase fluids flow in annuli. The experimental study consists of two-phase air-water, two-phase cutting-water and three-phase air-water-cutting experiments in large-scale annuli (2.91" X1.86", approximately 21' long) in horizontal, inclined and nearly vertical direction. Experiments were carried out with or without drill pipe rotation. For each experiment, average void fractions and total pressure drop along the flow loop was measured by using sensitive equipments.

Firstly, the two-phase air-water mixture flow patterns were identified in horizontal section by visual observations and they were plotted in the form of a two-dimensional plot of superficial liquid Reynolds number versus superficial gas Reynolds number. It is observed that the flow pattern boundaries proved to be shifted as compared to pipe flow, which necessitates the modification of flow transition criteria. After that, discriminant analysis was used to determine the boundaries, in predictor space, between various flow patterns. Then Lockhart & Martinelli (1969) and Beggs & Brill (1973) model was applied to predict pressure drop in annuli by using experimental parameters. By comparing the results obtained from Lockhart & Martinelli (1969) and Beggs & Brill (1973) model and observed pressure drop and liquid hold up data, it is detected that this method cannot be predicted the pressure drop and liquid hold up in annuli accurately. So it is necessary to develop a common

and proper model to explain the behavior of multiphase fluid flow through annuli in horizontal and inclined wells.

Secondly, some of the very-difficult-to-identify data for estimating total pressure drop and total cuttings concentration were determined for cutting-water two phase flows inside the horizontal wellbore. By comparing consecutive images, very valuable information has been collected about the accumulated cuttings amount, concentration of moving particles, their relative transport velocities, slip velocity between the phases, the friction factor on the stationary bed, etc. Since the images are digital, information collected is converted into numerical values, and semi-empirical equations are developed as a function of known drilling parameters. The obtained information is tested in simple mechanistic models for estimating pressure drop inside a wellbore with the presence of cuttings, and the performance of the model is tested by comparing the results with the measured ones. It is observed that, after supplying the very-difficult-to-identify information to the mechanistic model, the performance of the mechanistic model improved very significantly for cutting-water two phase flows inside the horizontal wellbore.

Finally, the hole cleaning process during the flow of a drilling fluid consist of a gas and a liquid phase through a horizontal inclined and nearly vertical wellbores were investigated. Experiments have been conducted using METU Multiphase Flow Loop under a wide range of air and water flow rates while injecting cuttings into the annulus with different rate of penetration. Data has been collected for steady state conditions, i.e., liquid, gas and cuttings injection rates are stabilized. Collected data include flow rates of liquid and gas phases, total pressure drop inside the test section, local pressures at different locations in the flow loop, and high-speed digital images for identification of solid, liquid and gas distribution inside the wellbore. Digital image processing techniques are applied on the recorded images not only for volumetric phase distribution inside the test section, but also examination of the transport velocities of cuttings particles, which are in dynamic condition. The effects of liquid and gas phases are investigated on cuttings transport behavior under different flow conditions. Observations showed that the major contribution for carrying the cuttings along the wellbore is the liquid phase. However, as the gas flow

rate is increased, the flow area left for the liquid phase drastically decreases, which leads to an increase in the local velocity of liquid phase causing the cuttings to be dragged and moved, or a significant erosion on the cuttings bed. Therefore, increase in the flow rate of gas phase causes an improvement in the cuttings transport although the liquid phase flow rate is kept constant. Based on the observations, a mechanistic model which estimates the total cuttings concentration inside the wellbore and developed total pressure loss is introduced for gasified fluids flowing through horizontal, inclined and nearly vertical wellbores. The model estimations are in good agreement with the measurements obtained from the experiments. Using the model, minimum liquid and gas flow rates are identified for having an acceptable cuttings concentration inside the wellbore as well as a preferably low frictional pressure drop. Thus, the information obtained from this study is applicable to any underbalanced drilling operation conducted with gas-liquid mixtures, for optimization of flow rates for liquid and gas phases in order to transport the cuttings in the horizontal sections in an effective way with a reasonably low frictional pressure loss.

CHAPTER II

LITERATURE REVIEW

There are some studies related to performance of gasified drilling fluid in cutting transport and its mechanisms in the literature. It is required to consider and to understand the studies which related to prediction of gas-liquid mixture fluid hydraulics behaviors and to determination of cutting transport mechanism of drilling fluid in horizontal and inclined wells before pointing out three phase flow studies. In the following pages, the literature review is divided into different sub-sections pertaining to different objectives, which were combined.

2-1 Gas-Liquid Two-Phase Flow in Pipe

Gas-liquid mixture (two phase) fluid mechanics in circular pipes, have been intensively investigated theoretical and experimental studies. Developed models can be divided into two major categories, general models and mechanistic models.

Previous developed models for two-phase fluid flow which named general model were independent from flow pattern description. These models considered two-phase fluid flow as single phase flow or a fluid flow consisted of separated two-phase flow. The most important of these models developed by Wallis (1969), Lochart and Martinelli (1949), and Duns and Ros (1963). These models are the starting point of development of two-phase fluid flow modeling.

Wallis (1969) study contained the most complete mechanistic description of the liquid holdup and pressure drop for all flow regimes. He introduced the “Homogeneous No-Slip Flow Model”, by the two phase mixture was treated as a pseudo single-phase fluid with average velocity and physical properties.

On the other hand, Lochart and Martinelli (1949) assumed that gas and liquid phases of two phase mixture flow separately from each other. Thus, in order to

utilize single-phase flow methods such as friction factor concept, each of the phases was analyzed individually. They established four flow mechanisms and suggested transition criteria between these flow mechanisms. Curves were presented for the prediction of pressure drop and the liquid level in the pipe.

Duns and Ros (1963) initiated “Dimensional Analysis” which was a technique to develop universal solutions by using experimental data. In this technique, governing dimensionless groups were generated in order to control a given flow system. Although application of dimensional analysis to various single-phase flow problems has been illustrated acceptable results, because of the large number of variables involved, it could not be applied straightforwardly in two-phase flow.

The studies were focused on the determination of the flow pattern named mechanistic models. For each flow pattern, the fluid mechanics of two phase flow systems are independently examined and main flow equations were obtained. In order to understand flow properties of two phase fluid systems exactly, comprehensive and unified models were developed. The main concern in mechanistic modeling is determination of the flow patterns properly. For the main flow conditions (liquid and gas flow rate, fluid properties, suitable pressure and temperature, pipe diameter, etc.), many studies were made with the aim of estimating the flow patterns of two-phase fluids in pipes. Beggs and Brill (1973), Mandhane et al. (1974), Taitel and Dukler (1976) and Barnea (1987) studies are the most important experiments in this issue. An extensive study was prepared in two-phase flow in circular pipes in an entire range of inclination angles by Beggs and Brill (1973). Firstly, they developed correlations to predict the existing flow pattern by using Froude number and no-slip holdup. Then, they suggested model to estimate the actual holdup and to determine the pressure loss for each flow pattern separately by developing a new friction factor for two phase flow.

Transition boundaries between the flow patterns were investigated based on conservation equations by Taitel and Dukler (1976). In this study, equilibrium condition for stratified flow was assumed. After that, the Lockhart and Martinelli

parameter was used in order to determine equilibrium liquid holdup. The Kelvin-Helmholtz in viscid theory was modified in order to predict the initiation of slugs. The transition of intermittent to annular flow is assumed to be dependent only on liquid level. Jeffrey's theory for wave initiation is used to determine the transition of stratified smooth to stratified wavy flow pattern. They investigated turbulent and buoyant forces acting on a gas pocket for the boundary between dispersed bubble flow and intermittent flow. Dimensionless parameters were also developed to express the transition conditions. The experiments in small diameter pipes under low-pressure conditions were conducted in order to verify developed model for Newtonian fluid flow.

Azbel (1981) has conducted extensive experiments involving flow, mass bubbling, and mass transfer during bubbling and in a liquid-solid system, and the calculation of bubbling reactors for the two-phase oxidation reaction. The behavior of bubbles-gas dispersion into a liquid, liquid entrainment from a gas-liquid dispersion, solid dispersion into a liquid, and mass transfer systems were investigated in his book. Azbel proposed equations for bubble motion, bubble size, bubble-size distribution, and pressure drop across a perforated plate. He studied the problem of steady and no uniform motion of solid particles in liquid and investigated the effect of system walls on particle velocities in a dilute suspension as well as obtained basic equation for the motion of micro- and macro-solid particles suspended in a turbulent flow.

Barnea (1987) studied the transition mechanisms for each individual boundary and proposed a unified model. The developed mechanisms were applicable for the whole range of pipe inclinations. The dimensionless maps were developed to incorporate the effects of flow rates, fluid properties, and pipe size and inclination angle. This model was verified with the conducted experiments.

Xiao et al (1990) developed a comprehensive mechanistic model for two-phase flow in horizontal and near horizontal pipes. Taitel and Dueller's (1976), and Barnea et al's (1987) dimensionless groups were used to predict flow pattern transitions. The models proposed by Baker et al (1998) and Andritsos and

Hanratty (1987) were applied for calculating interfacial friction factor in stratified flow, i.e. Also the effect of pipe roughness was taken into consideration during friction factor calculations. They suggested empirical correlations in order to predict the slug length and liquid holdup of the slug body and treated annular flow as stratified flow with different geometrical configuration. Liquid entrainment fraction (Oliemans et al (1986).) was also considered while calculating the liquid holdup in the gas core.

Ansari et al (1994) proposed a comprehensive model to predict the flow behavior for upward two-phase flow. This model is composed of a model for flow-pattern prediction and a set of independent mechanistic models for predicting such flow characteristics as holdup and pressure drop in bubble, slug, and annular flow. The comprehensive model was evaluated by using a well data bank made up of 1,712 well cases covering a wide variety of field data. Model performance was also compared with six commonly used empirical correlations and the Hasan-Kabir mechanistic model. Overall model performance is in good agreement with the data. In comparison with other methods, the comprehensive model performed the best.

Gomez et al (2000) developed a unified mechanistic model for horizontal to vertical upward flow of two-phase fluid systems. Unified transition flow pattern prediction model and unified individual models for each flow type were presented. Moreover, the proposed model implemented new criteria in order to eliminate the discontinuity problems. The model of Taitel and Dukler (1976), and Barnea et al (1987) were inherited to predict flow mechanisms in the flow pattern boundaries.

Petalas and Aziz (2000) proposed a mechanistic model applicable to a wide range of pipe geometries and fluid properties. Empirical correlations were developed for interfacial friction in stratified and annular-mist flows, for liquid entrainment fraction and distribution coefficient in intermittent flow. A large amount of experimental and field data were collected in order to develop these empirical correlations. The transition mechanisms between the flow patterns were presented in a similar way to Taitel and Dukler's (1976), and Barnea et al's (1987) models.

Garcia et al (2003) studied a large amount of two-phase flow data and developed composite analytical expressions for friction factor covering both laminar and turbulent flow regimes. Two different approaches were presented. The first method is the universal composite correlation for friction factor estimation regardless of the flow pattern. The second method represents the friction factor correlations for a given flow pattern. This Fanning friction factor definition was based on the mixture velocity and density.

J. Oriol et al. (2008) proposed a new method for the characterization of two phase flows in horizontal and vertical tubes by using a non-intrusive optical sensor associated to a liquid phase tracer experiment. The difference between refractive index of the two phases allows estimating the void fraction on the section illuminated by the optical sensor and permits to characterize two-phase flow regime from the signal characteristics. Signal analysis and treatment of the absorbance variation due to the colored tracer injected in the liquid phase permit to estimate the real liquid phase averaged velocity and consequently the real gas phase average velocity. They also calculated volumetric void fraction and compared it to usual correlations with a good agreement. Finally, the evolution of the experimental liquid phase Peclet number with the two-phase flow regime has been observed and qualitatively explained.

M. Bonizzi et al. (2009) developed model based on multi-field model (Ishii, 1975; Chan and Banerjee, 1980 and many others) to predict the development of flow regimes and various flow parameters without the need for maps, or the need to change closure relationships. To accomplish this, the model includes four fields, i.e. continuous and dispersed liquid, continuous and dispersed gas, as well as a set of appropriate closure relationships from the literature. The results indicate that the development of certain flow regimes, including transitions from bubbly to stratified flow and vice versa, slug flow including slug frequency and length, and the evolution of these parameters along a pipeline are well predicted by the model when compared to experimental data.

2-2 Gas-Liquid Two-Phase Flow in Annuli

There are a lot of works regarding two-phase fluids in circular pipes, however, limited researches are conducted for annular two-phase flow; Aziz et al. (1972), Beggs and Brill (1973), Sadatomi (1982), Caetano (1992) and Kabir (1988,1992). Very limited numbers of works are encountered in horizontal annular environments. Sunthakar (2002), modified Taitel and Dukler (1976)'s suggested transition equations between flow patterns to the annular geometry by using the definition of hydraulic diameter and also compared the results by conducting experiments. Later, Zhou (2004) suggested a similar approach like Sunthakar (2002)'s approach, and changed the model in order to use it at high pressure and temperature.

Moreover, experiments were performed under conditions of high temperature and pressure. Both of these two studies, significant differences were observed between pressure losses observed from experiments and pressure losses calculated theoretically based on friction. Lage et al. (2000) experimentally and theoretically worked on two-phase fluid mechanics in the horizontal and inclined eccentric annular. In order to determine flow patterns, equations from Taitel and Dukler (1976)'s study were used. Theoretically calculated pressure losses were compared with the experimental data and Aziz et al. (1972)'s model and Beggs and Brill (1973)'s model and developed model gave more successful results.

Sadatomi et al. (1982) were most probably the first one to develop the flow pattern maps for the flow through annuli. In this study, flow pattern maps were developed for vertical air-water mixture through various noncircular conduits including concentric annuli. In order to detect transition criteria between flow patterns, slug interval were determined by considering the slug frequency and the gas phase velocity. From these flow pattern maps, they concluded that the channel geometry has very little effect on the flow pattern transitions.

Barnea (1987) presented models for predicting flow-pattern transitions in steady gas-liquid flow in pipes. The effect of fluid properties, pipe size and the angle

of inclination were incorporated in these models in a unified for various range of pipe inclinations. He presented transition mechanisms for each individual boundary and suggested a logical path for systematic determination of the flow patterns. Although the Barnea (1987) unified model gives a good prediction for the transition from slug to dispersed bubble flow at low flow rates, but it shows an incorrect trend at high gas flow rates. The reason is that the model is based on the Hinze (1955) correlation which is valid for small gas fractions, and the gas fraction is not related to the required turbulent energy for dispersion.

Kelessidis and Dukler (1989, 1990) studied the factors affecting the flow pattern transition in vertical concentric and eccentric annuli. “Probability Density Function” (PDF) was used to identify the flow patterns and transition boundaries for both the concentric and eccentric annulus. Mathematical models for flow pattern prediction were developed based on the ideas presented by Taitel et al. (1980) by considering different factors affecting the flow pattern transition such as gas, liquid flow rates, void fraction etc;. They found out that the degree of eccentricity has a minor effect on the flow pattern transition.

Hasan and Kabir (1988) conducted experimental work using air-water system to develop a hydrodynamic model for estimating gas void fraction in bubbly and slug flow regimes. They concluded that the gas void fraction in a circular channel is similar to that of an annular channel, especially for a small ratio of casing-tubing diameters. In a later study, Hasan and Kabir (1992) recognized four major flow regimes-bubbly, slug, churn and annular from the estimated void fraction for air-water systems. In case of bubbly flow, they found out that the terminal rise velocity was not affected significantly by either the variation in the inner tube diameter or the channel deviation from the vertical. Similarly, in this regime they concluded that the void fraction was not affected by inclination angle.

Caetano et al. (1992a, b) carried out experimental and theoretical study of upward gas-liquid flow through vertical concentric and eccentric annuli with air-water and air-kerosene mixtures. They identified flow patterns and developed flow pattern maps based on visual observations in conducted experiments. Moreover, they

developed mechanistic models for prediction of average liquid holdup and pressure drop for each flow pattern in concentric and eccentric annular geometries. Their developed mechanistic models for each of the existing flow patterns in an annulus were based on the two-phase flow physical phenomenon and incorporated annulus characteristics like casing and tubing diameters and degree of eccentricity. The effect of fluid properties was observed as a result of the comparison of the developed flow pattern maps for water-air and kerosene-air mixtures. Experiments were conducted in a small scale experimental setup.

The effect of flow obstruction geometry on the flow pattern transition, pressure drop and void distribution was investigated in horizontal two-phase flow by Salcudean et al. (1983a, b). In this study, annular geometry was assumed as a central obstruction. They found out that, annular geometry significantly affected the stratified wavy-intermittent flow and stratified smooth stratified wavy flow transitions. So it was necessary to develop an individual model for two-phase flow through annular conduit. Additionally, they emphasized that the developed models for flow pattern prediction in pipe flow should not applied accurately accurate results in annuli.

Das et al. (1999a, b) have reported experimental and theoretical work related with vertical flow in concentric annuli. They used probability density function to identify the flow patterns and define flow pattern boundaries. Based on the experimental work, they developed models for flow transition boundaries as functions of annular dimensions, physical properties and velocities of both the phases.

Sunthakar (2000) carried out experimental study of the flow of air-water and air-non-Newtonian mud through horizontal and inclined annuli (8" X 4.5", approximately 90 ft long). Experiments for horizontal, inclined upward (45°) and inclined nearly vertical (15°) flow without and with inner drill pipe rotation were conducted. In this study, the model developed by Taitel and Dukler (1976) for flow pattern prediction for horizontal and near horizontal flow in pipes was modified for flow in annuli by incorporating annular geometry, inner pipe rotation and

eccentricity of the inner drill pipe. This modified model was implemented in a computational tool to predict pressure drop in annulus for given flow conditions and inclination angle. The performance of the proposed model was evaluated with the experimental data. It was concluded that the intermittent flow was different than that was defined for pipe flow, i.e., the Taylor bubble was distorted and the liquid slug was highly aerated. The developed flow pattern maps showed shifts when compared with the flow pattern transition boundaries of pipe flow.

Lage et al (2000) formulated a mechanistic model to predict the flow behavior of two-phase mixtures in horizontal or slightly inclined fully eccentric annuli. The model was composed of a procedure for flow pattern prediction and a set of independent models for calculating gas fraction and pressure drop in stratified, intermittent, dispersed bubble, and annular flow. Small-scale experimental data performed in a 50 m long straight 4" (101.6 mm) ID pipe containing a 2" (50.8 mm) OD tube lying at the bottom validate the predictions of the model. The results showed good agreement even though the number of data points did not permit the development of a complete and precise flow pattern map. The model performance was also compared with Beggs and Brill (1973) correlation and modified Aziz et al (1972) method. It was concluded that proposed model had better performance.

Lage et al (2000) proposed a mechanistic model to predict the mixture behavior for upward two-phase flow in concentric annulus. The model was composed of a procedure for flow pattern prediction and a set of independent mechanistic models for calculating gas fraction and pressure drop in bubble, dispersed bubble, slug and annular flow. In addition, some aspects of churn flow such as the slug/churn transition and the predictions of pressure drop were discussed. A comprehensive experimental program was also launched to collect data. The model was validated against the acquired database and shows a good performance for pressure drop prediction.

Güçüyener (2003) developed a multiphase hydrodynamic model for flow pattern identification and pressure loss determination through drill string and annulus in vertical and moderately deviated directional wells. The carrying capacity of the

aerated drilling fluid was evaluated by using two-phase flow properties and a cuttings transport model. Moreover, a computer program was developed for the prediction of flow patterns, circulating pressures, optimum two-phase flow requirements, bit hydraulics and hole cleaning. It was concluded that dispersed bubble flow did not develop in the drill string and the annulus, and that the multiphase models calculated lower bottom hole pressures compared to dispersed model.

Zhou (2004) studied cuttings transport with aerated mud in horizontal annulus under high pressures and temperatures. The two-phase flow patterns were identified by visual observations through the view port. Taitel and Dukler (1976)'s model was modified for annular two-phase flow like Sunthakar (2002)'s approach. A mechanistic model was developed to predict the volumetric cuttings concentration in the annuli and the critical pressure gradient for preventing cuttings from deposition based on conservation equations and existing two-phase pipe flow correlations. The developed model has been verified by conducted experiments. It was concluded that liquid flow rate, gas liquid ratio and temperature essentially affected the cuttings transport efficiency. Comparisons between predictions and measurements for aerated mud flow showed an average error of 12.2%.

D.J. Rodriguez, and T.A. Shedd (2004) used a backlit digital imaging technique to obtain images of bubbles within the liquid film of adiabatic air–water horizontal annular flow. In this study, a digital image processing algorithm that isolated bubble contours from other flow features was implemented. They concluded that the bubble size distribution within the liquid film was exponential, and the parameters of the distribution were observed to be dependent on air flow rate and essentially independent of liquid flow rate. The bubble data, together with fluorescent imaging of waves on the liquid film, indicated that gas entrainment in the film was primarily controlled by air flow rate and wave behavior.

Ozbayoğlu and Omurlu (2007) were formed a mechanistic model to determine the flow patterns and to calculate the pressure losses based on friction with gas-liquid mixture fluid in horizontally located annular. In addition, they performed

the experiments using air and water, experimental results and model results were compared, and matching between the model results and the experimental results was obtained in case of identification of annular with "effective diameter".

As a result of work, some differences between flow patterns within well and the flow patterns occurred in circular pipes are determined, and it is established that image processing techniques can be used successfully to detection accurately of gas-liquid volumes.

Gomez et al (2000) developed a unified steady-state two-phase flow mechanistic model for the prediction of flow pattern, liquid holdup and pressure drop that is applicable to the all range of inclination angles. It consisted of a unified flow pattern prediction model and unified individual models for stratified, slug, bubble, annular and dispersed bubble flow. New criteria for eliminating discontinuity problems, providing smooth transitions between the different flow patterns were implemented in this model. They incorporated both mixture velocity and inclination angle into an empirical correlation for the slug liquid holdup. However, parameters like surface tension and gas-liquid density difference were not considered in their correlation, and the model cannot be used for downward flow. The new model has been initially validated against existing, various, elaborated, laboratory and field databases. It was observed that the proposed model provided an accurate two-phase flow mechanistic model for research and design for the industry.

Oddie et al (2003) conducted Steady-state and transient experiments of water-gas, oil-water and oil-water-gas multiphase flows on a transparent 11 m long, 15 cm diameter, inclinable pipe using kerosene, tap water and nitrogen. The pipe inclination was varied from 0° (vertical) to 92° and the flow rates of each phase were varied over wide ranges. Extensive results for holdup as a function of flow rates, flow pattern and pipe inclinations are reported and the various techniques for measuring holdup are compared and discussed. The flow pattern and shut-in holdup are also compared with the predictions of a mechanistic model. Results show close agreement between observed and predicted flow pattern, and a reasonable level of agreement in holdup.

Abduvayt et al (2003) investigated the effects of pressure and pipe diameter on gas-liquid two-phase flow behaviors experimentally and theoretically for horizontal and slightly inclined pipelines. Based on analysis of the experimental observations, a flow pattern map was developed for each pressure, pipe diameter, and inclination. In the large-diameter-pipe experiments, stratified flow was observed at higher superficial liquid velocities than in small diameter. The average pressure did not show large influences on liquid holdup and pressure drop. Based on the experimental data, a mechanistic model was developed incorporating transition criteria for eight flow patterns, and individual flow models for estimating liquid holdup and pressure drop. The results predicted by the individual models demonstrated excellent agreements with the experimental data for each pressure and each inclination angle.

Zhang et al. (2003) developed a unified mechanistic model for slug liquid holdup based on a balance between the turbulent kinetic energy of the liquid phase and the surface free energy of dispersed spherical gas bubbles in pipe. The model has been verified by using experimental data acquired at TUFFP for slug flows at all inclinations. The model can also be used to predict the slug–dispersed bubble flow pattern transition boundary over the whole range of inclination angles. From comparison with previous experimental results, the model predictions are accurate for gas superficial velocities larger than 0.1 m/s.

Scott et al. (1989) studied slug characteristics for large-diameter pipes with data collected from flow lines in the Prudhoe Bay field in Alaska. A lot of data were collected and a data base was constructed. Based on observed data, slug characteristics were named as slug length, bubble length, and holdups. Data analysis revealed that the liquid slugs do not maintain a constant length and that the slugs tend to grow as they flow through the pipeline. An existing slug-length correlation was modified with these new data, and a term was added to account for the observed slug growth.

Evren M. Ozbayoglu, and Murat A. Ozbayoglu,(2007) presented experimental study which approached to estimate the flow pattern and frictional

pressure losses of two-phase fluids flowing through horizontal annular geometries using Artificial Neural Networks (ANN) rather than proposing a mechanistic model. In this study, flow was characterized using superficial Reynolds numbers for both liquid and gas phase for simplicity. The results showed that ANN could estimate flow patterns with a high accuracy (error is less than $\pm 5\%$), and frictional pressure losses with an error less than $\pm 30\%$.

D. Schubring, and T.A. Shedd(2008) measured non-intrusive pressure drop, liquid base film thickness distribution, and wave behavior for 206 horizontal annular two-phase (air–water) flow conditions in 8.8, 15.1, and 26.3 mm ID tubes. They collected a large bank of data from the fully annular regime in horizontal flow. Empirical correlations for wave velocity and wave frequency were presented.

Bolsover, (2007) developed mathematical model of the flow and cutting transport which consider the effects of drill string rotation and eccentricity. In this report, they considered only the rotational flow, not the axial flow.

J. Enrique et al, (2009) have investigated the axial development of flow regime of adiabatic upward air-water two-phase flow in a vertical annulus experimentally. The flow regime has been classified into four categories: bubbly, cap-slug, churn, and annular flows. In order to study the axial development of flow regime, area-averaged void fraction measurements have been performed using impedance void meters. The axial development of flow regime is quantified using the superficial gas velocity and void fraction values where the flow regime transition takes place. The predictions of the models are compared for each flow regime transition. In the current test conditions, the axial development of flow regime occurs in the bubbly to cap-slug (low superficial liquid velocities) and cap-slug to churn (high superficial liquid velocities) flow regime transition zones.

A. Cioncolini et al (2009) considered algebraic turbulence modeling in adiabatic gas–liquid annular two-phase flow. After reviewing the existing literature, two new algebraic turbulence models were proposed for both the liquid film and the droplet laden gas core of annular two-phase flow. Both turbulence models were

calibrated with experimental data taken from the open literature and their performance critically assessed. Although the proposed turbulence models reproduce the key parameters of annular flow well (average liquid film thickness and pressure gradient) and the predicted velocity profiles for the core flow compared favorably with available core flow velocity measurements, a more accurate experimental database is required to further improve the models accuracy and range of applicability.

H. Andersen et al (2009) presented a new technique to evaluate the impact of aerated mud hydraulic design on the drilling rate. In this study, classical theory of hydraulic optimization (i.e., maximum bit hydraulic horsepower/ jet impact force criteria) has been re-visited for possible modification and application in hydraulic optimization of aerated mud drilling. As for incompressible fluids, it was found that the parasitic pressure losses for aerated drilling fluids can be treated as a power law function of the total (gas + liquid) fluid flow rate. A new methodology has been suggested to determine optimum gas/liquid injection rates for maximizing drilling rate when drilling with aerated mud.

Yu et al (2009) developed a mechanistic model to predict flow patterns, pressure gradient and liquid holdup for gas-liquid flow in upward vertical annuli. The flow pattern transition model consists of modified Zhang et al. (2003a) unified model for dispersed bubble flow and annular flow pattern transitions, Caetano (1986) model for bubbly flow transition and modified Kaya et al. (2001) model for slug to churn flow transition. The hydrodynamic models are developed based on the dynamics of slug flow and the film zone is used as the control volume. The two liquid films are taken into account in the annulus slug flow and annular flow model developments. The churn flow model is developed based on the Zhang et al. unified model for pipe flow by using a much shorter slug length.

Hasan et al. (2007) presented a simplified two-phase flow model using the drift-flux approach to well orientation, geometry, and fluids. For estimating the static head, the model uses a single expression for liquid holdup, with flow-pattern-dependent values for flow parameter and rise velocity. The gradual change in the

parameter values near transition boundaries avoids discontinuity in the estimated gradients, unlike most available methods. Frictional and kinetic heads were estimated using the simple homogeneous modeling approach.

2-3 Flow in Eccentric Annuli and Conformal Mapping

W. Snyder and G. A. Goldstein (1965) presented an analysis of fully developed laminar flow in an eccentric annulus. An exact solution for the velocity distribution was presented. From this solution were obtained expressions for local shear stress on the inner and outer surfaces of the annulus, friction factors based on the inner and outer surfaces, and the overall friction factor. Curves of these data were presented covering a range of eccentricity values and radius ratio values.

Iyoho and Azar (1981) represented an approximate slot flow model for the flow of non-Newtonian fluids through an eccentric annulus and determined the velocity profile.

Ozgen and Tosun, (1987) presented a new approach in extrapolating the experimental data for laminar and turbulent flows in eccentric annuli by the use of an inversion technique. The geometric inversion transforms the eccentric annulus system to the symmetrical case, that is, the concentric system. This transformation is both involutory and isogonal. In this way, a rather complicated problem in bipolar coordinates can be solved easily in cylindrical coordinates.

Tosun,(1987) extended the method of Iyoho and Azar (1981) to calculate the approximate volumetric flow rate through an eccentric annulus as functions of eccentricity ratio and radius ratio. The results were shown to be in agreement with the exact values. An exact analytical expression for the volumetric flow rate was also presented.

Uner, et al. (1988) proposed an approximate solution to predict the relationship between volume rate of flow and pressure drop for steady-state laminar flow of non-Newtonian fluids in an eccentric annulus is described. An eccentric annulus was modeled as a slit of variable height, and the equations of continuity and

motion were solved for the power-law, Bingham-plastic, and Sutterby models. The results compare reasonably well with the previously published theoretical and experimental data for radius ratio greater than 0.5.

Matunobu, (1988) derived Pressure-flow relationships for the steady flow through an eccentric double circular tube whose cross section takes the form of an annulus bounded by two circles which are in general not concentric. In this study, the velocity distribution was obtained by solving a two-dimensional Poisson equation with the use of conformal mapping.

Haige and Yinao (1998) proposed the axial flow velocity distribution, the annular average velocity, the volumetric flow rate and the frictional pressure drop of non Newtonian fluid flow through eccentric by using the RS fluid rheological equation and the geometrical relationship of eccentric annular clearance with other parameters. Results show that the main difference between concentric annular flow and eccentric annular flow lies in that the velocity profile is substantially altered in the annulus when the inner pipe is no longer concentric and the velocity in the reduced region of eccentric annular is much smaller than that of the increased region.

Videnic and Kosel, (2004) presented an analytical solution of a shrink-fit problem between an eccentric and a centric circular annulus in the elastic domain. The problem was solved using complex variable functions, where conformal mapping of the centric circular annulus to the eccentric one can be used.

Park and Eom (2005) investigated an electrostatic potential penetration into an eccentric annular aperture in a thick conducting plane when an inner conductor is electrically floating. Conformal mapping was used to transform an eccentric annular aperture into a concentric aperture.

Feng, et al. (2007) performed numerical calculations to analyze the influence of the orbital motion of an inner cylinder on annular flow and the forces exerted by the fluid on the inner cylinder when it is rotating eccentrically.

Chen, et al. (2009) obtained the analytical solution for Laplace problem easily, by way of mapping in the complex plane by using transformation in a transformed plane in the complex variable theory. They focus on the connection between conformal mapping and curvilinear coordinates, and figure out the relation to take integration.

2-4 Cuttings Transport

Studies on cuttings transport have been in progress during the past 70 years. These studies can be separated into two basic approaches: i) empirical and ii) theoretical. Initially, terminal velocity determination was investigated for single-phase drilling fluids. In vertical wells, terminal velocity was enough to address most of the problems. As interest in directional and horizontal wells increased, studies were shifted to experimental approaches and mechanistic models trying to explain the cuttings transport phenomenon for all inclination angles. Later, underbalanced drilling became more important as an essential tool and the interest expanded to include cuttings transport with multi-phase fluids for inclined and horizontal wells.

2-4-1 Solid Transport with Drilling Fluid Flow in Pipes

Charles (1970) categorized solids transported in the form of capsules, settling slurries and non-settling slurries, and described the distinctions among homogenous suspensions, heterogeneous suspensions, sliding bed and stationary bed structures. He concluded that for short distances, settling slurries are more economic than the other forms, while for long distances, solids need to be transported in a non-settling form.

Wilson (1974) developed a mechanistic two-layer model consisting of a stationary solids bed and a suspension layer. The model results were verified with experimental data for a Newtonian fluid.

Wilson (1976-1987) introduced a bed-slip model that can determine the minimum fluid rate required for preventing a stationary solids bed. The model

equations were solved for an equilibrium point at which the bed just starts moving. Model results were compared with experimental data.

Televantos, et al. (1979) experimentally verified Wilson's (1974) two-layer model. They also determined in-situ concentrations and particle velocities.

Thondavadi and Lemlich (1985) studied the effect of solid particles in foams on pressure drop on horizontal pipes. They observed that up to 35% by weight of cuttings have no effect on pressure drop.

Doron, et al. (1987) developed a two-layer model that consists of a solids bed (either stationary or moving) and a suspension layer by using basic conservation principles. The model can be used for cases with a stationary bed, a moving bed and fully-suspended solids. They verified the model with experimental data.

Doron and Barnea (1993) improved their two-layer model by adding a third layer. The improved model assumes that there is a stationary bed, a moving bed and a heterogeneous layer. They verified the model with experimental data.

King, et al. (2000) experimentally analyzed the transport of solids with different multiphase fluids; i.e., water, oil, and CMC solutions, and a water-oil-air mixture. The experiments showed that in slug flow, water and oil are able to transport solids uphill, whereas neither high viscosity solution is able to transport the solids. They also observed that an increase in water fraction causes an increase in the mobility of the solids.

Datta et al. (2005) conducted an extensive laboratory study in order to develop a simple model for pressure drop calculation in pneumatic conveying based on classical Darcy's equation with some modifications. The predicted pressure values matched well with the test data. This article has tried to look at the possibility of a unified approach for two-phase flow.

Danielson et al. (2007) developed firstly a correlation for liquid-solid transport in pipe, based on data taken in the SINTEF STRONG JIP. Then they

presented a critical velocity correlation based on solid and fluid properties, and pipe diameter. Correlations were verified with experimental data and good fit to the data was obtained.

2-4-2 Solid-Liquid Two-Phase Flow in Wellbores

Tomren (1979) conducted an experimental study on cuttings transport in inclined wellbores. He included a radial component to the terminal settling velocity. He categorized the inclinations into three major groups; 0° - 30° , 30° - 50° and 50° - 90° . He observed that around 40° hole cleaning is the most difficult due to a sliding bed. He claims that cuttings transport velocities are constant even when the flow rates are changed because of the change in cross-sectional area of the fluid, which is one of the possible ways to explain the interfacial shear stress between the layers. Finally, he suggests that the focus in an inclined wellbore should be on in-situ cuttings concentration, not on the terminal velocity.

Iyoho (1980) studied the effects of flow rate, flow regime, eccentricity, rate of penetration and inclination on cuttings transport. He introduced a general cuttings transport ratio definition, which can be used for any inclination. Based on observations from experiments, he concludes that although laminar flow is enough to transport cuttings in a vertical well, turbulent flow is required for inclined wellbores.

Okranji (1981) focused on the effect of mud rheology on cuttings transport in directional wells by describing the mud properties in terms of the ratio of yield stress over plastic viscosity. He claims that increasing this ratio improved cuttings transport. He observed that mud rheology has no effect on cuttings transport in the turbulent flow regime. For laminar flow regime, yield stress improves the cuttings transport for low inclinations, and as the inclination increases, the effect of yield stress diminishes. He also observed that the inclinations of 45° - 55° are the hardest to clean.

Hareland (1985) compared oil-based muds and water-based muds. He observed that at low inclinations there is no difference in the performances of the two

muds. However, as the inclination increases, water-based muds show better cuttings transport. He also observed that the ratio of yield stress over plastic viscosity is detrimental to cuttings transport for medium and high inclinations.

Meano(1987) conducted an experimental study on shale cuttings transport in inclined wellbores. He studied the effects of flow rate, inclination, rate of penetration, eccentricity and fluid rheology on in-situ cuttings concentration. He observed a decrease in cuttings concentration with increasing yield stress. Also, an increase in inclination causes an increase in cuttings concentration. He did not measure a significant difference in concentration as rate of penetration was changed.

Becker (1987) developed mathematical models based on the previously conducted experiments. He studied the effect of mud rheology intensively by analyzing yield stress, plastic viscosity, behavior index, and consistency index and gel strengths separately. He observed that turbulent flow improved cuttings transport for highly-inclined wellbores. Also, the effects of fluid rheology dominated at low inclinations.

Bin-Haddah (1988) presented a mechanistic model based on the forces acting on a particle: gravitational force, buoyancy force, drag force and the lift force. He also presents another model derived from a slurry transport model which is valid for laminar and turbulent regimes. He introduces a suspension ratio term to estimate the bed thickness and cuttings concentration.

Brown, et al. (1989) studied cuttings transport with water and HEC-polymer muds. They developed a two-layer model with a stationary bed and a fluid layer, and compared the model results with experiments. Their observations include bed movement as a block or as dunes observed at high flow rates with low viscosity fluids. They also included the effect of eccentricity. They concluded that for low inclinations, HEC-polymer shows better cuttings transport performance, but at higher inclinations, water is more effective. They also noticed that when hole angles are 50°-60°, hole cleaning is the most difficult.

Seeberger, et al. (1989) conducted a study of cuttings transport with oil-based muds that are Power-Law fluids. They observed that bed development is different than when water is used. They reported bed problems at inclination angles between 35°-55°.

Larsen (1990) developed a study on cuttings transport based on critical and sub-critical velocities. He developed correlations as a function of rate of penetration, flow rate, plastic viscosity, yield stress, mud density, inclination and cuttings size. Since the model is based on experimental data, it only works for positive eccentricity and with inclination angles greater than 55°. He concluded that low viscosity muds reach the critical velocity at lower flow rates. He also observes that positive eccentricity has a detrimental effect on cuttings transport. He reported that smaller cuttings are harder to transport.

Stevenik (1990) studied the applicability of Larsen's findings to a large-scale system. He also analyzed the effect of pipe rotation, rate of penetration, eccentricity and fluid rheology on cuttings transport. He observed higher critical velocities than Larsen (1990).

Chin (1990) presented analytical solutions for flow of Power-Law fluids in a concentric annulus with pipe rotation and an eccentric annulus with the presence of a cuttings bed but without pipe rotation. He developed a simulator based on his analytical solutions. Sifferman and Becker (1990) used a statistical approach to analyze the effect of flow rate, mud density, mud rheology, cutting properties, rate of penetration, and pipe rotation and eccentricity on bed thickness. They observed that the bed thickness is not constant along the test section. They also noted that bed build-up is less when the pipe is rotated at high inclination angles with smaller cuttings and low rates of penetration.

Ford, et al. (1990) conducted an experimental study on cuttings transport. They introduced a minimum velocity definition to describe the interfacial shear stress. They observed the following flow patterns: homogenous and heterogeneous

suspensions, suspension and saltation, sand clusters, moving dunes, continuously moving bed and stationary bed.

Zamora and Hanson (1991) presented a list of rules of thumb for cuttings transport. They divide the inclinations into four categories: 0° - 10° , 10° - 30° , 30° - 60° and 60° - 90° . They note that wellbore angles 30° - 60° are the most difficult to clean the well. They also studied the effect of eccentricity, mud rheology and pipe rotation.

Hemphill (1990) studied cuttings transport with oil-based muds. He observed that as rheological properties (plastic viscosity and yield stress) increase, the critical flow rate also increases at high inclination angles.

Martins and Santana (1992) developed a two-layer model with the presence of cuttings in the upper layer. They determine the interfacial stress by using a friction factor definition which includes the effect of cuttings. The model requires simultaneous solution of five equations for five unknowns: bed thickness, average velocities, cuttings concentration in the upper layer and pressure drop. They define four flow patterns: a stationary bed, a moving bed, heterogeneous suspension, and homogenous suspension. They noted a decrease in pressure drop when the flow rate is increased in the presence of a thick bed.

Lou, et al. (1992) developed a mechanistic model addressing the question of minimum required flow rate for preventing bed development in a wellbore based on forces acting on a particle in a cuttings bed. They conducted experiments and observed flow patterns as heterogeneous, dunes and moving bed. They introduce a term called critical wall frictional velocity for determination of the drag and lift forces in terms of four dimensionless groups, which are a function of apparent viscosity, fluid density, cuttings diameter, cuttings density, eccentricity, inclination and frictional velocity. They also define a correction factor for matching data from their small flow loop to a large-scale system.

Hemphill (1992) summarized the work conducted on cuttings transport in horizontal wells. He notes the positive effect of pipe rotation on cuttings transport because of agitation.

Ford, et al. (1993) developed a mechanical model based on the forces acting on a particle. They use a friction factor between the cuttings bed and the wellbore. They also define the drag and lift forces based on the velocity and rheology of the fluid in the vicinity of the particle.

Iyoho and Takahashi (1993) studied modeling of unstable cuttings transport. They described the motion of a dune analytically.

Hemphill and Larsen (1993) compared the carrying capacity of water-based and oil-based muds. They concluded that the Bingham-Plastic Model is not accurate enough to analyze the hole cleaning phenomenon. Thus, the Yield-Power Law model should be used.

Jalukar (1993) studied the effect of hole size on critical and sub-critical velocities. He develops empirical equations for correcting a hole geometry that does not match the model. He observes that for sub-critical flow, there is no effect of hole size on bed thickness.

Azouz (1994) developed a numerical simulator using a finite-difference technique for laminar and turbulent flow in the wellbore. His model can be used in cases where a cuttings bed is present in an eccentric wellbore. In addition, the model permits the use of three rheological models: Bingham Plastic, Power Law and Yield-Power Law. He reports the importance of interfacial shear stress in studying cuttings transport.

Clark and Bickham (1994) developed a mechanistic model based on forces acting on a particle which they claim was developed for the entire well; i.e., from the bit to the surface. They define three modes for cuttings transport: rolling, lifting and settling. However, their model is developed only for pipe flow. Campos⁸⁵ developed two different mechanistic models for describing cuttings transport. The first model

considers average velocities and concentrations in the annulus. The second model, however, focused on cuttings concentration profiles and velocity distributions instead of average values. He used experimental data obtained by other researchers to verify his model.

Bassal (1996) studied the effect of pipe rotation on cuttings transport. Since the pipe was eccentric, he observed that due to orbital motion, cuttings transport improves with pipe rotation.

Sanchez (1997) studied the effect of pipe rotation on bed erosion. He observes that bed erosion is improved with pipe rotation. He notes that pipe rotation also causes irregularities in bed thickness along the test section.

Nguyen and Rahman (1996) developed a three-layer mechanistic model that is similar to the model developed in the present study. Their model consists of three components; a stationary bed, a dispersed layer and a fluid flow layer. Their model works for different modes of transport, ranging from a stationary bed condition to a fully suspended flow. As discussed in this study, determination of the shear stress on the stationary bed is very important. Nguyen and Rahman⁸⁸ describe the interfacial shear stress on the stationary bed in terms of two components: residual fluid shear stress and inter-granular shear stress. They presented the equations of the model for different transport modes. They did not verify their model with experimental data. However, they do present a computer simulator. They conducted a sensitivity analysis for their simulator, and they discussed effects of different variables, i.e., fluid density, fluid viscosity, eccentricity, cuttings density, etc., on the stationary bed.

Gavignet and Sobey (1996) introduced a two-layer model for explaining the cuttings transport phenomenon in an inclined wellbore. Their model consists of a stationary bed and pure fluid flow in the upper layer. They solved a force balance for each layer for pressure drop, and they mention that if the interfacial shear stress is determined, the bed thickness can be expressed as a function of rate of penetration, flow rate, inclination and wellbore geometry. Their model can also estimate the minimum required flow rate to prevent a cuttings bed.

Sanchez (1997) developed a cuttings simulator based on a layered approach emphasizing the importance of the interfacial shear stress. He also studied the effect of mud rheology and eccentricity on bed thickness.

Kamp and Rivero (1999) developed a two-layer mechanistic model that simulates a moving bed below a heterogeneous layer of mud and cuttings. They compared their model results with correlation-based models.

Kuru, et al. (1999) presented a review of foam and aerated drilling fluid technology. The review included an analysis of foam and aerated fluid rheology and flow-pressure loss models. Problems associated with the applications of current models were discussed in this study. They offered suggestions for possible model modifications and needs for future research.

Adari (2000) conducted an experimental study on bed erosion for polymer muds with no pipe rotation. He developed empirical equations to determine the minimum required time to clean the hole. However, his assumption about the mechanism of erosion was not observed during the experiments. Also, his equations are limited to the dimensions of the experimental facility.

Cho, et al. (2000) developed a three-layer model similar to Nguyen and Rahman's model. They developed a simulator and compared the results with existing models as well as the experimental data conducted by other researchers. They developed charts to determine the lowest possible pressure gradient to serve as an operational guide for drilling operations.

Subramanian and Azar (2000) conducted an extensive experimental study on friction pressure drop for non-Newtonian drilling fluids in pipe and annular flow in a fully instrumented 350 feet flow loop, consisting of two pipes and two annular flow test sections with five different muds.

The experimental data obtained were used to generate very useful plots of "friction factor" versus "generalized Reynolds number". For each of the mud systems, the plots offer a practical and accurate means in determining needed friction

factors for the calculation of pressure drops in pipe and annular flow. In addition, in this study, a comparative discussion was presented on measured friction pressure drop data, predicted by correlations such as the power law, Bingham plastic and yield power law. The importance of wall roughness on turbulent flow friction pressure drop calculations was also investigated.

Sapru (2001) studied the effect of pipe rotation on bed erosion for polymer muds. He observed a positive contribution of pipe rotation on bed erosion. He empirically correlated time and bed thickness for a given set of operating conditions.

Ramadan (2001) focused on three transport models, i.e., particle mechanics model which analysis forces acting on a cuttings particle on a bed (he verified the model predictions), layered model (he added the wellbore inclination to the existing layered approach) and convection diffusion model (he discussed turbulent and shear-induced diffusivity coefficients to increase the applicability of the model). He also conducted experiments at a flow loop to verify these different modeling techniques. He concluded that combining all three models, a hole cleaning simulator could be developed to predict critical velocity, transport rate, pressure drop and other related drilling parameters.

Li and Walker (2000) investigated the effects of the different parameters in two different modes: the circulation mode, that involves the development of a cuttings bed or build-up of cuttings in the wellbore, and hole cleaning mode, which is cleaning out an existing cuttings bed. It will be shown that the results indicate: 1) for the tested particle size range (0.150 – 7 mm), cleaning efficiency is partly dependent upon the particle's size, 2) with suitable agitation, a gelled fluid is more effective for cuttings transport than water in a highly deviated wellbore, 3) Pipe eccentricity has an effect on cuttings transport for different fluids and 4) for complete wellbore clean-up it requires many more hole volumes than previous 'rules of thumb' would indicate.

L.J. Leising, and I.C. Walton, (2002) introduced two novel approaches to understanding hole cleaning. First, for laminar flow, the distance that a particle will travel (downstream) before it falls across the annulus clearance is calculated with

Stokes' law and the local viscosity while flowing. This analysis may easily be applied to optimize mud selection and wiper trips. Applying this model to high low-shear-rate-viscosity (LSRV) gels shows that they may perform well inside casing but are expected to do a poor job of hole cleaning in a narrow, open hole, horizontal annulus without rotation. Second, for turbulent flow in horizontal wells, the concept of using annular velocity (AV) as a measure of hole cleaning is shown to be insufficient. A more complete term, annular velocity/root diameter (vARD), is introduced and should be used to compare cuttings transport in turbulent flow in horizontal wells of different cross-sectional areas.

Cho et al. (2002) proposed a new mathematical model to overcome the limitations in existing hydraulic models used to predict cuttings transport in coiled tubing horizontal or deviated well drilling. A new three-segment (a horizontal and near horizontal segment, a vertical and near vertical segment, and a transit segment) hydraulic model under two-phase (solid-liquid) flow in an annulus was developed to predict and interpret cuttings transport mechanisms.

Ramadana et al. (2004) presented a mechanistic model that predicts the critical velocity, which is required to initiate the movement of solid bed particles. The model was developed by considering fluid flow over a stationary bed of solid particles of uniform thickness, resting on an inclined pipe wall. Sets of sand bed critical velocity tests were performed to verify the predictions of the model.

Li et al. (2004) developed a one dimensional transient mechanistic model of cuttings transport with conventional (incompressible) drilling fluids in horizontal wells and solved it numerically to predict cuttings bed height as a function of drilling fluid flow rate and rheological characteristics (n , K), drilling rates, wellbore geometry and drill pipe eccentricity. They did not consider the effect of inner pipe rotation in this model.

Kelessidis et al. (2004) provided a critical review of the state-of-the-art modeling for efficient cuttings transport during Coiled-tubing drilling (CTD) and presented the critical parameters involved. They also proposed a different approach

for predicting the minimum suspension velocity by considering the effect of geometry.

Li et al. (2005) studied the effect of particle density and size on cutting transport. In this study, they presented the results of an experimental study on different density and different diameter particles ranging from 0.15 to 7 mm. From experimental results, it is concluded that particle density and size play a significant role on the solids transport. For a given flow rate, higher density solids result in higher in-situ solids concentrations and lower wiper trip speed (the wiper trip speed is the coiled tubing pull-out-of-hole (POOH) speed) and reduced transport efficiency. Wellbore deviation angle strongly influenced the solids transport for different particle sizes. In a near-vertical wellbore larger particles have the lower transport efficiency while in a horizontal wellbore the medium sized particles have the lowest transport efficiency. Based on experimental data, they developed new correlations in order to predict solids in-situ concentration, solids carrying capacity and optimum wiper trip speed for these tested solids under a given operating condition.

Ozbayoglu et al. (2007) conducted experimental study in order to estimate the critical fluid flow velocity for preventing the development of a stationary bed using empirical correlations that can be used easily at the field. Also, they introduced a rough estimation of bed thickness if the flow velocity is lower than the critical velocity.

Bilgesu et al. (2007) simulated annulus section by using Computational Fluid Dynamics (CFD) to determine the effects of different parameters such as fluid velocity, cutting size, rate of penetration, drill pipe rotation and inclination angle in deviated wells. From this study, it is found out that fluid flow rate, angle of inclination and rate of penetration have a major impact on cutting concentrations and proper prediction of these parameters are important to avoid formation of cutting beds. It is also noted that drill pipe rotation can enhance cutting transport but it generally has a greater effect on smaller sized particles.

Garcia-Hernandez et al. (2007) conducted extensive experiments in order to determine the cuttings lag or slip velocity in horizontal and high-angle borehole configurations with water and an aqueous polymer-based (PAC) drilling fluid. They concluded that the average cuttings lag was nearly 40% of the fluid velocity (i.e., the cuttings traveled at 60% of the fluid velocity). Pipe rotation increased the cuttings velocity even after accounting for the effect of cuttings bed height on the fluid velocity. A change in inclination from 90 deg (horizontal) to 70 deg reduced the slip velocity by 17%. A cuttings lag model was developed from the experimental data.

Yu et al. (2007) conducted experimental research and theoretical analysis to enhance cuttings transport capacity in oil and gas well drilling operations by considering the effects of drilling fluid rheology, mud density, temperature, borehole inclination, pipe rotation, eccentricity, rate of penetration (ROP) and flow rates. They concluded that drill pipe rotation, temperature and rheological parameters of the drilling fluids have significant effects on cuttings transport efficiency. They also developed correlations that can be used for field applications by conducting a dimensional analysis. A user-friendly simulator was developed based on the results of the dimensional analysis and correlations.

Kelessidis et al. (2007) studied phenomena occurring during the flow of dilute solid-liquid mixtures in a horizontal concentric and 100% eccentric annulus in small scale transparent annulus by using Newtonian and non-Newtonian fluid. The flow patterns at various experimental conditions were observed visually by video monitoring equipment and were analyzed to produce flow pattern maps. A method was presented for flow pattern detection using pressure drop measurements and the positive implications for real-life applications.

Li et al. (2007) developed a one-dimensional transient mechanistic model of cuttings transport with conventional (incompressible) drilling fluids in horizontal wells. The model was solved numerically to predict cuttings bed height as a function of drilling fluid flow rate and rheological characteristics (n , K), drilling rates, wellbore geometry and drill pipe eccentricity. The results of the sensitivity analysis showing the effects of various drilling operational parameters on the efficiency of

solids transport were presented. The model developed in this study can be used to develop computer programs for practical design purposes to determine optimum drilling fluid rheology (n , K) and flow rates required for drilling horizontal wells.

Ozbayoglu et al. (2008) investigated the effect of pipe rotation on hole cleaning for horizontal and directional wells. Cuttings transport experiments have been conducted at METU Cuttings Transport Flow Loop using pure water as well as water-based muds consist of different concentrations of xanthan bio-polymer, starch, KCl and soda ash, weighted with barite. Effect of pipe rotation have been observed for hole inclinations from horizontal to 50 degrees, for rate of penetrations from 15 to 45 ft/hr, for flow velocities from 2.1 ft/s to 7.2 ft/s, and for pipe rotations from 0 to 120 rpm. Pressure drop within the test section, and stationary and/or moving bed thickness were recorded besides the other test conditions. It has been observed that, pipe rotation has a significant improvement on cuttings transport, especially if the pipe was making an orbital motion. Also, pipe rotation drastically decreased the critical fluid velocity required to remove the stationary cuttings bed totally. However, after a certain rotation speed, no additional contribution of pipe rotation on hole cleaning was observed.

Duan, et al. (2008) studied the transport behavior of small cuttings in extended-reach drilling. During this study, the effects of cuttings size, drill pipe rotation, fluid rheology, flow rate, and hole inclination were investigated in cutting transport experimentally and theoretically. They concluded that smaller cuttings resulted in a higher cuttings concentration than larger cuttings in a horizontal annulus when tested with water. However, a lower concentration was achieved for smaller cuttings when 0.25-ppb polyanionic cellulose (PAC) solutions were used. Unlike the transport of large cuttings, which is mainly dominated by fluid flow rate, the key factors controlling small cuttings transport were found to be pipe rotation and fluid rheology. Based on experimental results, mathematical modeling was performed to develop correlations for cuttings concentration and bed height in an annulus for field applications. Predictions from a three-layer model previously developed for larger cuttings were also compared with experimental results. Differences (up to 80%)

indicate the need for improving the frequently used three-layer model by including correlations specifically developed for small cuttings to get a better design of extended-reach drilling.

Salazar-Mendoza et al. (2008) presented two-region hydraulic averaging model to analyze the problem of cuttings transport during horizontal well drilling. They applied the volume averaging method to obtain the volume-averaged transport equations for both the moving bed and the porous medium regions in the three main flow patterns of the horizontal cuttings transport process which were: Case 1 - fully suspended flow, Case 2 - flow with a stationary bed and Case 3 - flow with a moving bed. The one-dimensional models for all cases were solved numerically using the finite difference technique with an implicit scheme. The numerical results were compared with experimental data and theoretical results reported in the literature and a good agreement was found.

Scheid et al. (2009) presented an extensive experimental study aiming the evaluation of friction losses resulting from the flow of 4 different drilling fluids in use in deepwater operations through pipe and annular sections, besides accessories such as tool joints, bit jets and stabilizers. After a data analysis process, they collected a set of equations for prediction of relevant hydraulic calculations, such as: hydraulic diameter for annular flows, friction factors for turbulent pipe and annular flows and discharge coefficients for accessories.

Duan, et al. (2009) determined two critical conditions for efficient transport of small solids 1) the critical re-suspension velocity (CRV), the minimum fluid velocity necessary to initiate solids-bed erosion, 2) the critical deposition velocity (CDV), the minimum fluid velocity required to prevent bed formation. In order to determine CRV and CDV for 0.45-mm and 1.4-mm sands, Experiments were conducted in a field-scale flow loop (8×4.5 in., 100 ft long) in different fluids over a range of bed heights and hole inclinations. The results show that, depending on sand size and fluid properties, CDV is approximately two to three times larger than CRV. Water is more effective than low-concentration polymer solutions for bed erosion. However, polymer solutions are more helpful than water in preventing bed

formation. This indicates the need for different drilling fluids for cleanout and drilling operations. A mechanistic model was developed to predict CRV for a solids bed. Both experimental and theoretical results indicate the importance of inter-particle forces that are incorporated into the model. The model accounts for drill pipe eccentricity in any direction in an annulus, which is consistent with experimental observations. The model predictions are in good agreement with experimental results.

Ozbayoglu, et al. (2010) studied the effect of pipe rotation in the frictional pressure losses in horizontal and highly inclined wells in presence of cuttings. Experiments have been conducted on METU Cuttings Transport Flow Loop using pure water as well as numerous water based muds consist of different concentrations of xanthan bio-polymer, starch, KCl and soda ash, weighted with barite for various inclinations, flow rates, rate of penetrations and pipe rotation speeds They concluded that pipe rotation has a significant influence on decreasing critical velocity required to prevent stationary bed development, especially if the pipe is making an orbital motion. However, after a certain pipe rotation speed, no additional contribution of pipe rotation is observed on critical velocity. They also developed empirical correlations based on the experimental data for estimating pressure drop and verified developed correlation by conducted experimental results.

2-4-3 Solid Transport with Two-Phase Flow in Pipes

Barnea et al. (1986) presented a paper in which they investigate the effect of gas injection on the flow of liquid-solid mixtures. They observed that gas injection has two different effects on pressure drop. The first effect is a reduction of pressure drop due to formation of gas voids for a constant total flow rate. The second effect is a pressure drop increase due to acceleration losses associated with slug flow. It was concluded that the addition of gas, combined with an increase in pipe diameter, may be a practical way to reduce the pressure drop for a given slurry flow rate.

Rankin, et al. (1989) studied the effect of inclination on pressure loss and hole cleaning for underbalanced drilling conditions. The effects of cuttings are totally ignored in this study.

Gillies et al. (1997) presented the results of experiments conducted in order to investigate the ability of gas/liquid mixtures to transport sand in a horizontal pipe or well at low velocities. Using a 30-meter-long flow loop, they investigated the effects of gas addition on sand transport in laminar and turbulent liquid flow regimes. One of the main conclusions of the study is that gas injection has little influence on the ability of a laminar flow to transport sand at low superficial velocities. This is due to the fact that gas and the solids travel in different regions of the pipe. They also observed that gas injection increases the solids transport rate and the axial pressure gradient if the liquid flow is turbulent.

Tippetts et al. (1997) presented the results of experiments conducted by using a horizontal flow loop with flowing water, air and sand in pipes. They observed that at low gas and liquid superficial velocities, sand can form a uniform static bed of solids. They also observed that under other conditions a series of individual dunes appears and these migrate by particles being eroded from the upstream end and redeposit at the downstream end. Based on their experiments, they presented a flow pattern map for the solids movements in the pipe as function of the superficial liquid and gas velocities.

Tippetts et al. (1997) presented the results of experiments conducted by using a horizontal flow loop with flowing water, air and sand in pipes. They observed that at low gas and liquid superficial velocities, sand can form a uniform static bed of solids. They also observed that under other conditions a series of individual dunes appears and these migrate by particles being eroded from the upstream end and redeposit at the downstream end. Based on their experiments, they presented a flow pattern map for the solids movements in the pipe as function of the superficial liquid and gas velocities.

Matthew et al. (2000) presented a paper showing results from experiments performed on the BP Amoco 6" multiphase flow facility located at Sunbury, England. They investigated the transport of sand through a pipeline with a dip angle of one degree from horizontal. Several fluids were selected for these experiments to examine the influence of liquid viscosity on the results. Water, oil and two different carboxyl-methyl and cellulose solutions (150 and 300 CP) were used for the experiments. Experiments showed that, in slug flow, water and low viscosity oil were able to transport the solids. They also showed a model for solid transport used by BP Amoco based on the concept of minimum transport velocity, which is sufficient to prevent particles from forming a settled bed. The model was based on the criteria for solid transport with single phase (liquid) that was developed by Thomas (1962). He established a minimum pressure gradient that is required for solid transport.

2-4-4 Solid Transport with Two-Phase Flow in Wellbore

Krug and Mitchell, (1972) developed charts for estimating the required flow rates for foam drilling as a function of rate of penetration, depth and bottom hole pressure. They assumed that foam behaves as a Bingham Plastic. They ignore the effects of solids in their calculations.

Okpobiri and Ikoku,(1982-1983) developed a semi-empirical correlation to determine frictional pressure losses due to the solid phase in foam flow and by using this correlation, they predict the minimum volumetric requirements for foam drilling operations. Experimental results show that the friction factor of foam flow transporting cuttings can be expressed as the sum of friction factor of the foam plus the friction factor of solids. For a constant flow Reynolds number, they observed an increase in friction pressure losses with an increase in solid mass flow rate. They assume that all foam drilling operations are performed in the laminar flow region and that foam qualities vary between 55 % and 96 %. To keep quality between these boundaries, their model indicates a need to apply an annular backpressure. They concluded that volumetric requirements increase with increasing particle size. Also, they observed that an increase in penetration rate causes only minor increases in volumetric requirements.

S. Holte et al. (1987) experimentally investigated the motion of sand particles in horizontal pipelines. These tests were conducted in an experimental facility that was 30 m long and had an inside diameter of 100 mm. He conducted three phase flow experiments using water-air-sand and established gas and liquid limits for the formation of sand beds in pipe. One of the important observations in his study was that shear stress is the prime force to move particles in an upward direction.

Kundu and Peterson (1987) analyzed the performance of solid transportation with foam in pipelines. They conducted experiments and conclude that foam is a promising fluid as a transporting fluid in pipelines. Two of the advantages are reduced water and equipment requirements; however, a significant disadvantage is that pressure losses increase.

Buyon Guo et al. (1993), define the carrying capacity of the aerated mud as the maximum volume of cuttings that can be lifted by it. They calculated the terminal slip velocity using Rittenger's equation for vertical flat particles, where they assumed the drag coefficient to be 0.94.

$$V_{st} = 7.3 \sqrt{\frac{D_c(\rho_c - \rho_{mf})}{\rho_{mf}}}$$

They define the required cuttings transport velocity as follow:

$$V_t = \frac{ROP}{3600 \times C_c}$$

They consider the maximum admissible cuttings concentration (C_c) to be 4% by volume for vertical flow. If mixture velocity is greater than $V_{ts}+V_t$, the aerated mud should be capable of transporting the drilled cuttings to the surface. In this approach they treated the multiphase fluid as a homogeneous mixture of liquid, gas and solid, flowing in the bubbly flow regimen. The slippage between the liquid phase and gas phase and the different flow pattern was not considered. Treating the multiphase mixture as homogeneous is unrealistic, resulting in poor predictions of flow behavior.

Guo, et al. (1994) addressed the question of determination of bottom hole pressure when foam is used as a drilling fluid. They used an equation of state for foam, assumed a cuttings transport velocity around 1.5 ft/sec at the bottom hole and calculated hydrostatic head and frictional losses along the annulus by following an iterative procedure. They assumed foam is a Power-Law fluid. They also compare their proposed model with other models and calculation procedures.

Zhou, et al. (1996) applied multi-phase flow theory to calculate and control injection pressure, flow rate, frictional pressure losses inside the pipe and annulus, and pressure loss at the bit nozzles. They also analyzed rheology of the aerated mud, casing program, gas-liquid ratio, mud density and annulus back-pressure. They concluded that the flow pattern should be bubble-flow and/or slug-flow in the annulus for better cuttings transport.

Wilkes, et al.(1998) studied the design factors for foam and mist drilling. They suggested new procedures and equipment for more efficient drilling. They also compared model results with field information.

Tian, et al. (2000) developed a simulator that allows hydraulic design of underbalanced drilling systems to predict optimum circulating flow rate for any type of fluid. However, the paper provides no information about modeling. Moreover, they claim that foam has a better carrying capacity than any other aerated mud. However, this is valid only for vertical cases and low inclination angles.

Saintpere, et al. (2000) analyzed the hole cleaning with foam in inclined wells using a fluid mechanics approach ignoring the inertial effects. They introduce a few dimensionless parameters for describing the fluid rheology, foam properties, flowing time, etc. They observed the worst hole cleaning performance at angles 40°-60°. They claimed that by extrapolation of the information developed for inclined sections; this will give an idea about the minimum circulation time necessary to remove cuttings.

Vieria, (2000) conducted experiments of cuttings transport with air-water mixtures for horizontal and highly-inclined wellbores. He observed that the cuttings were carried by the liquid phase only. He also mentions that there is a minimum air-water combination required to prevent a stationary bed, which developed at the intermittent boundary of the flow pattern map.

Martins, et al. (2001) experimentally studied effective hole cleaning with foam. They developed empirical equations to predict the bed erosion capacity in horizontal wells as a function of foam quality and Reynolds number.

J.Li and S. Walker (2001) studied the effects of gas-liquid ratio, flow rate, phase slip velocities, rate of penetration, and inclination and fluid properties on cuttings bed thickness for aerated fluids systems. They observed that liquid is the dominating parameter for cuttings transport in aerated systems. As the liquid ratio increases, for a constant in-situ flow rate, cuttings transport improves.

Rodriguez (2001) carried out an experimental study in order to find the minimum air and water flow rates that effectively transport cuttings through highly inclined and horizontal wells. The experiments were carried out in a low pressure field scale flow loop. The model proposed in the study of Sunthankar (2000) was inherited for flow pattern identification and pressure loss determination. The model's results were compared with experimental data. It was concluded that the flow patterns of cuttings are dependent on the total flow rate of the liquid and gas phase. It was also concluded that in order to avoid the formation of a stationary cuttings bed, an approximate boundary of minimum flow rate of each phase can be determined. The minimum requirements for gas and liquid flow rates were found to be always in the intermittent flow regime.

Vieira et al. (2002) studied minimum air and water flow rates required for effective cuttings transport in high angle and horizontal wells. Extensive experiments were performed in a unique field-scale low-pressure flow loop. The effects of gas and liquid flow rates, drilling rate, inclination angle, pressure drop and flow patterns on cuttings transport were analyzed in this study. It was observed in the experiments,

for the range of volumetric flow rates used during these tests, that cuttings are only transported by the liquid phase. It was also found that it is possible to define a boundary for the minimum air and water velocities required to avoid the formation of a stationary cuttings bed. These minimum requirements exist in the intermittent flow region for the gas and liquid interface distribution. It was observed that the minimum requirements for air and water injection rates are also a function of the solids injection rate. It is postulated in this study that there is a minimum energy required for solids transport, and this is constant for a given solids injection rate. It was observed that the inclination effect for angles close to horizontal is negligible.

Doan, et al. (2003) presented the model in order to understand the mechanisms involved in the transport of cuttings in UBD. The model simulated the transport of drill cuttings in an annulus of arbitrary eccentricity and includes a wide range of transport phenomena, including cuttings deposition and re-suspension, formation, and movement of cuttings bed. The model consists of conservation equations for the fluid and cuttings components in the suspension and the cuttings deposit bed. Interaction between the suspension and the cuttings deposit bed, and between the fluid and cuttings components in the suspension, are incorporated. Solution of the model determines the distribution of fluid and cuttings concentration, velocity, fluid pressure, and velocity profile of cuttings deposit bed at different times. The model was used to determine the critical transport velocity for different hydrodynamic conditions. But, the effect of drill pipe rotation was not considered in their model. Results from the model approved quite closely, qualitatively, with experimental data obtained from a cuttings transport flow loop at the Technology Research Center of the Japan Natl. Oil Corp. (TRC/JNOC)'s Kashiwazaki Test Field in Japan.

Yu, et al. (2004) proposed technology which work to counteract the gravitational force while simultaneously increasing the drag force by attaching gas bubbles to drilled cutting particles with chemical surfactants. The gas bubbles will pull the cuttings upward because of their buoyancy in the drilling mud thereby counteracting the gravity force. They conducted laboratory experiments to determine

the effects of chemical surfactants, pH, and cutting particle size on the attachment of air bubbles to cutting particles. Two types of chemical surfactants, one to attach air bubbles to cutting particles and another to strengthen the air bubble, were necessary for attachment to occur.

Zhou et al. (2004) carried out experiments in a unique full-scale flow loop in different liquid and gas flow rates as well as elevated temperatures. The in-situ cuttings concentration (i.e. volumetric concentration) was determined by using a special designed multiphase measurement system. The results clearly show that in addition to liquid flow rate and gas-liquid ratio (i.e. injection gas volume fraction calculated at test temperature and pressure), temperature essentially affects the cuttings transport efficiency and the associated frictional pressure drop. The volume of cuttings which accumulated in the annulus was very sensitive to the liquid flow rate. Also in this study; a mechanistic model for cuttings transport with aerated fluids under EPET conditions has been developed to predict frictional pressure loss and cuttings concentration in the annulus. The model is based on mass and momentum conservation equations and wall equations.

Zhou et al. (2005) presented a mechanistic model for underbalanced drilling with aerated muds. The hydraulic model determines the flow pattern and predicts frictional pressure losses in a horizontal concentric annulus. The influences of gas liquid ratio (GLR) and other flow parameters on the frictional pressure loss are analyzed using this model. Also in this study, extensive experiments in a unique field-scale high pressure and high temperature flow loop were performed to verify the predictions of the model. Comparisons between the model predictions and experimental measurements show a satisfactory agreement. The present model is useful for the design of underbalanced drilling applications.

Lourenco et al. (2006) presented the analysis of the results from two sets of experimental tests performed at PETROBRAS real scale test facility aiming the evaluation of solids return times in aerated fluid drilling by considering the effect of liquid and gas injection rates, particle diameter, liquid phase viscosity and annular back pressure on the transport capacity of solids in a vertical well with aerated water

and polymer-based drilling fluids. They concluded that the gas has a major effect in accelerating the liquid phase, which would be responsible for carrying the particles to the surface. The trend was confirmed in the experiments with polymer-based mud.

Avila et al. (2008) presented a study of cuttings transport at intermediate inclinations using aerated fluid, to determine the amount of solids that exist in the wellbore and minimum flow requirements for "clean-hole" condition. The experiments were conducted in a large-scale facility [100-ft-long flow loop with 8-in. outer diameter (OD) casing and 4.5-in.-OD drill pipe] by considering pipe rotation at different pipe inclination and different liquid-and gas-flow-rate combinations. They initiated correlations to estimate the required critical-gas-flow rates for hole cleaning at specified liquid-flow rate and drill pipe-rotation combinations, and to predict volumetric cuttings concentration as a function of air and water flow rate, drill pipe-rotational speed, and inclination angle.

Zhou (2008) developed mechanistic model for cuttings transport by combining two-phase hydraulic equations, turbulent boundary layer theory, and particle transport mechanism. Effects of temperature, bottom hole pressure, liquid flow rate, gas injection rate, cuttings size and density, inclination angle, and rheological properties of drilling mud on hole cleaning were analyzed using this mechanistic model. The model was validated by available experimental data.

Falcone et al. (2008) presented a critical review of multiphase-flow loops around the world, highlighting the pros and cons of each facility with regard to reproducing and monitoring different multiphase-flow situations. They suggest a way forward for new developments in Multiphase-Flow Modeling area.

Avila, et al. (2008) presented an experimental study of cuttings transport at intermediate inclinations using aerated fluid, to determine the amount of solids that exist in the wellbore and minimum flow requirements for "clean-hole" condition.

CHAPTER III

STATEMENT OF THE PROBLEM

In depleted reservoirs, production is provided by secondary production techniques. In order to apply these methods, it is necessary to drill new wells. In conventional drilling operations, the hydrostatic pressure of drilling fluid is more than the pore pressure in the formation rock. However, in low-pressure reservoirs or depleted reservoirs, conventional drilling methods should cause to reduced or total absence of fluid flow up the annulus, and that cause pollution in the reservoir. Therefore, "underbalanced" drilling techniques are needed in such reservoirs. Generally, underbalanced drilling operation is applied with drilling fluid which consists of gas-liquid mixture, and by using this type of fluids, reservoir pollution is largely or completely eliminated. However, the drilling performed with gas-liquid mixture, calculating the pressure losses and the performance of cutting transportation is more difficult than single-phase fluid due to the characteristics of multi-phase fluid flow. In case configured drilling is directional or horizontal, these types of calculations are becoming more difficult depending on the slope of the wells. Both hydraulic behavior and mechanism of cutting transportation of the drilling fluids formed by gas-liquid mixture are not fully understood yet, especially there is a large uncertainty in selection of most appropriate flow regarding two phases.

Nowadays, technological achievements and increased energy demand play major roles in increase drilling operation in more deep and difficult locations. Especially there are horizontal and directional sections in almost all of drilling operations which conducted in offshore platforms. In addition, today's, the depth and length of drilled wells are increasing, and supply of hydraulic requirements, as well as effective well cleaning and cutting transport operations are essential aspects in order to realize and to minimize the drilling cost. Especially in horizontal and high-inclined sections of wells, created cutting bed will lead to many problems. During drilling insufficiently cutting transports can be generated many problems such as:

excessive speed bit wear, slow drill speed and formation cracking, as well as significantly increased the drilling costs.

Therefore, experimental and theoretical studies are required to comprehend the issues related to cuttings transport problems in gas-liquid mixture flow through vertical, horizontal and directional annular conduits.

In the literature, there are a little attempts made to describe cuttings transport with two-phase fluid flow in horizontal and inclined wellbores. Although, there are field applications of two-phase drilling fluids for directional and horizontal wells reported to be successful, there is a lack of understanding what is really happening in the wellbore. Since well costs increase drastically for directional and horizontal drilling operations, a proper understanding of such problems may decrease the drilling costs significantly.

CHAPTER IV

SCOPE OF THE STUDY AND APPROCH

The aims of this study are:

- to observe and analyze cutting transport performance of gas-liquid two phase drilling fluids experimentally,
- to identify the primary and essential effective variables in cutting transport performance of two phase drilling fluid,
- to conduct detailed cutting particle movement analysis by using digital image processing techniques,
- to identify the flow schemes of gasified fluids flowing inside an annulus,
- to determine the flow pattern transition boundary equations by discriminant analysis method
- to develop a mechanistic model using fundamental laws of physics and mathematics to predict the flow behavior for two-phase flow and three-phase flow through annular geometries based on obtained experimental findings, during drilling vertical, directional and horizontal wells.

Created mechanistic model can estimate the most appropriate gas and liquid flow rates, consequently, the cutting transport performance and developed pressure loss for two-phase drilling flow through vertical, directional and horizontal annulus by taking into account the different drilling conditions. The model estimations are in good agreement with the measurements obtained from the experiments.

During drilling, monitored data are gas and liquid flow rate of mixture, total measured depth and total vertical depth, rods and shaft diameter, drilling fluid of the gas and liquid phase of the rheological properties (usually the surface conditions are measured), the total pressure loss of system, well bottom pressure (MWD is being used), drilling speed, etc.. By using this information, the well-critical point in the hole cleaning, cut transportation performance and pressure loss estimates can be realized. Also, by performing developed mechanistic model, minimum liquid and gas

flow rates are identified for having an acceptable cuttings concentration inside the wellbore as well as a preferably low frictional pressure drop.

In order to attend to this problem, the following approach was adopted:

- Extensive study of underbalanced drilling technology
- Extensive study of multiphase flow and cuttings transport
- Development of empirical correlations in order to predict void fractions of each phase, and friction factors for two phase flow: cutting-liquid and gas-liquid
- Development of a mechanistic model describing cuttings transport in horizontal and inclined wellbores by considering the effect of eccentricity and pipe rotation
- Development of a computer program based on the proposed model
- Verification of the proposed model

CHAPTER V

EXPERIMENTAL SETUP

The unique experimental setup consisting of various equipments like pump, compressor, control valves, flow meters, pressure transducers etc. and a data acquisition system were used in this study. Experiments were conducted for providing the experimental database and for the verification of the developed empirical correlation and mechanistic model in this study. Experiments were categorized as:

- Air-water two phase flow experiments
- Cutting-water two phase flow experiments
- Cutting-Air-water three phase flow experiments

5.1 Experimental Setup

In order to conduct the experimental program, the Middle East Technical University Petroleum and Natural Gas Engineering Department cuttings transport facility (METU-PETE-CT) was modified to incorporate two-phase and three-phase flow experiments. The available METU-PETE-CT flow loop was completely dismantled and rebuilt with modifications. These performed modifications are listed as follow:

1. Connect the Annular Test section and air compressor (see Fig5.1&5.2)
2. Modify the shale shaker by adding a new vibrator motor and changing pathway of the bypass pipe in order to reduce cutting accumulation and decrease separation time shale shaker (see Fig 5.3)
3. Renew all electrical cables and lines which transfer data from measurement equipments to data logger system.
4. Install the new data acquisition system (National Instruments) and Lab View 8.2 software (see Fig 5.4)

5. Develop Lab View appropriate cods to logging and evaluating data acquired from different measurement equipments.
6. Paint and repair tanks, valves and pipes
7. Construct plat form for camera and annular test section in order to perform experiments in vertical and inclined positions (see Fig 5.5)



Figure5.1: METU-PETE-CT Flow Loop

Figure5.1 is show the modified METU-PETE-CT flow loop which can be used for both three-phase flow and two-phase flow experiments. The annular test section consist of approximately 21 ft. long with 2.91 inch I.D. transparent acrylic casing with a 1.85 in O.D. inner drill pipe. The inner pipe is attached to a variable speed motor, which enables the rotation of the drill pipe at variable speed. One side of the flow loop is mounted on a movable corner (Figure5.2) while the other is connected to the pulley which enables the investigator to incline the loop at any inclination ranging between approximately 10^0 (nearly vertical) to 90^0 (horizontal). The top part of the annular section (end of the transparent section of flow loop) is connected to the separation section which consists of liquid gas separator and shale shaker (see Fig5.3). The eccentricity of the drill pipe can vary from fully concentric to negative and positive eccentricities (see Fig.5.6).



Figure5.2: Annular Test Section Inlet and Movable Corner



Figure 5.3 Separation Section and Modified Shale Shaker



Figure5.4 Data Logger System (National Instruments NI SCXI-100)

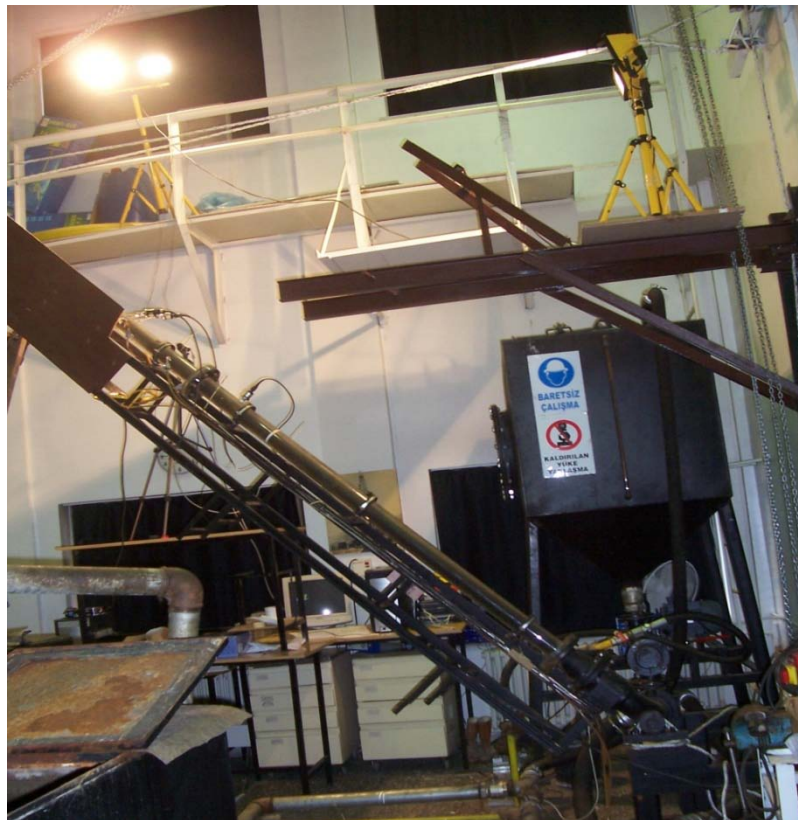


Figure5.5 Constructed Plat Form for Camera and Annular Test Section

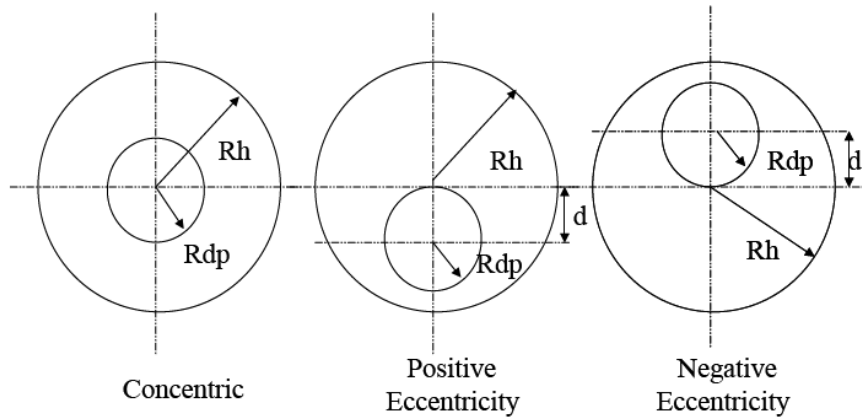


Figure 5.6 - Drill Pipe - Range of Eccentricities

The cuttings are injected into the annular section from a 550-gallon capacity injection tank using a rotating auger system (see Fig5.7). A shale shaker separates the fluid from the cuttings, which are then collected in a collection tank.



Figure 5.7 Cutting Injection Tank and Helicoids (Screw) Metal Chip Conveyor

The liquid collected in the mud tank is pumped and circulated through the loop. Two centrifugal pumps (maximum capacity of 250 gpm) (see Fig. 5.8) are used

periodically with a Fisher control valve (see Fig.5.9) to have a controlled circulation of liquid through the loop. The Fisher control valve controls the variable flow area in the pipe lines.



Figure 5.8 Centrifugal Pump for the Liquid Phase



Figure 5.9 Fisher Control Valve and Toshiba Flow Meter

A compressor (with working capacity of 0-1200 scfm at delivery pressure of 125 psi) is used to supply compressed air. The compressed air is stored into an accumulator tank and dehydrated by air dryer (see fig 5.10 A-B &5.11). The dried air is used to operate Fisher control valves and to inject air to annular section through experiments. The air compressed and dehydrated at a particular pressure is carried to

the bottom of the annular section where it is mixed with the liquid at the entrance of the annular section of flow loop. Before mixing with liquid phase, the air flow rate is controlled using a Fisher control valve for higher gas flow rates (200-1200 scfm) or a Brass Gas Ball Valve for lower flow rates (0-200 scfm) and gas mass flow meter (see fig 5.12).



Figure 5.10-A Air Compressor and Accumulator Tank



Figure 5.10-B Air Compressor and Accumulator Tank



Figure 5.11 Air Dryer and Air Pipe Line



Figure 5.12 Fisher Control Valve and ABB Gas Mass Flow Meter

A pressure regulator is used to control pressure of the gas phase before entering the test section as a safety measure. Usually the air pressure is decreased from 125 psi to 20-45 psi. Both the gas and liquid pipelines have check valves mounted on the lines to allow the flow in one direction and to prevent the fluids flowing in reverse direction. The flow rates of both the gas and liquid phases are measured by using mass flow meters (Cole Parmer Inc and Toshiba Inc. respectively). The liquid and air are mixed at an angle (inverted 'V'), which was specially devised to promote proper mixing of the two phases. During the flow tests, pressure drop is measured at a fully developed section on the test section using a

digital pressure transducer. A high-speed digital camera is also mounted to the test section in order to record the experiments.

The schematic diagram of the experimental facility is as shown in Fig 5.13. Two pair pressure taps are located in the middle and both sides of flow loop with suitable distance from the inlet and outlet of annular section in order to acquire perfect data from fully developed section and to neglect end effect. These taps are connected to differential pressure transducers (Honeywell Inc. and Cole Parmer Inc.) to measure a differential pressure by flexible lines filled with water. To eliminate the problem of contamination of the pressure taps with the test fluids, lines were bled regularly.

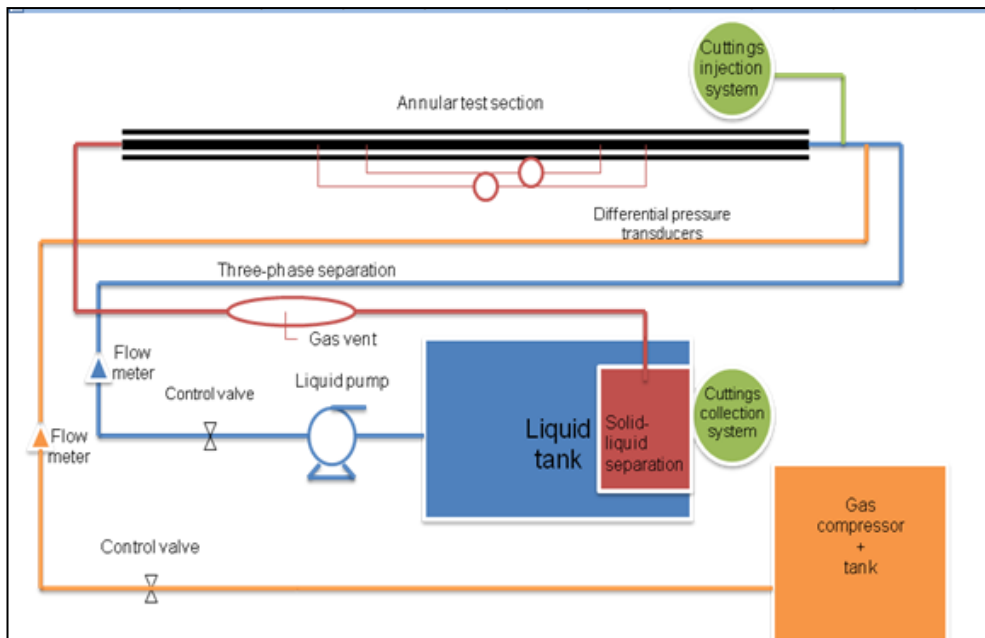


Figure 5.13 Schematic of Experimental Setup

The control panel located near the test section has a data acquisition system. The flow rates of air, water and cutting injection rate, drill pipe rotation and high speed camera can be controlled from the control panel by using two computers, National Instrument data logger and appropriate related softwares. The loop pressure, flow rates, injection and collection tanks weight, rate of penetration (ROP), inner pipe rotation speed (RPM) and the differential pressures can be measured using the

data acquisition system. 'Lab View8.2' data acquisition software is used for data logging and storage, real-time data display, on-line analysis, process monitoring, etc. To ensure accuracy, regular calibration checks are carried out on all the instrumentation. The capacity and brand name of each component in the experimental setup are presented in Table 5.1. Commercial gravel was used to simulate the drill bit cuttings. The solid particle has a roughly spherical shape. The summary of the solid particle characteristics that were used to simulate the drilled cuttings are shown in Table 5.2.

Table 5.1 Capacity and Brand Name of Experimental Components

Component	Brand Name	Capacity
Air Compressor	TAMSAN	3000 l/min at 6 atm
Air Accumulator Tank		
Air Dryer	OMI	700 l/min at 6 atm
Centrifugal Pump	DOMAK	1.136 m ³ /min
Liquid Tank		2000 m ³
Magnetic Liquid Flow Meter	TOSHIBA	1.136 m ³ /min
Volumetric Gas Flow Meter	COLE-PARMER INST. CO	0-1000 l/min at 25 psi
Electro pneumatic Control Valves	SAMSON	
Digital Differential Pressure Transducers	COLE-PARMER INST. CO	0-1 psi ,0-2.5 psi
Digital Differential Pressure Transducers	Honey Well INST. CO	0-2.5 psi
Load Cell	ESIT Elektronik LTD	0-5000kg
High-Accuracy Gauge Transmitter	COLE-PARMER INST. CO	0-30 psi ,0-60 psi

Table 5.2 the Solid Particle Characteristics

Particle Diameter(in)	Cutting Density(ppg)	Cutting Bed Porosity(%)
0.079	23.050	36.0

5-2 Installation of Data Acquisition System

Before starting this study, Elimko E-680 was used in METU-PETE-CT flow loop as data acquisition system. Since a lot of problems were occurred during the past studies because of low accuracy of this data acquisition system, it has been

decided to use the National Instrument SCXI-1000 chassis as hardware and NI-DAQ 8.X and Lab VIEW 8.2 as Software in order to improve accuracy of obtained data in presented study. The installation procedure is presented as follow:

- Install Application Software NI-DAQmx
- Install NI-DAQ 8.X
- Unpack the Devices, Accessories, and Cables
- Install the Devices, Accessories, and Cables
- Confirm that the Device is recognized
- Install Signal Conditioning or Switch Devices
- Attach Sensors and Signal Lines
- Run Test Panels
- Take an NI-DAQmx Measurement
- Use NI-DAQmx with Lab view 8.2
- Install Lab view 8.2
- Construct an NI-DAQmx task and Test the task
- Graph Data from DAQ Device
- Edit an NI-DAQmx Task
- Add the output measurement devices to the modulo channels and Build front and back panels of Lab View (See fig 5.14 & 5.15).

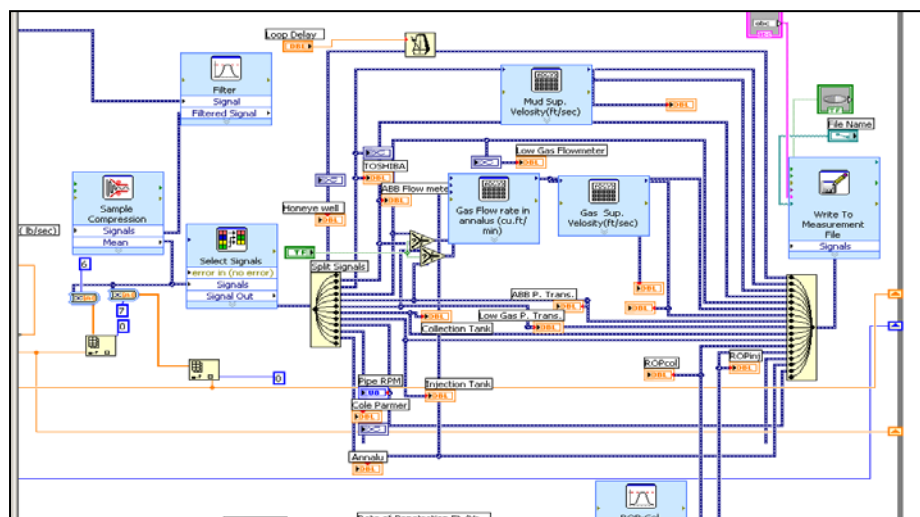


Figure 5.14 Back Panel of Lab View Designed by Researcher

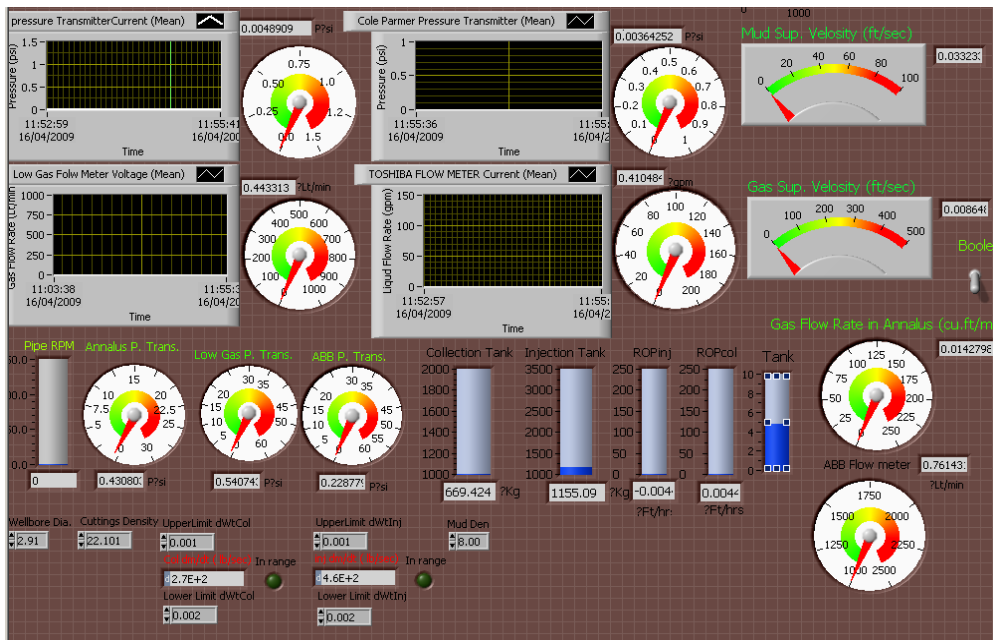


Figure 5.15 Front Panel of Lab View Designed by Researcher

5-3 Experimental Test Procedure and Data Acquisition

Two-phase flow experiments using air-water and cutting-water as well as three phase flow air-water-cutting were conducted at different gas and liquid flow rates, at cutting injection rate and at horizontal (89.6°), nearly vertical (12.5°) and three inclined (45.0°), (60.0°), (75.0°), test sections of the test section. In all test sections, the experiments were performed in an eccentric annulus with and without inner pipe rotation, at the room temperature $25\text{-}35^\circ\text{C}$ (298.15 K , 77°F). The eccentricity ratio (ϵ) in all test section is 0.623. The pressure in the annular test section was varied in the range of 15.7-27.7 psia depending on phases flow rate. Once the experimental setup was ready, the calibration of data acquisition system was carried out. It was ensured that the measurements of phase densities, pressure and phase flow rates were under acceptable accuracy limits, after calibrating the respective measuring devices in the control panel. The programmable logic control was used to control the flow rate from the control panel. Differential pressure transducers were calibrated and programmed into the Lab View data acquisition software. The accuracy of all the measuring devices was maintained by regular calibration checks. Some preliminary experiments with single-phase water flow were

conducted to validate the experimental setup along with the data acquisition system. Typical recorded data as a function of time during the two and three phase experiments were pressure losses for each set of transducers, inlet pressure and air and water flow rate and ROP. In order to examine the accuracy of recorded data, some of experiments were repeated one or two times. Some of the experimental data recorded and repeated is presented in Appendix A. The experimental test procedures for these experiments are described below.

5-3-1 Two-Phase Gas-Liquid Flow

The experiments were performed in an eccentric annulus using water-air mentioned positions, without inner pipe rotation. The standard experimental procedure adapted was as follows: Using centrifugal pump, the liquid was pumped at a constant flow rate in the range of 0-250 gpm. Then, the air was injected into the annular test section through a compressor with the working capacity of 0-50 psi and a flow rate range 0-100 scfm. Once both the air and liquid flow rates were stabilized, the data acquisition was activated in order to record flow rates, pressures at critical points, pressure drop inside the test section, etc. At the same time, high-speed camera was recording the flow in the test section for analysis of flow patterns and identification of gas and liquid volume fractions in dynamic conditions. These recordings were used later to confirm the visual observations of the flow patterns and to determine of void fraction of each phase.

5-3-1.1 Test Procedure for Gas-Liquid Two Phase Flow

The following procedure is used for gas-liquid two phase flow tests:

- 1) Prepare water in the main mud tank.
- 2) Flush differential pressure transducer lines with water.
- 3) Start data acquisition system.
- 4) Make sure flow is through only one pipe.
- 5) Start air compressor to support air for pneumatic valves and annular test section.
- 6) Start mud pump.
- 7) Set liquid flow rate to desired value.

- 8) Set air flow rate to desired value.
- 9) Start recording data.
- 10) Start high-speed camera to record the flow in the test section
- 11) As soon as the readings are stable, change air flow rate and set it to new value.
- 12) Repeat steps 9-10 until data is collected for all desired air flow rate values
- 13) Stop recording data.
- 14) Stop high-speed camera.
- 15) Set liquid flow rate to new desired value.
- 16) Repeat steps 8-15 until data is collected for all desired values ($Q_l=0-120\text{gpm}$).
- 17) Stop mud pump.
- 18) Stop compressor.

5-3-1.2 Test Matrix for Gas-Liquid Two Phase Flow

The test matrix for water and air tests is presented in Table 5.3.

Table 5.3 Test Matrix for Gas-Liquid Two Phase Flow Tests

	Minimum	Maximum
Average Water Annular Velocity (ft/s)	1	10
Average Gas Annular Velocity (ft/s)	1	120
Average Annular Pressure(Psig)	1	13
Temperature($^{\circ}\text{C}$)	25	35
eccentricity ratio	0.623	0.623

5-3-2 Test Matrix for Cutting-Liquid Two Phase Flow

The standard experimental procedure adapted was as follows. Using centrifugal pump, the liquid from the tank was pumped and passed through the loop at a specific flow rate using the mass flow meter and the Fisher control valve. Once the liquid flow rate was stabilized, the cuttings were injected into the flow loop. Once both the cuttings and liquid flow rates were stabilized and the flow was steady, the data acquisition was started and sufficient data observed. At the same time, High speed camera was recorded all step of experiments. These recordings were used later

to identify flow pattern and to determine the total and moving cutting concentrations, bed height, bed area and velocity of moved bed into the annulus section.

5-3-2.1 Test Procedure for Cutting-Liquid Two Phase Flow

The following procedure is used for gas-liquid two phase flow tests:

- 1) Prepare water in the main mud tank
- 2) Flush differential pressure transducer lines with water
- 3) Start data acquisition system
- 4) Make sure flow is through only one pipe
- 5) Start mud pump
- 6) Set liquid flow rate to desired value
- 7) Set pipe rotation to desired value
- 8) Inject cutting into annular test section and Set cutting flow rate to desired value
- 9) Start recording data
- 10) Start high-speed camera to record the flow in the test section
- 11) As soon as the readings are stable, change water flow rate and set it to new value
- 12) Repeat steps 9-10 until data is collected for all desired water flow rate values
- 13) Stop recording data
- 14) Stop high-speed camera
- 15) Set pipe rotation to new desired value
- 16) Repeat steps 8-15 until data is collected for all desired values
- 17) Stop mud pump
- 18) Stop compressor

5-3-2.2 Test Matrix

The test matrix for water and cuttings tests is presented in Table 5.4.

Table 5.4 Test Matrix for Cutting-Liquid Two Phases Flow Tests

	Minimum	Maximum
Average Water flow rate (gpm)	20	120
Average Water Annular Velocity (ft/s)	1	10
Average Cutting Rate of Penetration (ft/hrs)	60	120
Pipe Rotation(1/min)	0	120
Average Annular Pressure(Psig)	1	13
Temperature(°C)	25	30
eccentricity ratio	0.623	0.623

5-3-3 Three Phase Flow (Air-Water-Cutting)

The standard experimental procedure adapted for three phase flow was as follows: Using centrifugal pump, the liquid was pumped at a constant flow rate. Then, the air was introduced with the desired rate. Once both the air and liquid flow rates were stabilized, the cutting was injected from injection tank into the system. When the cutting, gas and liquid flow rates are stable, the data acquisition was activated in order to record flow rates, pressures at critical points, pressure drop inside the test section, etc. At the same time, high-speed camera was recording the activity in the test section for analysis of cuttings concentration in dynamic conditions. These digital images were used later to confirm the visual observations of the flow regimes and to develop a new method for cuttings concentration determination by using image analyzes technique.

In order to investigate the effects of all mentioned parameters, the above procedure was conducted in different water, gas and cuttings flow rates as well as various pipe rotation speeds. So, considerable data points which used to develop model for prediction of pressure drop and for optimization of flow rates for liquid and gas phases, were logged.

5-3-2.1 Test Procedure for Cutting-Liquid Two Phase Flow

The following procedure is used for gas-liquid two phase flow tests:

- 1) Prepare water in the main mud tank.
- 2) Flush differential pressure transducer lines with water.
- 3) Start data acquisition system.
- 4) Make sure flow is through only one pipe.
- 5) Start mud pump.
- 6) Set pipe rotation to desired value
- 7) Inject cutting into annular test section and Set cutting flow rate to desired value.
- 8) Set liquid flow rate to desired value.
- 9) Set air flow rate to desired value.
- 10) Start recording data.
- 11) Start high-speed camera to record the flow in the test section
- 12) As soon as the readings are stable, change air flow rate and set it to new value.
- 13) Repeat steps 10-12 until data is collected for all desired air flow rate values
- 14) Stop recording data.
- 15) Stop high-speed camera.
- 16) Set liquid flow rate to new value and repeat steps 8-15.
- 17) Change pipe rotation and set it to new desired value.
- 18) Repeat steps 7-16 until data is collected for all desired values (RPM=0-80-100-120 (1/min)).
- 18) Change Cutting injection rate and set it to new value and repeat steps 8-18 until data is collected for all desired values (ROP=80-100-120 (ft/hrs)).
- 17) Stop mud pump.
- 18) Stop compressor.

5-3-3.2 Test Matrix

The test matrix for three phases flow air, water and cuttings tests is presented in Table 5.5.

Table 5.5 Test Matrix for Gas-Cutting-Liquid Three Phases Flow Tests

	Minimum	Maximum
Average Water flow rate (gpm)	20	120
Average Water Annular Velocity (ft/s)	1	10
Average Gas Annular Velocity (ft/s)	1	120
Average Cutting Rate of Penetration (ft/hrs)	80	120
Pipe Rotation(1/min)	0	120
Average Annular Pressure(Psig)	1	13
Temperature(°C)	25	30
eccentricity ratio	0.623	0.623

5-4 Sensitivity Analysis of Experimental Data

A preliminary analysis of errors in measurement of various variables was carried out. The gas and liquid mass flow rates were measured using Micro-motion mass flow meters, which were designed to measure mass flow to an accuracy of 1% of reading. The acquired data showed that the accuracy affected by fluctuations and the dynamic disturbance varied with the flow readings. For liquid mass flow measurements, it was observed that for very low flow rates (<10 gpm) and high flow rates (>170 gpm) the accuracy was less while for the intermediate range (used in experiments) the accuracy was found to be $\pm 5\%$. In case of gas flow rate measurements, at very low flow rates (<10 scfm), the accuracy was very low ($\pm 15\%$) due to various inherent fluctuations inside the system. For higher gas flow rates, the fluctuations were observed, but their amplitude was less and the accuracy was up to $\pm 10\%$ (nevertheless, the running averages of all the fluctuations were accurate).

In case of differential pressure measurements, the accuracy of the pressure transducers was rated as $\pm 0.25\%$ of the full scale. Due to the flow rate fluctuations, the measured values showed that the accuracy was $\pm 1\%$ (or less) in case of horizontal flow for both pressure transducer in low gas flow rate. In high gas flow rate, because of low sensitivity and aged mechanism, the accuracy of Cole Parmer pressure transducer was less than that of Honey Well pressure transducer. So in these

conditions, the measured value by Honey Well pressure transducer is considered as accurate data.

An attempt was made to repeat all the tests (both air-water and air-water-cutting flow) to ensure the repeatability (and accuracy) of the acquired data.

The eccentricity of the annular geometry was measured by using Image Analysis Technique in the present experiments. The drill pipe was supported at both the ends without any centralizers in between. Since the drill pipe was empty inside, it was partially lifted up due to buoyancy when liquid was injected inside the annulus.

5-5 Experimental Data Analysis Procedure

As mentioned previously, NI-SCXI-1000 module and Lab View 8.2 were used as data acquisition system. This system can be able to log 1000 signals per second from each input channel and to process input signals. The signal processes steps are:

- Filtering unwanted signals or noise from the signal which are measured (A common use of a filter is to eliminate the noise from a 50 or 60 Hz AC power line).
- Calculating necessary variables from logged signals such as ROP and gas-liquid superficial velocities
- Computing the average of input and filtered signal and storing them in excel file in the manner of one data per second

In case of two-phase flow experiments, the liquid superficial velocity was fixed and controlled in constant value by fisher control valve and liquid mass flow meter. Then gas superficial velocity was increased from 1 to 800 ft/sec step by step. In each step, when the flow in test section was stabilized, data logger system was started to store data send from different measurement equipments in 60-100 sec periods. After that gas superficial velocity was increased and above procedure repeated for new situation. This procedure was recurred for different gas and liquid superficial velocity. Finally, there were 60-100 data sets corresponding to each gas

and liquid superficial velocities, In order to calculate the average of them, an excel macro was developed (Appendix B).

In this study, the measured total pressure difference is composed of changes in pressure due to gravitational, frictional and acceleration forces. The acceleration pressure change was assumed to be small as compared to the remaining two pressure components and can be neglected.

5.6 Methodology of Image Analysis Technique

As mentioned previously, in this study, image analysis technique was used in order to determine void fraction of each phase and to identify flow pattern dynamically. A high speed camera was used to record all experiments. All recorded videos were converted to frames by using Matlab video acquisition toolbox. Then the Image Processing Toolbox software was used to get Information about Image Pixel Values and Image Statistics which were discussed in details as stated below. In this study, the extracted frames were divided into different types based on their visual observation properties, and different algorithms were developed to analyze each type of frame individually.

5-6-1 Common Initial Steps for Algorithms

The common initial steps for all algorithms were extracting the annular section, cropping frames using the coordinates of annular (fig5.16.a.b.c) and obtaining the gray-level image from RGB image (fig5.17.a.b.c). Extracting the annular section was done one time because fixed camera and the annular section locations were not changed during recording the videos. However cropping frames using the coordinates of pipe and obtaining the gray-level image from RGB image steps were performed for each frame. Gray-level image was attained by decomposing the RGB image in order to get the red component. Details on the standard image processing operations used can be found in Appendix C, based on the work by Gonzalez and Woods (1993).

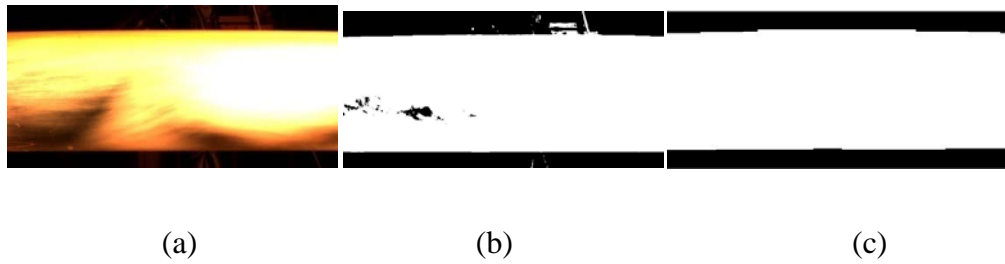


Figure 5.16 Finding Annulus

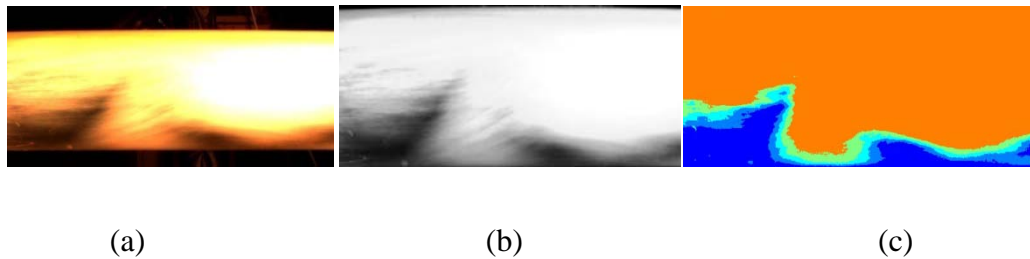


Figure 5.17 Pixel Intensity Labeling Algorithm

5-6-2 Liquid Hold up Determination by Using Image Analysis Technique applied in Gas-Liquid Two Phase Flow

In this section, the extracted frames were collected according to developed flow patterns. In order to label the area of each phase in frames, two different algorithms were developed: 1) labeling by using boundary, 2) labeling by using Pixel intensity After applying initial common steps pointed out in section 5-7-1 for each frame, these algorithms were implemented to each frame.

5-6-2.1 Labeling by Using Boundary

This algorithm was used for analyzing frames which recorded in stratified and plug flow patterns. After applying initial steps, firstly, the image edges were detected by using convolution operation with Sobel mask (Appendix C) (fig .5.18 c). Then by using global thresholding technique, the images were converted from gray-level to binary type (fig .5.18 d). After that, dilation and erosion operations were performed in order to highlight the boundary between air and liquid and ignore noises (Fig 5.18 e). By application of these steps, boundary between two phases was detected.

Finally, the pixels which located in the two sides of boundary were labeled as gas and water by using logical observation (fig 5.18 f).

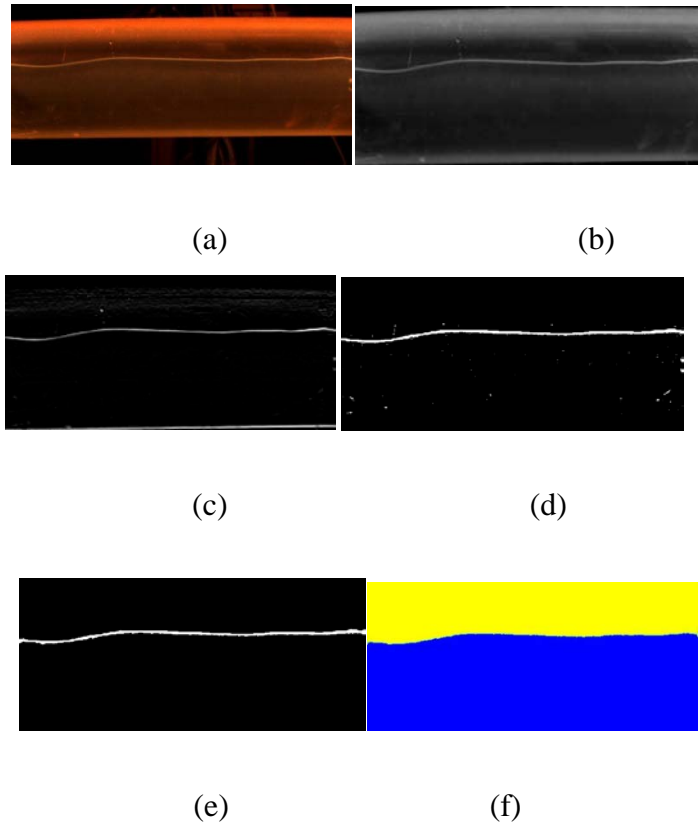


Figure 5.18 Labeling Using Boundary Algorithm

5-6-2.2 Labeling by Using Pixel Intensity

In order to analyze frames which were extracted from wavy annular, dispersed annular and dispersed bubble flow patterns recordings, this algorithm was applied. Since liquid and gas were mixed in these flow patterns, three individual phases; Liquid, Gas, and Mix phase were observed in each frame and apparent boundary among these phases were not identified. Also variety of pixel intensities was detected in mix phase of extracted frames. After applying initial steps and obtaining gray-level image, firstly, the pixels were classified in to six different levels according to their intensity values (Table 5.6).

Table 5.6: Labeling Levels and Intervals

Name	Interval
Gas and Liquid	$0 \leq x < 80$
Level 1	$80 \leq x < 105$
Level 2	$105 \leq x < 130$
Level 3	$130 \leq x < 160$
Level 4	$160 \leq x < 200$
Level 5	$200 \leq x \leq 255$

In Table 5.6, the interval values were formed by observation and examination of relevant frame types. Different combinations of levels were used to identify mix region for each frame based on flow patterns (Table 5.7). Finally the gas and liquid phases were labeled based on flow patterns definitions and logical observations. For example in dispersed bubble and dispersed annular frame types, after identifying the mix region, the remaining area was labeled as a liquid phase (Fig. 5.19). But in wavy annular frame types, the upper side of mix region was labeled as gas and lower side of it was labeled as liquid (fig. 5.18).

Table 5.7: Used Levels for Frame Types to Generate Gas and Liquid Mixture

<i>Frame Type</i>	<i>Used levels for liquid and gas mixture</i>
Dispersed Annular	Level 4 and Level 5
Wavy Annular	Level 3, Level 4 , Level 5
Dispersed Bubble	Level 1, Level 2, Level 3, Level 4 , Level 5



(a)

(b)

(c)

Figure 5.19 Partial Intensity Labeling Algorithm

The combination of these two algorithms were applied in order to label the area of each phase in the frames which extracted from slug and churn flow patterns (fig 5.20).

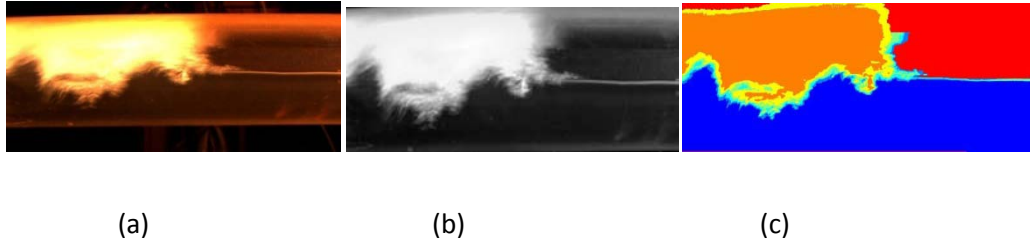


Figure 5.20 Combination of Partial Intensity Labeling and Labeling Using Boundary Algorithm

5-6-2-3 Determination of Gas and Liquid Ratio in Mixture

To accurately determine gas and liquid ratio in the mixture, a transparent acrylic pipe - representing a cross-section of annulus - was set up. This particular annulus was filled with a predetermined amount of liquid as such the liquid-gas ratio was set within the structure. As a result of this process constant volume of liquid and gas were captured in this transparent acrylic pipe. Then the pipe was shaken manually to obtain different flow patterns with known liquid-gas volumes. After shaking for different ratios of liquid and gas, frame types were captured by using the camera. This would give an idea of liquid-gas ratio of the mixture during real-time pipe flow when a particular flow pattern is observed.

5-6-2-4 Liquid Holdup Calculation

Information loss due to transformation of 3D image to 2D projection is a well-known problem in image processing applications. So the main assumption using these techniques is to have symmetrical flow within the pipe so that the visibility from one cross sectional view has the same projection on the other side. Also, the information loss due to cylindrical to rectangular conversion will be minimal as the geometry of the annular pipe structure is carefully measured. The volume calculations are done according to the particular pipe geometry of the given problem. For example, in the problem of an annular eccentric pipe flow (fig.5.21) the shaded

area is representing the volume between the inner and outer cylinder. Depending on the location within the rectangular projected image the corresponding volumes can be calculated. (Ozbayoglu 2002)

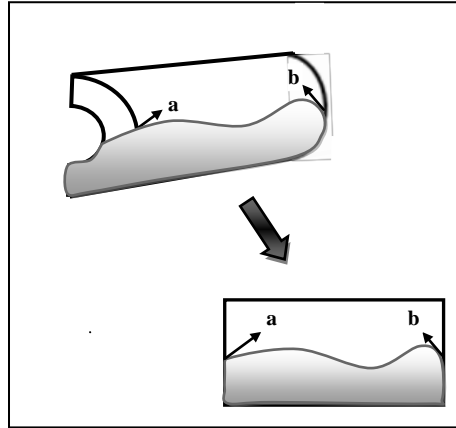


Figure 5.21 Three-Dimensional System to Two-Dimensional Frame

5-6-3 Cutting Concentration Determination by Using Image Analysis Technique Applied in Cutting- Liquid Two Phase Flow

In this section, the extracted frames were divided into three types: Stationary bed, moving bed and dispersed (fig. 5.22 – a, b, c, respectively) and different algorithms were developed to analyze each type of frame individually.

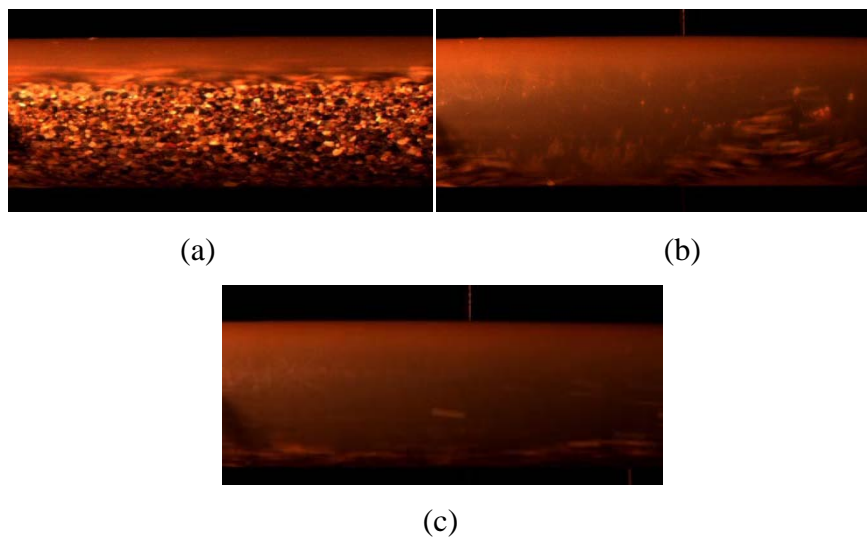


Figure 5.22 Flow Types (a) Stationary Bed (b) Moving Bed (c) Dispersed

5-6-3-2 Stable Cutting Algorithm

In stationary bed frame type, there is a stable cutting block at the bottom of the annulus. Moving cutting zone was located over that. After applying the common initial steps, the motion of moving cutting zone was found by using absolute difference between successive frames.

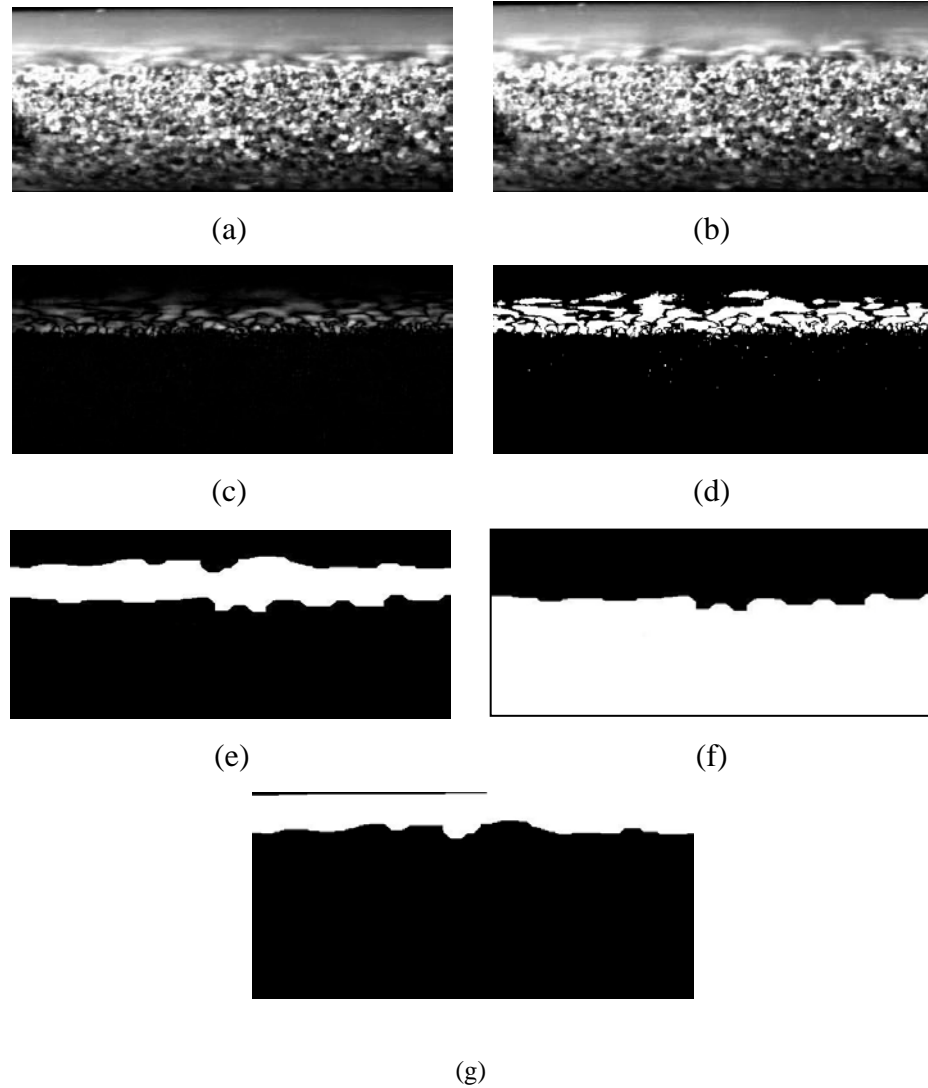


Figure 5.23 Stable Cutting Algorithms

Then by using global thresholding technique, gray-scale moving cutting zone was converted to binary image in which the lighter regions of the frame were separated from the dark background. Some binary morphological operations such as closing and opening operations were applied sequentially in order to enhance the

binary image. Finally, the pixels which were located in upper and below sections of moving cutting zone were detected as liquid and cutting respectively (fig. 5.23).

5-6-3-3 Moving cutting algorithm

In moving bed frame type, cuttings moved like a wave (sine wave) regularly through annular section (fig 5.22-b). Each wave consisted of a liquid core and cuttings accumulation around this core. The high frequency of the wave was depended on the rate of penetration and liquid flow rate. When the liquid flow rate was increased gradually, cuttings were dispersed roughly through the annular section. The frame which was extracted from this particular situation was named as dispersed frame type (fig 5.22-c). The aim of the moving cutting algorithm is to detect the cutting pieces for both moving bed and dispersed frame type. To analyze these types of frames, at first, the common initial steps were applied. After these steps, the absolute difference technique was applied by using frame and background that was estimated from all frames.

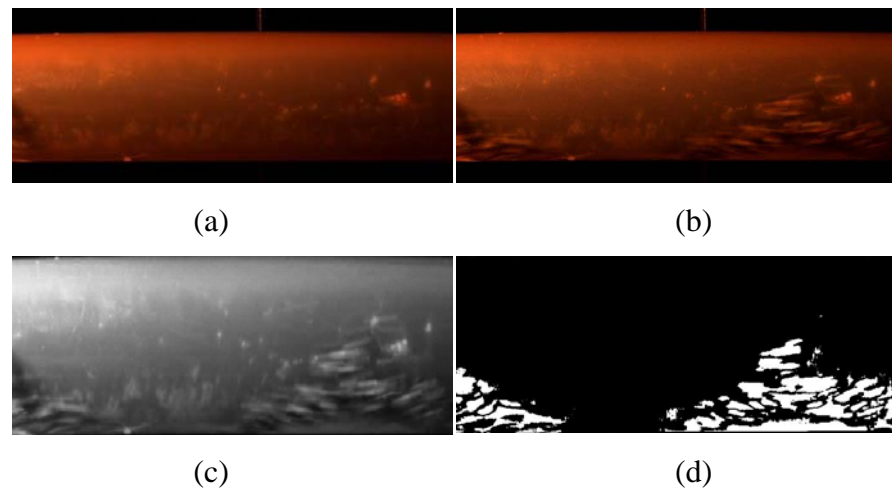


Figure 5.24 Moving Cutting Algorithm Applied to Slug Frame

Additionally, global thresholding technique was performed to detect cuttings in annular section as a binary image. Moving cutting algorithm that was applied to moving cutting and dispersed frame type was given in figures 5.24 and 5.25, respectively.

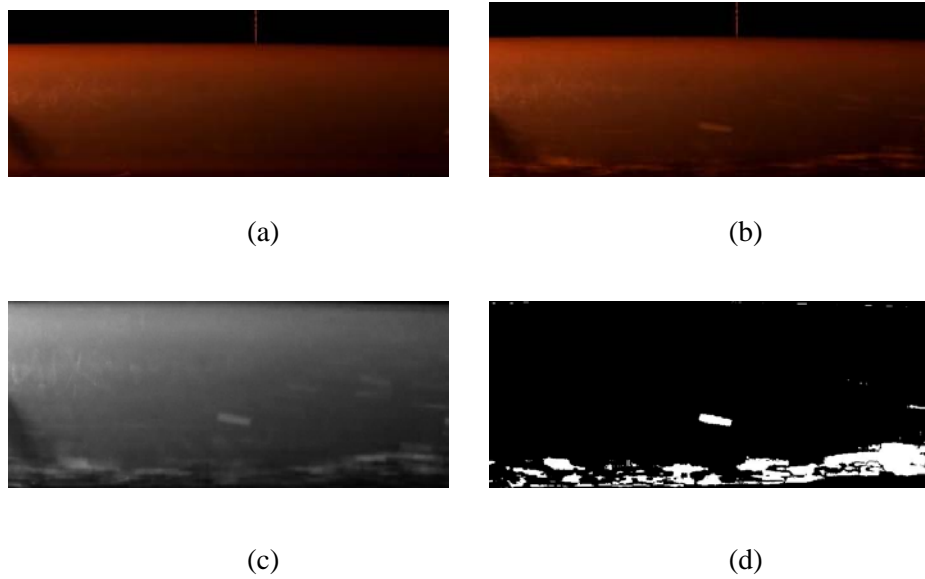


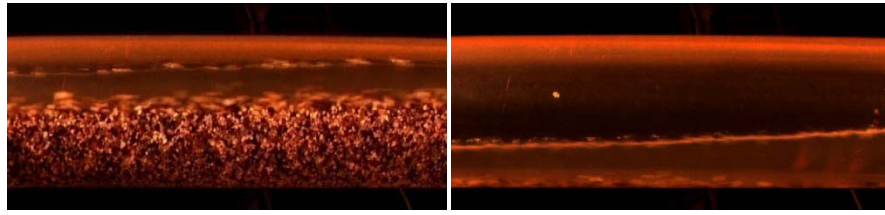
Figure 5.25 Moving Cutting Algorithm Applied to Dispersed Frame Type

5-6-3-4 Volume Calculation

In all analysis, after finding related regions such as cutting and liquid regions, volumes of these regions are calculated by using the method which introduced in section 5-7-2.4, for measurement of total and moving cutting concentrations, bed height and bed area.

5-6-4 Cutting Concentration Determination by Using Image Analysis Technique applied in Three Phase Flow

In this section, the extracted frames were divided into two types: stationary bed and dispersed (fig5.26.a.b, respectively) and different algorithms were developed to analyze each type of frame individually.



(a)

(b)

Figure 5.26 Flow Patterns (a) Stationary-Bed Flow (b) Dispersed Flow

5-6-4 -1 Stationary bed algorithm

In stationary bed frame type, a stable cuttings block was observed at the bottom of the annulus and moving cuttings zone and liquid zone was located over that. The gas region took place above the liquid phase. After applying common initial steps, edge detection process was applied with sobel filter in order to separate the gas and the liquid region and the liquid-gas boundary was obtained (fig5.27.e). The motion of moving cuttings zone was found by using the absolute difference between successive frames while considering the liquid-gas boundary. Then by using the global thresholding technique, gray-scale moving cuttings zone was converted to binary image in which the lighter regions of the frame were separated from the dark regions. Some binary morphological operations such as closing and opening operations were applied sequentially in order to enhance the binary image. After determining moving cuttings zone and the liquid-gas boundary, the segmentation process was applied in three steps for finding the phases separately. First, the pixels which were located above the liquid-gas boundary were found as the gas region. Second, the area between liquid-gas boundary and moving cuttings zone were detected as the liquid region. Last, the below part of moving cuttings zone was attained as the stationary cuttings region (fig5.27.a.b.c.d.e.f.g.h.i.j).

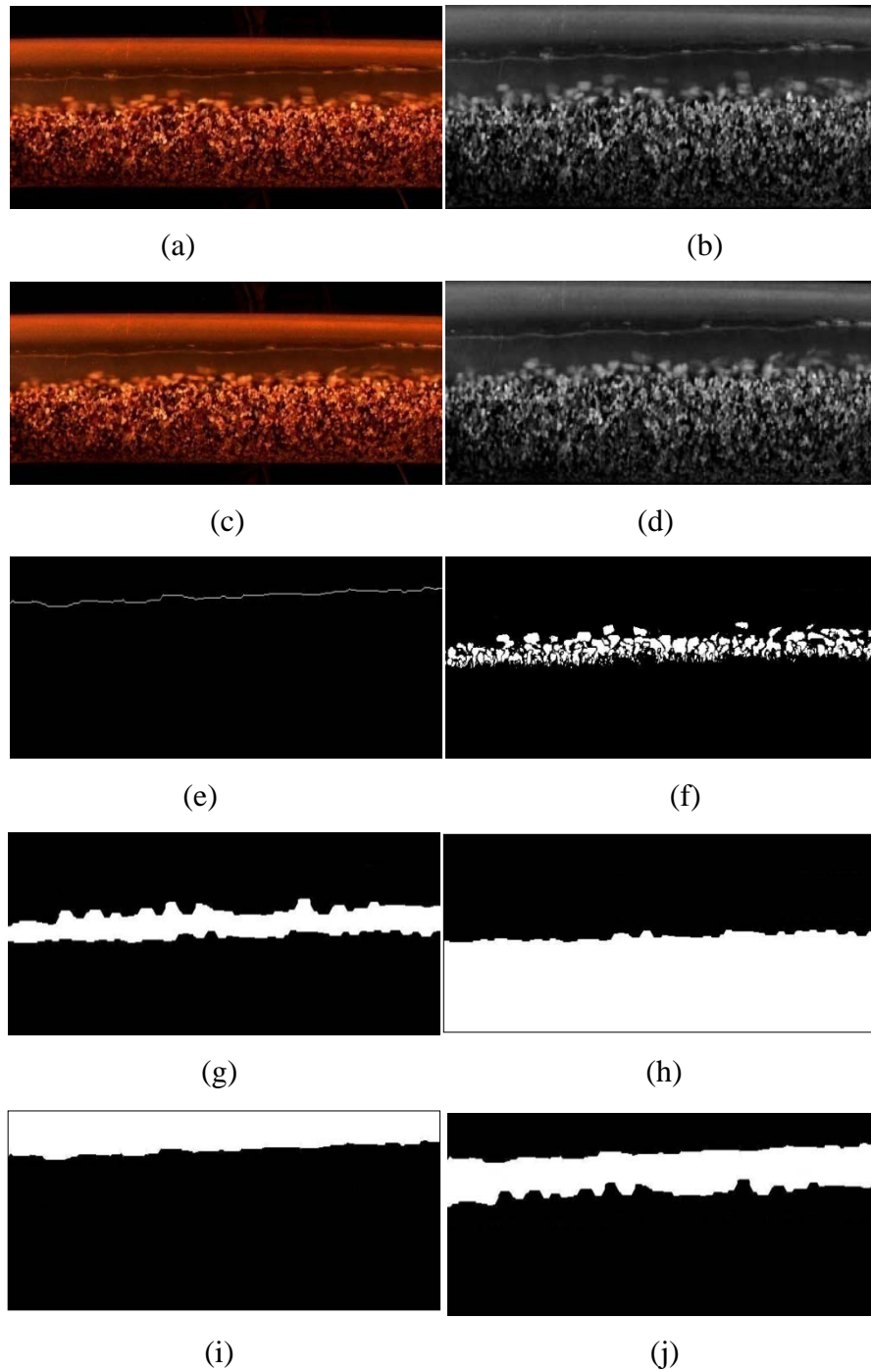


Figure 5.27 Stationary Bed Algorithms

5-6-4 -2 Dispersed algorithm

When the liquid flow rate was increased gradually, cuttings were dispersed roughly in liquid phase and gas phase was located above the liquid phase. The frame

which was extracted from this particular situation was named as dispersed frame type (fig 5.26-b). To analyze these types of frames, at first common initial steps were applied. To separate the gas and the liquid region, edge detection process was applied with sobel filter and the liquid-gas boundary is obtained (fig5.28.e).

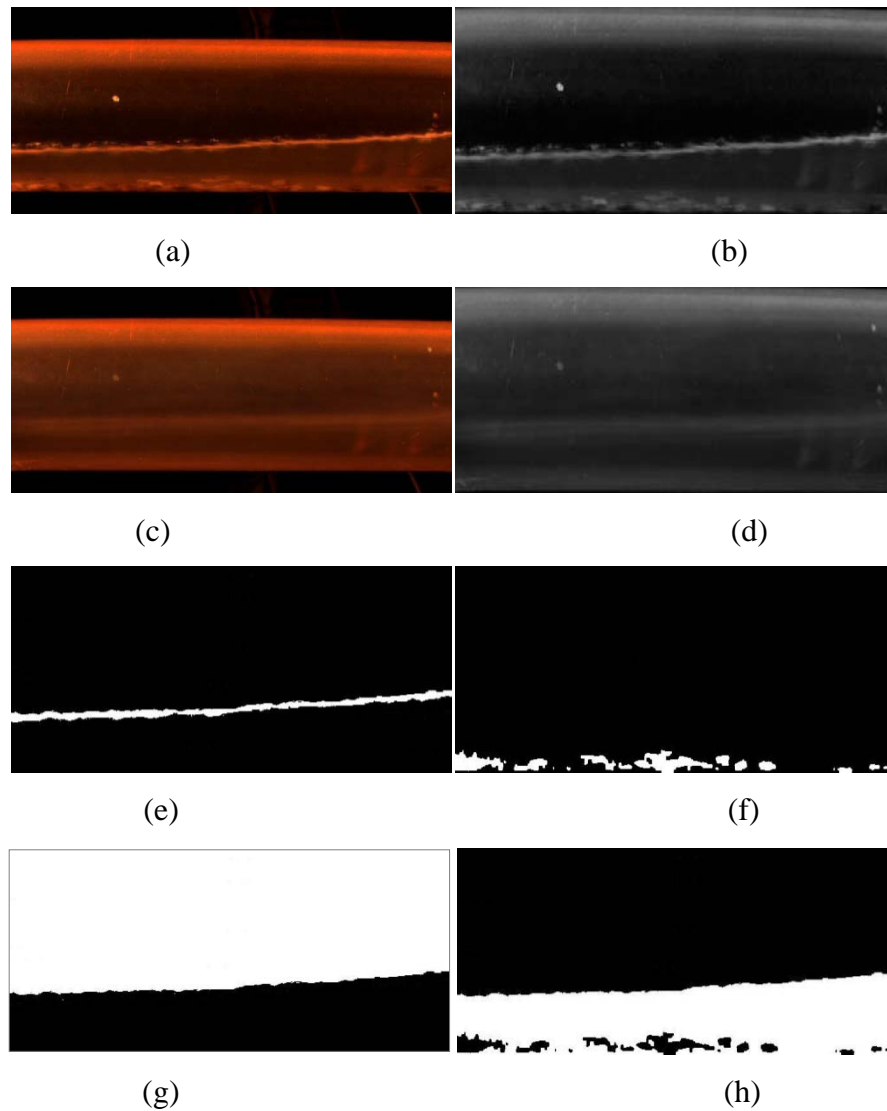


Figure 5.28 Dispersed Algorithms

After that, while considering the liquid-gas boundary, absolute difference and global thresholding techniques were performed to detect cuttings in annular section. After determining cuttings and the liquid-gas boundary, the segmentation process was implemented in two steps to find the phases separately. First, the pixels which were positioned above the liquid-gas boundary were found as the gas region. Second,

the area that existed below the liquid-gas boundary was detected as the liquid region (fig5.28.a.b.c.d.e.f.g)

5-6-4-3 Volume Calculation

In all analysis, after finding related regions such as cutting, liquid and gas regions, volumes of these regions are calculated by using the method which introduced in section 5-7-2.4, for measurement of total and moving cutting concentrations, bed height and bed area.

5-6-5 Calculating Cutting Velocity

To calculate velocity of cuttings, a Java application which was called “Pixel Distance Calculator” was developed by using Java Development Kit 1.6.0 (JDK 1.6.0) and Eclipse Integrated Development Environment 3.5.2 (Eclipse IDE Classic 3.5.2) (fig. 5.29). The aim of this application is calculating the velocity of a cutting. This is conducted by identifying the distance of two selected pieces from frames. The application detects the clicked location by an event mechanism, and each location consists of (X, Y) components. After selecting pieces, velocity of a piece pair calculated by using the equation below.

$$V_p = \text{EuclideanDistance}((x_1, y_1), (x_2, y_2)) * \text{Dif}_{\text{frames}} \times n_{\text{fps}} \times p_{\text{camera}}$$

V_p = Velocity of a pair

EuclideanDistance = Distance between two pieces:

$$d = \sqrt{(x_1 - x_2)^2 + (y_1 - y_2)^2}$$

$\text{Dif}_{\text{frames}}$ = Difference of frame numbers

n_{fps} = Frame per second (fps) value of relevant video that consisted of used frames

p_{camera} = calculated projection parameter of camera

The projection parameter of the camera is changed according to the position of camera. Using the projection parameter of the camera, unit is converted from pixel to centimeter. Similarly, using the video information, time is converted from fps to second. Following this process, the velocity of all pairs was found and the average velocity is calculated.

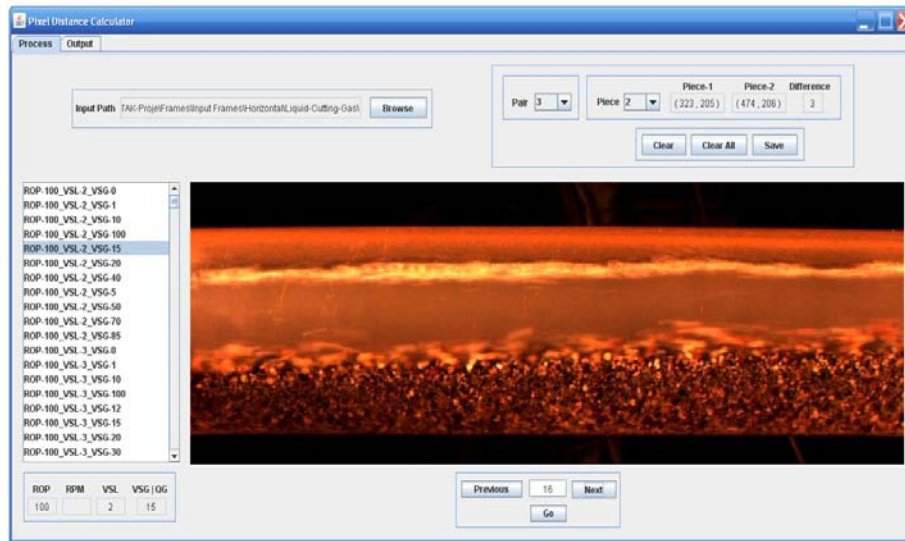


Figure 5.29 Pixel Distance Calculators

5-7 Initial Experiments: Single-phase Water Flow to Validate the Experimental Setup Along with the Data Acquisition System

The sensitivity analysis of the acquired data was carried out and the details are described in this section. Some preliminary experiments with single-phase water flow were conducted to validate the experimental setup along with the data acquisition system. Single-phase water flow experiments were conducted to check the equipment and data acquisition system. The pressure difference along the loop length (21 ft) was measured and compared with the theoretical calculations. The tests were repeated to ensure the repeatability of the experimental results. The results of these tests are shown in figure 5.30. The results show a good repeatability and except for the low liquid flow rates (where there was problem in accurately controlling the flow rates and where the flow might be in the transition zone), the measured pressure drop values were within the range ($\pm 5\%$) of the calculated values. Note that for calculating the theoretical values, the pipe roughness factor was assumed to be zero.

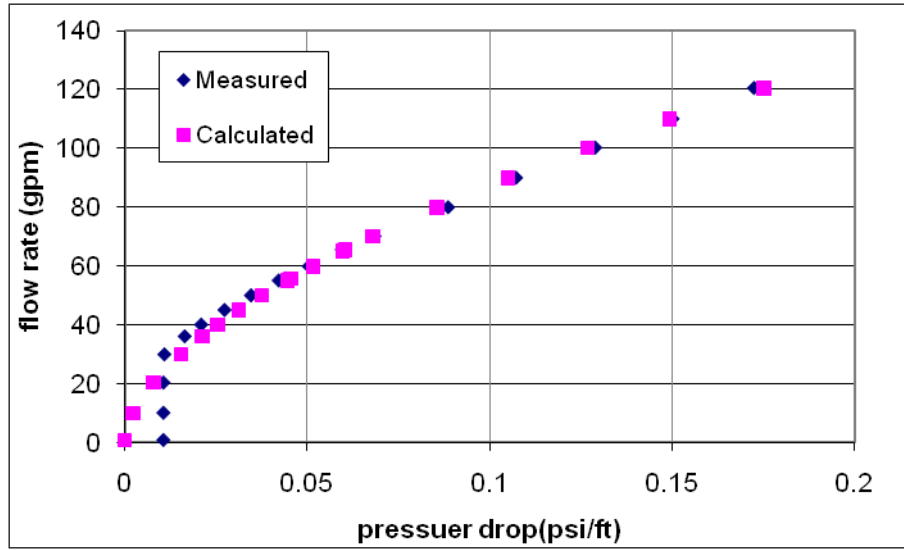


Figure 5.30 Comparing Measured and Calculated Single-Phase Friction Pressure Drop in Horizontal Test Section

CHAPTER VI

THEORY

Gasified (aerated) fluids, having 2-phases, are commonly used in drilling operations, especially for achieving underbalanced conditions. While adjusting the flow rates for each phase, common application is to adjust liquid phase for proper cuttings transport, and to adjust gas phase for controlling bottomhole pressure. Since each of these phases flow with relatively different local velocities, occurred various flow patterns leads to fluctuations in hole cleaning performance as well as frictional pressure losses. These flow patterns are influenced by hole inclination, geometry, and presence of cuttings.

In this chapter, the flow pattern determination, void fractions of each phase and the pressure loss estimation methods are presented in details for cutting-liquid and gas-liquid two phase Newtonian fluids flow in horizontal section. Also mechanistic models are proposed for estimating the pressure losses and void fractions of each phase based on fundamental of physics and mathematics for both gas-liquid two phase Newtonian fluids flow and cutting-gas-liquid two phases Newtonian fluids flow through eccentric annuli by considering the effect of inner pipe rotation in horizontal, inclined and vertical sections.

6-1 Flow Pattern Identification for Cutting-Liquid and Gas-Liquid Two Phase Flow

There is no standard method for classifying and defining the flow pattern, i.e., the investigator's personal interpretation is the usual approach for development of flow pattern map in annulus geometry (Sunthakar 2000). For a given flow condition, different observers may have different definitions of flow regime. In the present study, the flow patterns were defined base on the investigator's visual observations. Also the classification of these flow pattern and determination of boundaries between them were carried out by using quadratic discriminant analysis.

After analyzing the experimental results and verifying them using high speed camera recordings, the flow patterns observed in the horizontal annulus test section are described and named using the similar analogies with two phase flow in pipes. The proposed two-phase flow pattern classification is presented in figure 6.1 for gas-liquid two phase flow and in figure 6.2 for cutting-water two phase flow. Because the visually observed flow patterns were very similar to those observed in pipe flow, it was not required to describe them in details. Thus, the similar flow pattern classification terminology is used in this study. It was observed that, two or more flow patterns occurred at the same gas-liquid and cutting-liquid flow rate conditions, and none of them were fully developed, so they were termed to be the transition zones between those.

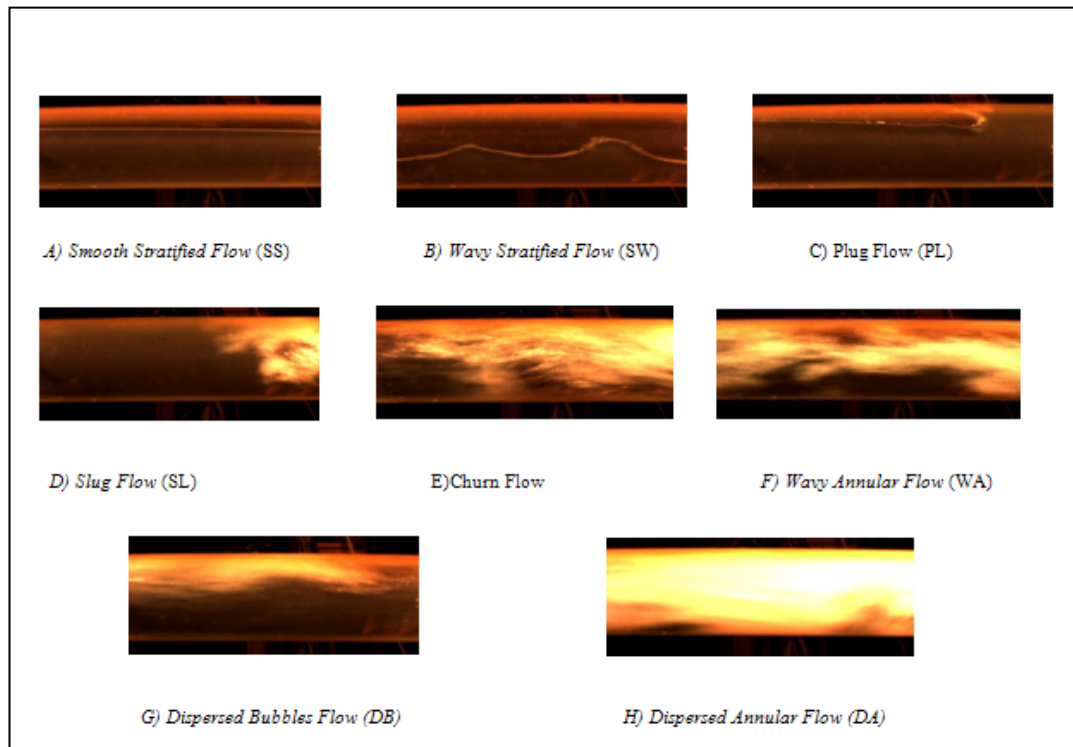


Figure 6.1 Flow Patterns for Horizontal (Air-Water) Flow without Drill pipe Rotation

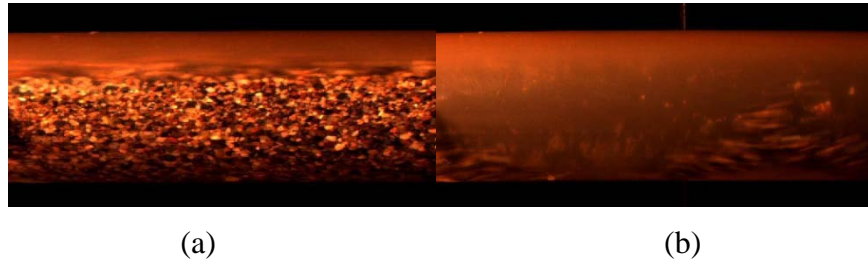


Figure 6.2 Flow Patterns for Horizontal (Cutting-Water) Flow with or without Drill pipe Rotation a) Flow with Bed Existence (b) Dispersed Flow

6-1-1 Discriminant Analysis

Originally developed in 1936 by R.A. Fisher, discriminant analysis is a statistical technique which allows the researcher to study the differences between two or more groups of objects with respect to several variables simultaneously. Discriminant analysis considers a set of vectors of observations x of an object or event, each of which has a known type y . This set is referred to as the training set. The problem is, then, to determine for a given new observation vector, what the best class should be. Based on the training set, the technique constructs a set of functions of the predictors, known as discriminant functions. There are different types of discriminant functions; mainly linear, quadratic, diagquadratic and mahalanobis. These discriminant functions are used to predict the class of a new observation with unknown class. For a k class problem, k discriminant functions are constructed. Given a new observation, all the k discriminant functions are evaluated and the observation is assigned to class I , if the i th discriminant function has the highest value. In quadratic discriminant analysis, there is no assumption that the covariance of each of the classes is identical. This property can be used in classification of flow patterns. Diagquadratic discriminant analysis is similar to 'quadratic', but with a diagonal covariance matrix estimate

6-1-2 Development of Flow Pattern Map by Using Discriminant Analysis Gas-Liquid Two Phase Flow in Horizontal Section

Definitely, classification of flow pattern as well as determination of transition conditions and boundary location has been an essential step in order to predict two-

phase flow behavior in annuli. In presented study, quadratic discriminant analysis method was used to conquer this issue. Through the conduction of experiments, data set containing measurements on several variables such as water and air flow rates and annular test section pressure and temperature were recorded for different flow patterns. Now the question is how we can determine the boundary of each flow pattern by using statistical method. This is the problem of classification. This section illustrates classification by applying it to current experimental data, using the Matlab Statistics Toolbox step by step. These data consists of measurements on the water and air flow rates and annular test section pressure and temperature of 400 data points. There are 15-70 specimens from each of seven groups. In order to consider the effect of flow geometry and annular section pressure, superficial Reynolds number of liquid and gas were calculated. These data were load in matlab statistical tool box and all flow patterns are indicated on the flow map of the superficial Reynolds number presented in figure 6.3.

```
load Lastflowpattern
NSg = Lastflowpattern(1:407,2);
NSl = Lastflowpattern(1:407,1);
group = Lastflowpattern(1:407,3);
h1 = gscatter(NSg,NSl,group, 'r','xosdhpv');
set(h1, 'LineWidth',2)
axis([10 98000 2500 85000])
xlabel('Gas Sup. Reynolds number ')
ylabel('Mud Sup. Reynolds number')
title(' Classification with Two Phase Flow Data')
```

As shown in flow pattern map, the flow pattern change do not occurred suddenly. It occurred gradually by forming a zone of transition. This transition zone was clearly observed between churn flow and wavy annular flow as well as between wavy annular and dispersed annular flow, but the difference between flow patterns can be distinguished. In this study, Figure 6.3 was obtained by using just the two columns containing experimental measurements. After obtaining superficial Reynolds number of liquid and gas from measured data, it is required to determine its corresponding flow pattern on the basis of those measurements.

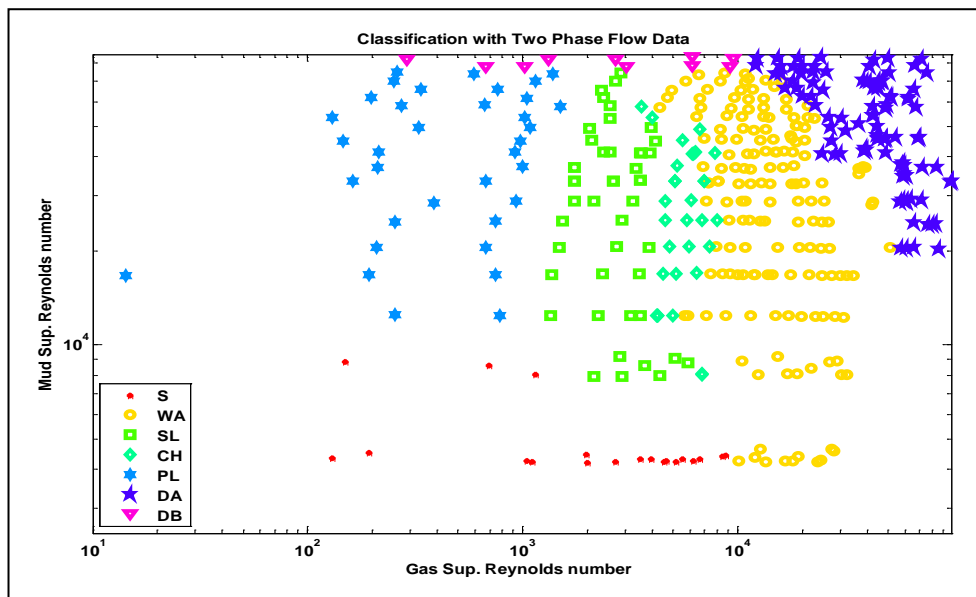


Figure 6.3 Flow Pattern Map for Horizontal Air-Water Flow without Drill Pipe Rotation

One approach to solving this problem is known as discriminant analysis. In matlab statistical tool box, the classify function can perform classification using different types of discriminant analysis. In this study, the superficial Reynolds number of liquid and gas data were classified using the default diagquadratic method.

```
[X,Y] = meshgrid(linspace(2500,83362),linspace(14,98053));
X = X(:); Y = Y(:);
[C,err,P,logp,coeff] = classify([X Y],[NSg NSl],...
                                group,'diagquadratic');
```

Classify also returns an estimate err of the misclassification error rate based on the training data. This function returns the apparent error rate, i.e., the percentage of observations in training that are misclassified, weighted by the prior probabilities for the groups. Of the 400 specimens, 11.45% or 44 specimens are misclassified by the diagquadratic discriminant function. This fact is indicated in workspace part of Matlab.

The diagquadratic discriminant function has separated the plane into regions divided by curves, and assigned different regions to different species

```
hold on;
K = coeff(1,2).const;
```

```

L = coeff(1,2).linear;
Q = coeff(1,2).quadratic;
f23 = sprintf('0 = %g+%g*x+%g*y+%g*x^2+%g*x.*y+%g*y.^2',...
             K,L,Q(1,1),Q(1,2)+Q(2,1),Q(2,2))
h3 = ezplot(f23,[8300 13000 16000 2500]);
set(h3,'Color','k','LineWidth',2)

```

One way to visualize these regions is to plot the borders of regions (see fig. 6.4) and to obtain the boundary equations as quadratic type equations (See equation 6.1). The equation coefficients obtained are given in table 6.1 for different flow patterns.

$$F = a + bN_{Re_{SG}} + cN_{Re_{SL}} + dN_{Re_{SG}}^2 + fN_{Re_{SL}}^2 \quad 6.1$$

Where $N_{Re_{sg}}$ and $N_{Re_{sl}}$ are described as follow:

$$N_{Re_{SG}} = \frac{V_{SG} \rho_G (D_{wh} - D_{dp})}{\mu_G} \quad 6.2$$

$$N_{Re_{SL}} = \frac{V_{SL} \rho_L (D_{wh} - D_{dp})}{\mu_L} \quad 6.3$$

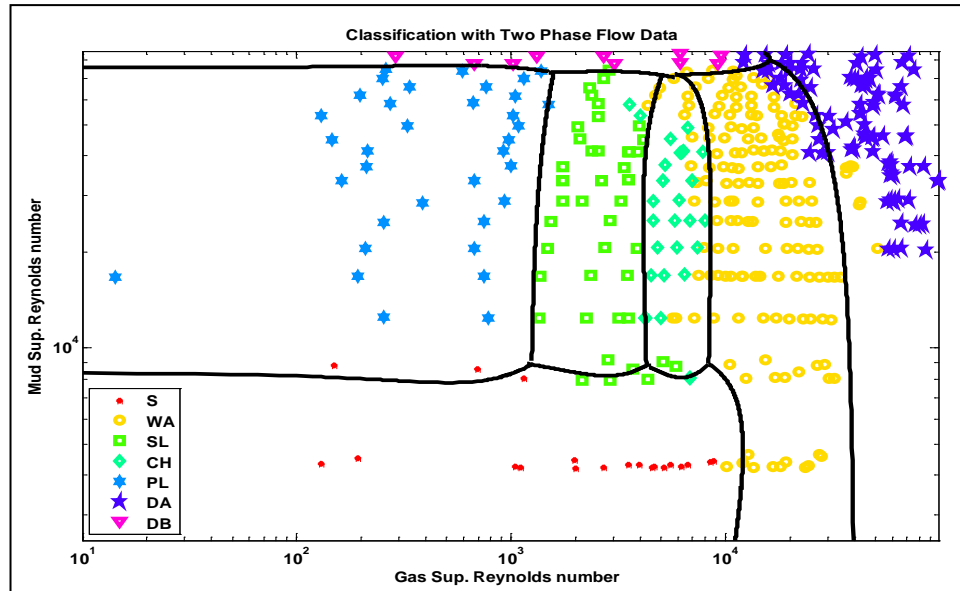


Figure 6.4 Boundaries between Various Flow Patterns Determined by Using Diagqu-adratic Discriminant Analysis Method

Table 6.1: Boundary Equation Coefficients

Boundary Equation Between	Function	a	b	c	d	f
S - PL	f26	-1.803	0.0032	0.002	3.12×10^{-6}	-2.1×10^{-7}
S - SL	f24	1.3584	-0.0026	0.0020	4.64×10^{-7}	-2.10×10^{-7}
S-CH	f25	9.9108	-0.0038	0.0020	3.04×10^{-7}	-2.1×10^{-7}
S-DA	f23	0.9667	0.0002	0.0020	-5.95×10^{-8}	-2.11×10^{-7}
PL- DB	f68	503.54	0.0033	-0.0125	-3.14×10^{-6}	7.78×10^{-8}
PL-SL	f46	-3.162	-0.0006	-1.72×10^{-5}	2.7×10^{-6}	-2.21×10^{-10}
SL-CH	f45	8.5524	-0.0012	-6.22×10^{-5}	-1.6×10^{-7}	1.2×10^{-9}
SH- DB	f48	500.38	0.0027	-0.0126	-4.89×10^{-7}	7.76×10^{-8}
DB-DA	f78	496.4	-0.0002	-0.0125	3.93×10^{-8}	7.77×10^{-8}
DB- WA	f83	-500.7	0.0001	0.0126	-3.39×10^{-8}	-7.80×10^{-8}
WA-CH	f35	8.944	-0.004	-7.4×10^{-5}	3.64×10^{-7}	1.45×10^{-9}
WA-DA	f37	4.403	0.0001	-7.18×10^{-5}	-5.48×10^{-9}	1.57×10^{-10}

For given liquid and gas superficial Reynolds numbers, the equation of boundaries which separated stratified flow from others, are calculated. If these are bigger than zero, the flow pattern is stratified. On the other hand, the other flow patterns boundary equation were investigated in the same way, until the true flow pattern was identified. An excel macro were developed to determined the flow pattern based on given liquid and gas superficial Reynolds numbers using flowchart shown in figure D-1 (See Appendix D). When the data points were considered in flow pattern map (figure 6.4), it is observed that determined boundaries were separated flow patterns from each other with an acceptable accuracy.

6-1-3 Development of Flow Pattern Map by Using Discriminant Analysis Cutting-Liquid Two Phase Flow in Horizontal Section

After analyzing the experimental results and verifying them using high speed camera recordings, two different and general types of regimes in the horizontal annular geometry were observed; i) flow with bed existence, and ii) dispersed flow regime. The proposed two-phase flow pattern classification is presented in figure 6.5.

In this section, diagquadratic discriminant analysis method mentioned in section 6-1-1 was used to determine the flow patterns for liquid and cuttings flow as a function of a dimensionless group for rotation and a dimensionless group for axial flow of mixture, as shown in fig.6–5. Data used for this purpose consists of measurements on the water and cutting flow rates and annular test section pressure and temperature of 250 data points.

One way to visualize these regions is to plot the borders of regions (see fig. 6.5) and to obtain the boundary equations as quadratic type equations (See eq.1)

$$F = 1.9 + 0.00035N_{Re_{CW,mix}} + 7.20 \times 10^{-7} N_{Re_{ro}} - 1.7 \times 10^{-8} N_{Re_{CW,mix}}^2 + 1.90 \times 10^{-10} N_{Re_{ro}}^2 \quad 6.4$$

Where $N_{Re_{CW,mix}}$ and $N_{Re_{ro}}$ are described as follow:

$$N_{Re_{CW,mix}} = \frac{V_z \rho_{mix} (D_{wh} - D_{dp})}{\mu_{C.Lmix}} \quad 6.5$$

$$N_{Re_{ro}} = \frac{V_\theta \rho_{mix} (D_{wh} - D_{dp})}{\mu_{C.Lmix}} \quad 6.6$$

Where ρ_{mix} and $\mu_{C.Lmix}$ are non slip mixture density and non slip mixture viscosity which determined by equations 6.7 and 6.8.

$$\rho_{mix} = \lambda_c \rho_c + (1 - \lambda_c) \rho_L \quad 6.7$$

$$\mu_{C.Lmix} = (1 + 2.5 \lambda_c + 10.05 \lambda_c^2 + 0.00273e^{(16.6 \lambda_c)}) \mu_L \quad 6.8$$

For given the Axial Mixture Reynolds number and tangential Reynolds number, the equation of boundary which separated flow with bed existence from dispersed flow, is calculated. If these are bigger than zero, the flow pattern is flow with bed existence. On the other hand, the flow pattern is dispersed flow.

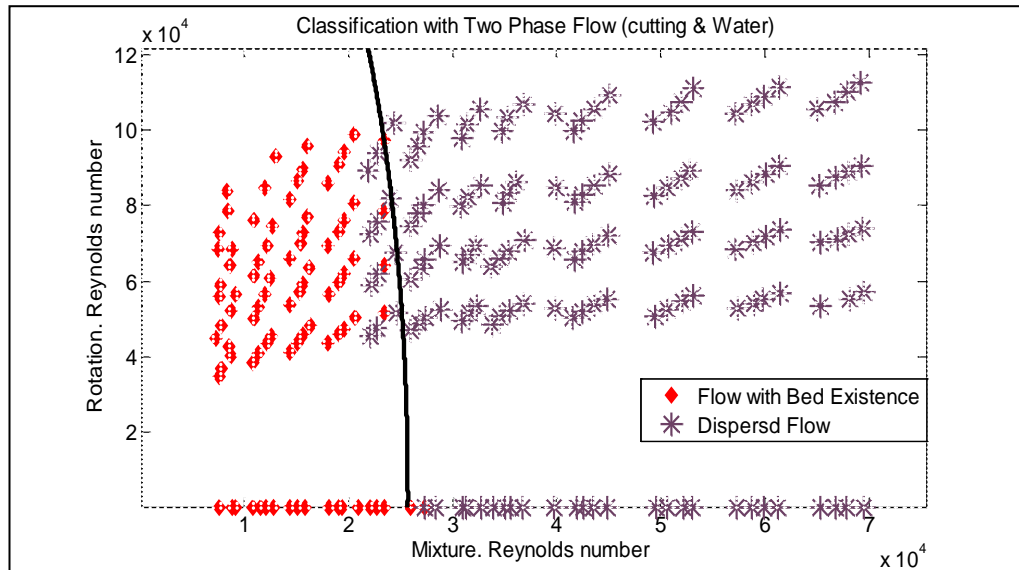


Figure 6.5 Flow Pattern Map for Horizontal Cutting-Water Flow with Drill Pipe Rotation

6-2 Dimensional Analysis to Estimate Liquid Hold up and Friction Pressure Loss in Gas-Liquid Two Phase Flow through Horizontal Eccentric Annuli

6-2-1 Liquid Hold up Prediction

6-2-1-1. Empirical correlation for estimation of liquid holdup for each flow pattern

In case of average volumetric liquid holdup, the experimental data acquired during this study and Sunthakar study (2002) were plotted against the dimensionless group, ratio of superficial liquid velocity to mixture velocity, to observe any correlation existing between phase velocities and liquid holdup (Fig 6.6). The figure shows the same trend between the holdup values against the velocity ratio for different radius ratios. So, it is possible to initiate a correlation.

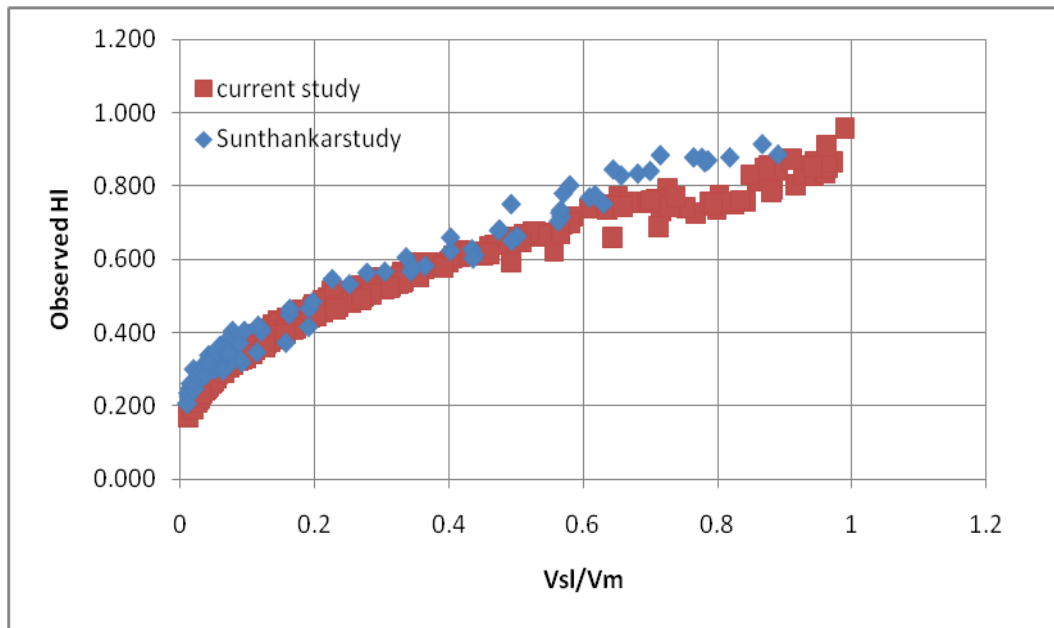


Figure 6.6 Relationships between the Liquid Hold up Values and the Velocity Ratio for Different Geometries

After determination of liquid holdup in previous section, Beggs & Brill (1973) and Lockhart & Martinelli (1949) liquid holdup methods were used to determine the liquid holdup in annuli, using the experimental data. The annular geometry was incorporated into these methods by considering the hydraulic diameter concept, which is used instead of pipe diameter. When obtained results from these methods and identified liquid holdup during the experiments were compared (see Figure 6.7), a considerable difference occurred between the estimated liquid holdup by Beggs & Brill (1973) model and the observed liquid holdup. Moreover, in the case of Lockhart & Martinelli (1969) method, the number of the data points in which liquid holdup could be predicted correctly was increased when compared with Beggs & Brill (1973) method. It is also observed that both models can be adjusted for annular geometries if the constant terms in the equations (equ. 6.9&6.10) are substituted with the proper values. Major reason for this difference is that, these models were developed for two-phase flow through pipes, and hydraulic diameter concept, apparently, was not good enough to explain the annular geometry by itself.

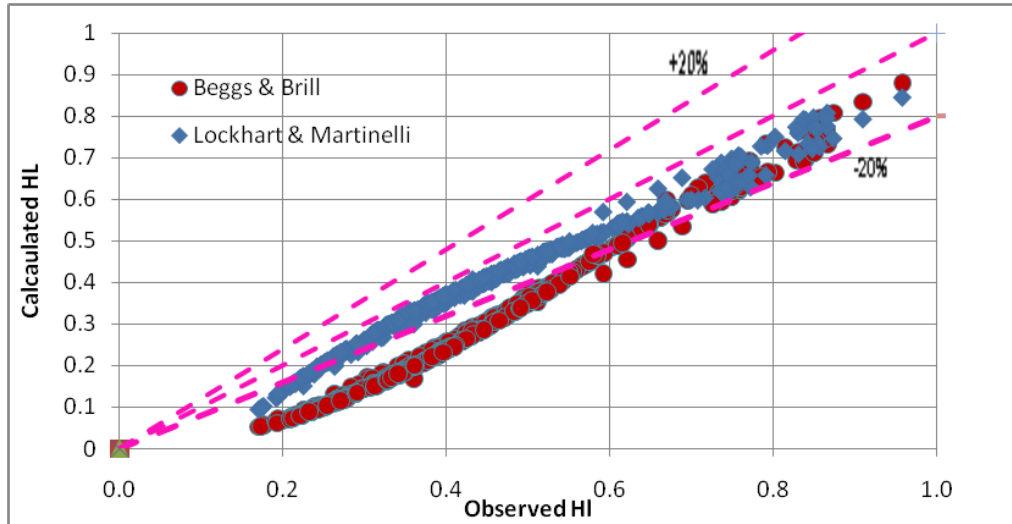


Figure 6.7 Comparisons between Experimental Liquid Hold up for Flow in Annuli and Estimated Liquid Hold up for Flow in Pipes (Beggs & Brill)

In order to determine constants and to modify these two methods, nonlinear least squares method was applied. A Matlab Cod was developed as well as by using Matlab Optimization tool box, the new constants were evaluated and presented in Tables 6.2 & 6.3.

$$H_L = \frac{a\lambda_L^b}{N_{Fr}^c} \quad 6.9$$

$$H_L = a - (1 + X^b)^c \quad 6.10$$

Table 6.2- Evaluated New Constants for Flow in Annuli (Beggs & Brill)

Flow Pattern	a	b	c
Stratified	0.862	0.342	0.014
Churn	0.849	0.341	0.008
Dispersed Bubble	0.901	0.494	-0.002
Plug	0.923	0.671	0.018
Wavy Annular	0.977	0.341	0.038
Slug	0.895	0.393	0.008
Dispersed Annular	0.967	0.314	0.043

Table 6.3- Evaluated New Constants for Flow in Annuli (Lockhart & Martinelli)

Flow Pattern	a	b	c
Stratified	1.000	0.912	-0.380
Churn	0.998	1.000	-0.337
Dispersed Bubble	1.000	1.000	-0.354
Plug	1.000	1.000	-0.332
Wavy Annular	1.000	0.767	-0.393
Slug	1.000	1.000	-0.355
Dispersed Annular	1.000	0.763	-0.380

After that, the modified Beggs & Brill and Lockhart & Martinelli methods were utilized to predict liquid holdup and the results were compared by observed liquid holdup (fig 6.8 & 6.9). As shown in figures 6.8 and 6.9, both modified methods can estimate liquid holdup in horizontal annuli successfully. Standard procedure to calculate liquid holdup for given liquid and gas superficial velocities by using modified Beggs & Brill model is presented as follows:

- a) Identification of flow pattern by applying flow pattern flow chart
- b) Selection of proper constants From table 6.2
- c) Calculation of liquid holdup by using equation 6.9

In order to confirm the accuracy of modified methods, both of them were applied to experimental data obtained from Sunthakar study (2002) (fig 6.10 & 6.11). As shown in these figures, developed methods can predict liquid holdup for different diameter ratios in horizontal annuli.

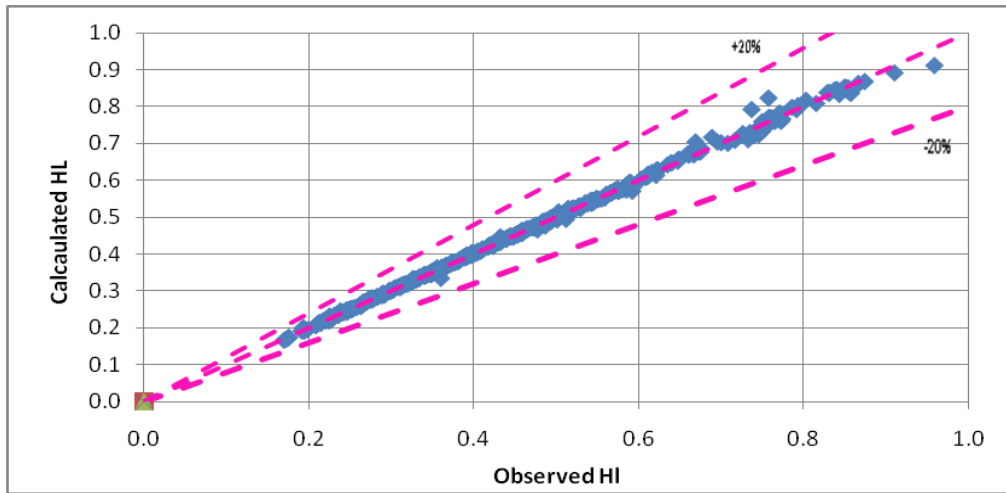


Figure 6.8 Comparisons between Experimental Liquid Hold up and Estimated Liquid Hold up for Flow in Annuli (Modified Beggs & Brill)

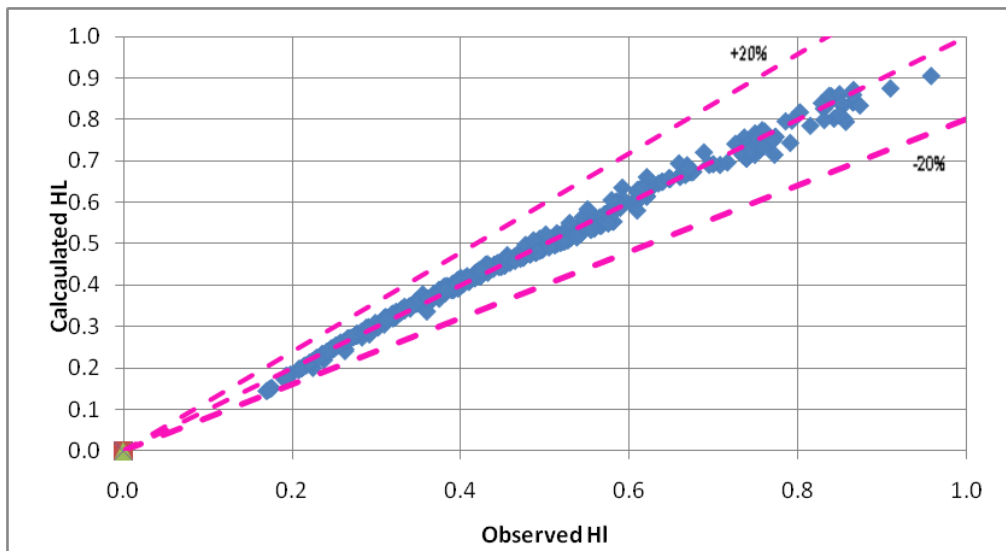


Figure 6.9 Comparisons between Experimental Liquid Hold up and Estimated Liquid Hold up for Flow in Annuli (Modified Lockhart & Martinelli)

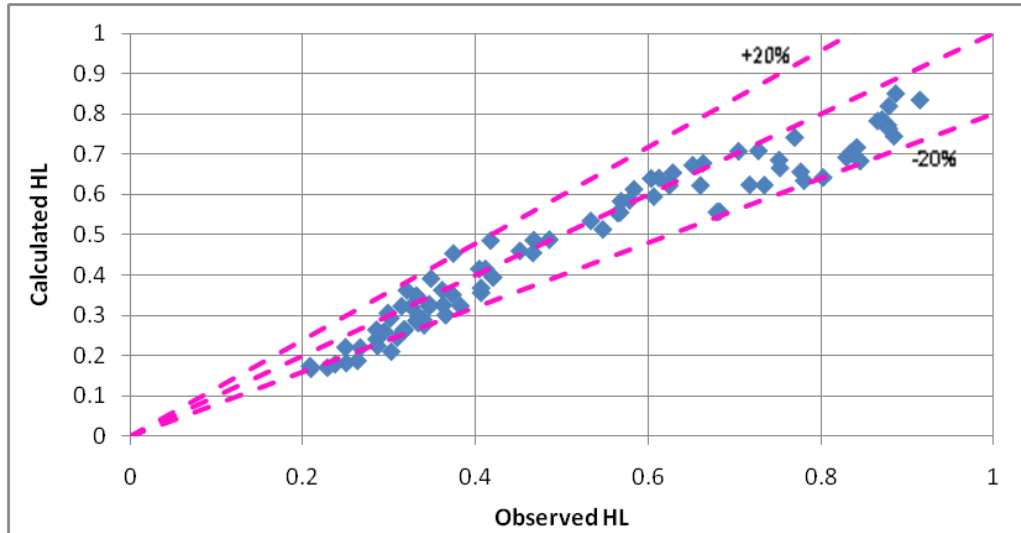


Figure 6.10 Comparisons between Experimental Data Obtained from Sunthankar Study and Estimated Liquid Hold up for Flow in Annuli (Modified Beggs & Brill)

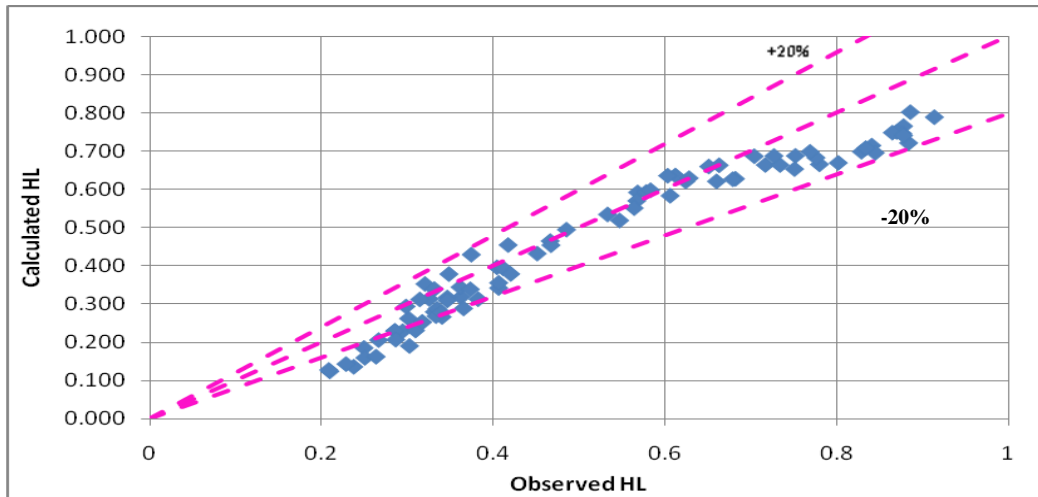


Figure 6.11 Comparisons between Experimental Data Obtained from Sunthankar Study and Estimated Liquid Hold up for Flow in Annuli (Modified Lockhart & Martinelli).

6-2-1-2. Empirical correlation for estimation of liquid holdup without consideration of flow pattern:

After determination of liquid holdup by using image analysis technique, and considering the relationship between no slip hold up and slip hold up (see fig.6.6), equation (6.11) was developed to describe the relationship between no slip liquid hold up and slip liquid hold up.

$$H_L = 0.841\lambda_L^{0.371} \tag{6.11}$$

Equation (6.11) was applied to experimental data obtained from this study and Sunthankar study (2002) (fig 6.12) in order to confirm the accuracy of its outcome. As shown in figure 6.12, developed equation can predict liquid holdup for different diameter ratios in horizontal annuli.

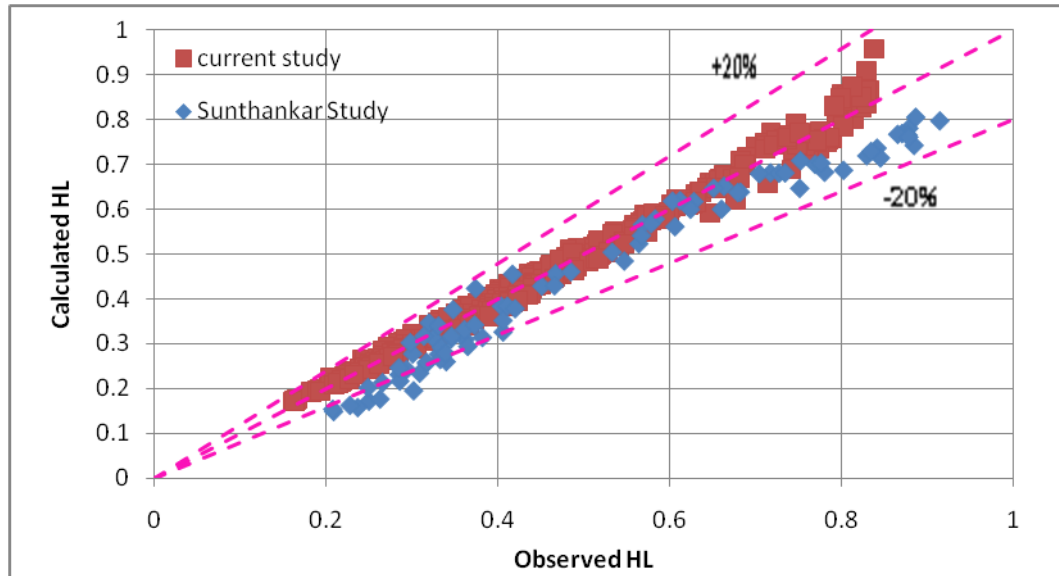


Figure 6.12 Comparisons between Experimental Data Obtained from Current Study and Sunthankar Study and Estimated Liquid Hold up for Flow in Annuli by Using Equation (6.11)

6-2-2 Friction Pressure Loss Prediction

The frictional pressure loss calculation for two-phase fluid flow is based on the same basic principles applied for the calculation of friction pressure loss for the single phase fluid flow. The most important factor which should be considered during the in calculation of pressure difference is the geometry of the flow field. Most of developed empirical and mechanistic methods so far are generally designed for the pipe and in order to calculate annular pressure loss, the general principles was to use the hydraulic diameter concept to introduce geometry of the flow field. Usually Beggs & Brill (1973) model is applied to estimate pressure drop though pipes in multiphase flow. Also this model sometimes used to predict the behavior of multiphase flow into the annuli by considering hydraulic diameter to describe annular geometry. In this study, Beggs & Brill (1973) model was applied to experimental data obtained from this study and Sunthankar study (2002) in order to estimate pressure drop in annular test section by taking into account the annular

geometry and experimental conditions. An excel macro was developed in order to perform this issue (Appendix E). After that, the resulted pressure drops were compared by observed pressure drop. It was observed that this model cannot be estimated pressure drop accurately in annulus geometry (see figures 6.13 & 6.14).

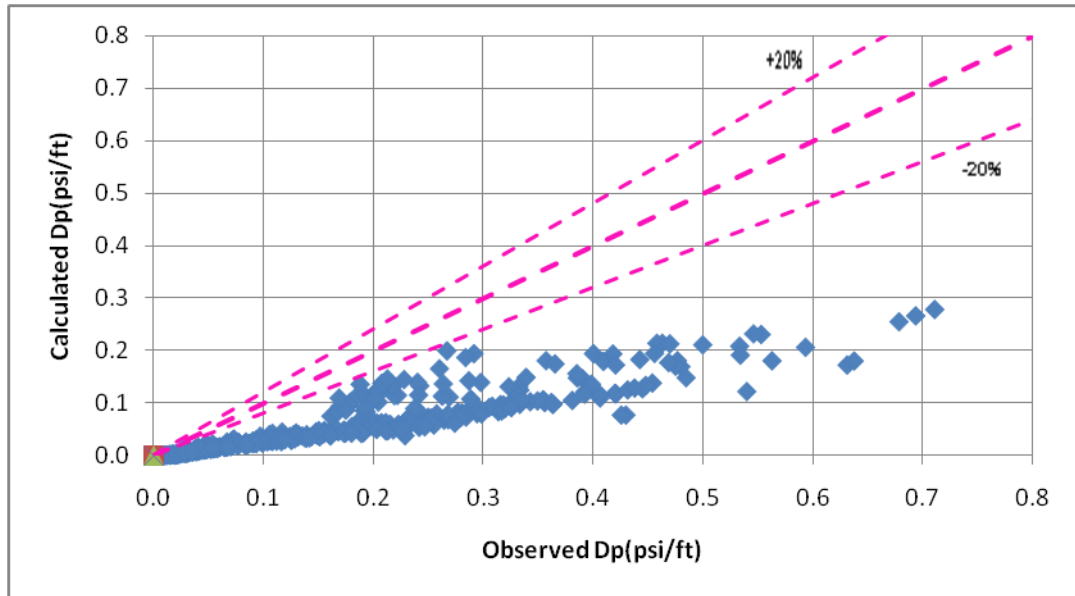


Figure 6.13 Comparisons between Experimental Data Obtained from Current Study and Estimated Friction Pressure Drop for Flow in Annuli by Using Beggs & Brill Method

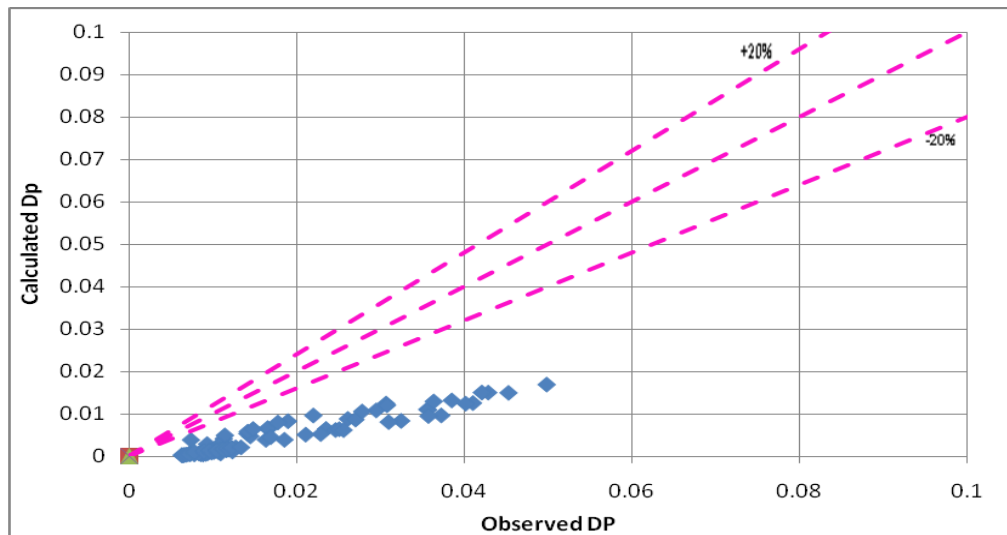


Figure 6.14 Comparisons between Experimental Data Obtained from Sunthakar Study (2002) and Estimated Friction Pressure Drop for Flow in Annuli by Using Beggs & Brill Method

So, in order to estimate the frictional pressure losses accurately, friction factor determined by Beggs & Brill (1973) as a function of Reynolds number and liquid hold up was modified by using presented experimental data. Flow pattern and holdup determination have already been described in previous sections. Neglecting the acceleration term, total pressure gradient (lb/ft²/ft) is equal to the frictional losses.

$$\left. \frac{\Delta P}{\Delta L} \right|_{total} = \frac{f_{TP} \rho_m V_m^2}{2gD_h} \quad 6.12$$

where V_m and f_{TP} are respectively mixture velocity and friction factor. Commonly used method for two-phase flow is to definition the homogeneous mixture density and velocity, as for two-phase flow density and velocity. The homogeneous mixture (mixture) density and velocity were calculated by using equations 6.13 and 6.14 respectively.

$$V_m = v_{SL} + v_{SG} \quad 6.13$$

$$\rho_m = \rho_L \lambda_L + \rho_G (1 - \lambda_L) \quad 6.14$$

During experiments, water and air flow rates and pressure loss were measured and recorded, in the pressure gradient equation; one unknown factor is the friction factor. Friction factors for each individual experiment were calculated and were saved as experimentally observed friction factors by considering equation 6.12, 6.13 and 6.14. In hydraulic calculations, friction factor usually associated with the Reynolds number and is defined as a function of it, Therefore, in this study, for the two-phase fluid, a "mixture" Reynolds number was defined, and the relationship between it and experimentally observed friction factor was analyzed.

"Mixture" Reynolds number and mixture viscosity can be determined by using equations 6.15 & 6.16.

$$N_{Re_{GW.mix}} = \frac{928 v_m \rho_m D_h}{\mu_m} \quad 6.15$$

$$\mu_m = \mu_L \lambda_L + \mu_G (1 - \lambda_L) \quad 6.16$$

Figure 6.15 is given the relationship between mixture Reynolds number and experimentally observed friction factor for current experimental data. As shown in Figure 6.14, although there is a relationship between the friction factor and mixture Reynolds number, the confusion and disorder is seen in part in which a small Reynolds number is smaller than 100000. In this case, an obtained friction factor for small Reynolds numbers may cause a serious error in pressure gradient calculation. Therefore, in order to obtain the friction factor, different correlations has been needed and discussed in later sections.

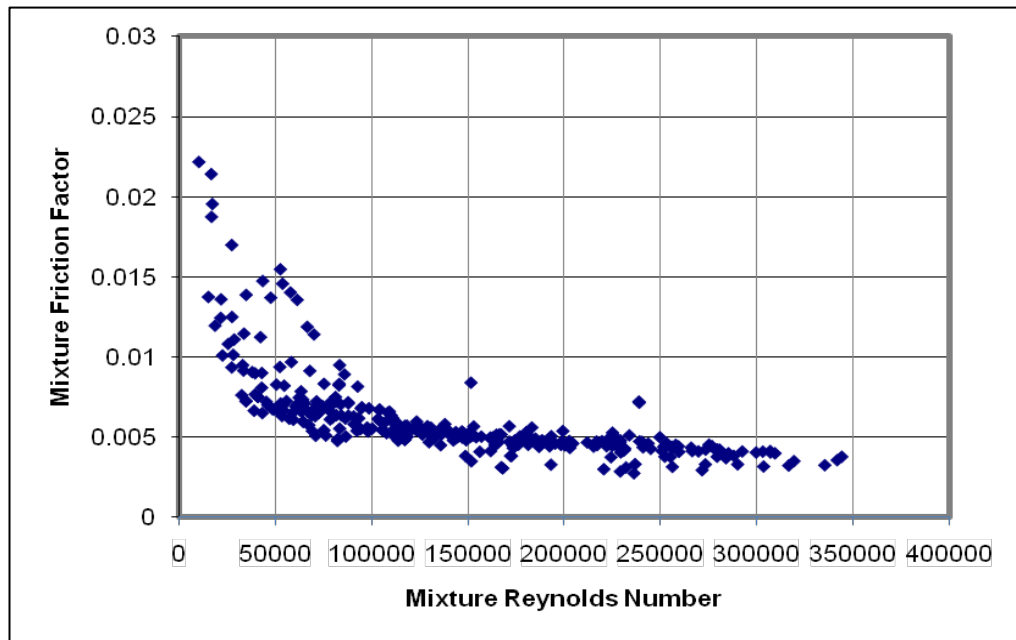


Figure 6.15 Relationships between Mixture Friction and Mixture Reynolds Num-ber

6-2-2-1 New Developed Friction Factor for Gas-Liquid Two Phase Flow in Horizontal Eccentric Annuli

In order to define accurate friction factor for two phase flow in annuli, firstly individual Reynolds numbers for liquid and gas phases was considered instead of a mixture Reynolds number and relationship between them and friction factor was investigated to create a useful correction by using Matlab statistical tool box and applying Robust regression (Appendix F) (Figure 6.16).

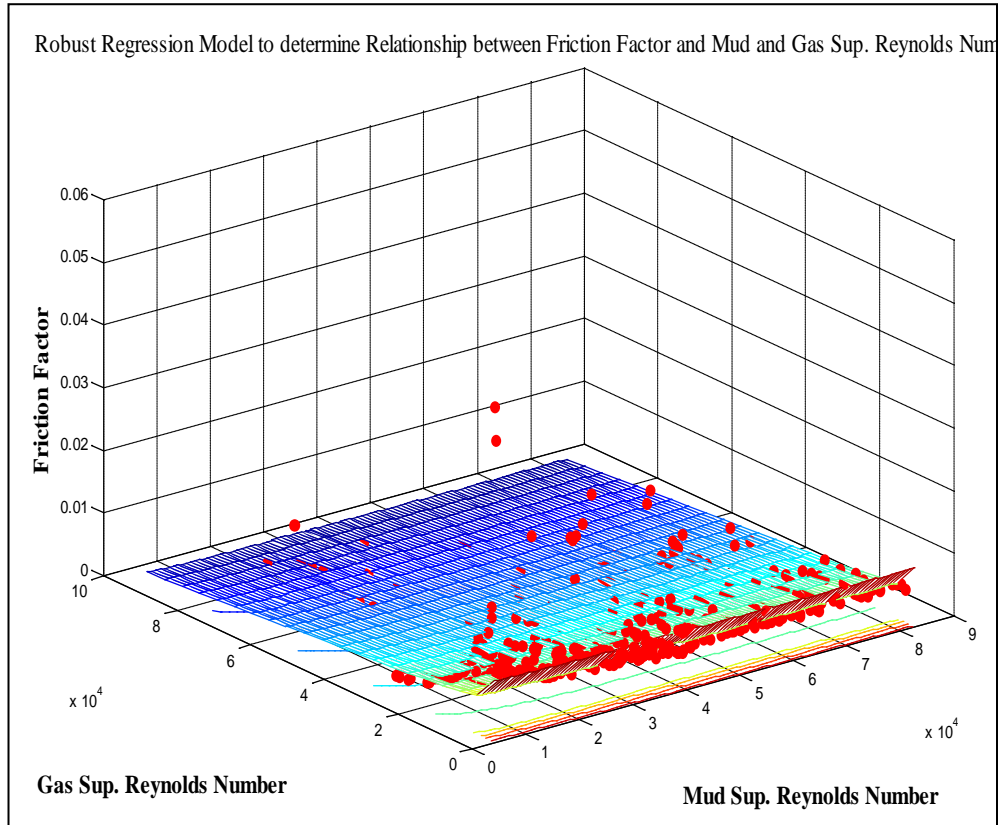


Figure 6.16 Relationships between Liquid and Gas Superficial Reynolds Number and Experimentally Observed Friction Factor for Current Experimental Data

Figure 6.16 is given the relationship between liquid and gas superficial Reynolds number and experimentally observed friction factor for current experimental data. Here, the red dots represent friction factor observed through experiments, and the surface is shown the generated correlation. Correlation obtained from figure 6.16 is presented in equation 6.17. The correlation's constants are summarized in the table 6.4.

$$f_f = a + b N_{Re_{SL}} + c N_{Re_{SG}} + d \ln(N_{Re_{SL}}^2) + e \ln(N_{Re_{SG}}^2) \quad 6.17$$

Figure 6.17 is given the comparison between the friction factor calculated by equation 6.17 obtained by applying robust regression analysis and experimentally observed friction factors.

Tablo-6.4 Equation Coefficients Obtained by Robust Regression

Constants	Robust regression
a	0,0140
b	6,50E-09
c	-3,42E-08
d	-0,0002
e	-0,0003

As seen in Figure-6.17, the friction coefficient was estimated successfully by using equation 6.17.

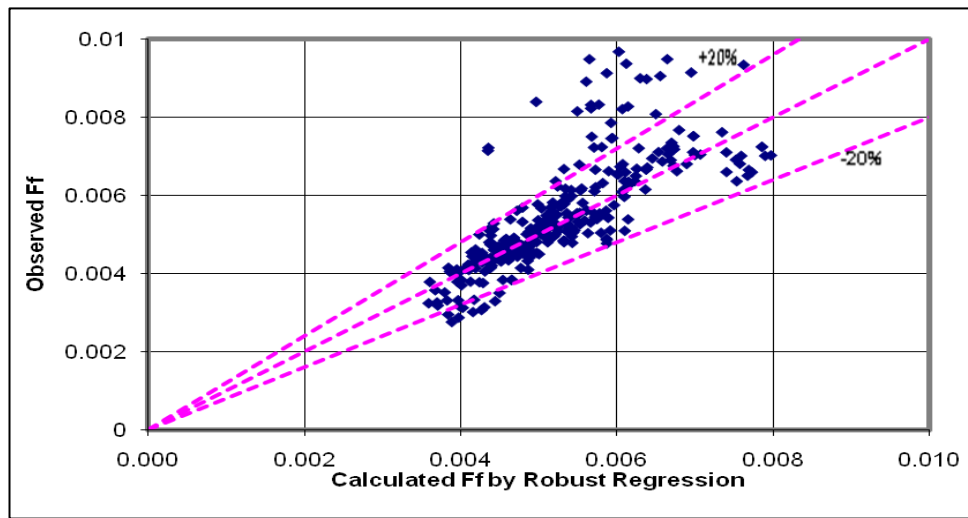


Figure 6.17 Comparisons between the Friction Factors Calculated by Equation 6.17 Obtained by Applying Robust Regression Analysis and Experimentally Observed Friction Factors

Figure 6.18 is given the comparison between calculated pressure gradients by using Friction coefficients obtained by this method and measured pressure gradients. As shown in Figure 6.18, pressure gradients calculated quite successfully. It can be concluded that robust regression analysis method estimate friction factor with an acceptable accuracy and equation 6.17 can be applied in order to estimate friction factor for two phase flow in horizontal annuli.

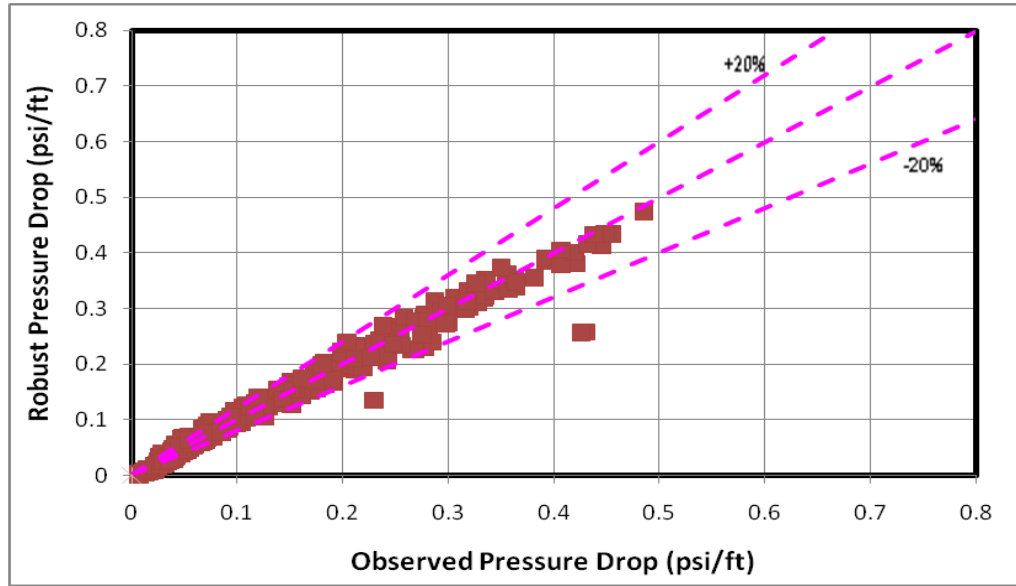


Figure 6.18 Comparison between Calculated Pressure Gradients by Using Friction Coefficients Obtained by Robust Regression Analysis Method and Measured Pressure Gradients

6-2-2-2 Modified Beggs & Brill (1973) Method

In the second part of this section, Based on experimentally observed friction factors, friction factor determined by Beggs & Brill (1973) was modified and redefined as a function of no slip liquid hold up, slip liquid hold up and Reynolds number by using Matlab optimization tool box and applying Nonlinear Least Squares Method (see equations 6.18, 6.19, 6.20 & 6.21)

$$y = \frac{\lambda_L}{H_L^3} \quad 6.18$$

$$S = \frac{\ln(y)}{-3.567 + 8.12 \ln(y) - 6.697 [\ln(y)]^2 + 1.915 [\ln(y)]^4} \quad 6.19$$

$$f_n = \frac{1}{\left[2 \log \left(\frac{N Re_{GW.mix}}{4.5223 \log(N Re_{GW.mix}) - 3.8215} \right) \right]^2} \quad 6.20$$

$$f_{TP} = f_n e^S \quad 6.21$$

By substituting calculated friction factor by equation 6.21 in equation 6.12 pressure drop can be estimated for two phase flow through horizontal annuli. Modified method for estimating frictional pressure losses are compared with experimental data obtained from this study and sunthankar study (2002) and it has been observed that the frictional pressure losses can be estimated with a reasonable accuracy(see fig 6.19 and 6.20).

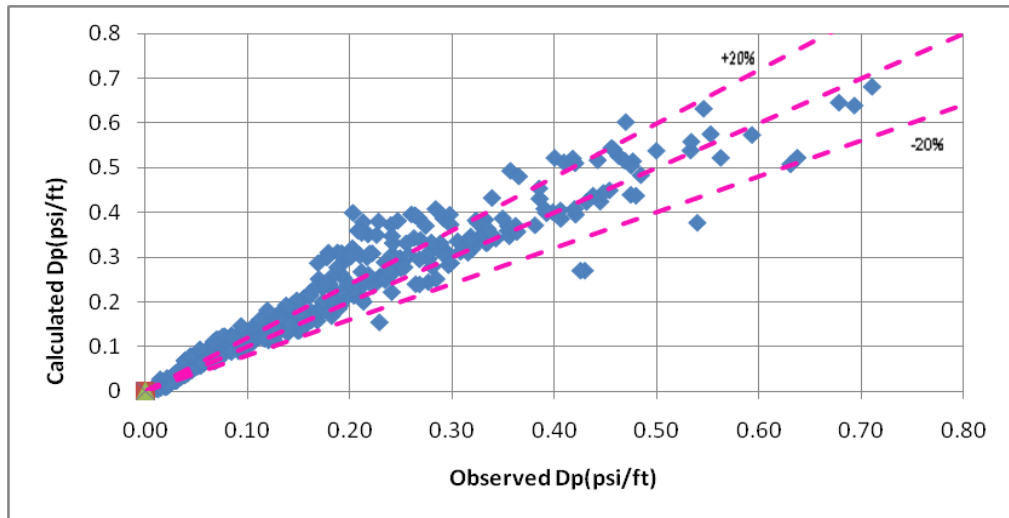


Figure 6.19 Comparisons between Experimental Data Obtained from Current Study and Estimated Friction Pressure Drop for Flow in Annuli by Using Modified Beggs & Brill Method

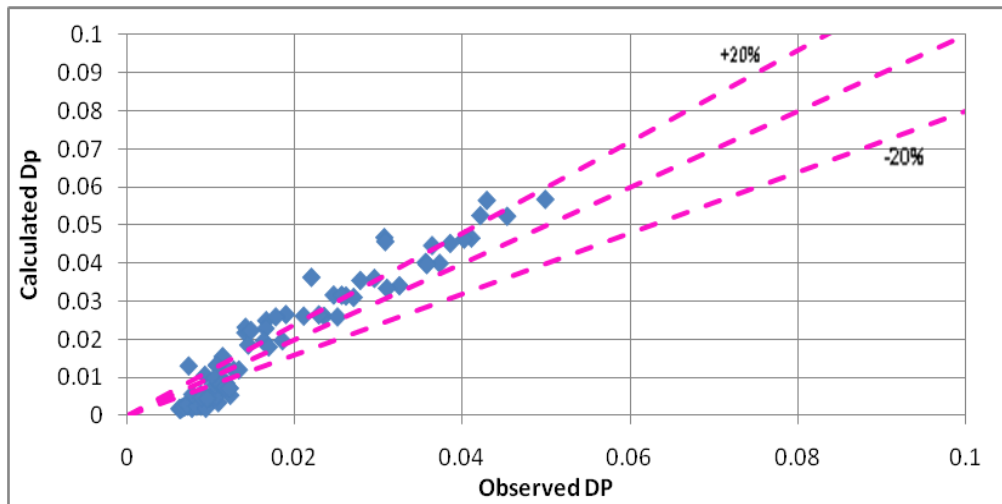


Figure 6.20 Comparisons between Experimental Data Obtained from Sunthankar Study and Estimated Friction Pressure Drop for Flow in Annuli by Using Modified Beggs & Brill Method

6-2-2-3 Modified Lockhart & Martinelli (1949) Method

Another method used to calculate the pressure gradient two phase flow in pipe posed by Lockhart & Martinelli (1949). In this method, total pressure gradient was obtained by multiplying liquid or gas surface pressure gradient and dimensionless pressure gradient parameters (ϕ_L & ϕ_G). Mathematical description of this method is given below.

$$\frac{\Delta P}{\Delta L} = \phi_L^2 \left(\frac{\Delta P}{\Delta L} \right)_{SL} = \phi_G^2 \left(\frac{\Delta P}{\Delta L} \right)_{SG} \quad 6.22$$

Where (ϕ_L) , (ϕ_G) , $\left(\frac{\Delta P}{\Delta L} \right)_{SG}$ and $\left(\frac{\Delta P}{\Delta L} \right)_{SL}$ are respectively liquid, gas dimensionless pressure gradient parameter and gas, liquid surface pressure gradients. Generally, dimensionless pressure gradient parameter (ϕ_L) is associated with Lockhart-Martinelli parameter (X) (see equ. 6.23).

$$X = \sqrt{\frac{\left(\frac{\Delta P}{\Delta L} \right)_{SL}}{\left(\frac{\Delta P}{\Delta L} \right)_{SG}}} \quad 6.23$$

Where

$$\left(\frac{\Delta P}{\Delta L} \right)_{SL} = \frac{2}{D_h g} C_L \left[\frac{1488 v_{SL} \rho_L D_h}{\mu_L} \right]^{-n} \rho_L v_{SL}^2 \quad 6.24$$

$$\left(\frac{\Delta P}{\Delta L} \right)_{SG} = \frac{2}{D_h g} C_G \left[\frac{1488 v_{SG} \rho_G D_h}{\mu_G} \right]^{-m} \rho_G v_{SG}^2 \quad 6.25$$

$C_L = C_G = 16$ and $m = n = 1$ for laminar flow, $C_L = C_G = 0.046$ and $m = n = 0.2$ for turbulent flow.

Lockhart-Martinelli parameter (X) and dimensionless pressure gradient parameter (ϕ_L) can be calculated for current experimental data by considering the

equations 6.23, 6.24, 6.25 and 6.22. The relationship between Lokhart-Martinelli parameter (X) and dimensionless pressure gradient parameter (ϕ_L) are shown figure 6.21 for current experimental data. As a result of this relationship equation between ϕ_L and X , are defined as follows.

$$\phi_L = 2.717X^{-0.5901} + 1.085 \quad 6.26$$

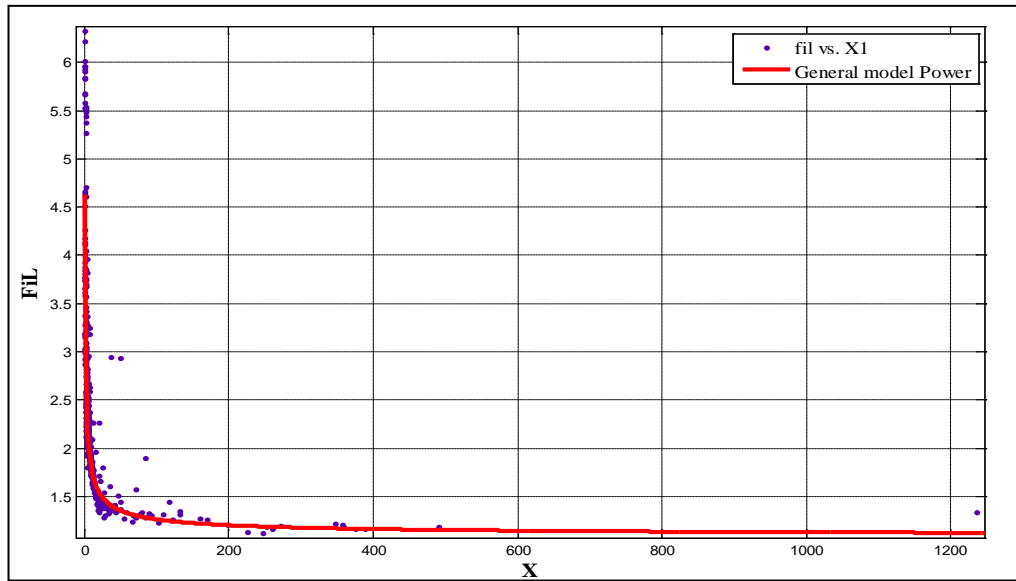


Figure 6.21 Relationship between Liquid Dimensionless Pressure Gradient Parameter and Liquid Surface Pressure Gradients

So, two phase flow pressure drop can be estimated though horizontal annuli by substituting calculated dimensionless pressure gradient parameter (ϕ_L) by equation 6.26 into equation 6.22. Estimated frictional pressure losses by Modified Lokhart-Martinelli method are compared with experimental data obtained from this study and Sunthakar study (2002) (see figures 6.22 and 6.23). As shown in Figures 6.22 and 6.23, estimated pressure gradient values by using equations 6.22 and 6.26 are in harmony with the measured values for both data sets. These figures also show that for higher gas flow rates, the comparison is better than that at lower gas flow rates.

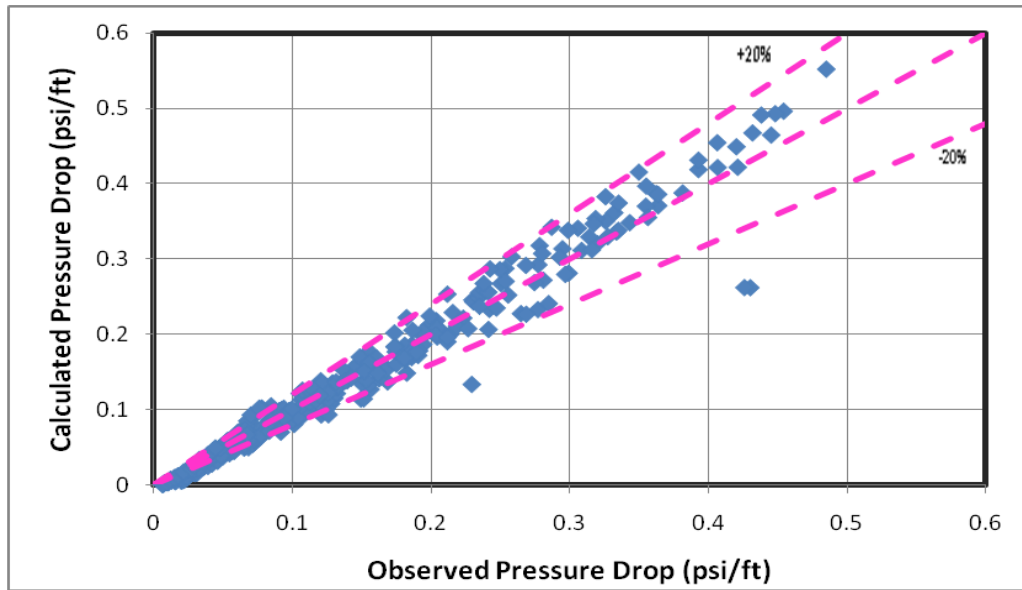


Figure 6.22 Comparisons between Experimental Data Obtained from Current Study and Estimated Friction Pressure Drop for Flow in Annuli by Using Modified Lockhart-Martinelli

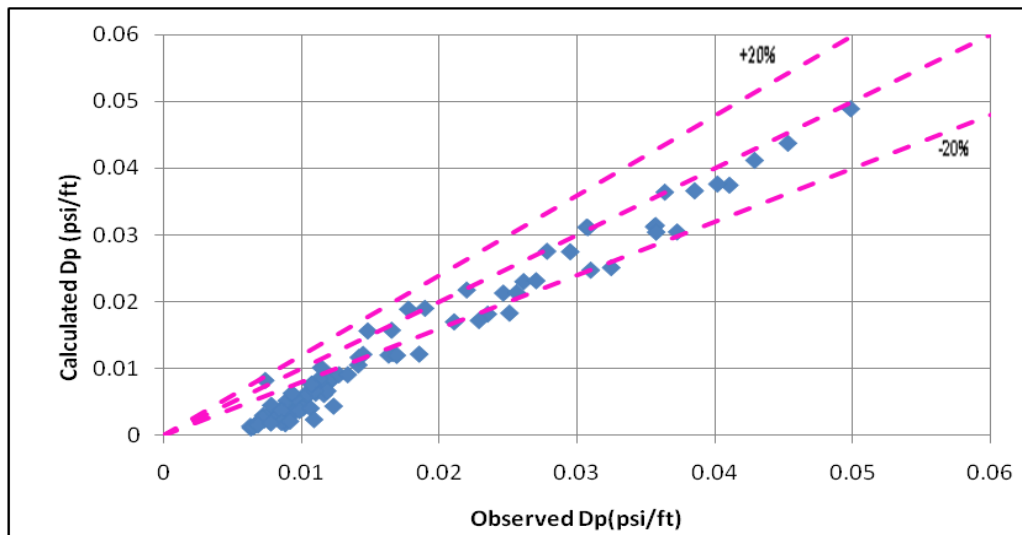


Figure 6.23 Comparisons between Experimental Data Obtained from Sunthankar Study (2002) and Estimated Friction Pressure Drop for Flow in Annuli by Using Modified Lockhart-Martinelli Method

6-3 Dimensional Analysis for Cutting-Liquid Two Phase Flow in Horizontal Eccentric Annuli

Empirical correlations were developed to estimate total and moving cutting concentrations, bed height, bed area and velocity of moving bed based on experimental data. In this section, also, calculation methodologies for predicting

interfacial friction factor for flow with bed existence and friction factor for dispersed flow pattern are also presented.

6-3-1 Development of Empirical Correlations to Estimate Parameters Measured by Using Image Analysis Technique

Based on the analysis of the influence of three independent variables on cutting concentration and cutting velocity; namely, liquid flow rate, ROP and pipe rotation speed; the following equations were developed to estimate the parameters of interest. In order to determine the equation constants, regression analysis method was applied based on the experimental data.

$$Y = 0.382 + 0.0167F_{C.Lr} - 1.27 \times 10^{-5}N_{Re_{CW.mix}} + 2.42 \times 10^{-7}N_{Re_{ro}} \quad 6.27$$

$$Z = 0.916 + 0.056F_{C.Lr} - 3.66 \times 10^{-5}N_{Re_{CW.mix}} - 4.8 \times 10^{-7}N_{Re_{ro}} \quad 6.28$$

$$C_c = -4.57Z^3 + 4.61Z^2 - 0.122Z + 0.0273 \quad 6.29$$

$$C_{cm} = -24.074Y^3 + 11.32Y^2 - 0.4Y + 0.035 \quad 6.30$$

$$\frac{V_{mact}}{V_z} = 1.835 + 0.072F_{C.Lr} - 4.32 \times 10^{-5}N_{Re_{CW.mix}} - 9.47 \times 10^{-7}N_{Re_{ro}} \quad 6.31$$

$$\frac{H_{bed}}{D_{wh}} = 0.891 + 0.099F_{C.Lr} - 3.7 \times 10^{-5}N_{Re_{CW.mix}} - 7.51 \times 10^{-7}N_{Re_{ro}} \quad 6.32$$

$$\frac{A_c}{A_w} = 0.32 - 0.0624F_{C.Lr} + 1.31 \times 10^{-5}N_{Re_{CW.mix}} - 3.72 \times 10^{-7}N_{Re_{ro}} \quad 6.33$$

where $N_{Re_{CW.mix}}$, $N_{Re_{ro}}$, and $F_{C.Lr}$ are dimensionless group – 1 (pseudo mixture Reynolds number), dimensionless group – 2 (pseudo tangential Reynolds number), and dimensionless group – 3 (pseudo Froude number), respectively. When drill pipe is rotated, it is necessary to consider the effect of both tangential and axial velocities during the calculations. The axial velocity component can be calculated from the average total flow rate (equation. 6.34). In order to determine the tangential velocity component, an annular rotational Couette (Slattery, 1999) flow model was considered (equation. 6.35) (Appendix G).

$$V_z = \frac{4(Q_L + Q_S)}{\pi(D_{wh}^2 - D_{dp}^2)} \quad 6.34$$

$$V_\theta = \frac{K^2 \omega [-D_{wh}^2 + D_{dp}^2 + 2D_{wh}^2 (\log D_{wh} - \log D_{dp})]}{(D_{wh}^2 - D_{dp}^2)(1 - K^2)} \quad 6.35$$

Where k is defined by equation 6.36 and ω is the drill pipe angular velocity.

$$K = \frac{D_{dp}}{D_{wh}} \quad 6.36$$

In general, the resultant velocity can be written as:

$$\vec{u}_m = \vec{V}_z + \vec{V}_\theta \quad 6.37$$

$$N_{Re_{CW.mix}} = \frac{V_z \rho_{mix} (D_{wh} - D_{dp})}{\mu_{C.Lmix}} \quad 6.38$$

$$N_{Re_{ro}} = \frac{V_\theta \rho_{mix} (D_{wh} - D_{dp})}{\mu_{C.Lmix}} \quad 6.39$$

$$F_{C.Lr} = \frac{V_z^2}{g(D_{wh} - D_{dp})} \quad 6.40$$

Where ρ_{mix} and $\mu_{C.Lmix}$ are non slip mixture density and non slip mixture viscosity which determined by equations 6.41 and 6.42.

$$\rho_{mix} = C_c \rho_c + (1 - C_c) \rho_L \quad 6.41$$

$$\mu_{C.Lmix} = (1 + 2.5 \lambda_c + 10.05 \lambda_c^2 + 0.00273 e^{(16.6 \lambda_c)}) \mu_L \quad 6.42$$

The developed empirical correlations were applied to predict parameters and the results were compared by experimental data (fig 6.24 and 6.27). As shown in these figures, developed empirical correlations can estimate mentioned parameters in horizontal annuli with or without inner pipe rotation with acceptable accuracy.

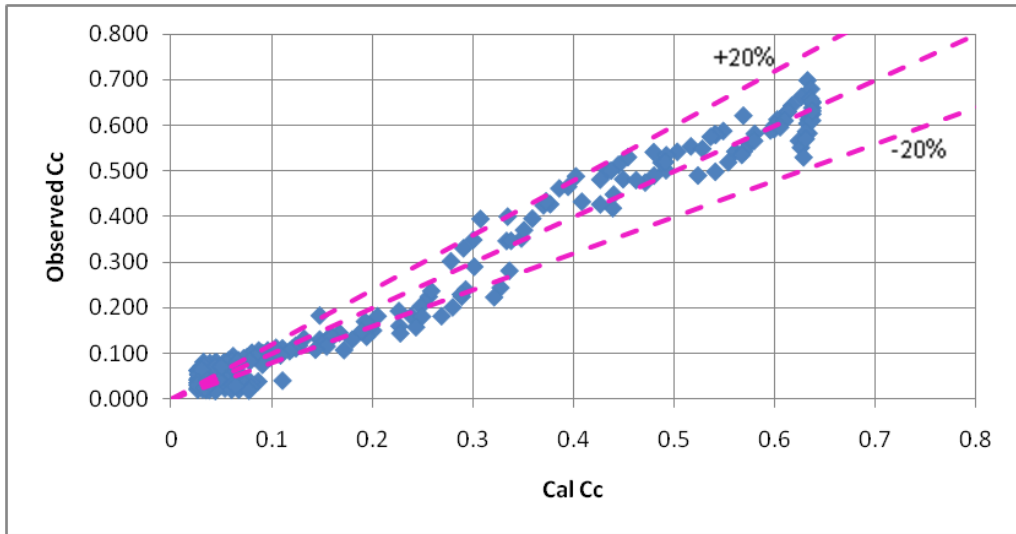


Figure 6.24 Comparisons between Experimental Data Obtained from Current Study and Estimated Cutting Concentration

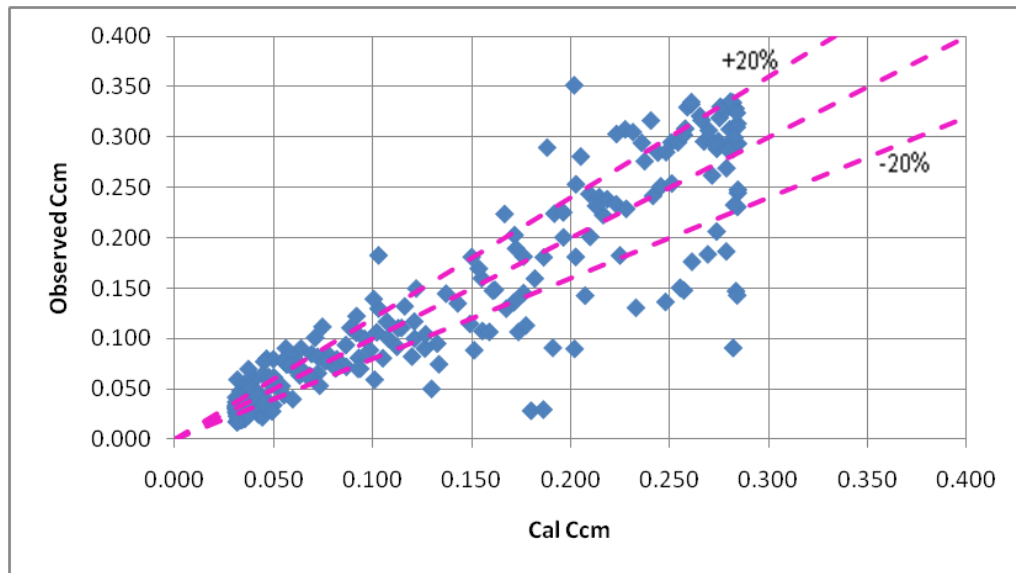


Figure 6.25 Comparisons between Experimental Data Obtained from Current Study and Estimated Moving Cutting Concentration

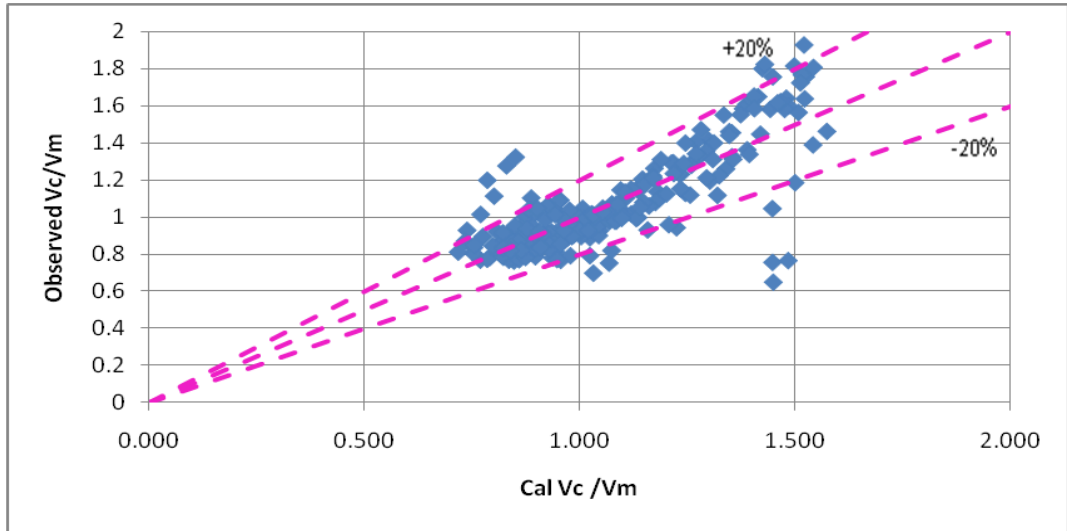


Figure 6.26 Comparisons between Experimental Data Obtained from Current Study and Estimated Ratio of Moving Cutting Velocity to Mud Axial Velocity

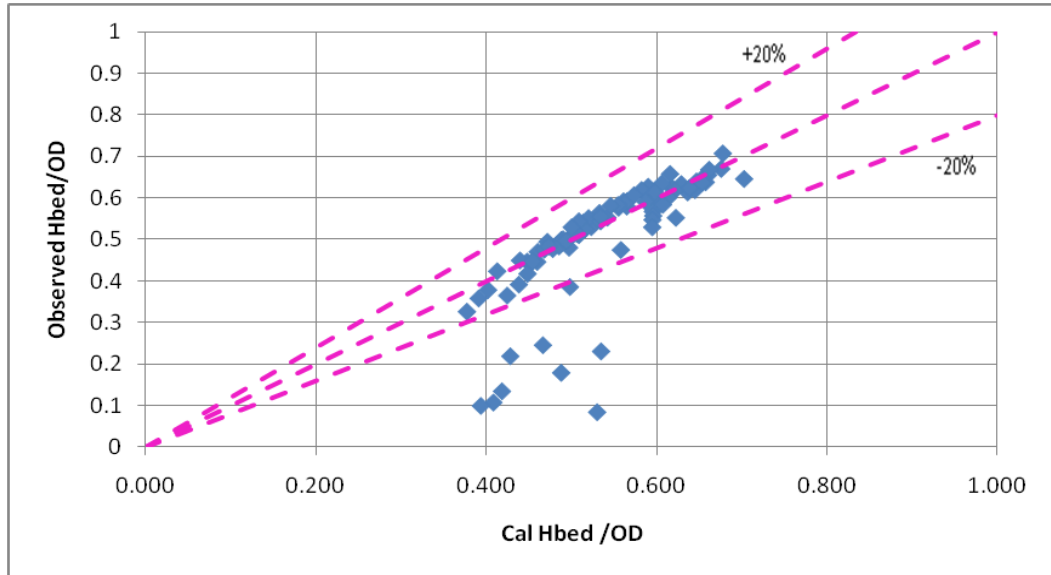


Figure 6.27 Comparisons between Experimental Data Obtained from Current Study and Estimated Ratio of Bed Height to Well Diameter

6-3-2 Determination of Friction Factor for Two Phase Cutting and Liquid Flow in Horizontal Eccentric Annuli

The total pressure gradient for steady-state flow is composed of three components: friction losses, gravity, and convective acceleration. Convective acceleration can be neglected for steady state cases, and long wellbore sections. So, only friction losses component is considered in a horizontal annulus. The friction

effect term is mainly contributed by the interfacial shear stress between the drilling fluid and the annuli walls, and between the drilling fluid and cutting bed.

6-3-2-1 Determination of Interfacial Friction Factor between the Drilling Fluid and Cutting Bed for Flow with Bed Existence Flow Pattern

Few attempts have been proposed to describe interfacial friction factor in the literature. One of the most popular and accepted method is layered models. In this study, a two-layered model is considered. A relationship between interfacial friction factor and dimensionless groups is proposed, initially using the momentum conservation for the layered model, and solving the balance for interfacial shear stress.

Gavignet and Sobey (1996) introduced a 2-layer cuttings transport model for horizontal wells. For each layer, momentum conservation equations are determined. The derived equations for fluid and the cuttings layers are

$$A_f \frac{\partial P}{\partial L} = -\tau_f S_f - \tau_i S_i \quad 6.43$$

$$A_c \frac{\partial P}{\partial L} = -\tau_c S_c + \tau_i S_i \quad 6.44$$

respectively. Here, A_f is the area of flow for the fluid, A_c is the bed area in the wellbore, τ_f is the shear stress due to the fluid, S_f is the surface where τ_f is acting on, τ_c is the shear stress due to the fluid, S_c is the surface where τ_c is acting on, τ_i is the interfacial shear stress between the layers, and S_i is the contact surface between the layers. The shear stresses can be determined using the well-known shear stress definitions as

$$\tau_f = \frac{1}{2} f_F \rho_{fm} u_{fm}^2 \quad 6.45$$

Where f_F is the friction factor between the fluid and moving cutting mixture and annular walls, which is a function of Reynolds number, ρ_{fm} is the fluid and

moving cutting mixture density which flow in upper layer and u_{fm} is the fluid and moving cutting mixture resultant velocity in the upper layer.

$$\rho_{fm} = C_{cm} \rho_C + (1 - C_{cm}) \rho_L \quad 6.46$$

$$u_{fm} = \sqrt{\left(\frac{Q_m}{(A - A_{bed})}\right)^2 + V_\theta^2} \quad 6.47$$

$$Q_m = Q_L + Q_c \quad 6.48$$

$$Q_c = \frac{\pi}{4} D_B^2 ROP \quad 6.49$$

where Q_L is fluid flow rate and Q_c is Cutting flow rate. In a similar manner,

$$\tau_c = \frac{1}{2} f_{Fc} \rho_{cm} u_{cm}^2 + k_f (\rho_C - \rho_L) g (A_c / S_c) (C_c - C_{cm}) \quad 6.50$$

Where f_{Fc} is the friction factor due to cuttings bed, which is a function of Reynolds number as well, and u_{cm} is the average velocity of the cuttings bed. The second term in this equation is due to the static friction between the bed and the wellbore. k_f has a value between 0.2 to 0.5.

$$\rho_{cm} = (C_c - C_{cm}) \rho_C + (1 - (C_c - C_{cm})) \rho_L \quad 6.51$$

$$u_{cm} = \sqrt{\left(\frac{Q_c}{(A)}\right)^2 + V_\theta^2} \quad 6.52$$

Finally, interfacial shear stress can be determined as

$$\tau_i = \frac{1}{2} f_{Fi} \rho_{fm} (u_{fm} - u_{cm})^2 \quad 6.53$$

In this study, following equations were used to calculate friction factor for laminar and turbulent flows in two layer model. For laminar flow

$$f_F = \frac{16}{N_{Re_{CW.mix.l}}} \quad 6.54$$

$$f_{Fc} = \frac{16}{N_{Re_{CW.mix.up}}} \quad 6.55$$

For turbulent flow

$$f_F = \frac{0.0466}{N_{Re_{CW.mix.l}}^{0.2}} \quad 6.56$$

$$f_{Fc} = \frac{0.0466}{N_{Re_{CW.mix.up}}^{0.2}} \quad 6.57$$

Where Reynolds numbers based on the hydraulic diameters of both layers

$$N_{Re_{CW.mix.l}} = \frac{\rho_{fm} u_{fm} (D_{uph})}{\mu_{fm}} \quad 6.58$$

$$N_{Re_{CW.mix.up}} = \frac{\rho_{cm} u_{cm} (D_{loh})}{\mu_{cm}} \quad 6.59$$

Where

$$\mu_{fm} = (1 + 2.5 C_{cm} + 10.05 C_{cm}^2 + 0.00273e^{(16.6 C_{cm})}) \mu_L \quad 6.60$$

$$\mu_{cm} = (1 + 2.5 (C_c - C_{cm}) + 10.05 (C_c - C_{cm})^2 + 0.00273e^{(16.6 (C_c - C_{cm}))}) \mu_L \quad 6.61$$

Equations (from 6.43 to 6.61) were solved by using experimental data in order to find interfacial friction factor by developing excel macro (Appendix H). Then, by applying regression analysis method and Matlab statistics tool box, interfacial friction factor can be predicted based on experimental data as follow:

Without pipe rotation

$$f_{Fi} = -0.26 \ln(N_{Re_{CW.mix}}) + 2.666 \quad 6.62$$

With pipe rotation

$$Z = 32.28 + 9.0 F_{C.Lr} - 0.0036 N_{Re_{CW.mix}} + 0.00025 N_{Re_{ro}} \quad 6.63$$

$$f_{Fi} = 0.88e^{(0.1644 Z)} \quad 6.64$$

As shown in figure 6.28, developed empirical correlation can estimate interfacial friction factor for water-cutting in horizontal annuli successfully.

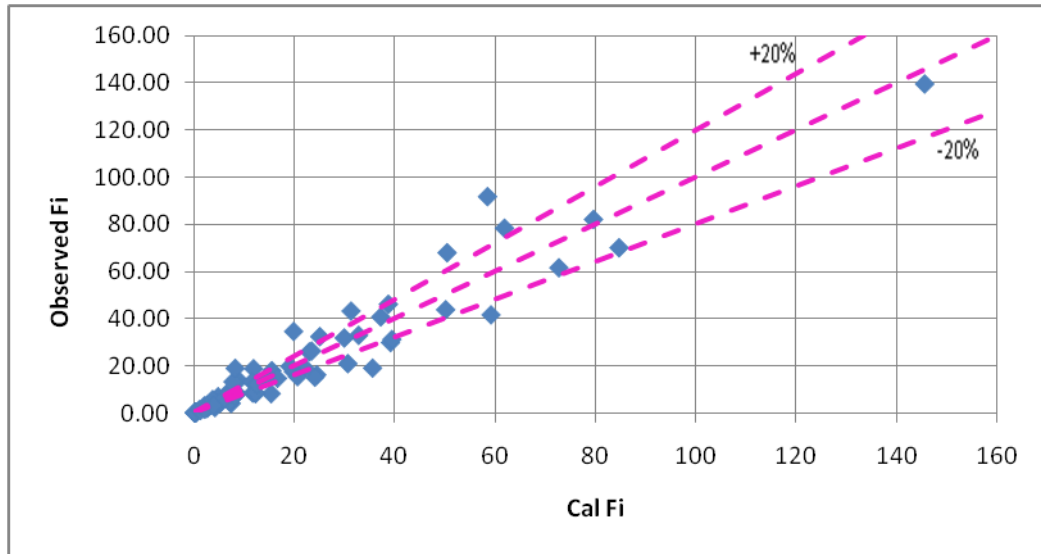


Figure 6.28 Comparisons between Experimental Data Obtained from Current Study and Estimated Interfacial Friction Factor

6-3-2-2 Determination of friction factor between the drilling fluid - cutting mixture and annuli walls for dispersed flow

In this study, it is assumed that cutting and the liquid phases mixed homogeneously in dispersed flow pattern. As a result of this assumption, it is reasonable to consider two phases flow as one homogeneous phase. The properties of gas and liquid mixture can be determined by using following formula:

$$\rho_{dm} = C_c \rho_C + (1 - C_c)\rho_L \quad 6.65$$

$$\mu_{dmix} = (1 + 2.5 (C_c) + 10.05 (C_c)^2 + 0.00273e^{(16.6 (C_c))}) \mu_L \quad 6.66$$

Also friction factor for one phase flow in horizontal annuli can be calculated by well known following equation

$$f_F = \frac{\left. \frac{\partial p}{\partial z} \right|_f (D_{wh} - D_{dp})}{2\rho_{dm} u_m^2} \quad 6.67$$

By considering the equations 6.65 - 6.67, friction factor can be determined for each experimental data point. Then, by applying regression analysis method and Matlab statistics tool box, interfacial friction factor can be predicted based on experimental data as follow:

With or without pipe rotation

$$Z_d = 0.002 - 1.13 \times 10^{-4} F_{C.Lr} + 1.13 \times 10^{-7} N_{Re_{CW.mix}} - 4.63 \times 10^{-8} N_{Re_{ro}} \quad 6.68$$

$$f_F = 0.0007 e^{(402Z_d)} \quad 6.69$$

Figure 6.29 shows that developed empirical correlation can estimate friction factor between the mixture and the wellbore walls in dispersed flow conditions for horizontal annuli reasonably accurate.

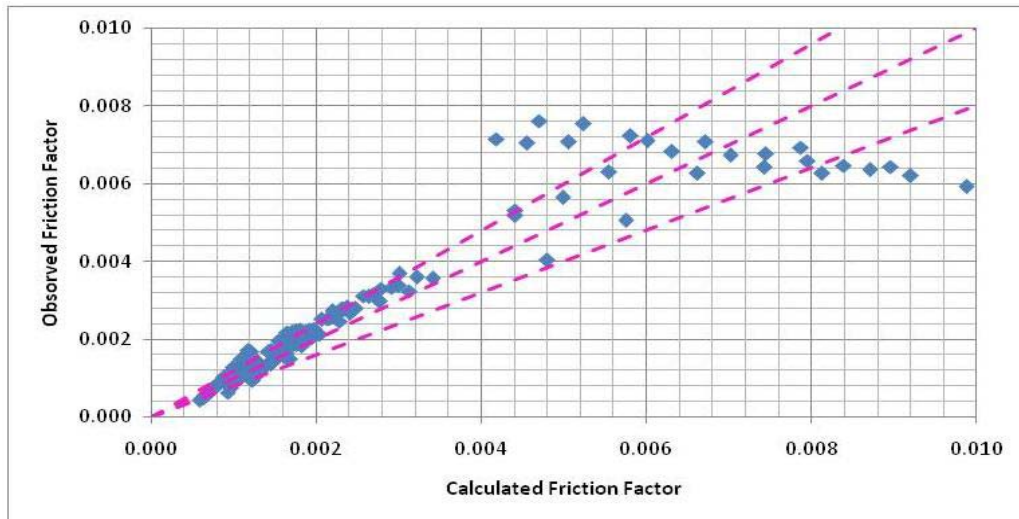


Figure 6.29 Comparisons between Experimental Data Obtained from Current Study and Estimated Friction Factor

It should be noted that all experiments have been conducted using water as the circulating fluid in this study. Therefore, the empirical equations presented in this study are mostly valid for low-viscosity fluids. If the fluid has a significant shear thinning tendency, or has a considerable yield stress, the equation coefficients may require an update.

6-4 Mechanistic Models

In section, developed mechanistic models to predict void fraction and pressure loss in horizontal, inclined and vertical sections for two and three phase flow are discussed in details.

6-4-1 Conformal Mapping

The most appropriate coordinate system to be used in analyzing fluid flow and heat transfer in an eccentric annulus is that of bipolar coordinates. However, in this coordinate system the solution of the equations of change appears to be lengthy and quite difficult if not impossible to obtain (fig. 6.30).

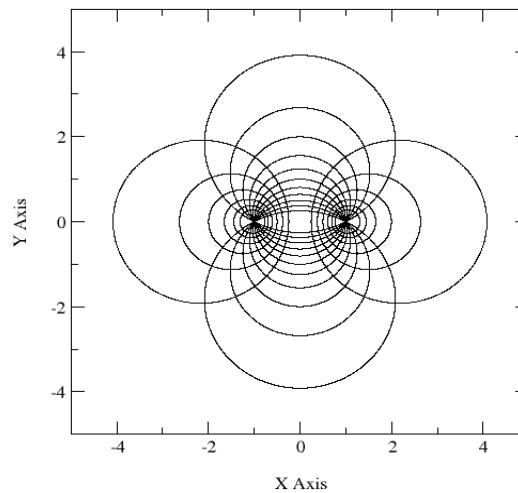


Figure 6.30 Bipolar Coordinate System (Jeng-Tzong Chen, Ming-Hong Tsai, Chein-Shan Liu 2009)

The bipolar coordinate's (η, ζ, z) are related to the rectangular coordinates (x, y, z) as follows:

$$x = \frac{a \sin h\eta}{\cos h\eta - \cos \xi} \quad 6.70$$

$$y = \frac{a \sin \xi}{\cos h\eta - \cos \xi} \quad 6.71$$

$$z = Z \quad 6.72$$

$$\eta = \frac{1}{2} \ln \frac{(x+a)^2 + y^2}{(x-a)^2 + y^2} \quad 6.73$$

$$\zeta = \arctan \frac{2ay}{x^2 + y^2 - a^2} \quad 6.74$$

$$Z = Z \quad 6.75$$

However, in this coordinate system the solution of the equations of change appears to be lengthy and quite difficult if not impossible to obtain. Thus, problems involving an eccentric annulus are solved approximately using cylindrical coordinates (Cheng and Hwang, 1968; Trombetta, 1971; Yao, 1980; Prusa and Yao, 1983).

The purpose of conformal mapping operation is to present a new approach in extrapolating the experimental data for laminar and turbulent flows in eccentric annuli by the use of an inversion technique. The geometric inversion transforms the eccentric annulus system to the concentric system. In this way, a rather complicated problem in bipolar coordinates can be solved easily in cylindrical coordinates (fig. 6.31).

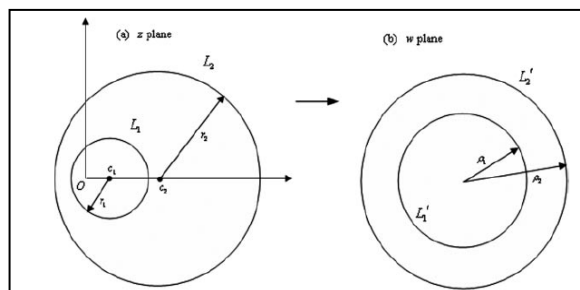


Figure 6.31 Mapping of the Eccentric Annulus to a Concentric Annulus (Jeng-Tzong Chen, Ming-Hong Tsai, Chein-Shan Liu 2009)

The eccentric annulus system is identified by two parameters; the radius ratio (r_e^*) and the eccentricity ratio (ϵ). These are defined by:

$$r_e^* = r_{ei} / r_{eo} \quad 6.76$$

$$\epsilon = \frac{e}{r_{eo} - r_{ei}} = \frac{\sinh(\eta_i - \eta_o)}{\sinh(\eta_i) - \sinh(\eta_o)} \quad 6.77$$

$$\cosh \eta_i = \frac{(1+r_e^*) - \epsilon^2(1-r_e^*)}{2\epsilon r_e^*} \quad 6.78$$

$$\cosh \eta_o = \frac{(1+r_e^*) + \epsilon^2(1-r_e^*)}{2\epsilon} \quad 6.79$$

When the point A(-a, 0) is taken as the center of inversion, the Apollonian circles representing constant η lines can be transformed into a set of concentric circles with centre at D(d, 0) and radius r, given by (fig.6.32): (Tosun and Ozgen (1987))

$$r_e = (a + d) \exp(\zeta - \eta) \quad 6.80$$

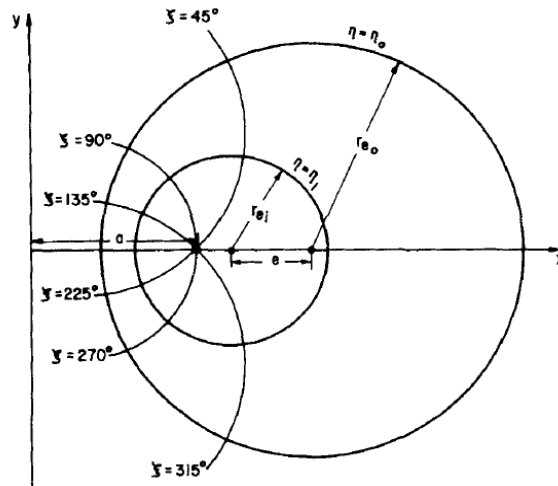


Figure 6.32 Geometry of Eccentric Annulus System (Tosun & Ozgen, 1987)

Tosun and Ozgen (1987) determined the region of applicability of the approximation presented in this work, as the values of the parameters ϵ and r_e^* vary. It is shown in Figure 6.33. In this study, the applicability of approximation for METU cutting transport loop is tested by intersecting its parameters ϵ and r_e^* (table 6.5) in Figure 6.33. It is observed that the intersected point located in two regions' boundary. So it was decided to use this approximation to convert eccentric annuli to concentric annuli.

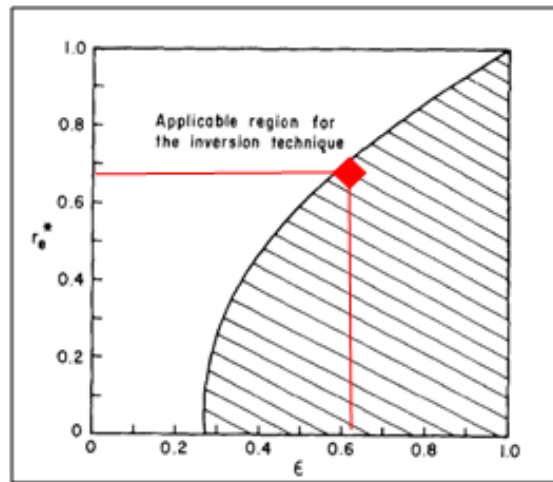


Figure 6.33 the Applicability Region for Conformal Mapping (Tosun & Ozgen, 1987)

By using the above equation, concentric annulus geometry properties (ID and OD) were calculated and presented in table 6.5 for METU Multiphase Flow Loop Annular test section. In order to simplify the solution of problem, it is proper to equalize the area of concentric annuli to the area of eccentric annuli. So this fact should be considered in the selection of $(a + d)$ value.

Table 6.5 New Concentric Annulus Geometry Properties for METU-PETE-CTFL Obtained by using Conformal Mapping Technique

ID	OD	(a+d)	e	r*	ϵ	η_i	η_o	New ID	New OD
1.85	2.91	3.85	0.33	0.64	0.62	1.25	0.89	2.21	3.15

6-4-2 Model Assumptions

For all mechanistic model proposed in this study (two phases and three phases flow), following assumption are considered:

- I. No mass transfer
- II. No difference between injected and produced liquid and gas flow rate
- III. Full developed steady state
- IV. Rotation in low angular velocity
- V. Interphase momentum transfer is due only to drag
- VI. Particles are spherical
- VII. The dispersed phase is assumed to instantaneously reach its terminal velocity, so the transient term on the drift velocity is neglected.
- VIII. Consideration of gas and liquid mixture as homogeneous turbulent flow

When there is intensive bubbling, it is best to consider the gas liquid mixture from the point of view of homogeneous isotropic turbulence. Because it is know that fully developed turbulence is in fact created as a result of the liquid agitation by moving the bubble. It is assumed that all gas kinetic energy is transferred to the liquid-particle mixture, eventually being dissipated by the turbulent motion (Azbel 1981).

6-4-3 Mechanistic Model for Gas-Liquid Two Phase Homogeneous Flow in Vertical and Inclined Eccentric Annuli

The increased application of multiphase flow in different industrial fields encouraged researchers to model the behaviors of multiphase flow in various ducts. Although flow of two-phase fluids is studied in detailed for pipes, not much is known for annular geometries. This section aims to present a developed mechanistic model which can estimate pressure drop and volume fraction of gas-liquid flow though vertical and inclined upward eccentric annulus.

6-4-3-1 Calculation of Gas Void Fraction

In this study, Azbel's mechanistic model is used to calculate gas void fraction in homogeneous liquid-gas two phases flow (Azbel, 1981). Azbel (1981) considered two limiting case of bubble regimes:

- Rapid bubbling ($N_{Fr} > 1$)
- Slow bubbling ($N_{Fr} < 1$).

Where

$$N_{Fr} = \frac{V_{SG}^2}{gh} \quad 6.81$$

Where h is liquid column height. In this study, it is the vertical length of annulus test section.

He obtained total energy equation of a two phase mixture by considering energy balance of a unit cross section of the differential later during bubbling process. After that, in order to find gas void fraction, he determined the minimum of total energy equation since for any steady state system, the available energy of the system must be at a minimum. In view of this fact, the following formulas for gas void fraction can be formed:

6-4-3-1-1 If $N_{Fr} > 1$ (Rapid bubbling)

For turbulent flow regime (for real liquid)

$$\varphi_{avg} = \frac{1}{1+(2N_{Fr})^{\frac{1}{2}}} \quad 6.82$$

6-4-3-1-2 If $N_{Fr} < 1$ (Slow bubbling)

$$\varphi_{avg} = (1 + ab) \left\{ 1 - \frac{(ab)^{\frac{1}{2}}}{2} \left[\sin^{-1} \left(\frac{1-ab}{1+ab} \right) + \frac{\pi}{2} \right] \right\} \quad 6.83$$

φ_{avg} :Relative density of two phase flow

A detailed derivation is presented in Azbel (1981).

6-4-3-1-1 Effect of Static Liquid Height and Equipment Diameter on Void Fraction

When the diameter of equipment is less than 0.2 m (7.88 in) and the static liquid level is less than 1 m (3.28 ft), Azbel (1981) introduced following correlation to consider the effects of static liquid height and equipment diameter on void fraction.

$$\phi_{\text{avg}} = 1 - K_d K_h \phi \quad 6.84$$

K_d : Correlation factor for duct diameter

K_h : Correlation factor for the static liquid level

$$K_d = 1 - \exp \left\{ -1.1 \left(\frac{V_{SG}}{V_b} \right)^{1/2} \left[\frac{(gd)^{1/2}}{V_{SG}} \right]^{3/4} \right\} \quad 6.85$$

$$K_h = 1 - \exp \left\{ -0.405 \left(\frac{V_{SG}}{V_b} \right)^{0.7} \left[\frac{(gd)^{1/2}}{V_{SG}} \right] \right\} \quad 6.86$$

$$V_b = 1.18 \left[\frac{g\sigma(\rho_L - \rho_G)}{\rho_L^2} \right] \quad 6.87$$

Where

$$a = \frac{3C_D}{8} \quad 6.88$$

$$b = V_{SG}^2 / gr_b \quad 6.89$$

6-4-3-1-2 Calculation of C_D and r_b :

In the range $500 < Re < 2 \times 10^2$: $C_D = 0.44$

$$V_b = \frac{2}{3} \left(\frac{4\sigma^2 g}{3S\rho_L \mu_L} \right)^{1/5} \quad 6.90$$

For spherical bubbles $S \approx 1$

$$r_b = \frac{C_D V_b^2}{4g} \quad 6.91$$

6-4-3-2 Definition of Gas and Liquid Homogeneous Mixture Properties

After calculation of liquid and gas void fractions by using equations (6.82-91), the properties of gas and liquid mixture can be determined by using following formulas:

$$\rho_{sm} = \phi_{avg} \rho_G + (1 - \phi_{avg}) \rho_L \quad 6.92$$

$$\mu_{sm} = \phi_{avg} \mu_G + (1 - \phi_{avg}) \mu_L \quad 6.93$$

$$V_{sm} = \frac{V_{SG} \rho_G + V_{SL} \rho_L}{\rho_{sm}} \quad 6.94$$

6-4-3-3 Determination of Pressure Loss for Two Phase Gas-Liquid Homogeneous Mixture

Friction losses, gravity losses and convective acceleration losses are the three components of total pressure gradient for steady-state flow. For higher pressure cases, it is proper to neglect acceleration losses term. So, friction losses and gravity losses components exist in vertical and inclined test sections. The friction and gravitation effects terms are defined by equations 6.96 and 6.97.

$$\left. \frac{dp}{dz} \right|_T = \left. \frac{dp}{dz} \right|_f + \left. \frac{dp}{dz} \right|_g \quad 6.95$$

$$\left. \frac{dp}{dz} \right|_g = g \rho_{sm} \quad 6.96$$

$$\left. \frac{dp}{dz} \right|_f = \frac{2f_F \rho_{sm} V_{sm}^2}{(D_{wh} - D_{dp})} \quad 6.97$$

Where for laminar flow

$$f_F = \frac{16}{N_{Re_{GW.mix}}} \quad 6.98$$

For turbulent flow (Blasius Formula)

$$f_F = \frac{0.0791}{N_{Re_{GW.mix}}^{0.25}} \quad 6.99$$

In equations 6.98 & 6.99, Gas-Liquid mixture Reynolds number can be calculated from equation 6.15 by considering the properties of gas and liquid mixture determined in equations 6.92,6.93,and 6.94. In order to apply and verify developed mechanistic model to experimental data, an excel macro was developed (Appendix I). Results are presented in result and discussion chapter (section7-2-2).

6-4-4 Solid-Gas-Liquid Three Phase Homogeneous Flow in Horizontal, Vertical and Inclined Eccentric Annuli

6-4-4-1 Calculation of Gas Void Fraction for Horizontal Test Section

In this section, it is assumed that the gas and the liquid phases travel at the same velocity into horizontal annuli. Physically, for no slip conditions, as both phases travel at the same velocity, liquid void fraction is simply equal to the ratio of the liquid volumetric flow rate to the total volumetric flow rate. No slip conditions will occur, for example, in homogeneous flow or dispersed bubble flow. So it is possible to consider that

$$\phi_{avL} = \lambda_L \quad 6.100$$

$$\phi_{avG} = 1 - \phi_{avL} \quad 6.101$$

6-4-4-2 Calculation of Gas Void Fraction for Vertical and Inclined Test Sections

In vertical and inclined test sections, gas void fraction can be calculated by using the formulas proposed in section 6-4-3-1(equations 6.81-91).

6-4-4-3 Definition of Gas and Liquid Homogeneous Mixture Properties

After calculation of liquid and gas void fractions by using above equations, the properties of gas and liquid mixture can be determined by using formulas (6.92-6.94) presented in section 6-4-3-2:

6-4-4-4 Calculation of Particle Relative Velocity into the Gas and Liquid Homogeneous Mixture

The determination of slip void fraction for each phase requires the knowledge of its distribution in annuli. Models for algebraic slip were first introduced by Ishii (1977) Manninen and Taivassalo (1996), providing a more general formulation which forms the basis for the implementation in this study. The phase and bulk momentum equations are first transformed to non conservative form by combining with the phase and bulk continuity equations.

Figure 6.34 show the free body diagram for a particle of dispersed phase (solid particle) in gas and liquid homogeneous mixture. Consider the non-deformable particle immersed in flowing gas-liquid homogeneous mixture. This particle is a part of dispersed phase in the continuous medium.

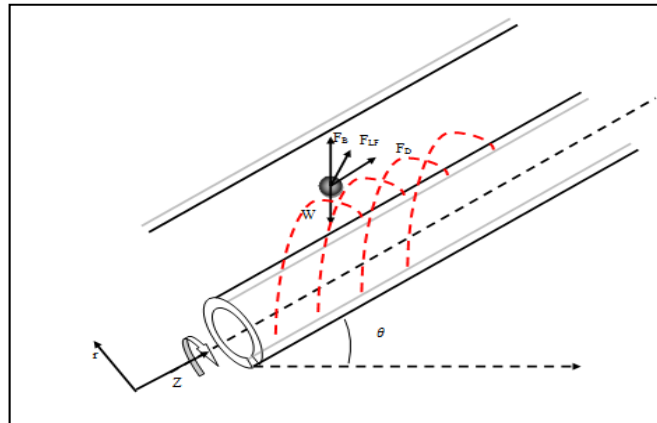


Figure 6.34 Free Body Diagram for a Particle of Dispersed Phase (Solid Particle) in Gas and Liquid Homogeneous Mixture

The general Lagrangian equation for the motion of the particle is:

$$m_p \frac{d\vec{v}_{SC}}{dt} = m_p \vec{g} + m_m \left[\frac{D\vec{v}_{sm}}{Dt} - \vec{g} \right] + \vec{F}_D + \vec{F}_{LF} \quad 6.102$$

Where

m_p = Mass of solid particle (dispersed phase)

m_m = Mass of the dispersed continues phase

v_{SC} = Solid particle velocity

v_{sm} = Gas- liquid mixture velocity

$\frac{D\vec{v}_{sm}}{Dt}$ = Lagrangian fluid acceleration $\frac{D\vec{v}_{sm}}{Dt} = \frac{\partial \vec{v}_{sm}}{\partial t} + \vec{v}_{sm} \cdot \nabla \vec{v}_{sm}$

\vec{F}_D = Drag forces

\vec{F}_{LF} = Lift forces

Since in this study, system assumed as steady stat system without acceleration, equation 6.102 simplifies to:

$$0 = m_p \vec{g} - m_m \vec{g} + m_m \vec{v}_{sm} \cdot \nabla \vec{v}_{sm} + \vec{F}_D + \vec{F}_{LF} \quad 6.103$$

The first term of equation 6.103 is gravitational force, the second term is buoyancy force and the thirty term is virtual mass effect. In this study, the effect of lift force is assumed negligible. The drag exerted by a single particle on the continuous phase is:

$$\vec{F}_D = C_D \rho_m \frac{\pi D_p^2}{8} |\vec{v}_{sm} - \vec{v}_p| (\vec{v}_{sm} - \vec{v}_p) \quad 6.104$$

Where $\vec{v}_{sp} = (\vec{v}_{sm} - \vec{v}_p)$ can be defined as particle relative velocity (slip velocity of solid particle) in gas-liquid mixture.

Several empirical correlations are available for drag coefficient. The one available in this study is due to Schiller and Naumann (1933). It can be written as follows:

$$C_{Dp} = \left(\frac{24}{N_{Re_p}} \right) \left(1 + 0.15 N_{Re_p}^{0.687} \right) + \frac{0.413}{1 + 16300 N_{Re_p}^{-1.09}} \quad 6.105$$

where

$$N_{Re_p} = \frac{\rho_{sm} (V_{sm}) (D_p)}{\mu_{sm}} \frac{1}{1-\varepsilon} \quad 6.106$$

The mass of each phase is the function of its density and volume.

$$m_p = \rho_c V_p \quad 6.107$$

$$m_m = \rho_{sm} V_p \quad 6.108$$

The volume of a single spherical particle V_p is given by:

$$V_p = \frac{\pi D_p^3}{6} \quad 6.109$$

By substituting equations 6.103-6.109 in equation 6.103, following equations can be considered.

$$(\rho_c - \rho_{sm}) \vec{g} V_p + \rho_{sm} V_p \vec{v}_{sm} \cdot \nabla \vec{v}_{sm} + C_D \rho_{sm} \frac{\pi D_p^2}{8} |\vec{v}_{sm} - \vec{v}_{SC}| (\vec{v}_{sm} - \vec{v}_{SC}) = 0 \quad 6.110$$

$$\text{In cylindrical coordinate: } \begin{cases} \vec{v}_{sm} = v_{smr} \vec{e}_r + v_{sm\theta} \vec{e}_\theta + v_{smz} \vec{e}_z \\ \vec{v}_{SC} = v_{SCr} \vec{e}_r + v_{SC\theta} \vec{e}_\theta + v_{SCz} \vec{e}_z \end{cases}$$

The consideration of model assumptions and mathematical operations lead to the following closed relationships for the particle relative velocity (slip velocity) in cylindrical coordinate:

$$\vec{v}_{spz} = - \frac{4}{3} \frac{\vec{g}_z}{C_D} \frac{D_p}{|v_{sp}|} \frac{(\rho_c - \rho_{sm})}{\rho_{sm}} \quad 6.111$$

$$\vec{v}_{spr} = -\frac{4}{3} \frac{D_p}{|v_{sp}| C_D} \left[\frac{(\rho_c - \rho_{sm}) \vec{g}_r}{\rho_{sm}} + \frac{V_\theta^2}{(D_{wh} - D_{dp})/2} \right] \quad 6.112$$

$$v_{sp} = \sqrt{v_{spr}^2 + v_{spz}^2} \quad 6.113$$

where $\vec{g}_r = \frac{v_\theta^2}{(D_{wh} - D_{dp})/2} - g \sin(\theta)$ is gravity in r direction.

By solving system of equations 6.111-6.113; slip velocity can be obtained.

6-4-4-5 Calculation of Gas, Particle and Liquid Slip Void Fraction into the Three Phase Mixture

Azbel (1981) verified the average fraction of particles in liquid flow by using the definition of the average relative velocity of the solid phase when velocities of the two phases are low and the duct is large enough (no wall effect) (equation 6.114). In this study, his derivation was used to calculate the particle slip void fraction in gas and liquid homogeneous mixture (equation 6.111-114) (see Appendix K for detailed derivation).

$$\Phi_{avp} = \frac{\vec{v}_{sp} - V_{sm} - V_{SC}}{2\vec{v}_{sp}} - \left[\left(\frac{\vec{v}_{sp} - V_{sm} - V_{SC}}{2\vec{v}_{sp}} \right)^2 + \frac{V_{SC}}{\vec{v}_{sp}} \right]^{1/2} \quad 6.111$$

$$\Phi_m = (1 - \Phi_{avp}) \quad 6.112$$

$$\Phi_{Gt} = \Phi_{avG} \Phi_m \quad 6.113$$

$$\Phi_{Lt} = 1 - \Phi_{Gt} - \Phi_{avp} \quad 6.114$$

6-4-4-6 Definition of Gas, Cutting and Liquid Homogeneous Mixture Properties

After calculation of liquid, gas and particle void fractions, the properties of gas, cuttings and liquid mixture can be determined by using the following formula:

$$\rho_{stm} = \phi_{avp} \rho_C + (1 - \phi_{avp}) \rho_{sm} \quad 6.112$$

$$\mu_{stm} = (1 + 2.5\phi_{avp} 10.05 (\phi_{avp})^2 + 0.00273e^{(16.6 (\phi_{avp}))}) \mu_{sm} \quad 6.113$$

$$V_{stm} = \frac{V_{SC} \rho_C + V_{sm} \rho_{sm}}{\rho_{stm}} \quad 6.114$$

6-4-4-7 Determination of Pressure Loss for Three Phase Gas, Cutting and Liquid Homogeneous Mixture

The total pressure gradient for steady-state flow is composed of three components: friction losses, gravity losses and convective acceleration losses. Convective acceleration losses can be neglected for higher pressure cases. So, only friction losses component exist in horizontal annuli cases and friction losses and gravity losses components exist in vertical and inclined test sections. The friction and gravitation effects term defined by equations 6.115 and 6.116, is mainly contributed by the interfacial shear stress between the drilling fluid and the annuli walls.

$$\left. \frac{dp}{dz} \right|_T = \left. \frac{dp}{dz} \right|_f + \left. \frac{dp}{dz} \right|_g \quad 6.115$$

$$\left. \frac{dp}{dz} \right|_g = g \rho_{stm} \quad 6.116$$

$$\left. \frac{dp}{dz} \right|_f = \frac{2f_F \rho_{stm} V_{stm}^2}{D_{wh} - D_{dp}} \quad 6.117$$

In this study, following equations were used to calculate friction factor for laminar and turbulent flows.

For laminar flow

$$f_F = \frac{16}{N_{Re_{th.mix}}} \quad 6.118$$

For turbulent flow (Chen, 1979)

$$\frac{1}{\sqrt{f_F}} = -4 \log \left(\frac{\delta/(OD-ID)}{3.7065} - \frac{5.0452}{N_{Re_{th.mix}}} \log(A) \right) \quad 6.119$$

$$A = \left(\frac{(\delta/(OD-ID))}{2.5497} \right)^{1.1098} + \left(\frac{7.1490}{N_{Re_{th.mix}}} \right)^{0.8981} \quad 6.120$$

Where $(\delta/(OD - ID))$ is relative wall roughness,

Or (Caetano, 1992)

$$\frac{1}{\left\{ f_F \left(\frac{16}{F_{CA}} \right)^{0.45 \exp \left(- \frac{(N_{Re_{th.mix}} - 3000)}{10^6} \right)} \right\}^{1/2}} = \quad 6.121$$

$$4 \text{Log} \left[N_{Re_{th.mix}} \left\{ f_F \left(\frac{16}{F_{CA}} \right)^{0.45 \exp \left(- \frac{(N_{Re_{th.mix}} - 3000)}{10^6} \right)} \right\}^{1/2} \right] - 0.395$$

Where Reynolds number based on the hydraulic diameter of cylinder for liquid, cutting and gas homogenous mixture is:

$$N_{Re_{th.mix}} = \frac{\rho_{stm} V_{stm}}{\mu_{stm} (D_{wh} - D_{dp})} \quad 6.122$$

Developed excel macro to apply and verify developed mechanistic model to cutting-liquid two phase and cutting-gas-liquid three phase experimental data, is explained in Appendix J. The model application results are presented in result and discussion chapter (section 7-2-3).

CHAPTER VII

RESULTS & DISCUSSIONS

In this chapter, experimental observations and sensitivity analysis are introduced in details. Also, the proposed models results are compared with the experimental data. Although all experiments were recorded by high speed camera, only the experiments conducted in horizontal test section were analyzed by using image analysis technique. So, the effects on volumetric cutting concentration or on liquid hold up in horizontal test section were investigated in sensitivity analysis section.

7-1 Experimental Observations and Sensitivity Analysis

After conducting extensive number of experiments with a wide range of air, water and cuttings injection rates, including pipe rotations from 0 to 120 rpm, the following observations have been obtained.

7-1-1 Cutting-Liquid Two Phase Flow

The effects of changes in the flow rate, rate of penetration, and pipe rotation on volumetric cutting concentration and pressure drop for a Newtonian fluid (water) were investigated.

7-1-1-1 Effects on Cutting Concentration in Horizontal Test Section

The experiments showed that there exists a direct relation between the total concentrations of cuttings present in the wellbore with the injection rate of cuttings, i.e., rate of penetration (ROP). As ROP increases, the total concentration of cuttings increases in the wellbore. As an example, shown in fig. 7.1, when the pipe rotation speed is kept constant, the total cuttings concentration in the wellbore shows an increase with increasing ROP values, for all flow rates. This effect vanishes as the fluid velocity is very high, and fully dispersed flow pattern is observed.

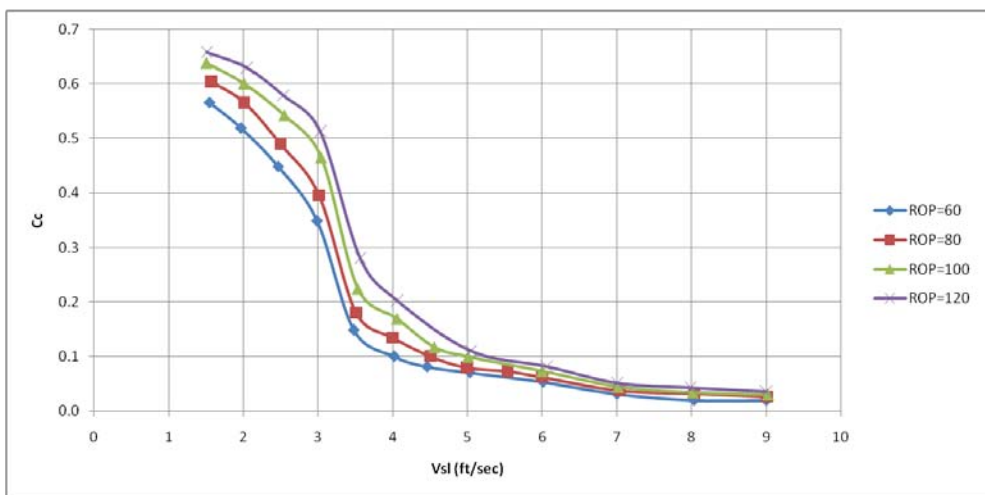


Figure 7.1 Ratio of Cutting Area Observed inside Wellbore from Image Analysis vs. Fluid Superficial Velocity in Horizontal Test Section ($\theta=0$) for RPM=80 (1/min), ROP=60, 80,100 &120 (ft/hrs)

When the effect of pipe rotation is analyzed, although the influence is relatively less, it has been observed that higher rotation speeds end up with less cuttings concentration inside the wellbore, especially when there is bed in the system. However, as the bed disappears and dispersed flow is achieved, no influence of pipe rotation is observed on total concentration in the wellbore, as seen from fig. 7.2.

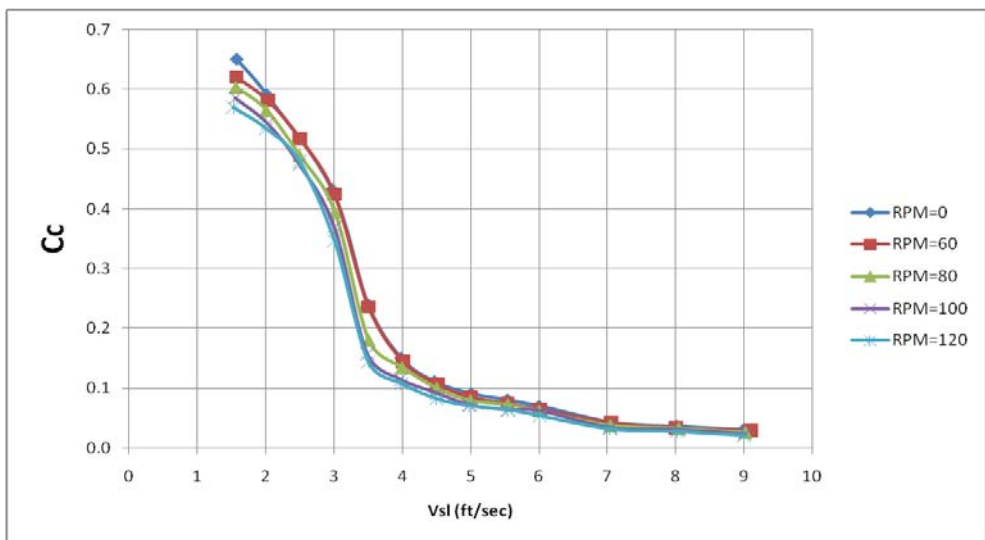


Figure 7.2 Ratio of Cutting Area Observed inside Wellbore from Image Analysis vs. Fluid Superficial Velocity in Horizontal Test Section ($\theta=0$) for ROP=80(ft/hrs) RPM=0, 60, 80, 100 & 120 (1/min)

7-1-1-2 Effects on Pressure Drop

Figure 7.3 ,7.4 and 7.5 show the alteration in the average pressure drop with the superficial liquid velocity for horizontal, nearly vertical and inclined ($\theta = 45.0$) solid (cutting)-water flow with different drill pipe rotation respectively.

In the case of the horizontal cutting-water flow(fig 7.3), in low liquid velocities ($V_{SL}=1.5-3$ ft/sec),there is slight increase in pressure drop because of cutting bed existence, after that, pressure drop decrease suddenly by disappearance cutting bed and increasing the liquid flow area. Finally, the friction pressure drop increase nearly linearly by increasing the liquid flow rate. In the case of the nearly vertical ($\theta=77.5$) cutting-water flow(fig 7.4), firstly pressure drop decrease with liquid superficial velocity increase, due to increase in turbulence effect, after that the gravitational pressure loss decrease because the cutting concentration decrease in the annulus test section as a result of liquid velocity increase. However, gravitational pressure loss reduction can be compensated by frictional pressure loss raise. So the total pressure loss starts to increase. In the case of inclined ($\theta=45.0$) cutting-water flow (fig 7.5, the increase in friction pressure loss neutralize the decrease in gravitational pressure loss. So the total pressure loss stays almost constant.

When the effects on pressure losses are analyzed, it can be seen that ROP has a direct impact on pressure losses (fig. 7.3, 7.4&7.5). As the total cuttings concentration in the wellbore increases due to the increase in ROP, higher pressure losses are observed as the other drilling parameters are kept constant. As the flow rates are increased, the difference between the pressure losses for different ROP values become less important.

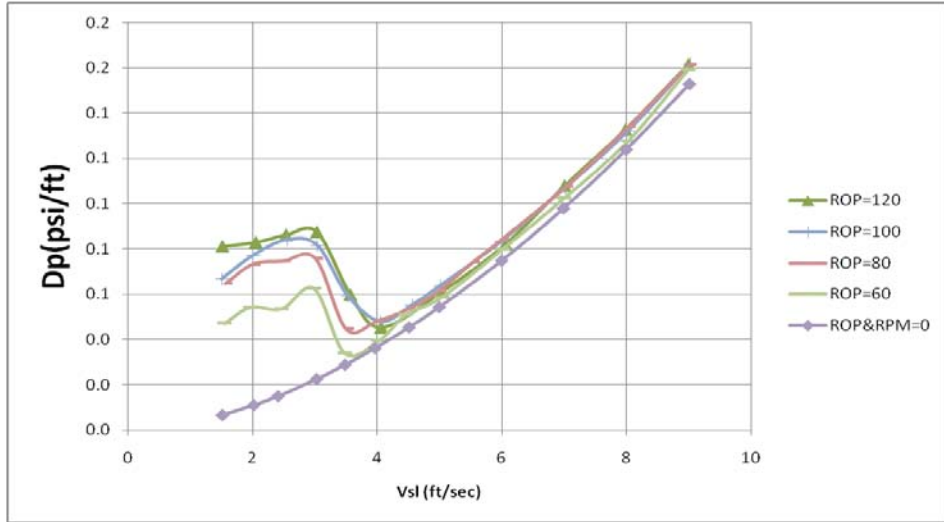


Figure 7.3 Measured Pressure Drop vs. Water Superficial Velocity in Horizontal Test Section ($\theta=0$) for RPM=80(1/min), ROP=60, 80,100 &120(ft/hrs)

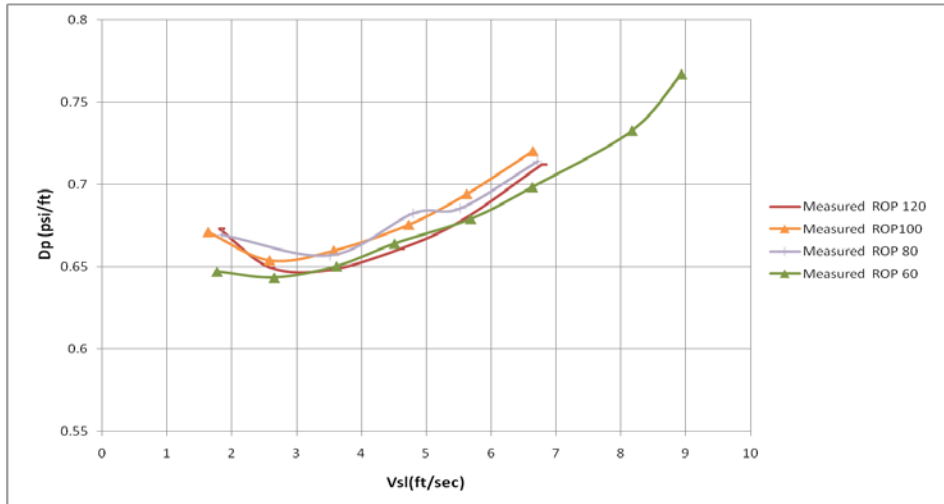


Figure 7.4 Measured Pressure Drop vs. Water Superficial Velocity in Nearly Vertical Test Section ($\theta=77.5$) for RPM=80(1/min), ROP=60, 80,100 &120(ft/hrs)

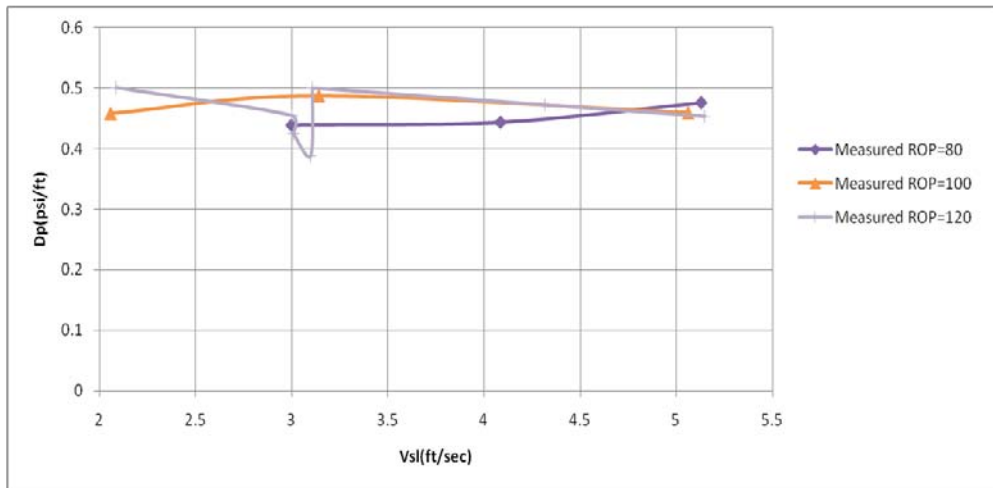


Figure 7.5 Measured Pressure Drop vs. Water Superficial Velocity in Inclined Test Section ($\theta=45.0$) for RPM=80(1/min), ROP=80,100 &120(ft/hrs)

The observations indicated that pipe rotation does not have a significant effect on pressure losses with the presence of cuttings for a constant ROP and a flow rate value (fig. 7.6, 7.7&7.8). It should be noted that the pipe lowest value of the pipe rotation is 60 rpm. For rotation speeds less than this value, there may be some influence; however, within the test matrix of this study, this observation could not be conducted due to time limitations.

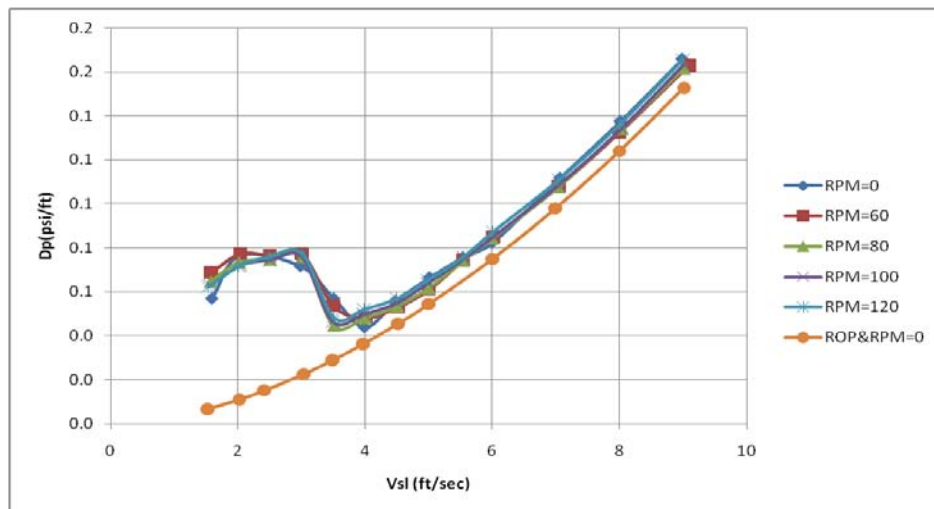


Figure 7.6 Measured Pressure Drop vs. Water Superficial Velocity in Horizontal Test Section ($\theta=0$) ROP=80(ft/hrs) RPM=0, 60, 80, 100 & 120 (1/min)

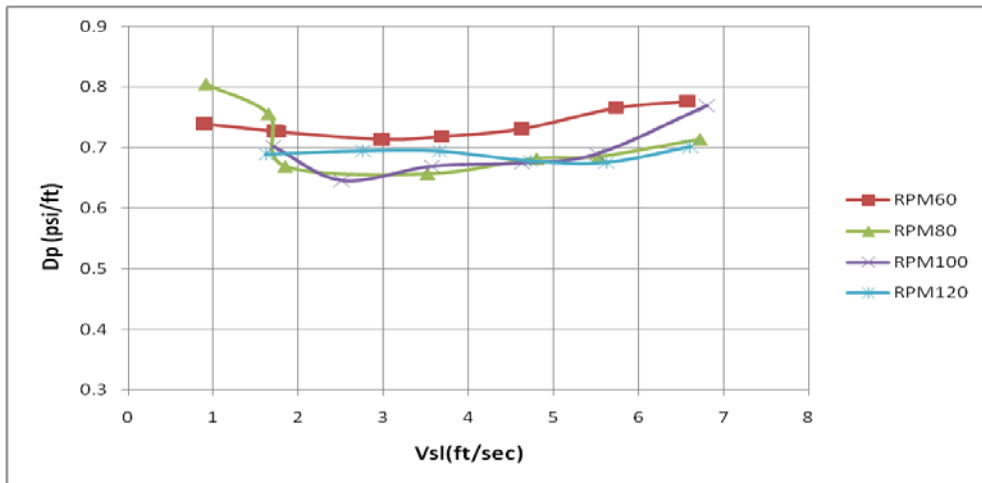


Figure 7.7 Measured Pressure Drop vs. Water Superficial Velocity in Nearly Vertical Test Section ($\theta=77.5$) ROP=80(ft/hrs), RPM=60, 80, 100 & 120 (1/min)

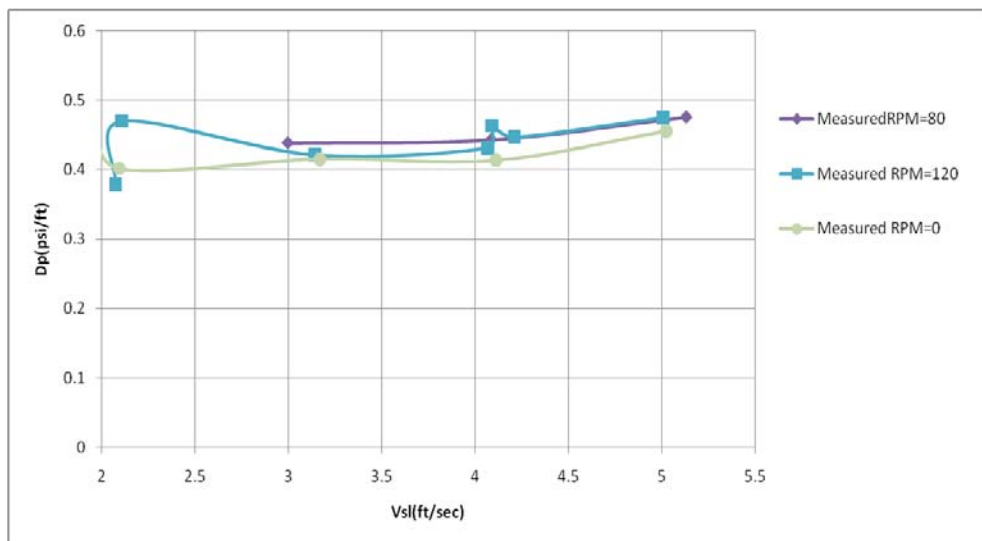


Figure 7.8 Measured Pressure Drop vs. Water Superficial Velocity in Inclined Test Section ($\theta=45.0$) ROP=80(ft/hrs) RPM=0, 80 & 120 (1/min)

From the comparisons among data for total pressure loss in the horizontal position, inclined position ($\theta=45.0$) and the nearly vertical position (77.5 degree from horizontal), it is observed that in horizontal by increasing the liquid velocity in wellbore, total pressure loss also increase due to friction pressure loss increase. But in inclined ($\theta=45.0$) and nearly vertical sections, by increasing liquid velocity, total pressure loss stays slightly constant, since decrease in gravitational pressure loss due to decrease in volumetric cutting concentration, can be compensated by increase in friction pressure loss due to mixture velocity increase.

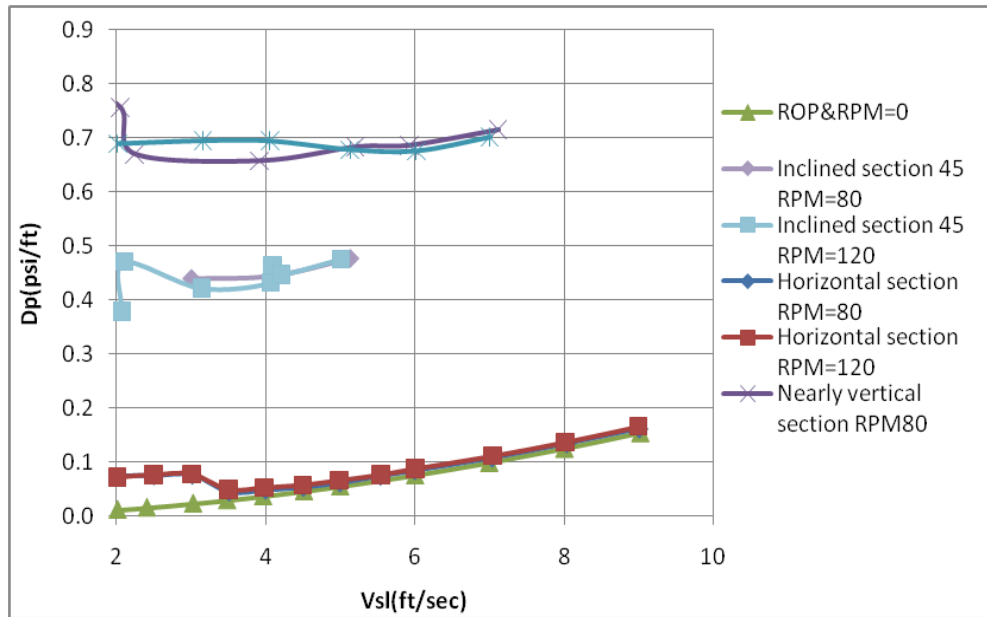


Figure 7.9 Measured Pressure Drop vs. Water Superficial Velocity in Horizontal ($\theta=0.$), nearly Vertical ($\theta=77.5$) and Inclined ($\theta=45.0$) Test Sections ROP=80(ft/hrs) RPM=80 & 120 (1/min)

7-1-1-3 Effects on Moving Cutting Velocity

One of the important achievements of this study is to identify the moving cuttings velocity in the wellbore under dynamic conditions, thanks to the image processing techniques. This piece of information is relatively less known and measured due to the technical limitations in most of the flow loops or test facilities all around the world. Densitometer measurements can give you an idea about the total concentration, or visual observations can give you the thickness of the moving layer. However, none of these are good enough to identify the moving cuttings velocity. Using image processing techniques, this piece of information is determined.

As seen from fig. 7.10, an increase in ROP causes a slight increase in moving cuttings velocity for a constant pipe rotation speed (including no rotation case). Another important observation is that, the increase in flow rate leads to an increased in the velocity of moving cuttings. Note that, this velocity is equal to the average transport velocity of the cuttings, which gives an idea about the slip between the fluid and the particles.

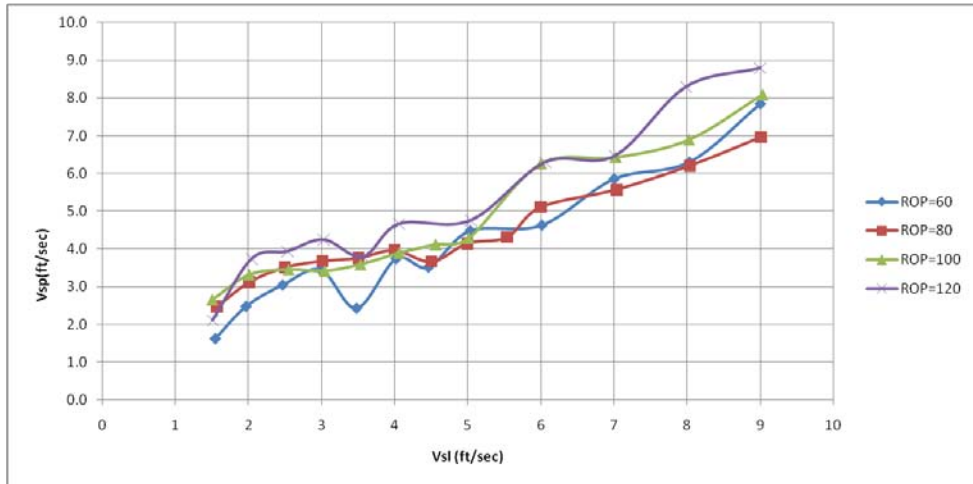


Figure 7.10 Measured Moving Cutting Velocity vs. Water Superficial Velocity in Horizontal Test Section ($\theta=0$) for RPM=80(1/min), ROP=60, 80,100 &120(ft/hrs)

Although it is not as clear as the effect of ROP, pipe rotation has a slight effect on moving cuttings velocity for a constant ROP value as shown in Figure 7.11. As the pipe rotation increases, a slight decrease in moving cuttings velocity is observed, which physically makes sense due to the decreasing influence of rotation speed on bed, which leads to an increase in fluid flow area, causing a decrease in the actual fluid velocity.

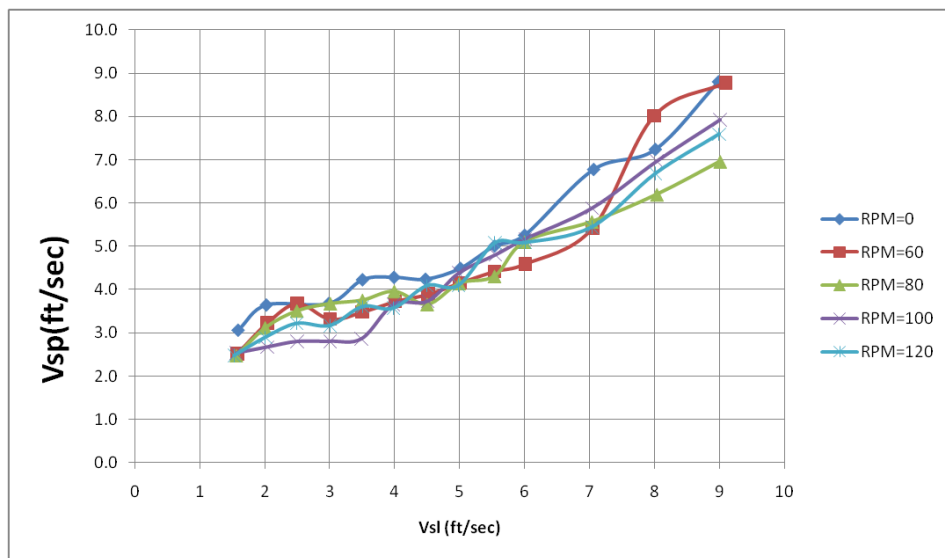


Figure 7.11 Measured Moving Cutting Velocity vs. Water Superficial Velocity in Horizontal Test Section ($\theta=0$) for ROP=80(ft/hrs) RPM=0, 60, 80, 100 & 120 (1/min)

7-1-2 Gas-Liquid Two Phase flow

The effects of changes in the liquid and gas flow rates, on liquid hold up and pressure drop for air-water two phase flows were investigated.

7-1-2-1 Effects on Liquid Holdup

The change in the average liquid holdup with the superficial gas velocity for a typical data set (horizontal air-water flow without drill pipe rotation) is shown in Fig 7.12. The figure shows that in constant liquid flow rate, by increasing the gas flow rate into the annulus test section, the liquid hold decreases because the volume of gas increase while the volume of liquid is constant into the system. Also, it can be observed from the plot that as the liquid flow rate is increased, the liquid holdup increases.

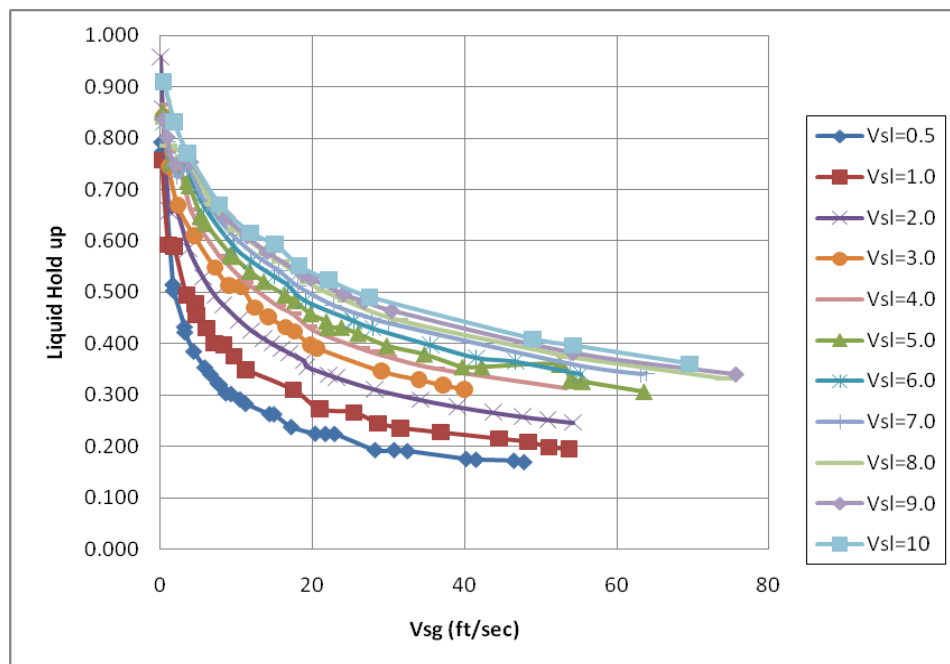


Figure 7.12 Measured Liquid Hold up vs. Gas Superficial Velocity in Horizontal Test Section ($\theta=0$) for Different Water Flow Rate

7-1-2-2 Effects on Pressure Drop

Figures 7.13 and 7.14 show the diagram of frictional pressure drop against the superficial gas velocities for different liquid velocities for horizontal flow and

near horizontal flow ($\theta = 15.0$) is. As shown in these figures, for the case of horizontal air-water flow without drill pipe rotation, the frictional pressure drop increases with the increase in gas superficial velocity in high liquid velocities, but in low liquid velocities, the change in friction pressure loss is inconsiderable by increasing the gas superficial velocity since in two phase flow, liquid phase play the major role in occurrence of friction pressure loss. Also, the frictional pressure drop was observed to be increasing with increase in the liquid superficial velocity.

For the case of nearly horizontal air-water flow ($\theta = 15.0$) without drill pipe rotation, the effect of gravitational pressure loss is low compared with effect of frictional pressure loss. So the same trend is observed in nearly horizontal air-water flow.

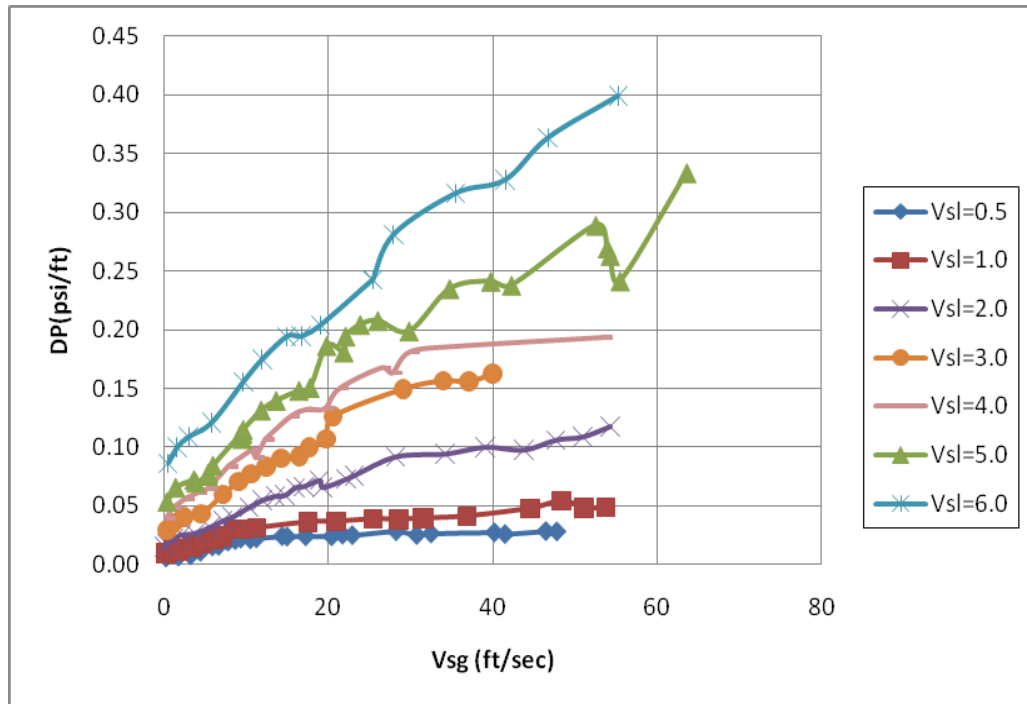


Figure 7.13 Measured Pressure Drop vs. Gas Superficial Velocity in Horizontal Test Section ($\theta=0$) for Different Water Flow Rate

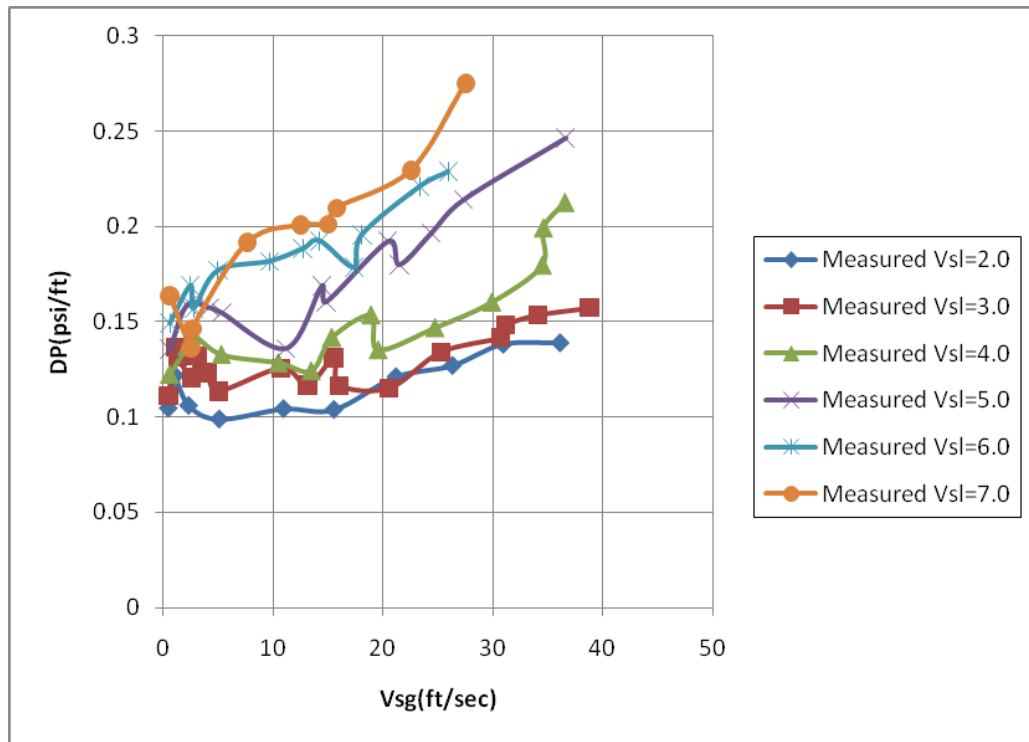


Figure 7.14 Measured Pressure Drop vs. Gas Superficial Velocity in Inclined Test Section ($\theta=15.0$) for Different Water Flow Rate

Figures 7.15, 7.16 and 7.17 show the diagrams of total pressure drop against the superficial gas velocities for different liquid velocities for nearly vertical ($\theta=77.5$) and inclined ($\theta=45.0$), ($\theta=30.0$) test sections respectively. Total pressure drop consist of gravitational and frictional pressure losses components. As shown in the figures, total pressure drop decrease by increasing the gas superficial velocity especially in low liquid velocities, since although the friction pressure loss increase by increasing gas flow rate, the gravitational pressure loss decrease due to mixture density reduction. These components neglect the effect of each other. When the liquid superficial velocity increases, the gravitational and frictional pressure losses components start to raise. So total pressure loss increase by injecting more liquid into the annulus test section.

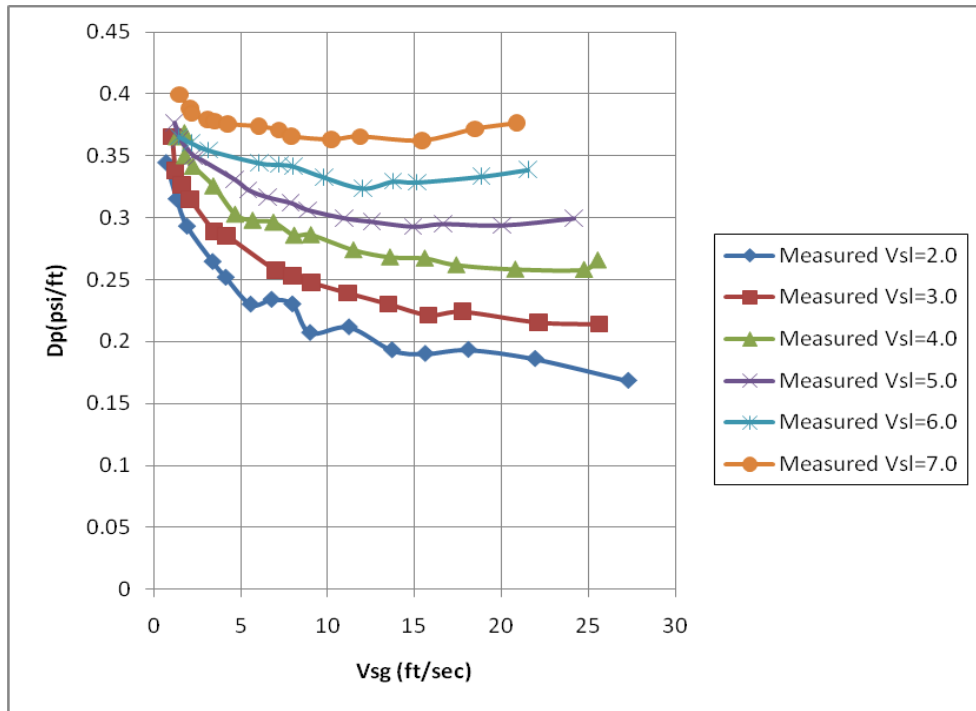


Figure 7.15 Measured Pressure Drop vs. Gas Superficial Velocity in Nearly Vertical Test Section ($\theta=77.5$) for Different Water Flow Rate

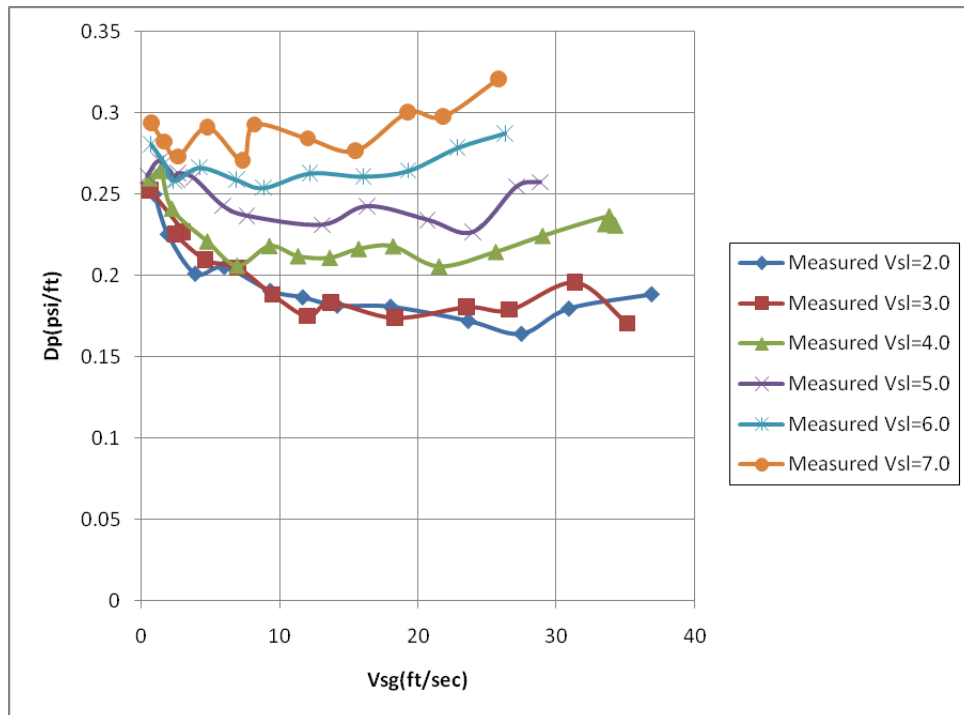


Figure 7.16 Measured Pressure Drop vs. Gas Superficial Velocity in Inclined Test Section ($\theta=45.0$) for Different Water Flow Rate

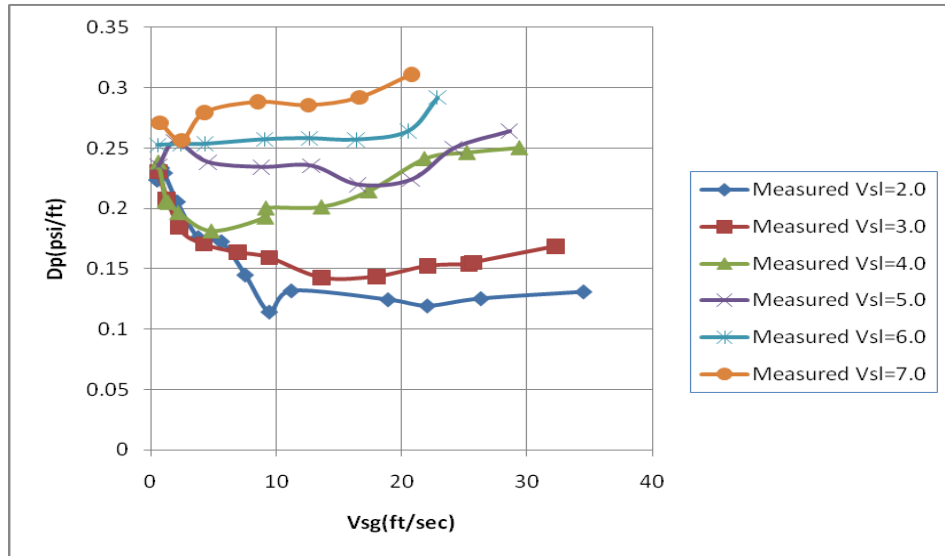


Figure 7.17 Measured Pressure Drop vs. Gas Superficial Velocity in Inclined Test Section ($\theta=30.0$) for Different Water Flow Rate

From the comparisons among data for total pressure loss in the horizontal position, inclined positions and the nearly vertical position (77.5 degree from horizontal) (Fig 7.18), it is observed that in horizontal and nearly horizontal ($\theta=15.0$) sections, by increasing the gas velocity in wellbore, total pressure loss also increase. But in inclined ($\theta=45.0$ & 30.0) and nearly vertical sections, by increasing gas velocity, total pressure loss decrease significantly, since the big part of total pressure loss is gravitational pressure loss in these inclinations.

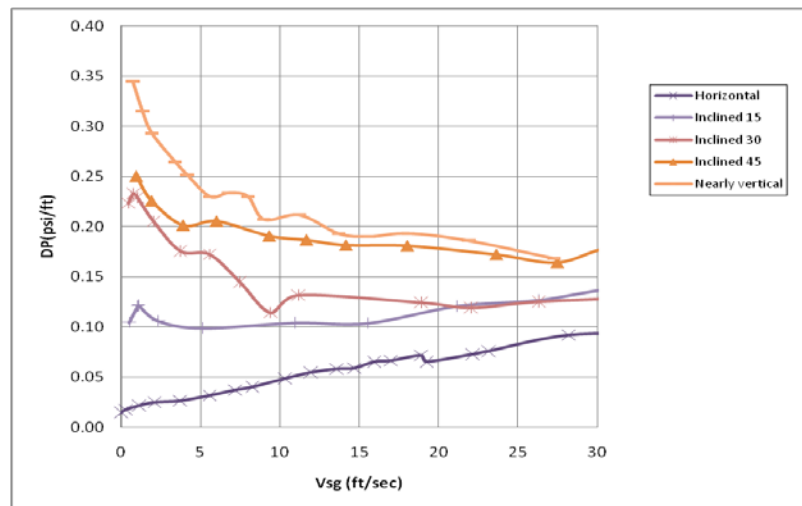


Figure 7.18 Measured Pressure Drop vs. Gas Superficial Velocity in Horizontal ($\theta = 0.0$), nearly Vertical ($\theta = 77.5$) and Inclined ($\theta = 45.0, 30.0$ & 15.0) Test Sections for $V_{SL}=2.0$ (ft/sec)

7-1-3 Cutting-Gas-Liquid Three Phase flow

The effects of changes in the gas and liquid flow rates, rate of penetration, and pipe rotation on volumetric cutting concentration and pressure drop for water, air and cutting, three phases flow were investigated. In this section, examples are given for by considering the effects of different drilling parameters on pressure drop and cutting concentration in various inclinations.

7-1-3-1 Effects on Cutting Concentration

The below figures illustrate the effects of mentioned drilling parameters in volumetric cutting concentration for horizontal three phase flow. As seen in these figures, the injection of gas into the system has significant effect in reduction of total volumetric cutting concentration for all cases, because addition of gas increase the carrying capacity of liquid by raising turbulence effect.

Figures 7.19 and 7.20 show the effect of pipe rotation on the change of volumetric cutting concentration for different liquid velocities and different rate of penetration. The inconsiderable influence of pipe rotation is observed on total concentration in the wellbore.

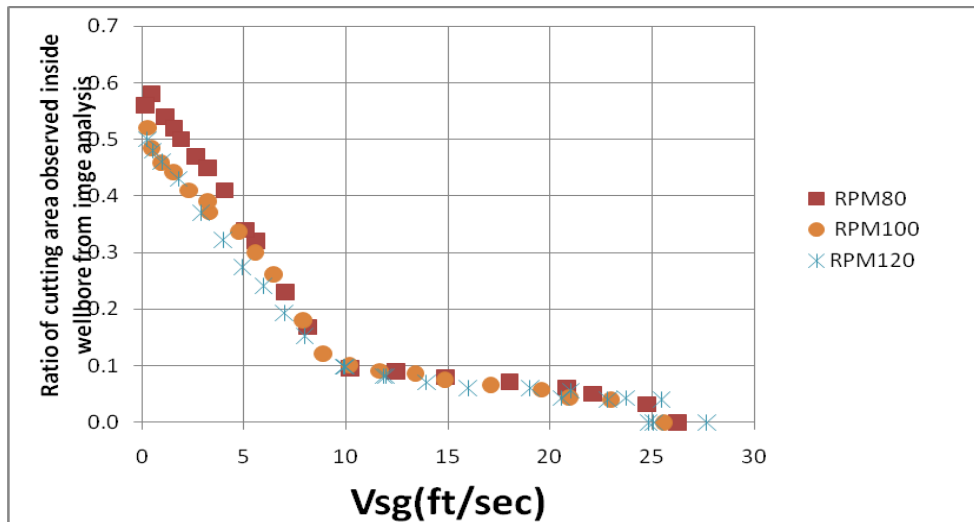


Figure 7.19 Ratio of Cutting Area Observed Inside Wellbore from Image Analysis vs. Air Superficial Velocity in Horizontal Test Section ($\theta=0$) for $V_{SL}=2.0$, $ROP=100$ (ft/hrs) $RPM=80$, 100 & 120 (1/min)

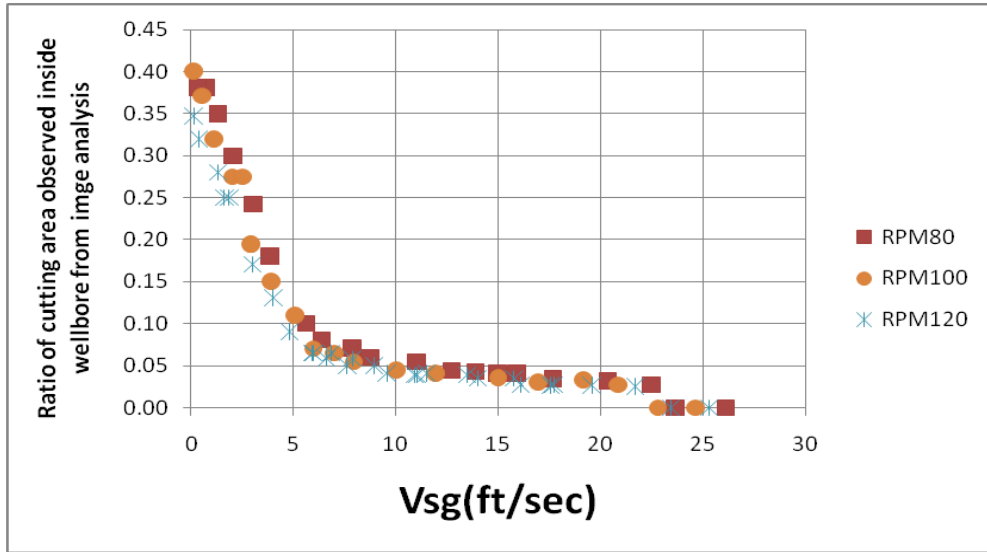


Figure 7.20 Ratio of Cutting Area Observed inside Wellbore from Image Analysis vs. Air Superficial Velocity in Horizontal Test Section ($\theta=0$) for VSL= 3.0, ROP=100(ft/hrs) RPM=80, 100 & 120 (1/min)

When the effect of penetration rate on volumetric cutting concentration is analyzed, it can be seen that ROP has a direct impact on volumetric cutting concentration (fig.7.21&7.22), since the total cuttings concentration in the wellbore increases due to the raise in ROP.

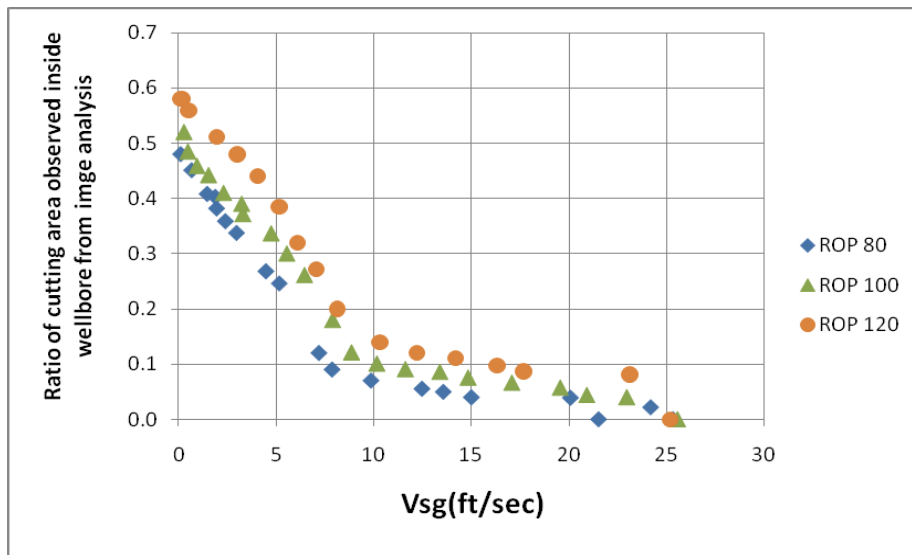


Figure 7.21 Ratio of Cutting Area Observed inside Wellbore from Image Analysis vs. Air Superficial Velocity in Horizontal Test Section ($\theta=0$) for VSL=2.0, RPM=100(1/min) ROP=80, 100 & 120 (ft/hrs)

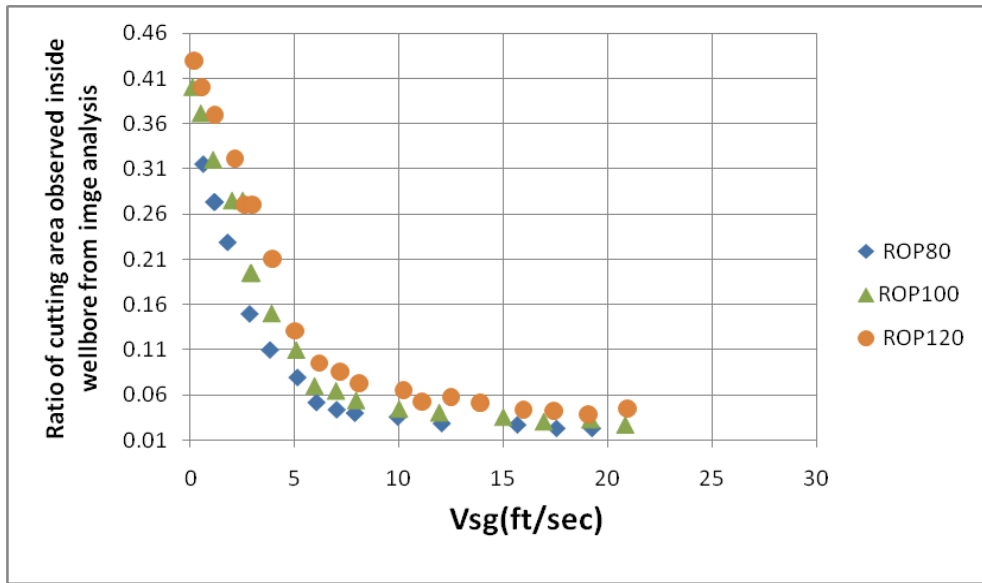


Figure7.22 Ratio of Cutting Area Observed inside Wellbore from Image Analysis vs. Air Superficial Velocity in Horizontal Test Section ($\theta=0$) for VSL=3.0, RPM=100(1/min) ROP=80, 100 & 120 (ft/hrs)

The effect of liquid velocity on volumetric cutting concentration can be seen in figure 7.23. By increasing the liquid flow rate, the carrying capacity of water-gas mixture is raised dramatically due to increase in water- gas mixture density. So, liquid velocity increase plays the major role in the hole cleaning performance of liquid-gas mixture.

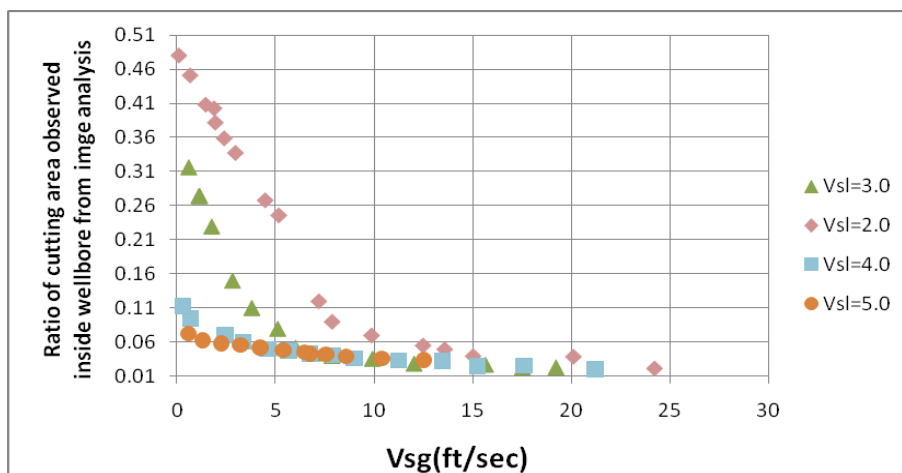


Figure7.23 Ratio of Cutting Area Observed inside Wellbore from Image Analysis vs. Air Superficial Velocity in Horizontal Test Section for Different Liquid Superfi-cial Velocity ROP=80(ft/hrs) RPM=100 (1/min)

7-1-3-2 Effects on Pressure Drop

The examples of experimental pressure loss data for experiments conducted using METU Multiphase Flow Loop are compared in figures 7.24-7.34 for different inclinations. The following important observations also can be made from these diagrams.

- a) The pressure gradient curve does not decrease monotonically with the gas superficial velocity in horizontal sections (see figure 7.24-7.27), because increase in gas superficial velocity decrease the cutting bed thickness in the first step and increase the flow area, after disappearing cutting bed, by increasing the gas velocity, friction pressure loss raise. This is unlike single-phase flow.
- b) There is a minimum in the pressure characteristic (at constant cuttings injection rate and pipe rotation speed). This point also corresponds to the lowest hydraulic power consumption for frictional losses inside the annulus, which leads to the minimum equivalent circulating density at the bit. The corresponding gas flow rate in this point is identified as the optimum gas flow rate since the frictional pressure drop has the minimum value while the cuttings concentration inside the wellbore is at an acceptable level. As obvious from figures 7.24-7.26, this point can be observed in lower gas velocity as liquid flow rate increase.
- c) As shown in Figures 7.24-7.27, it is also observed that by increasing pipe rotation rate and rate of penetration, total pressure drop, including friction and gravitation terms, was not considerably changed in horizontal annuli, as the liquid and gas flow rates are kept constant because of high turbulence effect due to gas presence in the system. The same observation can be seen in different inclinations as shown in Figures 7.29, 7.30, 7.32 and 7.33.
- d) Figures 7.28, 7.31 and 7.34 show the effect of liquid velocity in friction pressure loss in the constant rate of penetration and pipe rotation for three phase flow in horizontal inclined and nearly vertical eccentric annuli. It is observed that liquid superficial velocity increase cause raise in total pressure loss dramatically in the constant gas superficial velocity due to increase in mixture density and Reynolds number.

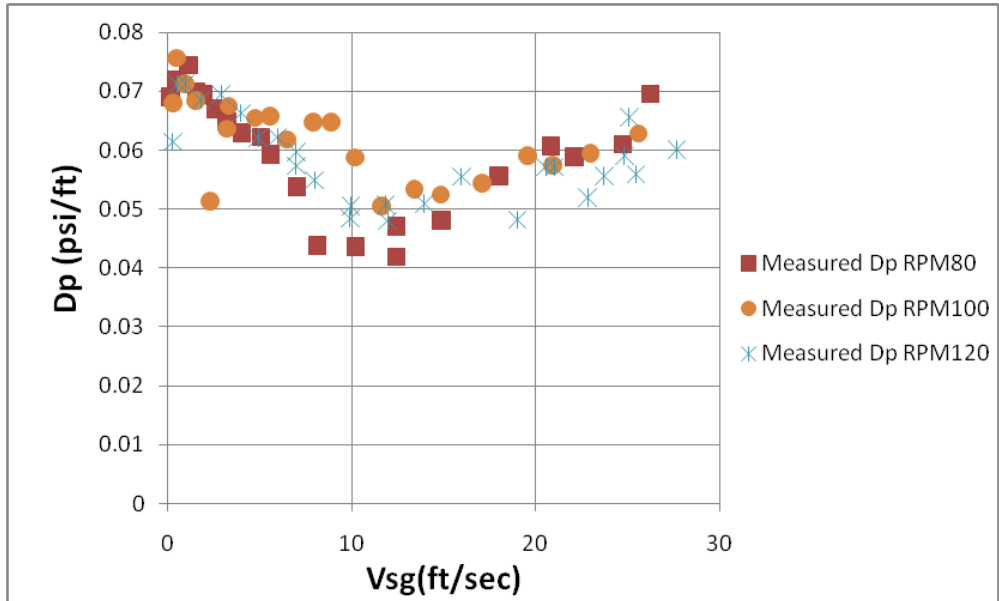


Figure 7.24 Measured Pressure Drop vs. Gas Superficial Velocity in Horizontal Test Section ($\theta=0$) $V_{SL}=2.0$ (ft/sec), ROP=100(ft/hrs) and RPM=80,100,120 (1/min)

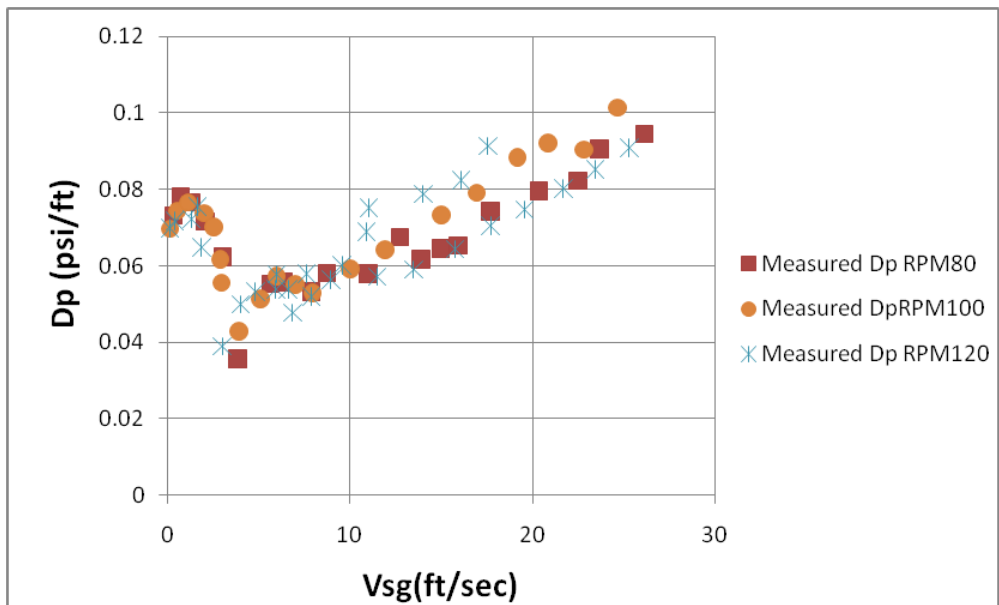


Figure 7.25 Measured Pressure Drop vs. Gas Superficial Velocity in Horizontal Test Section ($\theta=0$) $V_{SL}=3.0$ (ft/sec), ROP=100(ft/hrs) and RPM=80,100,120 (1/min)

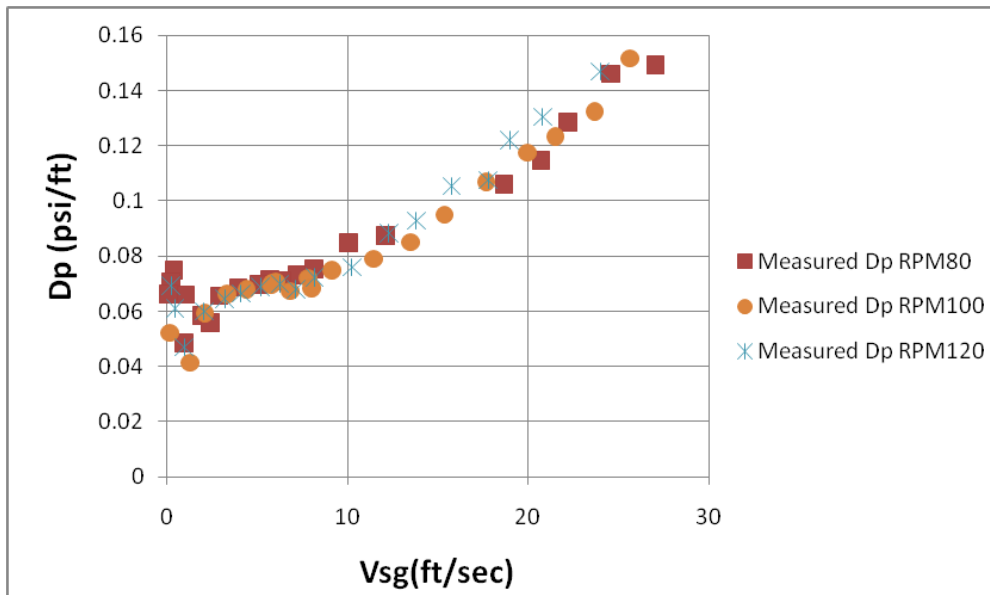


Figure 7.26 Measured Pressure Drop vs. Gas Superficial Velocity in Horizontal Test Section ($\theta=0$) $V_{SL}=4.0$ (ft/sec), ROP=100(ft/hrs) and RPM=80,100,120 (1/min)

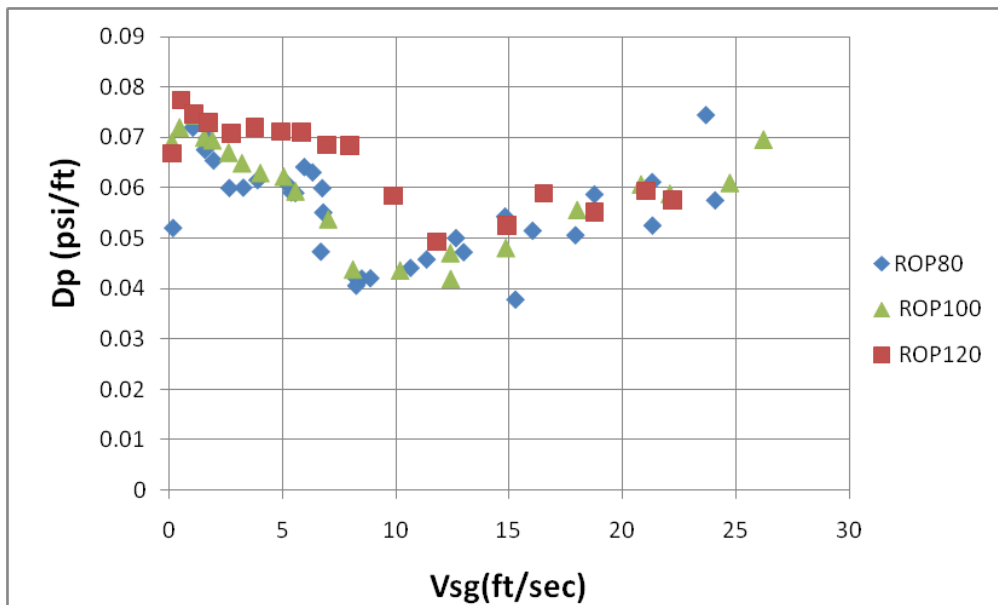


Figure 7.27 Measured Pressure Drop vs. Gas Superficial Velocity in Horizontal Test Section ($\theta=0$) $V_{SL}=2.0$ (ft/sec), RPM=80 (1/min) and ROP=80,100,120(ft/hrs)

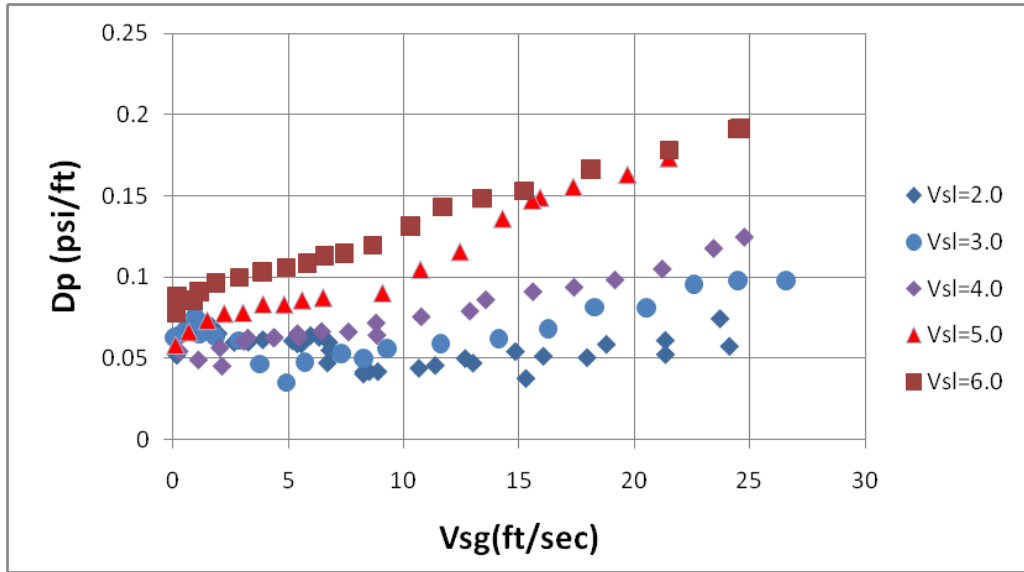


Figure 7.28 Measured Pressure Drop vs. Gas Superficial Velocity in Horizontal Test Section ($\theta=0$) $V_{SL}=2.0, 3.0, 4.0, 5.0$ and 6.0 (ft/sec), $ROP=80$ (ft/hrs) and $RPM=80, (1/min)$

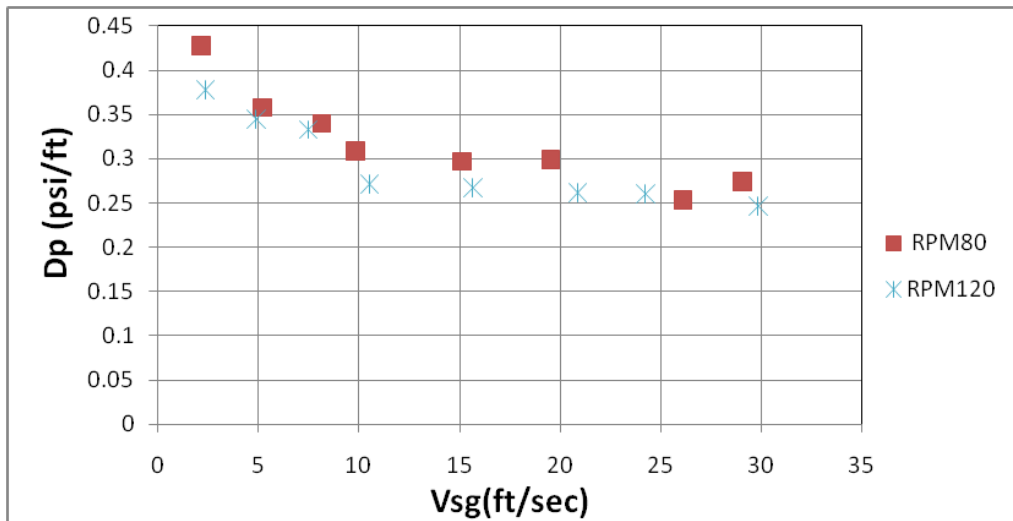


Figure 7.29 Measured Pressure Drop vs. Gas Superficial Velocity in Inclined Test Section ($\theta=45.0$) $V_{SL}=2.0$ (ft/sec), $ROP=120$ (ft/hrs) and $RPM=80, 120$ (1/min)

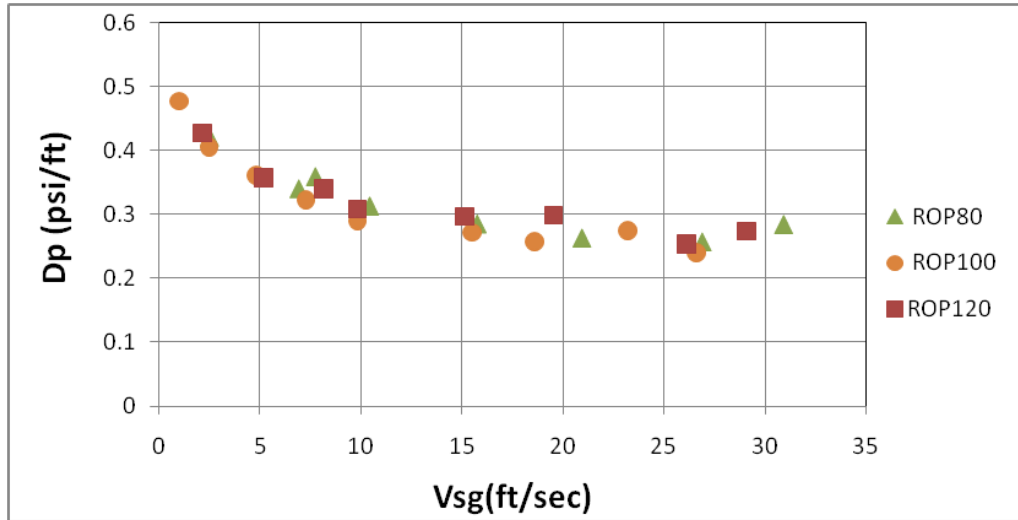


Figure 7.30 Measured Pressure Drop vs. Gas Superficial Velocity in Inclined Test Section ($\theta=45.0$) $V_{SL}=2.0$ (ft/sec), RPM=80 (1/min) and ROP=80,100,120 (ft/hrs)

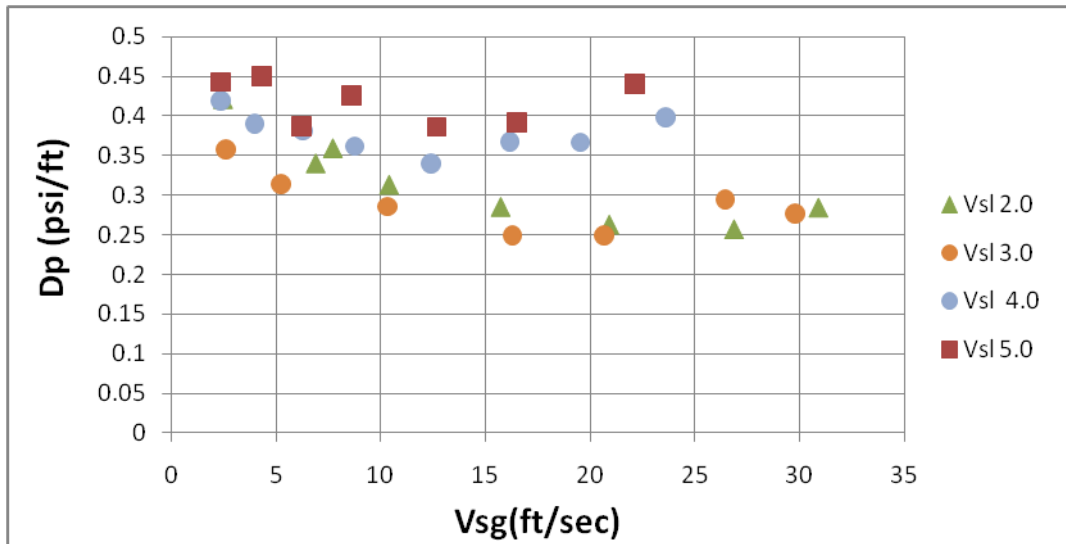


Figure 7.31 Measured Pressure Drop vs. Gas Superficial Velocity in Inclined Test Section ($\theta=45.0$) $V_{SL}=2.0, 3.0, 4.0$ & 5.0 (ft/sec), RPM=80 (1/min) and ROP=80 (ft/hrs)

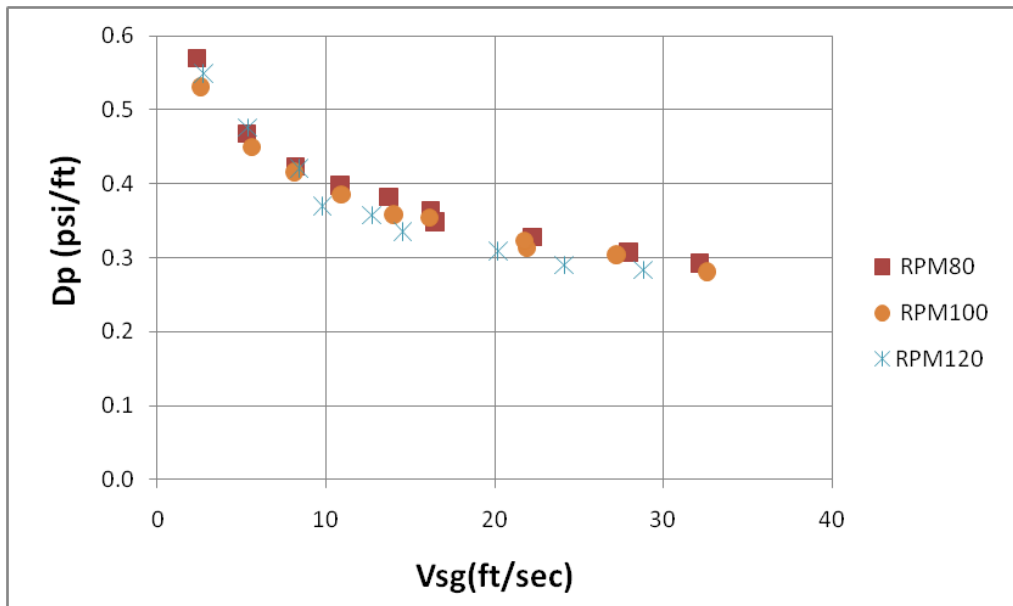


Figure 7.32 Measured Pressure Drop vs. Gas Superficial Velocity in Nearly Vertical Test Section ($\theta=77.5$) $V_{SL}=2.0$ (ft/sec), ROP=120(ft/hrs) and RPM=80,100,120(1/min)

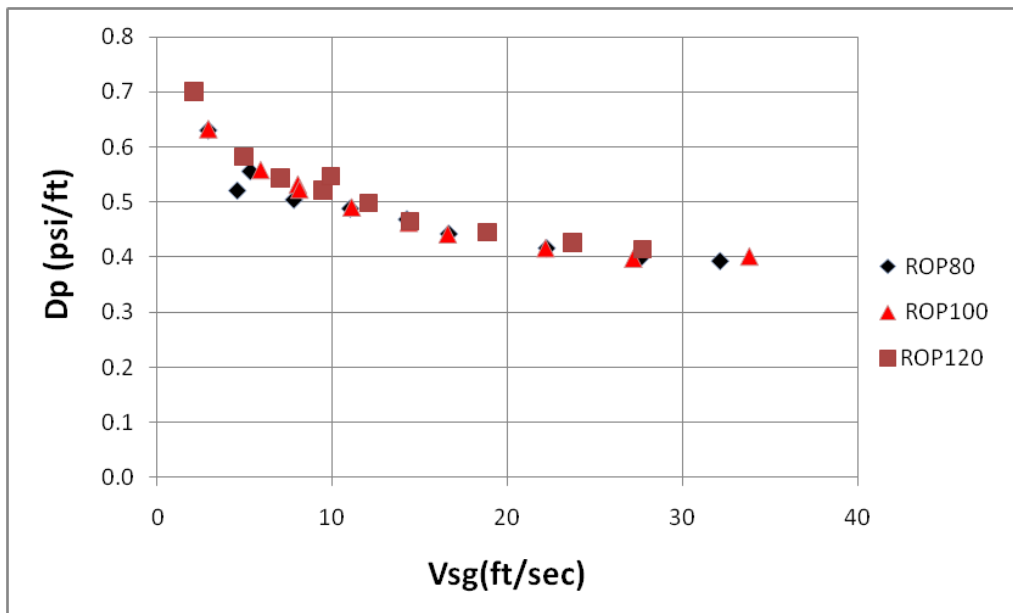


Figure 7.33 Measured Pressure Drop vs. Gas Superficial Velocity in Nearly Vertical Test Section ($\theta=77.5$) $V_{SL}=3.0$ (ft/sec), RPM=80 (1/min) and ROP=80,100,120(ft/hrs)

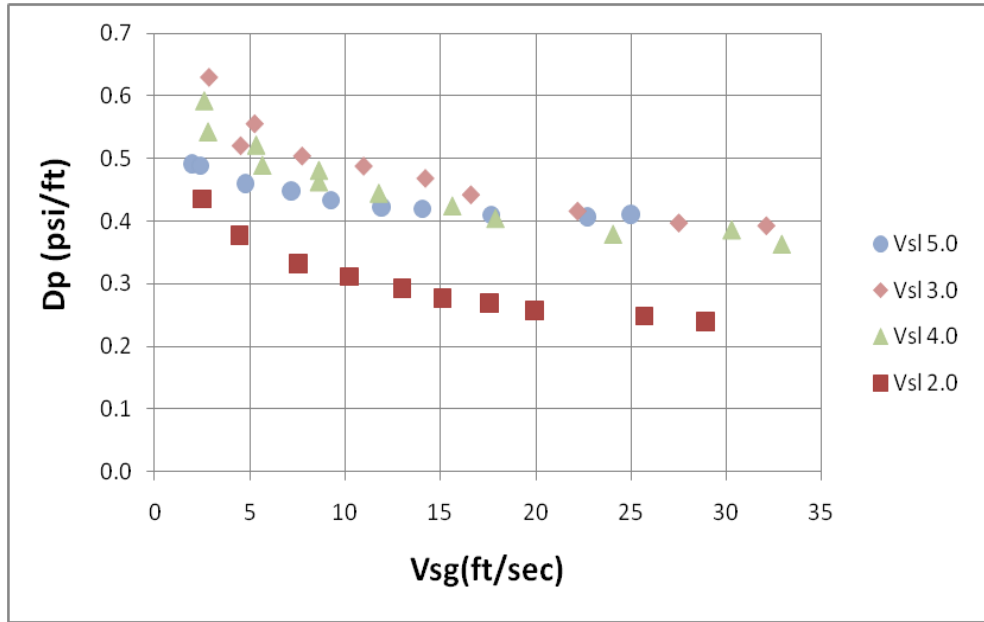


Figure 7.34 Measured Pressure Drop vs. Gas Superficial Velocity in Nearly Vertical Test Section ($\theta=77.5$) VSL=2.0, 3.0, 4.0&5.0 (ft/sec), RPM=80 (1/min) and ROP=80 (ft/hrs)

Figure 7.35 shows the comparisons among data for total pressure loss in the horizontal position, inclined positions and the nearly vertical position (77.5 degree from horizontal) for three phases flow in eccentric annuli, it is observed that in horizontal section, by increasing the gas velocity in wellbore, total pressure loss change modestly, since the only effective term in pressure drop is friction pressure loss and its change is small when compared with pressure drop changes in other inclination sections. But in inclined ($\theta=45.0, 15.0$ & 30.0) and nearly vertical sections, by increasing gas velocity, total pressure loss decrease significantly, gravitational pressure loss decrease due to mixture density reduction in these inclination sections.

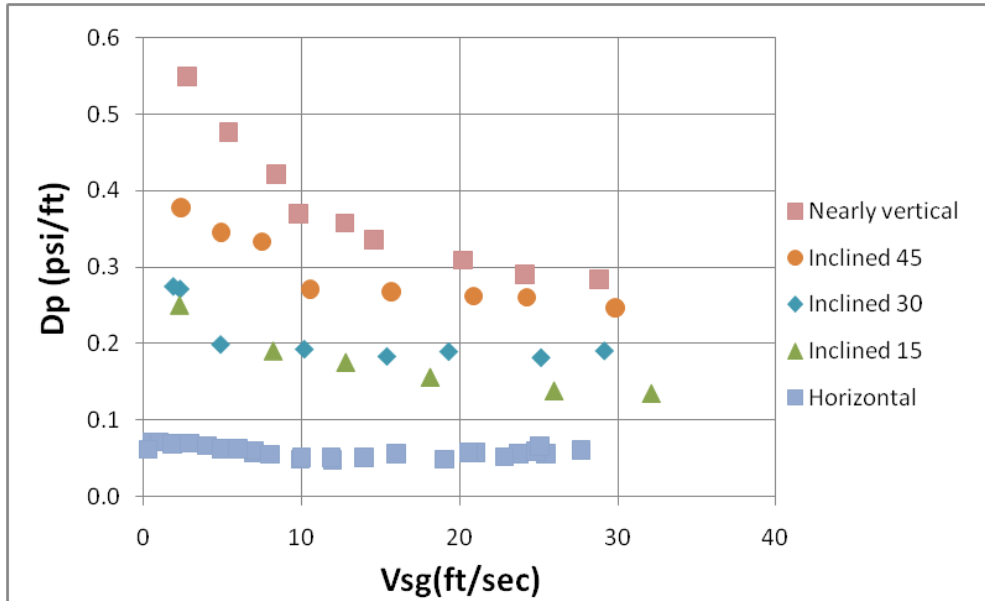


Figure 7.35 Measured Pressure Drop vs. Gas Superficial Velocity in Nearly Vertical ($\theta=77.5$) and Inclined ($\theta=45.0, 30.0$ & 15.0) Test Section for VSL=2.0 (ft/sec), RPM=120 (1/min) and ROP=120 (ft/hrs)

7-2 Comparison between Mechanistic Models Results and the Experimental Data

7-2-1 Solid (cutting)-Liquid Two Phase Flow

Comparison of model results and the experimental results for cuttings transport tests with water are presented from Figure 7.36 to Figure 7.38 in terms of measured total pressure drop versus calculated total pressure drop for horizontal ($\theta=0$), nearly vertical ($\theta=77.5$) and inclined ($\theta=45.0$) wellbore inclinations with inner pipe rotation.

For two phase flow in nearly vertical and inclined sections, the model slightly overestimates pressure losses in the system. But the difference between the experimental data and the estimated results are mostly less than of 20%, as shown in Figure 7.37 & 7.38. However in horizontal ($\theta=0$) section as shown in Figure 7.36, some of the experimental and compared results are different with an error of 50%. Most of these data points belong to the annular section for high pipe rotation speeds. The major reason for this high error is the presence of certain assumptions in

mechanistic model which neglect the effects of some drilling parameters. Although the model is developed for three phase fluid flow, the model can be used confidently for cutting- liquid two phase fluids as well except horizontal section.

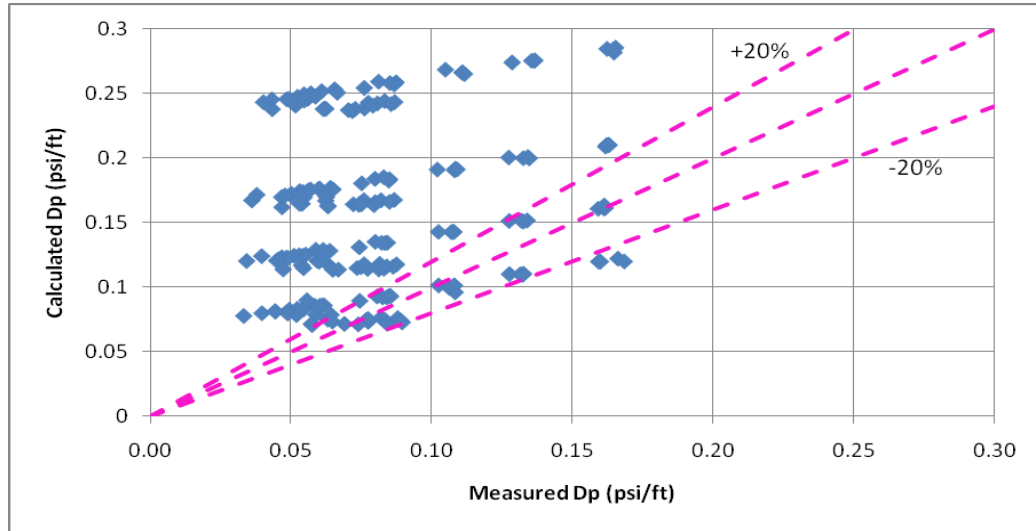


Figure 7.36 Comparisons between Experimental Data Obtained from Current Study and Estimated Friction Pressure Loss for Horizontal ($\theta=0$) Water-Solid (Cutting) Flow in Annuli with Inner Pipe Rotation by Using Developed Mechanistic Method (Presented in Section 6-4-4)

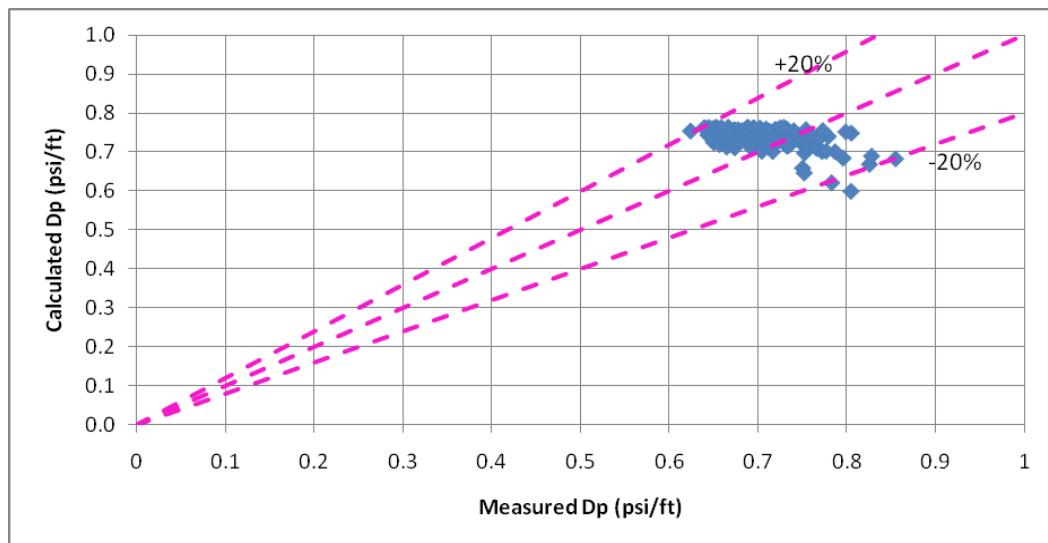


Figure 7.37 Comparisons between Experimental Data Obtained from Current Study and Estimated Total Pressure Loss for Nearly Vertical ($\theta=77.5$) Water-Solid (Cutting) Flow in Annuli with Inner Pipe Rotation by Using Developed Mechanistic Method (Presented in Section 6-4-4)

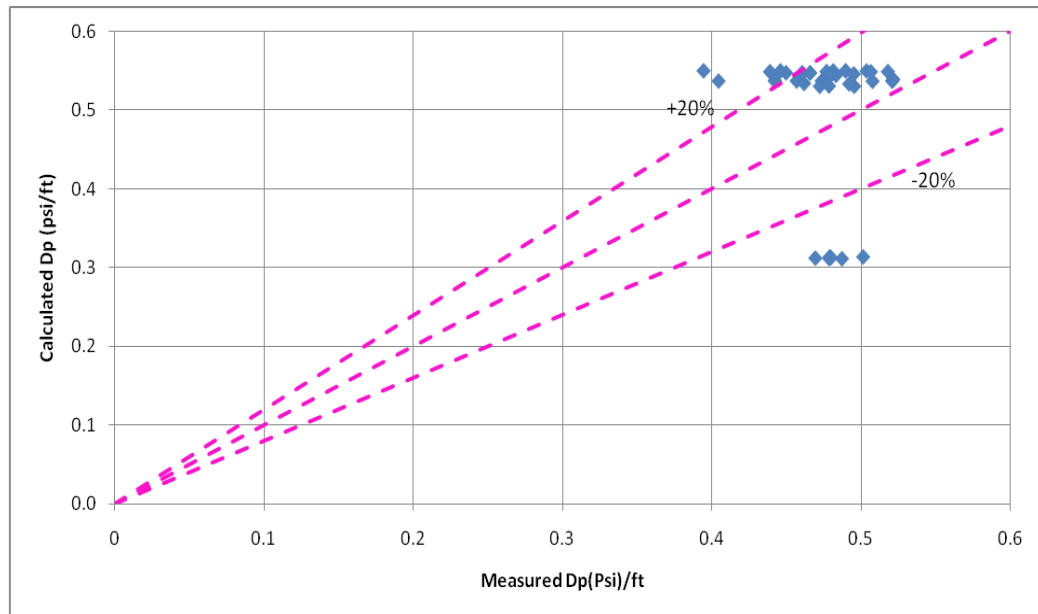


Figure 7.38 Comparisons between Experimental Data Obtained from Current Study and Estimated Total Pressure Loss for Inclined ($\theta=45.0$) Water-Solid (Cutting) Flow in Annuli with Inner Pipe Rotation by Using Developed Mechanistic Method (Pre-sented in Section 6-4-4)

7-2-2 Gas-Liquid Two Phase Flow

The experimental pressure loss data and model predictions for experiments conducted using METU Multiphase Flow Loop are compared in Figure 7.39 to Figure 7.42 in terms of measured total pressure drop versus calculated total pressure drop for nearly horizontal ($\theta=15.0$), nearly vertical ($\theta=77.5$), inclined ($\theta=30.0$) and inclined ($\theta=45.0$) wellbore inclinations without inner pipe rotation.

As shown in these Figures, the model slightly underestimates pressure losses in the system. But the difference between the experimental data and the estimated results are mostly less than of 20%.

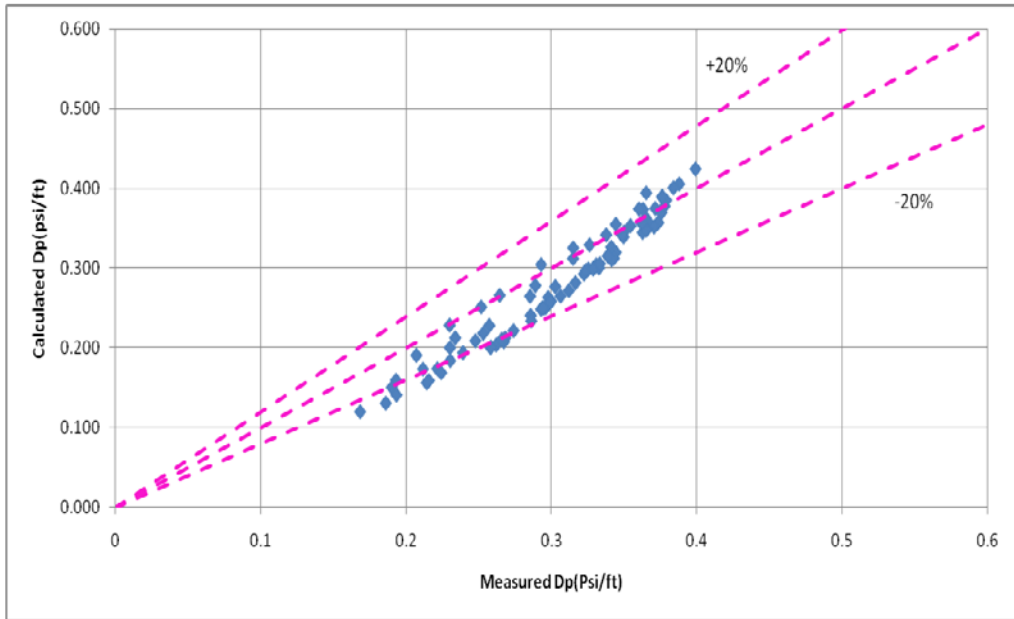


Figure 7-39 Comparisons between Experimental Data Obtained from Current Study and Estimated Total Pressure Loss for Nearly Vertical ($\theta=77.5$) Water-Air Flow in Annuli without Inner Pipe Rotation by Using Developed Mechanistic Method (Pre-sented in Section 6-4-3)

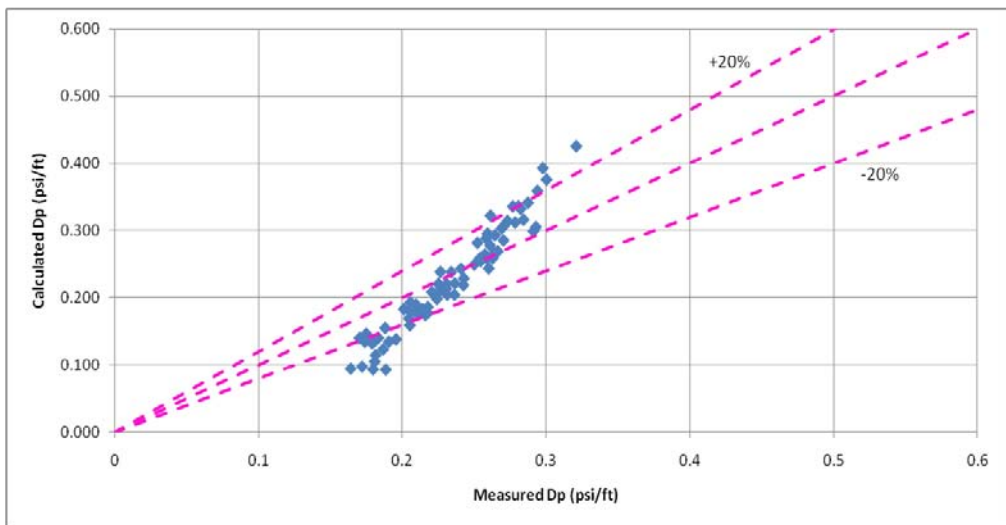


Figure 7.40 Comparisons between Experimental Data Obtained from Current Study and Estimated Total Pressure Loss for Inclined ($\theta=45.0$) Water-Air Flow in Annuli without Inner Pipe Rotation by Using Developed Mechanistic Method (Presented in Section 6-4-3)

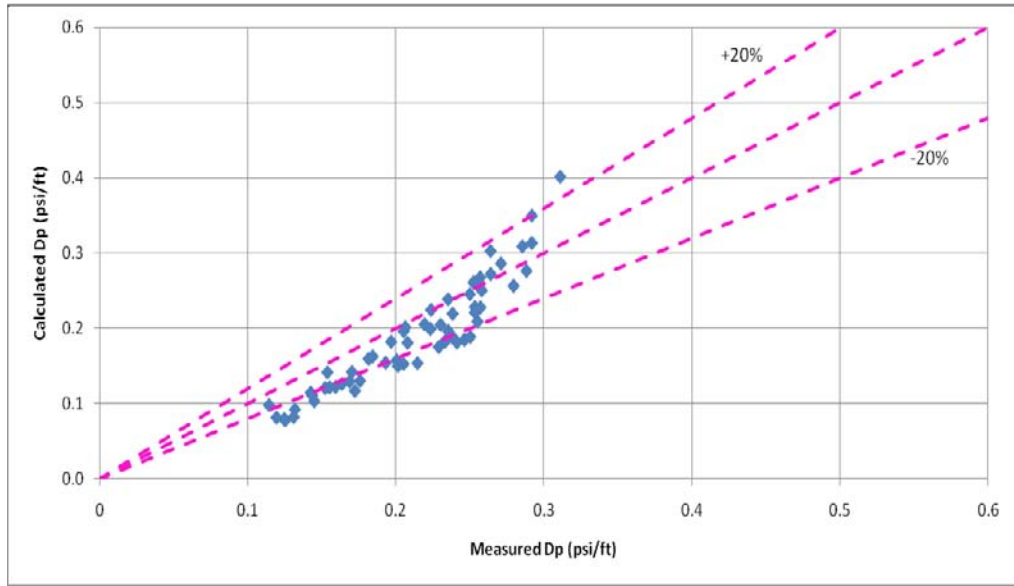


Figure 7.41 Comparisons between Experimental Data Obtained from Current Study and Estimated Total Pressure Loss for Inclined ($\theta=30.0$) Water-Air Flow in Annuli without Inner Pipe Rotation by Using Developed Mechanistic Method (Presented in Section 6-4-3)

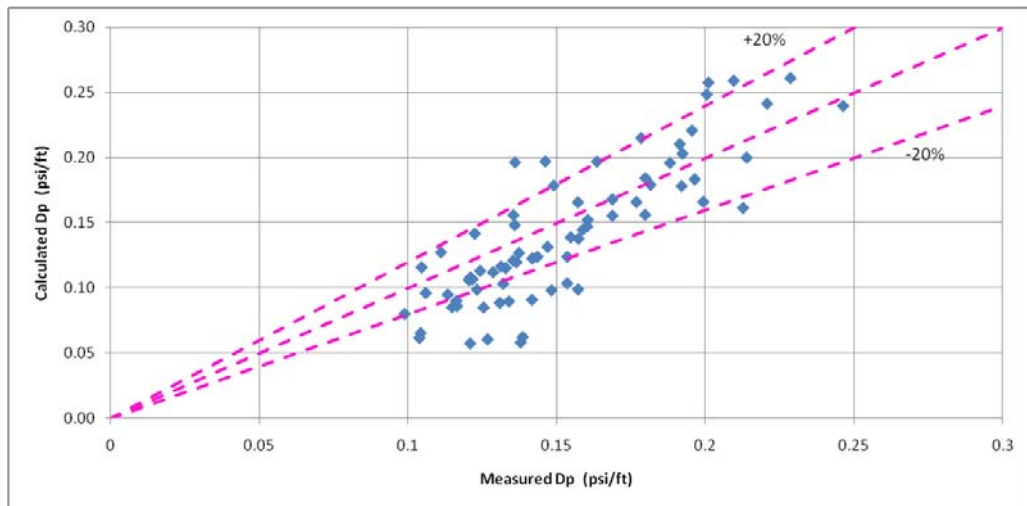


Figure 7.42 Comparisons between Experimental Data Obtained from Current Study and Estimated Total Pressure Loss for Inclined ($\theta=15.0$) Water-Air Flow in Annuli without Inner Pipe Rotation by Using Developed Mechanistic Method (Presented in Section 6-4-3)

7-2-3 Cutting-Gas-Liquid Three Phase Flow

The developed mechanistic model was applied to predict the total cuttings concentration inside the wellbore and developed total pressure loss using the experimental data. Analysis is conducted for three different cuttings injection rates,

and three pipe rotation speeds. Here, examples are given for different liquid flow rates and inclination sections.

In the case of horizontal section, as shown from Figures 7.43, 7.44 and 7.45, mechanistic model can estimate the total cuttings concentration in horizontal annuli with acceptable accuracy considering liquid-gas flow with presence of cuttings and pipe rotation in low liquid velocity (see figure 7.43&7.44). For high liquid velocity (see figure 7.45) probably because of neglecting the effects of lift force and some other drilling parameters, the model overestimate the total cutting concentration in the system. It is also observed that by increasing pipe rotation rate, total cuttings concentration, including stationary and moving particles, was not considerably changed in horizontal annuli, as the cuttings injection, liquid and gas flow rates are kept constant. This observation was confirmed by the results obtained from the experiments and the mechanistic model (figures 7.43, 7.44 and 7.45.). These figures also show that there is a relation between the cuttings concentration and observed area occupation by the cuttings determined from digital images.

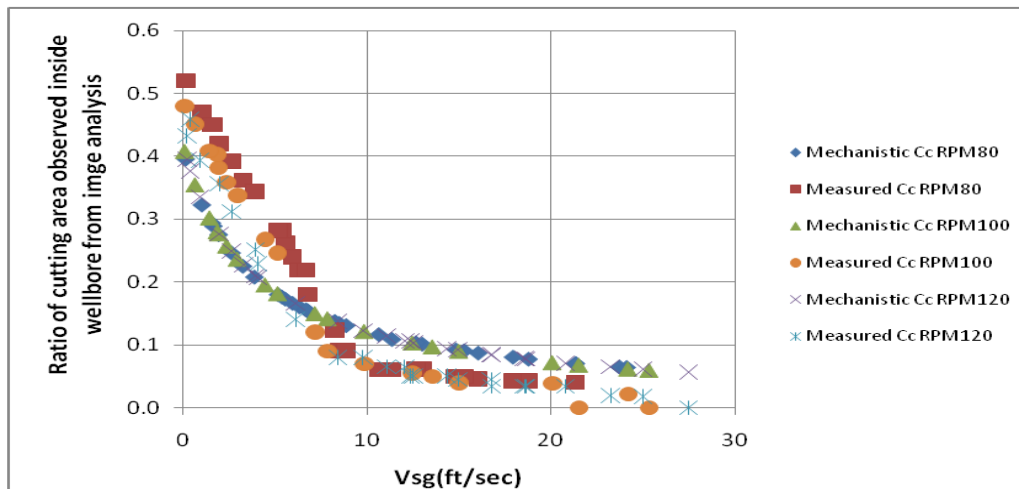


Figure 7.43 Ratio of Cutting Area Observed inside Wellbore from Image Analysis and Calculated Cutting Concentration by Mechanistic Model vs. Gas Superficial Velocity for VSL=2.0 (ft/sec), ROP=80(ft/hrs), RPM=80,100 &120 (1/min) for Horizontal Water-Air and Cutting Three Phases Flow in Eccentric Annuli with Inner Pipe Rotation by Using Developed Mechanistic Method

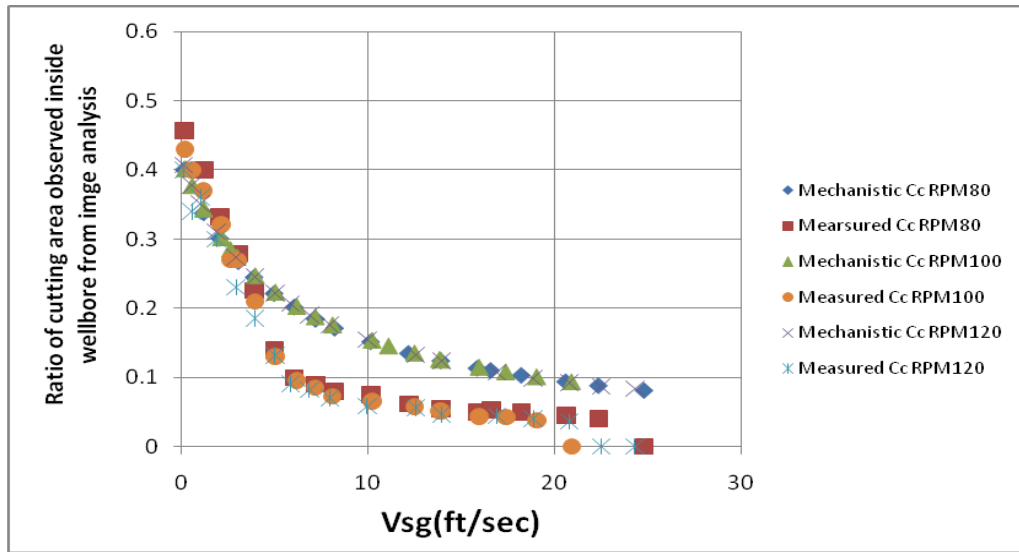


Figure 7.44 Ratio of Cutting Area Observed inside Wellbore from Image Analysis and Calculated Cutting Concentration by Mechanistic Model vs. Gas Superficial Velocity for VSL=3.0 (ft/sec), ROP=120(ft/hrs), RPM=80,100 &120 (1/min) for Horizontal Water-Air and Cutting Three Phases Flow in Eccentric Annuli with Inner Pipe Rotation by Using Developed Mechanistic Method

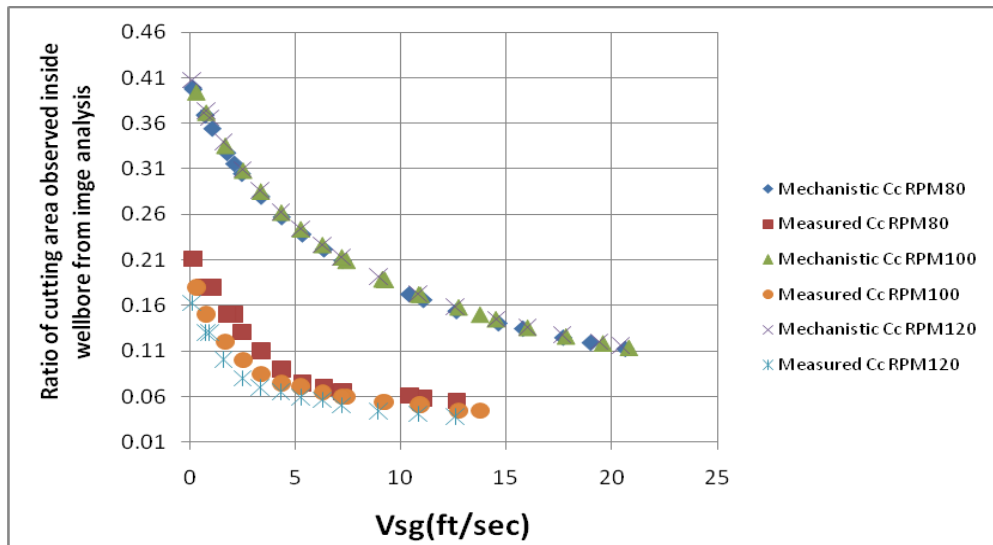


Figure 7.45 Ratio of Cutting Area Observed inside Wellbore from Image Analysis and Calculated Cutting Concentration by Mechanistic Model vs. Gas Superficial Velocity for VSL=4.0 (ft/sec), ROP=120(ft/hrs), RPM=80,100 &120 (1/min) for Horizontal Water-Air and Cutting Three Phases Flow in Eccentric Annuli with Inner Pipe Rotation by Using Developed Mechanistic Method

Figure 7.46 shows calculated cutting concentration by mechanistic model in different inclination sections for constant drilling parameters. It is observed that volumetric cutting concentration is increased by increasing inclination from horizontal section, since in high inclinations (from horizontal) gravity force applied

to solid particles cause to accumulate them into wellbore when gasified fluids are used as drilling fluid, as the inclination decrease the effect of gravity reduces and volumetric cutting concentration also decrease compared by vertical section.

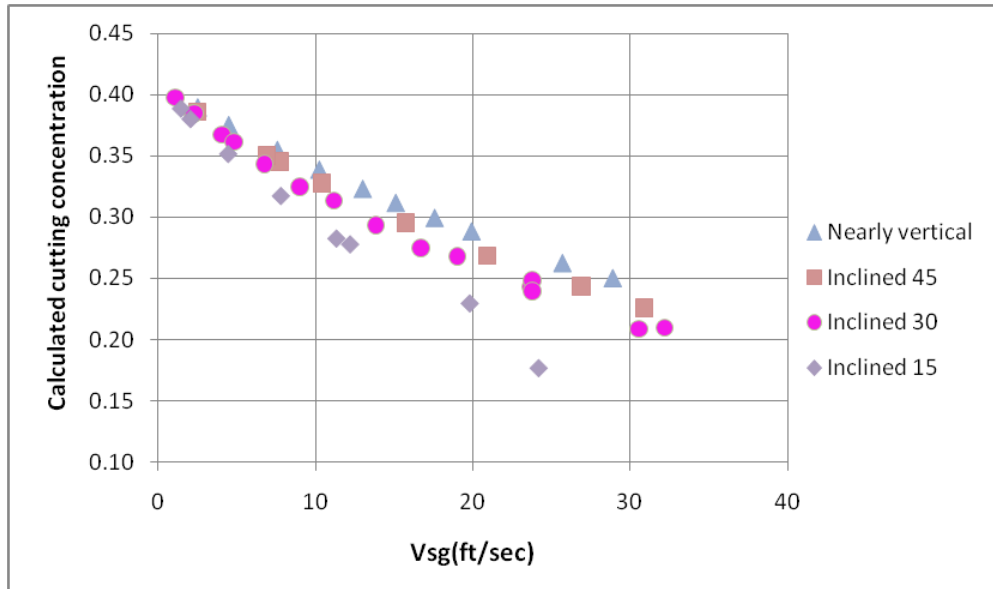


Figure 7.46 Calculated Cutting Concentration by Mechanistic Model vs. Gas Superficial Velocity for VSL=2.0 (ft/sec), ROP=80(ft/hrs), RPM=80 (1/min) in Horizontal ($\theta=0.$), Nearly Vertical ($\theta=77.5$) and Inclined ($\theta=45.0,30.0\&15.0$) Test Sections for Water-Air and Cutting Three Phases Flow in Eccentric Annuli with Inner Pipe Rotation by Using Developed Mechanistic Method

The experimental pressure loss data and model predictions for experiments conducted in horizontal section using METU Multiphase Flow Loop are compared in Figures 7.47-51. These figures show that the mechanistic model can estimate frictional pressure losses successfully for a given cuttings injection, liquid and gas flow rates, including pipe rotation in high gas superficial velocity. In low gas superficial velocity, because of failure in volumetric cutting concentration, the model overestimates the friction pressure loss.

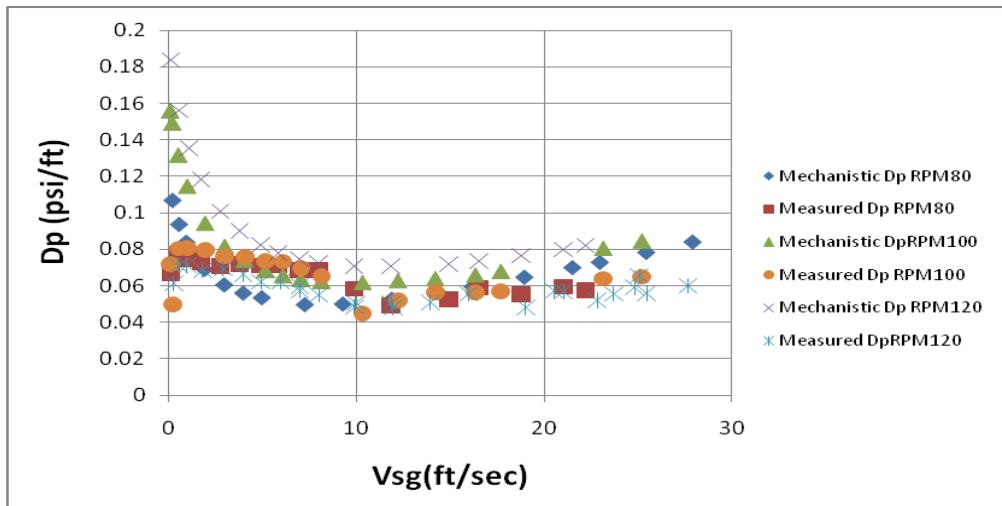


Figure 7.47 Measured and Predicted Pressure Drop vs. Gas Superficial Velocity by Mechanistic Model vs. Gas Superficial Velocity for VSL=2.0 (ft/sec), ROP=120(ft/hrs), RPM=80,100 &120 (1/min) for Horizontal Water-Air and Cutting Three Phases Flow in Eccentric Annuli with Inner Pipe Rotation by Using Developed Mechanistic Method (presented in section 6-4-4)

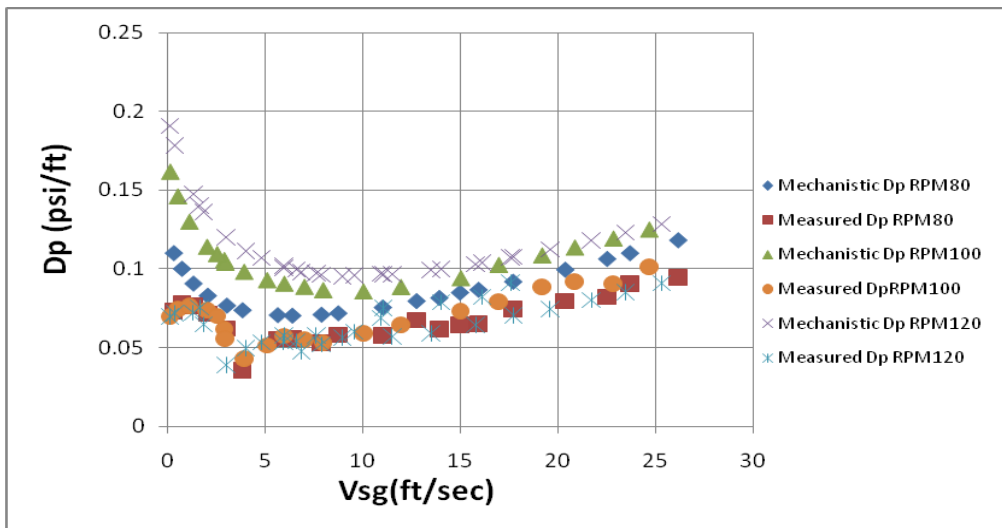


Figure 7.48 Measured and Predicted Pressure Drop vs. Gas Superficial Velocity by Mechanistic Model vs. Gas Superficial Velocity for VSL=3.0 (ft/sec), ROP=100(ft/hrs), RPM=80,100 &120 (1/min) for Horizontal Water-Air and Cutting Three Phases Flow in Eccentric Annuli with Inner Pipe Rotation by Using Developed Mechanistic Method (presented in section 6-4-4)

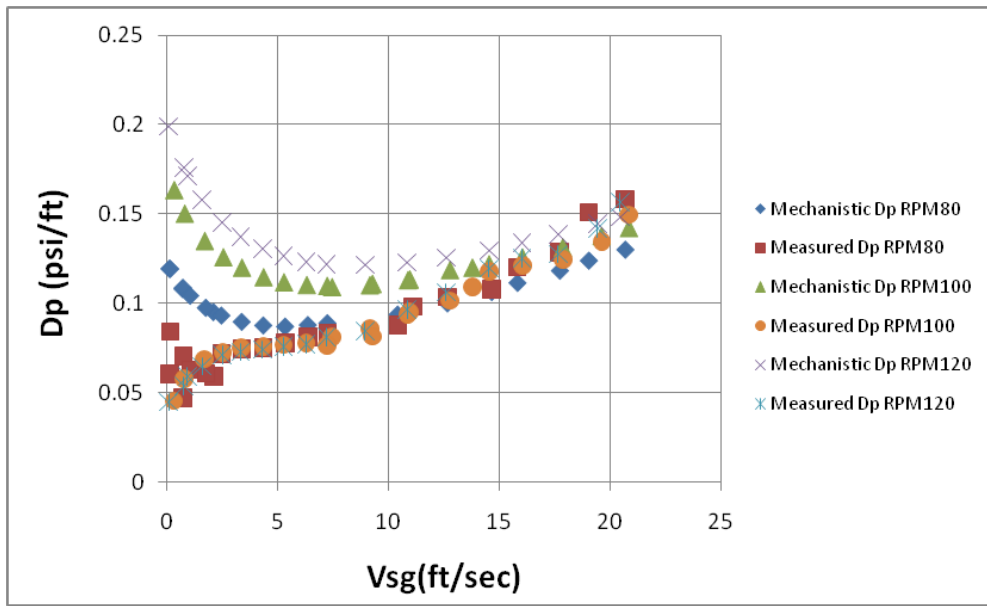


Figure 7.49 Measured and Predicted Pressure Drop vs. Gas Superficial Velocity by Mechanistic Model vs. Gas Superficial Velocity for VSL=4.0 (ft/sec), ROP=120(ft/hrs), RPM=80,100 & 120 (1/min) for Horizontal Water-Air and Cutting Three Phases Flow in Eccentric Annuli with Inner Pipe Rotation by Using Developed Mechanistic Method (presented in section 6-4-4)

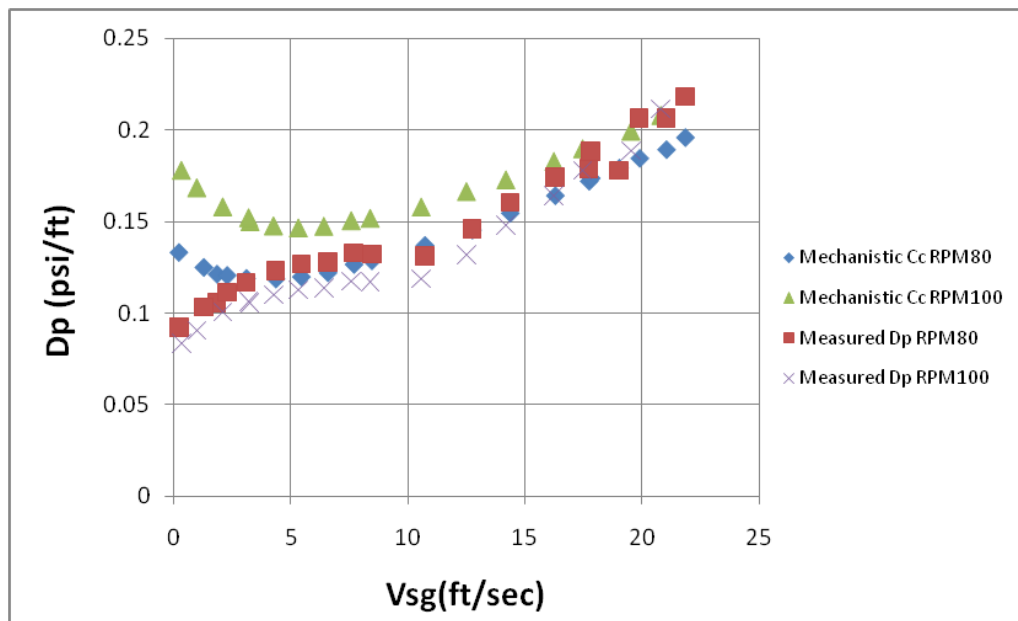


Figure 7.50 Measured and Predicted Pressure Drop vs. Gas Superficial Velocity by Mechanistic Model vs. Gas Superficial Velocity for VSL=6.0 (ft/sec), ROP=100(ft/hrs), RPM=80&120 (1/min) for Horizontal Water-Air and Cutting Three Phases Flow in Eccentric Annuli with Inner Pipe Rotation by Using Developed Mechanistic Method (presented in section 6-4-4)

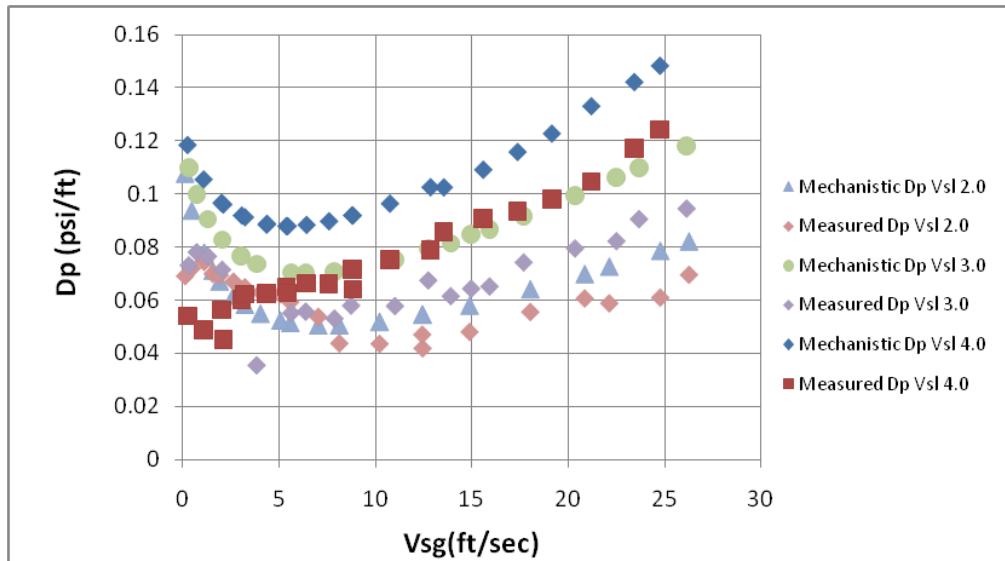


Figure 7.51 Measured and Predicted Pressure Drop vs. Gas Superficial Velocity by Mechanistic Model vs. Gas Superficial Velocity for VSL=2.0, 3.0, 4.0(ft/sec), ROP=100(ft/hrs), RPM=80 (1/min) for Horizontal Water-Air and Cutting Three Phases Flow in Eccentric Annuli with Inner Pipe Rotation by Using Developed Me-CHANISTIC Method (presented in section 6-4-4)

Based on observations mentioned in section 7-1-3-2 about minimum gas superficial velocity corresponding to minimum pressure drop, the minimum gas superficial velocity for each constant liquid flow rate can be calculated, for instance, table 7.1 shows the minimum gas superficial velocity for various liquid flow rate at constant pipe rotation speeds (RPM=80 1/min) and rate of penetration (ROP=100 ft/hr). It is observed that at a liquid flow rate, the predicted and observed minimum gas superficial velocities are close to each other.

Table 7.1 -Minimum Gas Superficial Velocity for Three Phase Flow in Horizontal Eccentric Annuli $V_{SL}=3$ ft/s, ROP=80 ft/hr

ROP	RPM	Vsl	DP	Model			Experiments	
				Min VSL	Cc	DP	Min VSL	Cc
100.0	80.0	2.0	0.050	7.037	0.153	0.044	8.127	0.168
100.0	80.0	3.0	0.070	5.634	0.210	0.055	5.634	0.100
100.0	80.0	4.0	0.092	3.073	0.288	0.060	3.073	0.080

Figures 7.52, 7.53, 7.54 and 7.55 show that in all inclination sections, most of total pressure drop estimations are close to the experimental data, with a difference less than 20%, but some points are out of the $\pm 25\%$ window, as seen in Figures 7.53,

7.54 and 7.55. Most of these data points belong to the annular section for high inner pipe rotation. The major reason for this high error is the presence of mechanical difficulties in the flow loop; it is not easy to control vibrations created in high inner pipe rotations. These vibrations affect the accuracy of the pressure transducers.

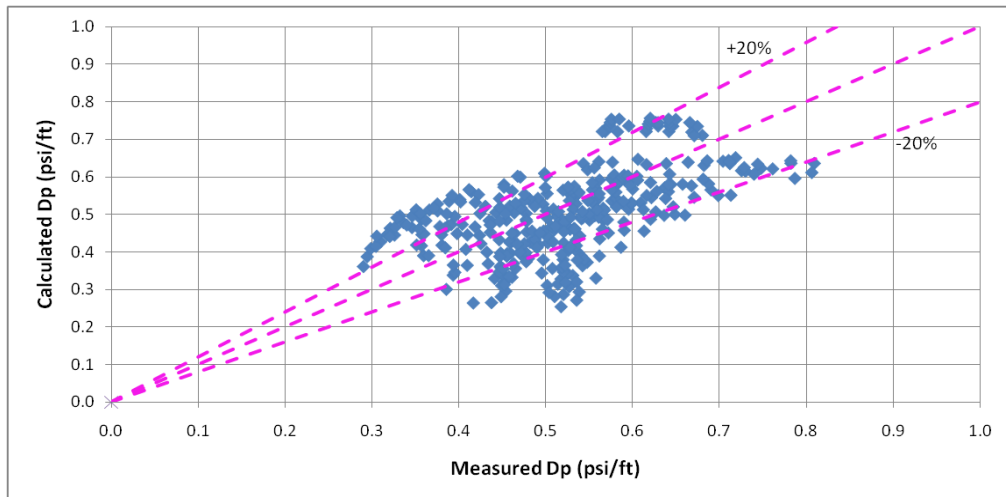


Figure 7.52 Measured and Predicted Pressure Drop vs. Gas Superficial Velocity by Mechanistic Model vs. Gas Superficial Velocity for VSL=2.0, 3.0, 4.0,5.0(ft/sec), ROP=80,100,120(ft/hrs), RPM=80,100,120 (1/min) for Nearly Vertical ($\theta=77.5$) Water-Air and Cutting Three Phases Flow in Eccentric Annuli with Inner Pipe Rotation by Using Developed Mechanistic Method

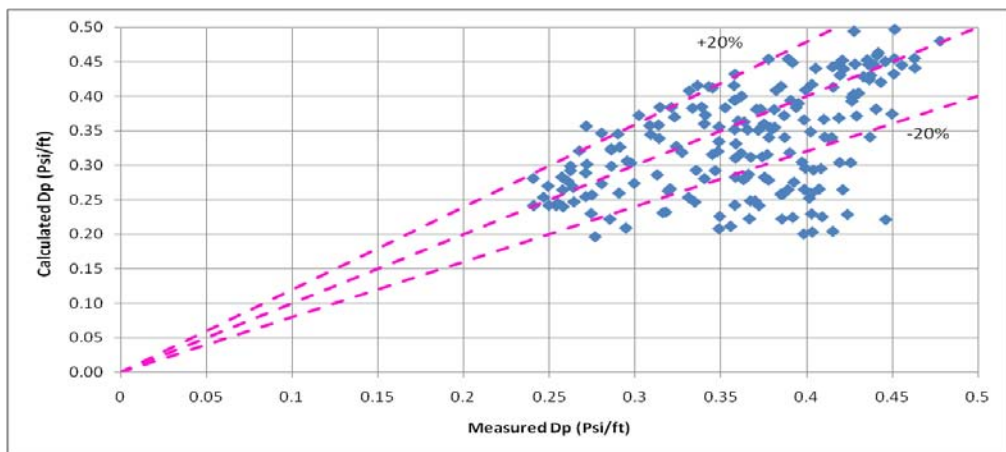


Figure 7.53 Measured and Predicted Pressure Drop vs. Gas Superficial Velocity by Mechanistic Model vs. Gas Superficial Velocity for VSL=2.0, 3.0, 4.0,5.0(ft/sec), ROP=80,100,120(ft/hrs), RPM=80,100,120 (1/min) for Inclined ($\theta=45.0$) Water-Air and Cutting Three Phases Flow in Eccentric Annuli with Inner Pipe Rotation by Us-ing Developed Mechanistic Method

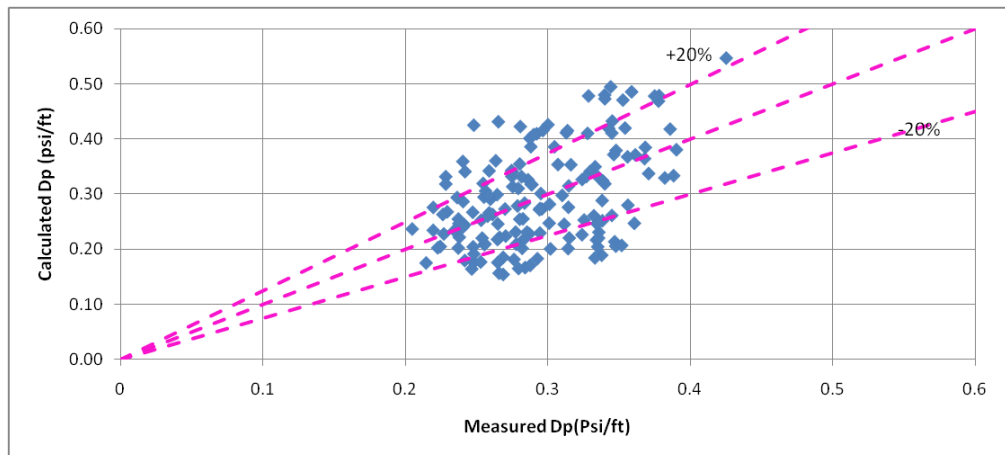


Figure 7.54 Measured and Predicted Pressure Drop vs. Gas Superficial Velocity by Mechanistic Model vs. Gas Superficial Velocity for VSL=2.0, 3.0, 4.0,5.0(ft/sec), ROP=80,100,120(ft/hrs), RPM=80,100,120 (1/min) for Inclined ($\theta=30.0$) Water-Air and Cutting Three Phases Flow in Eccentric Annuli with Inner Pipe Rotation by Us-ing Developed Mechanistic Method

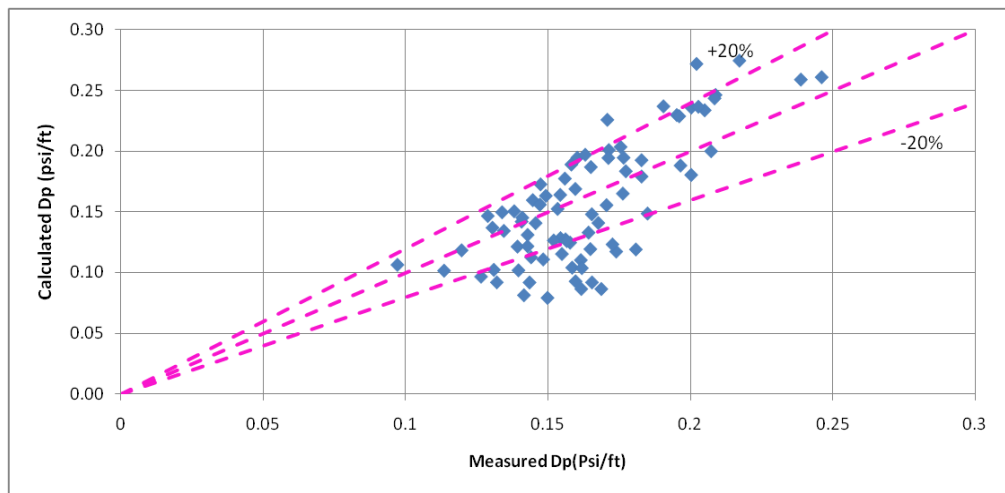


Figure 7.55 Measured and Predicted Pressure Drop vs. Gas Superficial Velocity by Mechanistic Model vs. Gas Superficial Velocity for VSL=2.0, 3.0, 4.0,5.0(ft/sec), ROP=80,100,120(ft/hrs), RPM=80,100,120 (1/min) for Nearly Horizontal ($\theta=15.0$) Water-Air and Cutting Three Phases Flow in Eccentric Annuli with Inner Pipe Rota-tion by Using Developed Mechanistic Method

CHAPTER IX

CONCLUSION

This study aims to address the hydrodynamic behavior of 2-phase drilling fluids in horizontal, inclined and vertical wellbores with the presence of cuttings and inner pipe rotation. Extensive experiments were conducted at a cuttings transport flow loop using air-water mixtures under a wide range of air and water flow rates, rate of penetrations (ROP), pipe rotations and hole inclinations. All experiments were recorded using a high-speed digital camera, and the images were analyzed using digital image processing techniques (DIPT). With the help of these images, flow patterns were classified for various flow conditions. Volumetric concentrations and local velocities of liquid, gas and cuttings phases inside the wellbore were detected. The experimental data was also used to investigate the cuttings transport mechanisms for different flow patterns. During the experiments, pressure losses, in-situ flow rates for each phase, ROP, inclination and pipe rotation speed were recorded.

Experimental study of the flow of air-water through horizontal annuli was carried out. The two-phase flow configurations, called as flow patterns, were identified by visual observations and the flow pattern maps were developed by using diagraphic discriminant analysis method. In case of air-water flow without drill pipe rotation, the observed flow patterns were defined in a similar way to those defined for pipe flow. New flow pattern map can be estimated the two phase flow regime in horizontal annuli successfully.

At the same time video recordings acquired for different flow patterns were analyzed frame by frame and water, gas levels along with liquid holdup measurements were obtained by using image processing techniques. The analysis of the frame images indicate that by using appropriate image processing techniques on experimental multi-phase flow data, similar measurements of flow parameters were obtained when compared to theoretical data and other flow experiments.

By comparing the measured liquid hold up and pressure gradients though both studies and calculated liquid hold up and pressure gradients by traditional methods which developed for pipe flow, it is observed that these methods cannot estimated liquid hold up and pressure gradient for two phase flow in eccentric annular geometry with an acceptable accuracy. In this study, Lockhart & Martinelli (1969) and Beggs & Brill (1973) were modified and analyzed by using experimental data obtained from this study and sunthankar study (2002). Additionally, new correlations were developed in order to estimate liquid hold up and pressure gradient by using Matlab and statistical methods.

In this study, also, cuttings transport experiments have been conducted in horizontal annulus using water and cuttings for various flow rates, rate of penetration values, pipe rotation speeds. Image processing techniques have been applied for determining cuttings concentrations, moving cuttings concentrations, transport velocity of the cuttings and amount of developed bed by the help of a high speed digital camera, which is used during the tests. Finally, discriminant techniques are applied for developing equations to estimate these parameters as a function of dimensionless groups obtained considering superficial conditions. The followings are majorly concluded:

- As the ROP increases, total cuttings concentration in the wellbore increases
- Increasing total cuttings concentration leads to an increase in frictional pressure losses
- Increase in flow rate causes an increase in transport velocity of the cuttings
- Empirical equations can estimate the desired hard-to-identify drilling parameter with a reasonable accuracy

Based on the obtained results from this study, a mechanistic model was developed to predict the volumetric distribution of each phase in three phase flow and to estimate frictional pressure drop for horizontal well sections by considering the effects of drill pipe rotation and eccentricity.

The following important conclusions also can be made from the experimental and theoretical studies.

- Conformal mapping technique can be applied in order to contribute the effect of eccentricity in three phase flow behavior.
- The effect of pipe rotation rate was investigated and it is also observed that by increasing pipe rotation rate, total cuttings concentration, including stationary and moving particles, was not considerably changed in horizontal annuli, as the cuttings injection, liquid and gas flow rates are kept constant.
- By using the information obtained from this study, the minimum gas superficial velocity for a constant liquid flow rate can be calculated for optimization of flow rates for liquid and gas phases in order to obtain the minimum frictional pressure losses inside the horizontal section while transporting the cuttings in an effective way.

Thus, the information obtained from this study is applicable to any underbalanced drilling operation conducted with gas-liquid mixtures, for optimization of flow rates for liquid and gas phases in order to transport the cuttings in the horizontal, inclined and vertical sections in an effective way with a reasonably low frictional pressure loss. At the same time, by using obtained results from the digital image processing techniques, cutting particles movements and cutting transport mechanism within the well can be recognized more realistic.

CHAPTER X

RECOMMENDATIONS

- The rheological parameters presented in this study are valid for the Newtonian fluid used. Determination of universal rheological parameters for any non-Newtonian fluid must be included in the models.

- The accuracy of the proposed models can be improved by focusing on the friction factors between the cuttings bed and the second layer, drag and lift coefficients, interactions between cuttings and the concept of wall slip in the wellbores.

- More accurate and successful results can be achieved for determination of cutting concentration by using two or three more high speed camera recording experiments from different directions in annulus test section

- Effect of low pipe rotation and temperature should be investigated on gasified fluid flow with cuttings.

- More work is needed for cuttings transport with gasified fluid at wellbore inclinations between 20° and 70° from horizontal

REFERENCES

- Abduvayt P., Manabe R. and Arihara N.: "Effects of Pressure and Pipe Diameter on Gas-Liquid Two-Phase Flow Behavior in Pipelines", SPE 84229, Society of Petroleum Engineering, 2003.
- Adari R.B., .Development of Correlations Relating Bed Erosion to Flowing time for Near Horizontal Wells., M.S. Thesis, The University of Tulsa, Tulsa (2000)
- Andrea Cioncolini, John R. Thome, Carlo Lombardi " Algebraic turbulence modeling in adiabatic gas-liquid annular two-phase flow" International Journal of Multiphase Flow 35 (2009) 580-596
- Andersen H., A. Vigrestad, E. Kuru, , "Hydraulic Optimization of Aerated Mud Drilling for Maximum Drilling Rate" IADC/SPE Managed Pressure Drilling and Underbalanced Operations Conference & Exhibition, 12-13 February 2009, San Antonio, Texas
- Andritsos, N., and Hanratty, T. J.: "Influence of Interfacial Waves in Stratified Gas-Liquid Flows," AICHE J. 33, No. 3, 444-454 (1987).
- Ansari A.M., Sylvester N.D., Cem Sarica, Ovadia Shoham, J.P. Brill, "A Comprehensive Mechanistic Model for Upward Two-Phase Flow in Wellbores" Journal SPE Production & Facilities, Volume 9, Number 2, May 1994
- Antonio C.V.M. Lage, Rune W. Time, "an Experimental and Theoretical Investigation of Upward Two-Phase Flow in Annuli" SPE Asia Pacific Oil and Gas Conference and Exhibition, 16-18 October 2000, Brisbane, Australia
- Avila R., Pereira E., Miska S., Takach N., Saasen A., "Correlations and Analysis of Cuttings Transport With Aerated Fluids in Deviated Wells" Journal SPE Drilling & Completion Volume 23, Number 2, Pages: 132-141, June 2008
- Azbel D.: "Two-Phase Flow for chemical engineering" Cambridge University Press, 1981. PP 121-123&147
- Azouz, I., .Numerical Simulation of Laminar and Turbulent Flows of Wellbore Fluids in Annular Passages of Arbitrary Cross-Section., Ph.D. Dissertation, University of Tulsa, Tulsa (1994)
- Baker, A., Nielsen, K., and Gabb, A.: "Pressure loss, Liquid Holdup Calculations developed," Oil & Gas J., 55-59 (March 14, 1998).

Barnea D.' 'A unified model for predicting flow-pattern transitions for the whole range of pipe inclinations' Int. J. Multiphase Flow 13 (1987), pp. 1–12.

Barnea, D., Shoham, O., and Taitel, Y.: "Flow Patter Transition for Vertical Downward Inclined Two-Phase Flow; Horizontal to Vertical," Chem. Eng. Sc. 37, No. 5, 735-740 (1982).

Barnea D., Granica D., Doron P. and Taitel Y. "Hydraulic Transport of Course Particles with Gas Injection" 10th International Conference on the Hydraulic Transport of Solid in Pipes, Innsbruck, Austria: 29-31 October 1986

Bassal, A. A., .The Effect of Drill pipe Rotation on Cuttings Transport in Inclined Wellbores., M.S. Thesis, University of Tulsa, Tulsa (1996)

Becker, T. E., .Correlations for Drill-Cuttings Transport in Directional-Well Drilling., Ph.D. Dissertation, University of Tulsa, Tulsa (1987)

Beggs, H.D., and Brill, J.P.: "A Study of Two-Phase Flow in Inclined Pipes," JPT (May 1973) 607; Trans., AIME, 255.

Bilgesu H.I., Mishra N., Ameri S., "Understanding the Effect of Drilling Parameters on Hole Cleaning in Horizontal and Deviated Wellbores Using Computational Fluid Dynamics" Eastern Regional Meeting, 17-19 October 2007, Lexington, Kentucky USA

Bin-Haddah, A. S., .Development of Models for Drill Cuttings Transport in Inclined Wells Based on Deposition Critical Velocity Concept., M.S. Thesis, University of Tulsa, Tulsa (1988)

Bonizzi a M., P. Andreussi a, b, S. Banerjee "Flow regime independent, high resolution multi-field modeling of near-horizontal gas-liquid flows in pipelines" International Journal of Multiphase Flow 35 (2009) 34–46

Brown, N. P., Bern, P. A., and Weaver, A., .Cleaning Deviated Holes: New Experimental and Theoretical Studies., SPE/IADC 18636, Presented at the 1989 Drilling Conference, New Orleans-Louisiana (February 28 - March 3, 1989)

Buyon Guo, Geir Hareland, Jerzy Rajtar. "Computer Simulator Predicts Unfavorable Mud Rate and Optimum Air Injection Rate for Aerated Mud Drilling". Paper SPE 26892 presented at the Eastern Regional Conference & Exhibition held in Pittsburgh, PA. U.S.A., 2-4 November 1993

Caetano, E.F.; Shoham, O.; Brill, J.P.; 1992a, "Upward Vertical Two-Phase Flow through an Annulus, Part-I: Single Phase Friction Factor, Taylor Bubble Velocity and Flow Pattern Prediction", J. Energy Resour. Technol., 114, pp 1-13.

Caetano, E.F.; Shoham, O.; Brill, J.P.; 1992b, "Upward Vertical Two-Phase Flow through an Annulus, Part-II: Modeling Bubble, Slug and Annular Flow", *J. Energy Resour. Technol.*, 114, pp 14-30.

Charles M.E., .Transport of Solids by Pipeline., Presented at the 1st International Conference on the Hydraulic Transport of Solids in Pipes, University of Warwick (September 1-4, 1970)

Chen, N.H., "An explicit equation for friction factor in pipe" *Ind. Eng. Chem. Fund.* 18(3), 296, 1979

Chin, W. C., .Exact Cuttings Transport Correlations Developed for High Angle Wells., *Offshore Magazine*, pp. 67-70 (May, 1990)

Cho H., Shah S.N., Osisanya S.O., .A Three-Layer Modeling for Cuttings Transport with Coiled Tubing Horizontal Drilling., SPE 63269, Presented at the 2000 SPE Annual Technical Conference and Exhibition, Dallas-Texas (October 1-4, 2000) and *Journal of Canadian Petroleum Technology*, Volume 41, Number 6, June 2002

Clark, R. K., and Bickham, K. L., .A Mechanistic Model for Cuttings Transport., SPE 28306, Presented at the 69th Annual Technical Conference and Exhibition, New Orleans-Louisiana (September 25-28, 1994)

Daniel J. Rodríguez and Timothy A. Shedd "Entrainment of gas in the liquid film of horizontal, annular, two-phase flow " *International Journal of Multiphase Flow* Volume 30, Issue 6, June 2004, Pages 565-583

Danielson Thomas J., "Sand Transport Modeling in Multiphase Pipelines" *Offshore Technology Conference*, 30 April-3 May 2007, Houston, Texas

Datta B.K., Ratnayake C., Tek T., Saasen A., Omland T.H., "Hole Cleaning and Pressure Loss Prediction from a Bulk Transport Perspective" *Offshore Europe*, 6-9 September 2005, Aberdeen, United Kingdom

Das, G.; Das, P.K.; Purohit, N.K.; Mitra, A.K.; 1999a, "Flow Pattern Transition during Gas Liquid Upflow through Vertical Concentric Annuli - Part I: Experimental Investigations", *Journal of Fluids Eng.*, 121, December 1999, pp. 895-901.

Das, G.; Das, P.K.; Purohit, N.K.; Mitra, A.K.; 1999a, "Flow Pattern Transition during Gas Liquid Up flow through Vertical Concentric Annuli - Part II: Mechanistic Models", *Journal of Fluids Eng.*, 121, December 1999, pp. 902-907.

Doan Q.T.,M. Oguztoreli, Y. Masuda, T. Yonezawa, A. Kobayashi, S. Naganawa," Modeling of Transient Cuttings Transport in Underbalanced Drilling (UBD)" *SPE Journal* Volume 8, Number 2 ,June 2003, Pages:160-170

Doron P., Granica D., Barnea D., .Slurry Flow in Horizontal Pipes-Experimental and Modeling., *International Journal of Multiphase Flow*, Volume 13, pp.535- 547 (1987)

Doron P. and Barnea D., .A Three-Layer Model for Solid-Liquid Flow in Horizontal Pipes., International Journal of Multiphase Flow, Volume 19, pp.1029-1043 (1993)

Duan M., Miska S., Yu M., Takach N., and Ramadan A., "Critical Conditions for Effective Sand-Sized Solids Transport in Horizontal and High-Angle Wells" SPE Drilling & Completion Volume 24, Number 2 pp. 229-238 June 2009

Duan M., Miska S., Yu M., Takach N., and Ramadan A., "Transport of Small Cuttings in Extended-Reach Drilling" SPE Drilling & Completion Volume 23, Number 3, pp. 258-265 September 2008

Duns, H.Jr. and Ros, N.C.J.: "Vertical Flow of Gas and Liquid Mixtures in Wells," Proc., Sixth world Petroleum Congress, Frankfurt-am-Main, Germany (1963) 451.

Enrique Julia, Basar Ozar, Abhinav Dixit, Jae-Jun Jeong, Takashi Hibiki, Mamoru Ishii "Axial Development of Flow Regime in Adiabatic Upward Two-Phase Flow in a Vertical Annulus" J. Fluids Eng. - February 2009 - Volume 131, Issue 2,

Falcone G., Teodoriu C., Reinicke K.M., Bello O.O., "Multiphase-Flow Modeling Based on Experimental Testing: An Overview of Research Facilities Worldwide and the Need for Future Developments" SPE Projects, Facilities & Construction Volume 3, Number 3, pp. 1-10,

Fisher, R. A., 1936 "The Use of Multiple Measurements in Taxonomic Problems" (PDF) Annals of Eugenics 7: 179–188. <http://hdl.handle.net/2440/15227>. Retrieved on 2009-05-09

Ford, J. T., Peden, J. M., Oyeneyin, E. G., and Zarrouh, R., .Experimental Investigation of Drilled Cuttings Transport in Inclined Boreholes., SPE 20421, Presented at the 65th Annual Technical Conference, New Orleans-Louisiana (September 23-26, 1990)

Ford, J., Gao, E., Oyeneyin, M. B., and Peden, J. M., .The Development of Mathematical Models Which Describe Cuttings Transport in Inclined Boreholes., Paper 93-1102, CADE Conference, Calgary-Canada (April 1993)

Garcia-Hernandez A., Miska S. Z., Yu M., Takach N. E., Zettner C., "Determination of Cuttings Lag in Horizontal and Deviated Wells" SPE Annual Technical Conference and Exhibition, 11-14 November 2007, Anaheim, California, U.S.A.

Garcia, F., Garcia, R., Padrino, J.C., Mata, C., Trallero, J.L. and Joseph, D.D.: "Power Law and Composite Power Law Friction Factor Correlations for Laminar and Turbulent Gas-Liquid Flow in Horizontal Pipelines," Int. J. Multiphase Flow 29, 1605-1624 (2003).

Gavignet, A. A. and Sobey, I. J., .A Model for the Transport of Cuttings in Highly Deviated Wells., SPE 15417, Presented at the 61st Annual Technical Conference and Exhibition, New Orleans-Louisiana (October 5-8, 1996)

Gillies R.G., McKibben M.J., Shook C.A., "Pipeline Flow of Gas, Liquid and Sand Mixture at Low Velocities" The Journal of Canadian Petroleum Technology, 39 (9), 36-42

Gou B., Miska S., Harelard G., "A Simple Approach to Determination of Bottom Hole Pressure in Directional Foam Drilling", ASME, Jan., (1994)

Gomez L.E., Shoham O., Schmidt Z., Chokshi R.N. and Northug T.: "Unified Mechanistic Model for Steady-State Two-Phase Flow: Horizontal to Vertical Upward Flow", Society of Petroleum Engineering, SPE Journal 5 (3), September 2000.

Gomez L.E. Gomez, O. Shoham and Y. Taitel, Prediction of slug liquid holdup: horizontal to upward vertical flow. Int. J. Multiphase Flow 26 (2000), pp. 517-521.

Gonzalez R. and Woods R., "Digital image processing" Addison-Wesley, 1993

Gucuyener, I.H.: "Design of Aerated Mud for Low Pressure Drilling," SPE 80491 presented at the SPE Asia Pacific Oil and Gas Conference, Jakarta, 15-17 April 2003,

Harelard, G., "A Comparative Drilled Cuttings Transport Study In Directional Drilling Using Invert Emulsion Mineral Oil-Base Mud and Water-Base Muds Having Similar Rheological Properties.", M.S. Thesis, University of Tulsa, Tulsa (1985)

Hasan, A.R. and Kabir, C.S.; 1992, "Two-Phase Flow in Vertical and Inclined Annuli", Int. J. Multiphase Flow, 18, pp 279-293.

Hasan, A.R.; Kabir, C.S.; Rahman, R.; (Feb., 1988), "Predicting Liquid Gradient In A Pumping-Well Annulus", SPE Prod. Eng., 3, pp 113-120.

Hasan A.R., Kabir C.S., Sayarpour M., "A Basic Approach to Wellbore Two-Phase Flow Modeling" SPE Annual Technical Conference and Exhibition, 11-14 November 2007, Anaheim, California, U.S.A

Hemphill, T., "Tests Determine Oil-Mud Properties to Watch in High-Angle Wells.", Oil & Gas Journal, pp. 64-70 (November 26, 1990)

Hemphill, T., "Research Solving Problems in Cuttings Transport.", The American Oil & Gas Reporter, pp. 32-37 (August, 1992)

Hemphill, T. and Larsen, T. I., "Hole-Cleaning Capabilities of Oil-Based and Water-Based Drilling Fluids: A Comparative Experimental Study.", SPE 26328, Presented at the 65th Annual Technical Conference and Exhibition, Houston- Texas (October 3-6, 1993)

Hinze J.O. "Fundamentals of the hydrodynamic mechanism of splitting in dispersion processes" AIChE J. 1 (1955), p. 289.

Holte S., et al (1987), "Sand Bed Formation in Horizontal and Near Horizontal Gas-Liquid-Sand Flow" European Two-Phase Group Meeting, Trondheim, June 1987

Ishii, M., “One-dimensional drift-flux model and constitutive equations for relative motion between phases in various two-phase flow regimes”, Argonne National Laboratory ANL-77-47, 1977.

Iyoho, A. W., .Drilled-Cuttings Transport by Non-Newtonian Drilling Fluids Through Inclined Eccentric Annuli., Ph.D. Dissertation, University of Tulsa, Tulsa (April 1980)

Iyoho, A. W., and Takahashi, H., .Modeling Unstable Cuttings Transport in Horizontal Eccentric Wellbores., SPE 27416 Submitted to the SPE for possible publication in the SPE Journal, (July 1993)

Iyoho, A. W., and J. J. Azar, “an Accurate Slot-Flow Model for Non-Newtonian Fluid Flow through Eccentric Annuli” SOC. Pet. Eng. 21,565 (1981).

Jalukar, L. S., .A Study of Hole Size Effect on Critical and Sub-critical Drilling Fluid Velocities in Cuttings Transport for Inclined Wellbores., M.S. Thesis, University of Tulsa, Tulsa (1993)

Jean Oriol, Jean Pierre Leclerc, Christian Jallut, Patrice Tochon, Patrice Clement “Characterization of the two-phase flow regimes and liquid dispersion in horizontal and vertical tubes by using colored tracer and non-intrusive optical detector” Chemical Engineering Science 63 (2008) 24 – 34

JENG-TZONG CHEN, MING-HONG TSAI, CHEIN-SHAN LIU “Conformal Mapping and Bipolar Coordinate for Eccentric Laplace Problems” Computer Applications in Engineering Education, vol. 17, pp. 314-322., 2009

Kamp A.M., and Rivero M., .Layer modeling for Cuttings Transport in Highly inclined Wellbores, SPE 53942, Presented at the 1999 Latin American and Caribbean Petroleum Engineering Conference, Caracas-Venezuela (April 21-23, 1999)

Kelessidis V.C., Bandelis G.E., “Flow Patterns and Minimum Suspension Velocity for Efficient Cuttings Transport in Horizontal and Deviated Wells in Coiled-Tubing Drilling”, SPE Drilling & Completion, Volume 19, Number 4, December 2004

Kelessidis V. C., Bandelis G. E., Li J.,’ Flow of Dilute Solid-Liquid Mixtures in Horizontal Concentric and Eccentric Annuli” Journal of Canadian Petroleum Technology, Volume 46, Number 5, May 2007

Kelessidis, V.C. and Dukler, A.E.; 1989, “Modeling Flow Pattern Transitions for Upward Gas-Liquid Flow In Vertical Concentric And Eccentric Annuli”, Int. J. Multiphase Flow, 15, pp 173-191.

Kelessidis, V.C. and Dukler, A.E.; 1990, “Motion of Large Gas Bubbles through Liquids in Vertical Concentric and Eccentric Annuli”, Int. J. Multiphase Flow, 16, pp 375-390.

King M.J.S., Fairhurst C.P., Hill T.J., .Solids Transport in Multiphase Flows- Application to High Viscosity Systems., Presented at the Energy Sources Technology Conference and Exhibition, New Orleans-Louisiana (February 14-17,2000)

Krug, J.A., and Mitchell, B.J., “Charts Help Find Volume Pressure Needed for Foam Drilling” OGI, pp.61-64, (February 7, 1972)

Kundu N., and Peterson G.P., .Transmission of Solid Particles Using a Two- Phase Medium., Journal of Energy Resources Technology, Volume 109, pp.35- 39 (March, 1987)

Kuru E., Miska S., Pickell M., Takach N., Volk M., “New Directions in Foam and Aerated Mud Research and Development” SPE 53963 Presented at the 1999 Latin American and Caribbean Petroleum Engineering Conference, Caracas-Venezuela (April 21-23, 1999)

Lage, A.C.V.M., Rommetveit, R. and Time, R.W. “An Experimental and Theoretical Study of Two-Phase Flow in Horizontal or Slightly Deviated Fully Eccentric Annuli,” SPE paper 62793, IADC/SPE Asia Pacific Drilling Technology, 11-13 September, Kuala Lumpur, Malaysia.

Larsen, T. I., .A Study of Critical Fluid Velocity in Cuttings Transport For Inclined Wellbores., M.S. Thesis, University of Tulsa, Tulsa (1990)

Leising L.J., and Walton I.C.,” Cuttings-Transport Problems and Solutions in Coiled-Tubing Drilling” SPE Drilling & Completion, March 2002

Li J., Walker S., “Sensitivity Analysis of Hole Cleaning Parameters in Directional Wells” SPE Journal, Volume 6, Number 4, December 2001

Li J. and Wilde G., “Effect of Particle Density and Size on Solids Transport and Hole Cleaning With Coiled Tubing” SPE/ICoTA Coiled Tubing Conference and Exhibition, 12-13 April 2005, the Woodlands, Texas

Li Y., Bjorndalen N., Kuru E., “Numerical Modeling of Cuttings Transport in Horizontal Wells Using Conventional Drilling Fluids” Canadian International Petroleum Conference, Jun 8 - 1, 2004, Calgary, Alberta and Journal of Canadian Petroleum Technology Volume 46, Number 7, July 2007

Lockhart, R.W., and Martinelli, R.C.: “Proposed Correlation of Data for Isothermal Two-Phase, Two-Component Flow in Pipes,” Chemical Engineering Progress 45, No. 1, 39-48 (1949).

Lourenco A.M.F., Martins A.L., Andrade Jr. P.H., Nakagawa E. Y., IADC “Investigating Solids-Carrying Capacity for an Optimized Hydraulics Program in Aerated Polymer-Based-Fluid Drilling” SPE Drilling Conference, 21-23 February 2006, Miami, Florida, USA

Luo, Y., Bern, P. A., and Chambers, B. D., .Flow-Rate Predictions for Cleaning Deviated Wells., IADC/SPE 23884, Presented at the 1992 Drilling Conference, New Orleans-Louisiana (February 18-21, 1992)

Manninen, M. and Tavassalo, V., “On the Mixture Models for Multiphase Flow”, VTT Publications, 1996.

Martins A.L., Lourenco A.M.F., de Sa C.H.M., .Foam Property Requirements for Proper Hole Cleaning While Drilling Horizontal Wells in Underbalanced Conditions., SPE Drilling and Completion (December 2001)

Martins, A. L., and Santana, C., .Evaluation of Cuttings Transport in Horizontal and Near Horizontal Wells-A Dimensionless Approach., SPE 23643, Presented at the 2nd Latin American Petroleum Engineering Conference, Caracas-Venezuela (March 8-11, 1992)

Matthew J. S. King, C. Paul Fairhurst and Trevol J. Hill, “Solids Transport in Multiphase Flows Application to High Viscosity System” Paper submitted to the Energy Sources Technology Conference and Exhibition, New Orleans, Feb 14-17, 2000.

Meano, W. J., .Experimental Study of Shale Cuttings Transport in an Inclined Annulus Using Mineral Oil-Base Mud., M.S. Thesis, University of Tulsa, Tulsa (1987)

Meena S., Kandaswamy P. “Hydromagnetic flow between rotating eccentric cylinders with suction at the porous walls”*Forschung im Ingenieurwesen* 67 (2002) 123 – 128 _ Springer-Verlag 2002

Mengjiao Yu, Daniel Melcher, Nicholas Takach, Stefan Z. Miska, Ramadan Ahmed, “A New Approach to Improve Cuttings Transport in Horizontal and Inclined Wells” SPE Annual Technical Conference and Exhibition, 26-29 September 2004, Houston, Texas

Nguyen, D., and Rahman, S. S., .A Three-Layer Hydraulic Program for Effective Cuttings Transport and Hole Cleaning in Highly Deviated and Horizontal Wells., IADC/SPE 36383, Presented at the 1996 Asia Pacific Drilling Technology, Kuala Lumpur-Malaysia (September 9-11, 1996)

Oddie G., Shi H., Durlofsky L.J., Aziz K., Pfeffer B. and Holmes J. A.: ”Experimental Study of Two and Three- Phase Flows in Large Diameter Inclined Pipes”, *International Journal of Multiphase Flow* 29(2003) 527-558, 2003.

Okpobiri, G.A., .Experimental Determination of Solids Friction Factors and Minimum Volumetric Requirements in Foam and Mist Drilling and Well Cleanout Operations., Ph.D. Dissertation, University of Tulsa, Tulsa, (1982)

Okpobiri G.A., and Ikoku C.U., .Experimental Determination of Friction Factors for Mist and Foam Drilling and Well Cleanout Operations., *Journal of Energy Resources Technology*, Dec., Volume105, pp.542-553 (1983)

Okranji, S. O., .Mud Cuttings Transport Study in Directional Well Drilling., Final Report for Amoco Production Company, University of Tulsa, Tulsa (January 1981)

Oliemans, R.V., A., Pots, B.F., and Trope, N.: "Modeling of Annular Dispersed Two-Phase Flow in Vertical Pipes," Int. J. Multiphase Flow 12, No. 5, 711-732 (1986).

Ozbayoglu E. M., Saasen A., Sorgun M., and Svanes K., "Estimating Critical Velocity to Prevent Bed Development for Horizontal-Inclined Wellbores" SPE/IADC Middle East Drilling and Technology Conference, 22-24 October 2007, Cairo, Egypt

Ozbayoglu M.E., Saasen A., Sorgun M., Svanes K., "Effect of Pipe Rotation on Hole Cleaning for Water-Based Drilling Fluids in Horizontal and Deviated Wells" IADC/SPE Asia Pacific Drilling Technology Conference and Exhibition, 25-27 August 2008, Jakarta, Indonesia

Ozbayoglu E. M., Sorgun M., "Frictional Pressure Loss Estimation of Water-Based Drilling Fluids at Horizontal and Inclined Drilling With Pipe Rotation and Presence of Cuttings" SPE Oil and Gas India Conference and Exhibition, 20-22 January 2010, Mumbai, India

Ozbayoglu M.E., and Omurlu C., "Two-Phase Flow Through Fully Eccentric Horizontal Annuli: A Mechanistic Approach", SPE 107076, presented at SPE/ICOTA Coiled Tubing and Well Intervention Conference and Exhibition, The Woodlans, Texas, 20-21 March, 2007

Ozbayoglu Evren M., and Murat A. Ozbayoglu, "Flow Pattern and Frictional-Pressure-Loss Estimation Using Neural Networks for UBD Operations" IADC/SPE Managed Pressure Drilling & Underbalanced Operations, 28-29 March 2007, Galveston, Texas, U.S.A

Ozgen C., Tosun I. "Application of Geometric Inversion to the Eccentric Annulus System" AIChE Journal November 1987 Vol. 33, No. 11

Paul Bolchover, "Cuttings transport with drill string rotation" Schlumberger Technical Report 2007 <http://www.maths-in-industry.org/miis/135/1/cuttings.pdf> Access Date 12.08.2010

Petalas, N., and Aziz, K.: "A Mechanistic Model for Multiphase Flow in Pipes," JCPT 39, No. 6, 43-55 (2000).

Ramadan A.M., .Mathematical Modeling and Experimental Investigation on Solids and Cuttings Transport., Ph.D. Dissertation, Norwegian University of Science and Technology, 2001

Ramadana A., Skalle P., Johansen S. T., "A mechanistic model to determine the critical flow velocity required to initiate the movement of spherical bed particles in inclined channels" Chemical Engineering Science 58 (2003) 2153 – 2163

Rankin M.D., Friesenhahn T.J., Price W.R., "Lightened Fluid Hydraulics and Inclined Boreholes", SPE/IADC 18670, Presented at the 1989 SPE/IADC Drilling Conference, New Orleans-Louisiana (February 28-March 3, 1989)

Rodriguez, P. V.: "Experimental Determination of Minimum Air and Water Flow Rates for Effective Cutting Transport in High Angle and Horizontal Wells", MSc. Thesis, 2001, The University of Tulsa.

Sadatomi, M., Sato, Y., and Saruwatari, S.: "Two-Phase Flow in Vertical Noncircular Channels," Int. J. Multiphase Flow 8, 641-655 (1982).

Saintpere S., Marcillat Y., Bruni F., Toure A., .Hole Cleaning Capabilities of Drilling Foams Compared to Conventional Fluids., SPE 63049, Presented at the 2000 SPE Annual Technical Conference and Exhibition, Dallas-Texas (October 1-4, 2000)

Salazar-Mendoza R., Garcia-Gutierrez A., "A Two-Region Hydraulic Averaging Model for Cuttings Transport During Horizontal Well Drilling" Journal of Canadian Petroleum Technology Volume 47, Number 3 March 2008

Salcudean, M., Chun, J.H., and Groeneveld, D.C.: "Effect of Flow Obstructions on Void Distribution in Horizontal Air-Water Flow," Int. J. Multiphase Flow 9, 91-96 (1983).

Sanchez, R. A., Azar, J. J., Bassal, A. A., and Martins, A. L., .The Effect of Drill pipe Rotation on Hole Cleaning during Directional Well Drilling., SPE 37626, Presented at the 1997 Drilling Conference, Amsterdam-Holland (March 4- 6, 1997)

Sanchez A.R., .Modeling of Drilled Cuttings Bed Erosion in Highly-inclined Wells., M.S. Thesis, The University of Tulsa, Tulsa (1997)

Sapru A., "Study of Effect of Drill pipe Rotation on Cuttings Bed Erosion in horizontal Wells" M.S. Thesis, The University of Tulsa, Tulsa (2001)

Scheid C.M., Calcada L.A., Rocha D.C., Aranha P.E., Aragao A.F.L., Martins A.L., "Prediction of Pressure Losses in Drilling Fluid Flows in Circular and Annular Pipes and Accessories" Latin American and Caribbean Petroleum Engineering Conference, 31 May-3 June 2009, Cartagena de Indias, Colombia

Schubring D., Shedd T.A., "Wave behavior in horizontal annular air-water flow" International Journal of Multiphase Flow 34 (2008) 636-646

Scott, S.L., Shoham, O. and Brill, J.P.: "Prediction of Slug Length in Horizontal Large Diameter Pipes," SPE Production Engineering, 4, 335-340, August, 1989

Schiller L. and Naumann A., Über die grundlegenden berechnungen bei der schwerkraftaufbereitung, Vereines Deutscher Ingenieure 77 (1933), pp. 318-3

Seeberger, M. H., Matlock, R. W., and Hanson, P. M., .Oil Muds in Large- Diameter, Highly Deviated Wells: Solving the Cuttings Removal Problem., SPE/IADC 18635, Presented at the 1989 Drilling Conference, New Orleans- Louisiana (February 28 - March 3, 1989)

Shunxin Feng, Qibing Li, Song Fu, ‘‘on the orbital motion of a rotating inner cylinder in annular flow’’ *Int. J. Numer. Meth. Fluids* 2007; 54:155–173

Sifferman, T. R., and Becker, T. E. ‘‘Hole Cleaning in Full-Scale Inclined Wellbores’’, SPE 20422, Presented at the 65th Annual Technical Conference, New Orleans-Louisiana (September 23-26, 1990)

Stenevik, B. C., .Design and Construction of a Large-Scale Wellbore Simulator and Investigation of Hole Size Effects on Critical Cuttings Transport Velocity in Highly-inclined Wells., M.S. Thesis, University of Tulsa, Tulsa (1990)

Subramanian R., and Azar J. J.,’’ Experimental Study on Friction Pressure Drop for Non-Newtonian Drilling Fluids in Pipe and Annular Flow’’ SEP 64647, presented at the SPE International Oil & Gas Conference and Exhibition in China held in Beijing, China, 7-10 November 2000.

Sunthakar, A.A.: ‘‘Study of the Flow of Aerated Drilling Fluids in Annulus under Ambient Temperature and Pressure Conditions,’’ Ms. Thesis, the University of Tulsa, 2000.

Taitel, Y., and Dukler, A.E.: ‘‘A Model for Predicting Flow Regime Transition in Horizontal and Near Horizontal Gas-Liquid Flow,’’ *AIChE J.* (1976) 22 No. 1, 47.

Televantos Y., Shook C., Carleton A., Streat M., .Flow of Slurries of Coarse Particles at High Solids Concentrations., *The Canadian Journal of Chemical Engineering*, Volume 57, pp.255-262 (June, 1979)

Thondavadi N.N., and Lemlich R., .Flow Properties of Foam With and Without Solid Particles., *Ind. Eng. Chem. Process Des. Dev.* 24, pp.748-753 (1985)

Tian S., Medley G.H., Stone C.R., .Optimization Circulation While Drilling Underbalanced., *World Oil* (June, 2000)

Tippetts, J. R. & Priestman, G. H., "Mobility of Solids in Multiphase undulating pipe flow" Paper presented at the 7 International Conference of Multiphase Production, Cannes, France 18-20 June 1997

Tomren, P. H., .The Transport of Drilled Cuttings in an Inclined Eccentric Annulus., M.S. Thesis, University of Tulsa, Tulsa (1979)

Tosun I. ‘‘ Axial Laminar Flow in an Eccentric Annulus: an Approximate Solution’’, *AIChE Journal* (Vol. 30, No. 5) September, 1984

Uner D., Ozgen C., Tosun I.,’’ An Approximate Solution for Non-Newtonian Flow in Eccentric Annuli’’ *Ind. Eng. Chem. Res.* 1988, 27, 698-701

Vieira P., Miska S., Reed T., Kuru E., "Minimum Air and Water Flow Rates Required for Effective Cuttings Transport in High Angle and Horizontal Wells" IADC/SPE Drilling Conference, 26-28 February 2002, Dallas, Texas

Vieria P "Determination of Minimum Water-Air Rates Required for Effective Cuttings Transport in High Angle and Horizontal Wells" M.S. Thesis, the University of Tulsa, Tulsa (2000)

Videnic T., Kosel F., "A shrink-fit problem between an eccentric and a solid of hollow shaft annulus", 2004, J. Strain Analysis Vol. 39 No. 6

Wallis, G.B.: "One-Dimensional Two-Phase Flow," McGraw-Hill Book Co. Inc., New York City (1969).

Walker S., Li J., "the Effects of Particle Size, Fluid Rheology, and Pipe Eccentricity on Cuttings Transport" SPE/ICoTA Coiled Tubing Roundtable, 5-6 April 2000, Houston, Texas

Wang Haige, Su Yinao " FLOW OF ROBERTSON-STIFF FLUIDS THROUGH AN ECCENTRIC ANNULUS" Applied Mathematics and Mechanics Vol. 19, No. 10, Oct. 1998

Wilkes M., Watson R.W., Graham R.L., "A New Improvement for the Design and Field Implementation of Air-Mist Drilling", IADC/SPE 39301, Presented at the 1998 IADC/SPE Drilling Conference, Dallas-Texas (March 3-6, 1998)

WILLIAM T. SNYDER, GERALD A. GOLDSTEIN "an Analysis of Fully Developed Laminar Flow in an Eccentric Annulus" AIChE Journal, Vol. 11, No. 3, May, 1965, Pages: 462-467

Wilson K.C., .Co-ordinates for the Limit of Deposition in Pipeline Flow., Presented at the 3rd International Conference on the Hydraulic Transport of Solids in Pipes, Colorado School of Mines (May 15-17, 1974)

Wilson K.C., .A Unified Physically-Based Analysis of Solid-Liquid Pipeline Flow., Presented at the 4th International Conference on the Hydraulic Transport of Solids in Pipes, Colorado School of Mines (May 18-21, 1976)

Wilson K.C., .Bed Load Transport at High Shear Stress., Proceedings of ASCE, Journal of Hydr. Div., 113 (1), pp.97-103 (1987)

Xiao, J.J., Shoham, O., and Brill, J.P.: "A Comprehensive Mechanistic Model for Two-Phase Flow in Pipelines." Paper SPE 20631 presented at the 1990 SPE Annual Technical Conference and Exhibition, New Orleans, 23-26 September.

Yaso'o MATUNOBU "Pressure-flow relationships for steady flow through an eccentric double circular tube" Fluid Dynamics Research 4 (1988) 139-149

Yong B. Park, Hyo J. Eom "Electric Polarity for a Thick Eccentric Annular Aperture with a Floating Inner Conductor" IEEE MICROWAVE AND WIRELESS COMPONENTS LETTERS, VOL. 15, NO. 4, APRIL 2005

Yu M., Takach E., Nakamura D. R., Shariff M.M., "an Experimental Study of Hole Cleaning Under Simulated Downhole Conditions" SPE Annual Technical Conference and Exhibition, 11-14 November 2007, Anaheim, California, U.S.A

Yu T.T., Zhang H.Q., Li M.X., SPE, and C. Sarica, "A Mechanistic Model for Gas/Liquid Flow in Upward Vertical Annuli" SPE Annual Technical Conference and Exhibition, 4-7 October 2009, New Orleans, Louisiana

Zamora, M. and Hanson, P., "Rules of Thumb to Improve High-Angle Hole Cleaning," Petroleum Engineer International, pp. 44-51 (January 1991)

Zhang, H., Wang, Q., Sarica, C. and Brill, J. P. "A Unified Mechanistic Model for Slug Liquid Holdup and Transition Between Slug and Dispersed Bubble Flows," International Journal of Multiphase Flow, Volume 29, Issue 1, January 2003, Pages 97-107.

Zhou L., Wang J., Hao J., "Calculation and Design of Flow Parameters for Two-Phase Flow in Aerated Drilling", SPE 37044, Presented at the 1996 SPE International Conference on Horizontal Well Technology, Calgary-Alberta- Canada (November 18-20, 1996)

Zhou L., Ahmed R.M., Miska S.Z., Takach N.E., Yu M., Pickell M.B., "Experimental Study and Modeling of Cuttings Transport with Aerated Mud in Horizontal Wellbore at Simulated Down hole Conditions" SPE Annual Technical Conference and Exhibition, 26-29 September 2004, Houston, Texas

Zhou L., Ahmed R.M., Miska S.Z., Takach N.E., Yu M., Saasen A., "Hydraulics of Drilling with Aerated Muds under Simulated Borehole Conditions" SPE/IADC Drilling Conference, 23-25 February 2005, Amsterdam, Netherlands

Zhou L., "Hole Cleaning During Underbalanced Drilling in Horizontal and Inclined Wellbore" SPE Drilling & Completion Volume 23, Number 3, pp. 267-273, September 2008

Zhou, L.: "Cuttings Transport with Aerated mud in Horizontal Annulus under Elevated Pressure and Temperature Conditions," PhD Dissertation, The University of Tulsa, 2004.

Zhou, L., Ahmed, R.M., Miska, S.Z., Takach, N.E., Yu, M. and Pickell, M.B. "Experimental Study of Aerated Mud Flows under Horizontal Borehole Conditions," paper SPE 89531, presented at the SPE/ICoTA Coiled Tubing Conference and Exhibition held in Houston, Texas, U.S.A., 23-24 March 2004

APPENDIX A
RESULTS OF EXPERIMENTS

Two-phase Flow Experimental Data

Table A.1 Two-phase Flow Experimental Data for Horizontal Eccentric Annulus (00.0°) Air-Water Flow without Drill pipe Rotation

<i>Mud Flow Rate(gpm)</i>	<i>Mud Sup. Vel.(ft/sec)</i>	<i>Gas Flow rate (gpm)</i>	<i>Gas Sup. Vel(ft/sec)</i>	<i>Annulus P. Tran.(Psig)</i>	<i>dp (psi/ft)</i>	<i>Flow Pattern</i>
6.836	0.553	3.651	0.298	2.980	0.007	Stratified
6.530	0.529	2.467	0.201	2.822	0.006	Stratified
6.434	0.521	20.667	1.686	2.219	0.008	Wavy Stratified
6.365	0.515	21.762	1.775	2.214	0.007	Wavy Stratified
6.332	0.513	40.112	3.272	1.967	0.010	Wavy Stratified
6.742	0.546	39.572	3.228	1.886	0.008	Wavy Stratified
6.381	0.517	54.668	4.459	1.726	0.011	Wavy Stratified
6.497	0.526	72.482	5.912	1.613	0.015	Wavy Stratified
6.498	0.526	81.729	6.666	1.545	0.016	Wavy Stratified
6.380	0.517	93.942	7.662	1.493	0.020	Wavy Stratified
6.431	0.521	96.484	7.869	1.438	0.020	Wavy Stratified
6.985	0.566	268.082	21.865	1.212	0.025	Wavy Annular
6.405	0.519	379.446	30.948	1.174	0.025	Wavy Annular
6.457	0.523	512.133	41.770	1.079	0.026	Wavy Annular
6.392	0.518	496.126	40.464	1.130	0.027	Wavy Annular
6.894	0.558	589.946	48.116	1.112	0.028	Wavy Annular
7.012	0.568	573.555	46.780	1.115	0.028	Wavy Annular
6.625	0.536	401.028	32.708	1.119	0.026	Wavy Annular
11.967	0.969	42.720	3.484	2.088	0.015	Slug
11.959	0.968	58.021	4.732	1.953	0.019	Slug
13.881	1.124	56.322	4.594	1.990	0.018	Slug
12.952	1.049	74.866	6.106	1.825	0.022	Slug
13.691	1.108	103.259	8.422	1.735	0.030	Slug
25.373	2.054	26.052	2.125	2.709	0.025	Slug
25.451	2.061	45.938	3.747	2.404	0.026	Slug
13.249	1.073	119.164	9.719	1.652	0.030	Slug
25.471	2.062	68.959	5.624	2.233	0.032	Slug
30.944	2.505	27.963	2.281	2.854	0.033	Slug
31.041	2.513	52.936	4.318	2.585	0.033	Slug
62.322	5.046	118.288	9.648	3.270	0.115	Wavy Slug+Annular
61.866	5.009	145.305	11.851	3.327	0.132	Wavy Slug+Annular
56.424	4.568	97.585	7.959	3.135	0.094	Wavy Slug+Annular
50.385	4.079	96.361	7.859	3.004	0.084	Wavy Annular+Slug
50.489	4.088	131.766	10.747	3.020	0.098	Wavy Annular+Slug
18.713	1.515	100.191	8.172	1.915	0.033	Wavy Annular+Slug
18.794	1.522	4.719	0.385	3.322	0.012	Elongated Bubble
18.725	1.516	14.899	1.215	2.913	0.016	Elongated Bubble+ Slug
25.201	2.040	0.260	0.021	3.640	0.015	Bubble
42.851	3.469	7.053	0.575	3.509	0.033	Bubble
43.478	3.520	17.294	1.411	3.212	0.041	Elongated Bubble
25.241	2.044	3.570	0.291	3.386	0.018	Bubble
25.347	2.052	14.078	1.148	3.109	0.022	Elongated Bubble
50.324	4.074	2.931	0.239	3.694	0.039	Bubble
50.324	4.074	2.931	0.239	3.694	0.039	Bubble
87.603	7.092	4.785	0.390	4.282	0.113	Bubble
87.483	7.083	26.591	2.169	4.177	0.140	Bubble
88.100	7.133	11.689	0.953	4.214	0.126	Bubble
50.399	4.080	12.371	1.009	3.448	0.048	Elongated Bubble
50.399	4.080	12.371	1.009	3.448	0.048	Elongated Bubble
55.835	4.520	3.813	0.311	3.711	0.045	Bubble
74.723	6.050	5.894	0.481	3.975	0.086	Bubble
74.596	6.039	19.489	1.590	3.917	0.100	Elongated Bubble
55.965	4.531	18.367	1.498	3.399	0.057	Elongated Bubble
100.050	8.100	661.859	53.982	8.026	0.477	Dispersed Annular
99.966	8.093	656.031	53.506	7.050	0.410	Dispersed Annular
99.479	8.054	677.928	55.292	7.379	0.443	Dispersed Annular
104.827	8.487	277.525	22.635	7.033	0.382	Dispersed Annular
103.854	8.408	337.847	27.555	7.516	0.421	Dispersed Annular
104.153	8.432	585.200	47.729	10.894	0.632	Dispersed Annular
105.509	8.542	608.118	49.599	11.190	0.638	Dispersed Annular
104.872	8.491	616.168	50.255	9.640	0.563	Dispersed Annular
104.741	8.480	571.599	46.620	8.384	0.476	Dispersed Annular

Table A.2 Two-phase Flow Experimental Data for Inclined (15.0°) (From Horizontal) Eccentric Annulus Air-Water Flow without Drill pipe Rotation

Mud Flow Rate(gpm)	Mud Sup. Vel.(ft/sec)	Gas Flow rate (gpm)	Gas Sup. Vel(ft/sec)	Annulus P. Tran.(Psig)	dp (psi/ft)	Flow Pattern
25.529	2.067	12.984	1.051	5.705	0.121	Plug
24.533	1.986	13.671	1.107	5.739	0.122	Slug
25.513	2.066	29.067	2.353	5.159	0.106	Slug
25.221	2.042	63.476	5.139	4.493	0.099	Slug
25.310	2.049	135.604	10.979	3.962	0.104	Slug
25.799	2.089	192.099	15.552	3.644	0.104	Slug
24.691	1.999	261.659	21.184	3.415	0.121	Churn
26.164	2.118	325.091	26.320	3.401	0.127	Wavy annular
24.841	2.011	381.880	30.917	3.265	0.138	Wavy annular
25.818	2.090	445.580	36.075	3.248	0.139	Wavy annular
38.877	3.148	14.634	1.185	5.206	0.137	Plug
37.070	3.001	16.331	1.322	5.320	0.131	Plug
36.811	2.980	31.887	2.582	5.352	0.121	Plug
36.810	2.980	37.930	3.071	5.181	0.132	Plug
36.947	2.991	62.335	5.047	4.832	0.113	Plug
36.879	2.986	132.093	10.694	4.404	0.126	Slug
39.376	3.188	197.945	16.026	4.214	0.116	Churn
36.633	2.966	253.923	20.558	3.957	0.115	Wavy Annular
37.037	2.999	312.125	25.270	3.971	0.134	Wavy Annular
35.914	2.908	379.476	30.723	3.916	0.142	Wavy Annular
37.860	3.065	384.909	31.163	4.024	0.148	Wavy Annular
38.328	3.103	421.428	34.119	4.079	0.154	Wavy Annular
35.806	2.899	479.134	38.791	3.964	0.157	Dispersed Annular

Table A.3 Two-phase Flow Experimental Data for Inclined (30.0°) (From Horizontal) Eccentric Annulus Air-Water Flow without Drill pipe Rotation

Mud Flow Rate(gpm)	Mud Sup. Vel.(ft/sec)	Gas Flow rate (gpm)	Gas Sup. Vel(ft/sec)	Annulus P. Tran.(Psig)	dp (psi/ft)	Flow Pattern
25.358	2.053	9.661	0.782	5.662	0.226	Bubble
25.243	2.044	12.617	1.022	5.490	0.222	Bubble
24.940	2.019	25.321	2.050	5.028	0.201	Slug
24.586	1.990	46.112	3.733	4.499	0.177	Slug
26.530	2.148	69.022	5.588	4.187	0.177	Slug
24.546	1.987	92.515	7.490	3.923	0.194	Slug
26.195	2.121	116.282	9.414	3.757	0.134	Slug
25.813	2.090	138.031	11.175	3.629	0.152	Churn
25.054	2.028	233.598	18.912	3.371	0.148	Churn
26.482	2.144	272.308	22.046	3.343	0.145	Wavy Annular
25.412	2.057	325.167	26.326	3.244	0.151	Wavy Annular
25.798	2.089	426.609	34.539	3.220	0.159	Wavy Annular
35.858	2.903	15.214	1.232	5.430	0.214	Bubble
36.471	2.953	27.560	2.231	5.298	0.198	Slug
37.042	2.999	51.752	4.190	4.917	0.186	Slug
37.106	3.004	85.551	6.926	4.513	0.181	Slug
38.775	3.139	116.420	9.426	4.399	0.179	Churn
37.685	3.051	168.239	13.621	4.156	0.169	Churn
36.647	2.967	222.016	17.975	3.991	0.174	Churn
38.558	3.122	272.844	22.090	4.023	0.184	Wavy Annular
42.365	3.430	313.510	25.382	4.269	0.196	Wavy Annular
37.665	3.049	317.483	25.704	3.995	0.185	Wavy Annular
37.174	3.010	399.221	32.321	4.001	0.198	Dispersed Annular

Table A.4 Two-phase Flow Experimental Data for Inclined (77.5°) (From Horizontal) Eccentric Annulus Air-Water Flow without Drill pipe Rotation

<i>Mud Flow Rate(gpm)</i>	<i>Mud Sup. Vel.(ft/sec)</i>	<i>Gas Flow rate (gpm)</i>	<i>Gas Sup. Vel(ft/sec)</i>	<i>Annalus P. Tran.(Psig)</i>	<i>dp (psi/ft)</i>	<i>Flow Pattern</i>
25.309	2.049	9.121	0.738	5.449	0.345	Bubble
25.303	2.049	16.520	1.337	5.179	0.315	Slug
38.273	3.099	86.751	7.023	4.271	0.257	Slug
37.954	3.073	98.365	7.964	4.214	0.253	Slug
37.716	3.054	111.784	9.050	4.148	0.248	Slug
37.444	3.031	137.888	11.164	4.041	0.239	Churn
38.182	3.091	166.723	13.498	3.937	0.230	Churn
37.447	3.032	195.162	15.800	3.856	0.222	Churn
37.774	3.058	219.282	17.753	3.848	0.224	Annular
37.328	3.022	273.304	22.127	3.803	0.216	Annular
37.629	3.046	316.443	25.620	3.832	0.214	Annular
50.430	4.083	16.257	1.316	2.766	0.365	Bubble
52.090	4.217	21.686	1.756	1.640	0.368	Bubble
48.994	3.967	21.971	1.779	4.650	0.350	Bubble
50.362	4.077	27.791	2.250	4.968	0.341	Slug
49.959	4.045	42.239	3.420	4.888	0.326	Slug
49.434	4.002	57.643	4.667	4.745	0.303	Slug
49.284	3.990	70.107	5.676	4.651	0.298	Slug
49.491	4.007	84.931	6.876	4.621	0.296	Slug
49.605	4.016	99.687	8.071	4.548	0.286	Slug
49.671	4.021	111.565	9.032	4.532	0.286	Churn
50.075	4.054	141.817	11.482	4.467	0.274	Churn
74.155	6.004	38.840	3.145	5.154	0.355	Dispersed Bubble
74.759	6.053	74.882	6.063	5.248	0.344	Dispersed Bubble
74.831	6.058	89.019	7.207	5.297	0.343	Dispersed Bubble
75.530	6.115	99.180	8.030	5.350	0.342	Dispersed Annular
86.134	6.974	26.712	2.163	5.273	0.384	Dispersed Bubble
86.596	7.011	38.041	3.080	5.207	0.379	Dispersed Bubble
86.407	6.996	43.390	3.513	5.394	0.378	Dispersed Bubble
86.511	7.004	52.236	4.229	5.514	0.376	Dispersed Bubble
87.200	7.060	74.614	6.041	5.628	0.374	Dispersed Bubble
87.039	7.047	88.790	7.189	5.713	0.371	Dispersed Bubble
87.001	7.044	97.578	7.900	5.720	0.366	Dispersed Annular
86.347	6.991	126.136	10.212	5.843	0.363	Dispersed Annular
86.619	7.013	146.416	11.854	6.047	0.365	Dispersed Annular

Table A.5 Two-phase Flow Repeated Experimental Data for Inclined (77.5°) (From Horizontal) Eccentric Annulus Air-Water Flow without Drill pipe Rotation

<i>Mud Flow Rate (gpm)</i>	<i>Mud Sup. Vel.(ft/sec)</i>	<i>Gas Flow Rate(gpm)</i>	<i>Gas Sup. Vel(ft/sec)</i>	<i>Annalus P. Tran (psig)</i>	<i>Ave Dp (Psi/ft)</i>	<i>Flow Pattern</i>
26.108	2.114	35.324	2.860	4.474	3.667	Slug
25.454	2.061	76.711	6.211	3.918	5.064	Slug
24.886	2.015	108.436	8.779	3.655	6.217	Slug
48.745	3.946	102.652	8.311	4.453	6.382	Slug
51.286	4.152	152.410	12.339	4.455	8.397	Slug
51.713	4.187	199.063	16.116	4.487	10.302	Slug
51.029	4.131	200.623	16.243	4.465	10.354	Slug
49.307	3.992	200.861	16.262	4.365	10.313	Slug
61.198	4.955	192.209	15.561	4.946	10.254	Slug
60.921	4.932	147.498	11.942	4.826	8.384	Slug
61.596	4.987	124.780	10.102	4.830	7.466	Slug
74.106	6.000	120.460	9.753	5.284	7.518	Slug
74.006	5.992	141.538	11.459	5.372	8.415	Slug
74.168	6.005	181.882	14.725	5.604	0.436	Slug
86.353	6.991	94.187	7.625	5.670	6.648	Slug
99.080	8.022	92.398	7.481	6.174	6.827	Slug
99.020	8.017	134.877	10.920	6.589	8.754	Slug

Table A.6 Two-phase Flow Experimental Data for Inclined (45.0°) (From Horizontal) Eccentric Annulus Air-Water Flow without Drill pipe Rotation

<i>Mud Flow Rate</i>	<i>Mud Sup. Vel.</i>	<i>Annulus P. Transmitter</i>	<i>Pipe RPM</i>	<i>Motor ROP</i>	<i>Dp(psi/ft)</i>
23.09	1.87	3.62	0	61	0.55
23.20	1.88	3.60	0	61	0.54
33.78	2.73	1.13	0	61	0.54
32.32	2.62	0.73	0	61	0.52
31.37	2.54	0.68	0	61	0.53
31.27	2.53	0.66	0	61	0.52
37.04	3.00	0.68	0	61	0.54
42.24	3.42	0.68	0	61	0.53
50.33	4.08	0.59	0	61	0.53
61.97	5.02	0.62	0	61	0.54
74.38	6.02	0.81	0	61	0.55
86.20	6.98	1.12	0	60	0.57
105.35	8.53	1.69	0	60	0.61
117.51	9.51	2.15	0	60	0.63
21.90	1.77	3.94	59	60	0.65
27.00	2.19	2.00	59	60	0.60
27.12	2.20	0.54	59	60	0.58
30.49	2.47	0.80	59	60	0.58
39.66	3.21	1.09	59	60	0.61
47.45	3.84	0.87	59	60	0.61
60.62	4.91	0.84	59	60	0.61
72.66	5.88	1.03	59	60	0.63
87.78	7.11	1.42	59	60	0.66
103.77	8.40	1.90	59	60	0.69
114.16	9.24	2.29	59	60	0.71
26.82	2.17	0.37	81	60	0.59
37.72	3.05	0.84	81	60	0.58
49.58	4.01	0.81	81	60	0.59
60.64	4.91	0.79	81	60	0.60
75.12	6.08	1.06	81	60	0.62
86.85	7.03	1.25	81	60	0.63
105.85	8.57	2.76	81	60	1.02
115.27	9.33	2.29	81	60	0.70
27.46	2.22	0.24	99	60	0.58
25.89	2.10	0.32	99	60	0.58
37.55	3.04	1.00	99	60	0.59
51.28	4.15	0.85	99	60	0.59
60.40	4.89	0.77	99	60	0.60
73.16	5.92	0.99	99	60	0.62
85.66	6.94	1.31	99	60	0.64
28.38	2.30	0.70	120	60	0.57
33.27	2.69	0.91	120	60	0.58
37.41	3.03	1.51	120	60	0.83
52.19	4.23	0.74	120	60	0.59
59.63	4.83	0.78	120	60	0.60
61.67	4.99	0.81	120	60	0.60

**Table A.7 Two-phase Flow Experimental Data for Horizontal (00.0°) (From Horizontal)
Eccentric Annulus Cutting-Water Flow**

Flow rate(qpm)	Mud Sup. Vel.(ft/sec)	Average Cc(%)	Moving Cc(%)	Dp(psi/ft)	ROP	RPM	Flow Pattern
18.91	1.52	61.23%	9.09%	0.046	60	0	stationaryBed
25.18	2.02	55.93%	17.65%	0.059	60	0	stationaryBed
30.07	2.41	50.11%	13.07%	0.073	60	0	stationaryBed
37.76	3.03	39.95%	11.32%	0.065	60	0	stationaryBed
43.45	3.49	18.27%	18.27%	0.031	60	0	dispersed
49.44	3.97	12.99%	12.99%	0.030	60	0	dispersed
56.25	4.51	10.11%	10.11%	0.041	60	0	dispersed
62.29	5.00	7.97%	7.97%	0.054	60	0	dispersed
74.78	6.00	5.94%	5.94%	0.084	60	0	dispersed
87.14	6.99	3.87%	3.87%	0.112	60	0	dispersed
99.68	8.00	2.50%	2.50%	0.138	60	0	dispersed
112.35	9.02	2.22%	2.22%	0.161	60	0	dispersed
18.07	1.45	58.21%	24.46%	0.057	60	60	stationaryBed
24.79	1.99	54.19%	26.20%	0.057	60	60	stationaryBed
30.75	2.47	48.14%	24.17%	0.065	60	60	stationaryBed
37.40	3.00	39.44%	22.53%	0.063	60	60	stationaryBed
43.53	3.49	16.00%	16.00%	0.033	60	60	dispersed
50.27	4.03	11.08%	11.08%	0.040	60	60	dispersed
55.50	4.45	9.38%	9.38%	0.049	60	60	dispersed
62.52	5.02	8.09%	8.09%	0.058	60	60	dispersed
74.86	6.01	5.55%	5.55%	0.081	60	60	dispersed
87.29	7.01	3.46%	3.46%	0.103	60	60	dispersed
100.13	8.04	2.32%	2.32%	0.128	60	60	dispersed
112.32	9.01	2.05%	2.05%	0.160	60	60	dispersed
19.27	1.55	56.54%	24.78%	0.047	60	80	stationaryBed
24.50	1.97	51.86%	28.84%	0.054	60	80	stationaryBed
30.73	2.47	44.80%	25.12%	0.054	60	80	stationaryBed
37.21	2.99	34.84%	25.32%	0.063	60	80	stationaryBed
43.33	3.48	14.85%	14.85%	0.034	60	80	dispersed
50.07	4.02	10.02%	10.02%	0.039	60	80	dispersed
55.58	4.46	8.11%	8.11%	0.051	60	80	dispersed
62.70	5.03	7.04%	7.04%	0.059	60	80	dispersed
74.90	6.01	5.33%	5.33%	0.080	60	80	dispersed
87.23	7.00	3.14%	3.14%	0.102	60	80	dispersed
100.06	8.03	1.98%	1.98%	0.128	60	80	dispersed
112.13	9.00	1.95%	1.95%	0.159	60	80	dispersed

Table A.8 Two-phase Flow Experimental Data for Inclined (77.5°) (From Horizontal) Eccentric Annulus Cutting-Water Flow

<i>Mud Flow Rate(gpm)</i>	<i>Mud Sup. Vel.(ft/sec)</i>	<i>P. Transmitter(psig)</i>	<i>Pipe RPM (1/min)</i>	<i>ROP(ft/hrs)</i>	<i>Dp(psi/ft)</i>
23.09	1.87	3.62	0	61	0.55
23.20	1.88	3.60	0	61	0.54
33.78	2.73	1.13	0	61	0.54
32.32	2.62	0.73	0	61	0.52
31.37	2.54	0.68	0	61	0.53
31.27	2.53	0.66	0	61	0.52
37.04	3.00	0.68	0	61	0.54
42.24	3.42	0.68	0	61	0.53
50.33	4.08	0.59	0	61	0.53
61.97	5.02	0.62	0	61	0.54
74.38	6.02	0.81	0	61	0.55
86.20	6.98	1.12	0	60	0.57
105.35	8.53	1.69	0	60	0.61
117.51	9.51	2.15	0	60	0.63
21.90	1.77	3.94	59	60	0.65
27.00	2.19	2.00	59	60	0.60
27.12	2.20	0.54	59	60	0.58
30.49	2.47	0.80	59	60	0.58
39.66	3.21	1.09	59	60	0.61
47.45	3.84	0.87	59	60	0.61
60.62	4.91	0.84	59	60	0.61
72.66	5.88	1.03	59	60	0.63
87.78	7.11	1.42	59	60	0.66
103.77	8.40	1.90	59	60	0.69
114.16	9.24	2.29	59	60	0.71
26.82	2.17	0.37	81	60	0.59
37.72	3.05	0.84	81	60	0.58
49.58	4.01	0.81	81	60	0.59
60.64	4.91	0.79	81	60	0.60
75.12	6.08	1.06	81	60	0.62
86.85	7.03	1.25	81	60	0.63
105.85	8.57	2.76	81	60	1.02
115.27	9.33	2.29	81	60	0.70
27.46	2.22	0.24	99	60	0.58
25.89	2.10	0.32	99	60	0.58
37.55	3.04	1.00	99	60	0.59
51.28	4.15	0.85	99	60	0.59
60.40	4.89	0.77	99	60	0.60
73.16	5.92	0.99	99	60	0.62
85.66	6.94	1.31	99	60	0.64
28.38	2.30	0.70	120	60	0.57
33.27	2.69	0.91	120	60	0.58
37.41	3.03	1.51	120	60	0.83
52.19	4.23	0.74	120	60	0.59
59.63	4.83	0.78	120	60	0.60
61.67	4.99	0.81	120	60	0.60
73.29	5.93	1.01	120	60	0.62
88.32	7.15	1.26	120	60	0.59

Table A.9 Two-phase Flow Experimental Data for Inclined (45.0°) (From Horizontal) Eccentric Annulus Cutting-Water Flow

Mud Flow Rate(gpm)	Mud Sup. Vel.(ft/sec)	Pipe RPM (1/min)	ROP(ft/hrs)	P. Transmitter(psig)	Dp(psi/ft)	FlowPattern
24.27602534	1.965410865	0.068072904	79.7860723	1.957196204	0.506767161	Stationary Bed
25.872019	2.094624167	0.067090667	79.86556267	2.447908833	0.418587249	Stationary Bed
39.14046753	3.168850694	0.067772612	84.78184024	2.131505041	0.432465489	Moving Bed
50.78631719	4.111710127	0.068268556	79.59477584	1.346118476	0.430656739	Moving Bed
62.03809219	5.022664901	0.065562838	81.28840135	1.409673697	0.474432885	Moving Bed
37.03189208	2.998138371	80.33734194	81.36212805	2.122984097	0.456730374	Moving Bed
50.45707782	4.085054548	80.31840045	79.93109524	1.446320065	0.461712736	Moving Bed
63.33794919	5.127902569	80.37877892	81.56704032	1.586208486	0.495334023	Dispersed
25.63431267	2.075379	120.0212623	80.74773033	5.797929667	0.394301107	Moving Bed
26.05640577	2.10955217	120.0192081	80.72045883	4.252208511	0.489599874	Dispersed
38.82243671	3.143102604	119.7631423	81.4795153	2.066055369	0.43883576	Moving Bed
50.25402005	4.068614792	119.5953873	81.39565034	5.672397766	0.449608109	Moving Slug
50.50451998	4.088895595	110.2512924	81.27165894	1.407806905	0.483084097	Moving Slug
52.01594814	4.211262293	119.5366369	81.65060153	2.25302681	0.465645485	Moving Bed
61.83722304	5.00640237	119.7541137	81.68995311	1.438331519	0.495016911	Dispersed
24.77443668	2.00576272	0.068180787	99.87556263	5.425352947	0.546214862	Stationary Bed
25.82883443	2.091127824	0.066818757	99.10281276	1.304084811	0.506607886	Stationary Bed
37.56289214	3.041128627	0.066983018	100.6396207	1.499102745	0.480767646	Moving Bed
52.13071713	4.220554078	0.0675521	101.8052583	1.441145656	0.478485769	Moving Bed
64.96714118	5.259803571	0.066500796	102.5094077	5.579785653	0.46196703	Dispersed
65.02313933	5.264337178	0.067125356	102.5417829	1.632654111	0.487106944	Dispersed
25.3856788	2.055249463	80.98235623	99.53248613	4.944795352	0.476934673	Moving Bed
38.77209233	3.139026613	80.36567823	101.6270123	2.148373699	0.507611699	Moving Bed
62.52165603	5.0618147	80.73293508	100.9416417	1.475467275	0.478419114	Dispersed
24.72044367	2.001391393	119.3364757	99.51640466	6.47499418	0.503597207	Moving Bed
25.136463	2.035072736	119.326468	99.52063245	6.997821698	0.44585124	Moving Bed
38.18632123	3.091602	120.0475228	100.9050864	3.564449851	0.517926633	Moving Bed
38.57139031	3.122777632	120.296497	102.1653429	2.218567747	0.476781146	Moving Bed
39.23992414	3.176902818	119.7825278	100.3102778	2.144671091	0.506524553	Moving Bed
50.68112463	4.103193651	119.927195	101.0719042	1.44717914	0.460442663	Moving Bed
63.35050479	5.128919121	119.7321954	100.9838279	1.510183603	0.480026344	Dispersed
25.13383143	2.034859646	0.068467798	120.8523658	2.358151859	0.515620588	Stationary Bed
37.42376073	3.029864433	0.066381667	119.4679133	1.186725867	0.478952229	Moving Bed
39.01175789	3.158430205	0.067007812	120.2037794	2.085474017	0.501334712	Moving Bed
39.01175789	3.158430205	0.067007812	120.2037794	2.085474017	0.501334712	Moving Bed
49.64598328	4.019387583	0.067129833	119.7920579	1.452096097	0.479720393	Moving Bed
63.84244441	5.168747	0.066074023	120.6288441	1.516201341	0.469270578	Moving Bed
64.20386936	5.198008266	0.066560469	120.6285475	1.454986297	0.445275319	Moving Bed
25.77571353	2.086827086	80.3539328	121.0791608	5.8111927	0.521485652	Moving Bed
37.05130572	2.999710116	80.39289784	119.775666	1.56652076	0.473562491	Moving Bed
37.15860237	3.008396951	81.14023337	120.1669836	5.692753173	0.442087084	Moving Bed
37.15860237	3.008396951	81.14023337	120.1669836	5.692753173	0.442087084	Moving Bed
38.26186907	3.097718492	80.39823926	119.776803	5.693743852	0.404366208	Moving Bed
38.37009216	3.106480354	81.13932124	120.1848585	2.582534	0.520855785	Moving Bed
38.37009216	3.106480354	81.13932124	120.1848585	2.582534	0.520855785	Moving Bed
53.32521019	4.317261403	80.63988444	120.1745945	2.275111306	0.491939506	Moving Bed
63.58564762	5.14795648	80.42449512	122.5325543	1.557194757	0.472259186	Moving Bed
25.71530317	2.081936214	119.4238613	121.1049898	4.181783619	0.481296091	Moving Bed
52.67146498	4.264333564	120.3129101	120.2564466	1.564024356	0.465747445	Moving Bed
63.64662052	5.152892955	120.2186549	122.6196957	1.573145364	0.478805832	Dispersed

Three-phase Flow Experimental Data

Table A.10 Three-phase Flow Experimental Data for Horizontal (00.0°) (From Horizontal) Eccentric Annulus Cutting-Gas-Water Flow

Mud Flow Rate(gpm)	Mud Sup. Vel.(ft/sec)	Annulus Gas Flow rate(gpm)	Gas Sup. Vel(ft/sec)	Pipe RPM (1/min)	ROP(ft/hrs)	P. Transmitter(psig)	Dp(psi/ft)
22.114	1.790	5.899	3.989	80.468	81.759	3.296	0.052
23.880	1.933	38.432	25.665	1575.197	0.004	0.400	0.072
23.949	1.939	398.290	269.314	80.598	82.998	3.062	0.046
24.551	1.988	209.002	141.322	80.691	86.239	3.698	0.064
24.574	1.990	297.922	201.448	80.591	82.916	3.416	0.042
24.589	1.991	221.900	150.043	80.583	82.886	3.606	0.063
24.591	1.991	236.776	160.102	80.693	86.236	3.651	0.060
24.597	1.991	238.378	161.186	80.695	86.239	3.585	0.055
61.826	5.006	196.410	15.902	80.787	80.352	2.824	0.149
61.922	5.013	243.046	19.677	80.795	80.368	2.863	0.163
62.086	5.027	192.140	15.556	80.776	80.327	3.046	0.147
62.366	5.049	1.631	0.132	80.697	80.174	3.374	0.058
73.797	5.975	165.445	13.395	81.161	81.109	3.131	0.148
73.942	5.986	72.120	5.839	81.092	81.088	3.576	0.109
73.977	5.989	223.828	18.121	81.187	81.117	5.686	0.167
73.989	5.990	14.152	1.146	81.564	81.798	5.370	0.091
74.034	5.994	60.724	4.916	81.083	81.091	4.854	0.106
74.127	6.001	35.745	2.894	81.066	81.089	4.500	0.100
74.173	6.005	47.773	3.868	81.073	81.085	4.153	0.103
37.778	3.059	99.949	8.092	98.557	119.998	3.546	0.058
37.780	3.059	48.656	3.939	98.569	120.008	4.029	0.078
37.794	3.060	76.255	6.174	98.564	120.009	3.704	0.042
37.820	3.062	62.006	5.020	98.566	120.014	3.852	0.051
37.855	3.065	36.611	2.964	98.578	120.013	4.227	0.082
48.856	3.955	257.301	20.831	99.003	120.861	4.923	0.150
48.945	3.963	220.447	17.848	99.009	120.837	4.969	0.124
48.959	3.964	242.063	19.598	99.006	120.842	4.904	0.135
49.198	3.983	197.907	16.023	99.014	120.875	5.056	0.121
49.621	4.017	179.343	14.520	99.019	120.886	5.193	0.118
49.763	4.029	170.061	13.768	99.024	120.888	3.710	0.109
49.768	4.029	91.849	7.436	99.043	120.885	6.087	0.081
49.775	4.030	112.926	9.143	99.037	120.906	5.826	0.086
49.781	4.030	134.150	10.861	99.031	120.900	5.359	0.094
49.945	4.044	135.116	10.939	98.970	120.570	5.528	0.095
50.101	4.056	114.364	9.259	98.971	120.615	5.887	0.081
50.186	4.063	9.694	0.785	98.981	120.814	11.281	0.058

**Table A.11 Three-phase Flow Experimental Data for Inclined (77.5°) (From Horizontal)
Eccentric Annulus Cutting-Gas-Water Flow**

Mud Flow Rate(gpm)	Mud Sup. Vel.(ft/sec)	Annular Gas Flow rate(gpm)	Gas Sup. Vel(ft/sec)	P. Transmitter(psig)	Pipe RPM (1/min)	ROP(ft/hrs)	Flow Pattern	Dp(psi/ft)
25.629	2.075	339.530	27.489	3.522	0	59	Annular	0.213
25.534	2.067	297.527	24.088	3.603	0	60	Annular	0.235
25.613	2.074	227.245	18.398	3.815	0	60	Slug	0.256
25.483	2.063	206.201	16.694	3.912	0	60	Slug	0.261
25.638	2.076	169.313	13.708	4.061	0	60	Slug	0.273
25.724	2.083	143.177	11.592	4.292	0	60	Slug	0.289
25.438	2.059	115.615	9.360	4.475	0	60	Slug	0.296
25.333	2.051	86.201	6.979	4.719	0	60	Slug	0.313
25.269	2.046	56.131	4.544	5.166	0	60	Slug	0.343
25.024	2.026	27.033	2.189	5.925	0	60	Slug	0.398
37.136	3.007	95.843	7.760	4.840	80	80	Slug	0.419
37.309	3.021	65.119	5.272	5.221	80	80	Slug	0.464
37.004	2.996	35.529	2.876	5.843	80	80	Slug	0.532
37.403	3.028	135.714	10.988	4.649	80	80	Slug	0.403
37.922	3.070	205.229	16.616	4.292	80	80	Slug	0.362
37.611	3.045	175.712	14.226	4.469	80	80	Slug	0.385
37.384	3.027	339.933	27.521	4.084	80	80	Annular	0.320
37.291	3.019	274.360	22.212	4.109	80	80	Annular	0.337
37.860	3.065	396.683	32.116	4.067	80	80	Annular	0.314
37.781	3.059	417.351	33.789	4.154	80	104	Annular	0.324
37.399	3.028	335.520	27.164	4.101	80	104	Annular	0.321
38.090	3.084	273.786	22.166	4.187	80	104	Annular	0.340
37.759	3.057	204.770	16.578	4.336	80	104	Annular	0.363
37.901	3.069	177.387	14.361	4.497	80	104	Slug	0.384
37.577	3.042	169.651	13.735	4.596	120	123	Slug	0.448
37.769	3.058	337.684	27.339	4.183	120	123	Annular	0.374
38.009	3.077	134.519	10.891	4.754	120	123	Slug	0.472
37.483	3.035	101.019	8.179	5.016	120	123	Slug	0.503
37.425	3.030	66.625	5.394	5.391	120	123	Slug	0.545
37.025	2.998	31.463	2.547	6.067	120	123	Slug	0.626
49.877	4.038	333.074	26.966	4.393	0	-30	Annular	0.349
49.989	4.047	343.989	27.850	4.641	0	81	Annular	0.408
51.063	4.134	341.781	27.671	4.727	0	81	Annular	0.404
48.462	3.924	338.406	27.398	4.548	0	81	Annular	0.402
50.200	4.064	241.401	19.544	4.581	0	81	Annular	0.429
49.356	3.996	291.647	23.612	4.535	0	81	Annular	0.400
49.487	4.007	179.112	14.501	4.567	0	81	Annular	0.432
49.854	4.036	150.918	12.218	4.660	120	123	Slug	0.363
50.342	4.076	366.676	29.686	4.362	120	123	Slug	0.315
50.435	4.083	117.523	9.515	4.821	120	123	Slug	0.373
49.619	4.017	232.197	18.799	4.419	120	123	Slug	0.339
50.019	4.050	76.451	6.190	5.124	120	123	Slug	0.400
49.726	4.026	190.497	15.423	4.558	120	123	Slug	0.349
49.593	4.015	38.697	3.133	5.641	120	123	Slug	0.445
62.157	5.032	27.419	2.220	5.162	0	80	Dispersed Bubble	0.461
62.612	5.069	49.870	4.038	5.137	0	80	Dispersed Bubble	0.440
61.908	5.012	75.862	6.142	5.034	0	80	Dispersed Bubble	0.425
61.770	5.001	105.035	8.504	5.001	0	80	Dispersed Bubble	0.417
63.287	5.124	130.796	10.589	5.063	0	80	Dispersed Bubble	0.421
61.597	4.987	151.694	12.281	5.050	0	80	Dispersed Bubble+Slug	0.412
61.527	4.981	209.250	16.941	5.190	0	80	Annular	0.411

**Table A.12 Three-phase Flow Experimental Data for Inclined (45.0°) (From Horizontal)
Eccentric Annulus Cutting-Gas-Water Flow**

Mud Flow Rate(gpm)	Mud Sup. Vel.(ft/sec)	Annular Gas Flow rate(gpm)	Gas Sup. Vel.(ft/sec)	P. Transmitter(psig)	Pipe RPM (1/min)	ROP(ft/hrs)	Flow Pattern	Dp(psi/ft)
25.522	2.066	322.551	26.114	3.932	80	121	Wavy Annular+Dispersed	0.254
25.986	2.104	241.129	19.522	4.186	80	121	Slug+Dispersed	0.299
25.041	2.027	121.209	9.813	4.875	80	121	Slug+Dispersed	0.309
24.859	2.013	186.735	15.118	4.402	80	121	Slug+Dispersed	0.297
25.101	2.032	358.928	29.059	3.837	80	121	Wavy Annular+Dispersed	0.274
25.138	2.035	100.781	8.159	5.142	80	121	Slug+Dispersed	0.340
25.373	2.054	64.118	5.191	5.674	80	121	Slug+Dispersed	0.358
25.293	2.048	26.708	2.162	6.694	80	121	Slug+Moving bed	0.428
25.641	2.076	30.793	2.493	6.355	81	81	Moving bed C+Slug	0.421
25.501	2.065	194.416	15.740	4.319	81	81	Dispersed C+Slug	0.286
25.481	2.063	128.685	10.418	4.764	81	81	Dispersed C+Slug	0.314
25.671	2.078	95.520	7.733	5.084	81	81	Dispersed C+Slug	0.360
25.648	2.076	258.451	20.924	3.990	81	81	Dispersed C+Slug	0.264
26.116	2.114	85.396	6.914	5.217	81	81	Wavy Slug C+Slug	0.341
26.052	2.109	178.581	14.458	4.520	120	81	Dispersed C+Slug*****	0.324
25.672	2.078	90.527	7.329	5.084	120	81	Dispersed C+Slug*****	0.339
25.585	2.071	59.128	4.787	5.522	120	81	Moving bed C+Qg=0	0.343
25.279	2.047	30.267	2.450	6.408	120	81	Moving bed C+Qg=0	0.421
36.981	2.994	33.287	2.695	5.768	80	102	Slug+Moving bed	0.437
37.620	3.046	64.905	5.255	5.211	80	102	Slug+Dispersed	0.394
37.895	3.068	174.322	14.113	4.572	80	102	Wavy Annular+Dispersed	0.366
37.685	3.051	86.006	6.963	4.989	80	102	Slug+Dispersed	0.375
37.546	3.040	116.392	9.423	4.793	80	102	Slug+Dispersed	0.358
37.287	3.019	233.953	18.941	4.323	80	102	Wavy Annular+Dispersed	0.331
37.747	3.056	289.167	23.411	4.314	80	102	Wavy Annular+Dispersed	0.349
37.175	3.010	34.977	2.832	5.745	120	101	Slug+Moving bed	0.415
37.555	3.040	59.818	4.843	5.307	120	101	Slug+Dispersed	0.382
38.177	3.091	85.900	6.955	4.987	120	101	Slug+Dispersed	0.371
36.820	2.981	33.025	2.674	5.714	120	102	Slug+Moving Bed	0.436
36.914	2.989	33.635	2.723	5.612	120	102	Slug+Moving Bed	0.439
49.340	3.995	29.051	2.352	5.631	80	80	Slug+Dispersed	0.419
49.336	3.994	49.308	3.992	5.428	80	80	Slug+Dispersed	0.391
49.304	3.992	77.463	6.271	5.238	80	80	Slug+Dispersed	0.381
51.894	4.201	108.053	8.748	5.128	80	80	Slug+Dispersed	0.362
49.879	4.038	153.111	12.396	4.928	80	80	Slug+Dispersed	0.340
49.388	3.998	199.775	16.174	4.937	80	80	Wavy Annular+Dispersed	0.367
50.575	4.095	241.137	19.523	4.975	80	80	Wavy Annular+Dispersed	0.366
49.315	3.993	291.317	23.585	5.017	80	80	Wavy Annular+Dispersed	0.398

APPENDIX B

Developed Excel Macro to Calculate the Average of Experimental Data

```
Sub Project()  
,  
' Project Macro  
' Macro recorded 23.03.2009 by Reza E. Osgouei  
,  
' Keyboard Shortcut: Ctrl+b  
,  
  
    Dim Num, Num2, Num3, sayi, bul1 As Long  
  
    Range("T2").Select  
    sayi = Range("T2").Value  
    Range("T4").Select  
    Limit = Range("T4").Value  
    cvp = 1  
    bul2 = 2  
    For Num = bul2 To sayi  
        Range("a" & Num).Select  
        bul1 = Range("a" & Num).Value  
        Num3 = Num + 1  
        Range("a" & Num3).Select  
        Num2 = Range("a" & Num3).Value  
        If Num2 - bul1 > Limit Then  
            cvp = cvp + 1  
            Sum1 = 0  
            Sum2 = 0  
            Sum3 = 0  
            Sum4 = 0  
            Sum5 = 0  
            Sum6 = 0  
            Sum7 = 0  
            Sum8 = 0  
            Sum9 = 0  
            Sum10 = 0  
            Sum11 = 0  
            Sum12 = 0  
            Sum13 = 0  
            Sum14 = 0  
            Sum15 = 0  
            Sum16 = 0  
            Sum17 = 0
```

```

Sum18 = 0
For i = bul2 To Num
Sum1 = Sum1 + Range("A" & i).Value
Sum2 = Sum2 + Range("B" & i).Value
Sum3 = Sum3 + Range("C" & i).Value
Sum4 = Sum4 + Range("D" & i).Value
Sum5 = Sum5 + Range("E" & i).Value
Sum6 = Sum6 + Range("F" & i).Value
Sum7 = Sum7 + Range("G" & i).Value
Sum8 = Sum8 + Range("H" & i).Value
Sum9 = Sum9 + Range("I" & i).Value
Sum10 = Sum10 + Range("J" & i).Value
Sum11 = Sum11 + Range("K" & i).Value
Sum12 = Sum12 + Range("L" & i).Value
Sum13 = Sum13 + Range("M" & i).Value
Sum14 = Sum14 + Range("N" & i).Value
Sum15 = Sum15 + Range("O" & i).Value
Sum16 = Sum16 + Range("P" & i).Value
Sum17 = Sum17 + Range("Q" & i).Value
Sum18 = Sum18 + Range("R" & i).Value
Next i
Range("S" & Num).Select
FlowPatern = Range("S" & Num).Value
TimeAvg = Sum1 / (Num + 1 - bul2)
HoneywellPressureTransmitterAvg = Sum2 / (Num + 1 - bul2)
MudFlowrateAvg = Sum3 / (Num + 1 - bul2)
MudSupVelAvg = Sum4 / (Num + 1 - bul2)
ABBGasFlowRatAvg = Sum5 / (Num + 1 - bul2)
LowGasFolwAvg = Sum6 / (Num + 1 - bul2)
AnnalusGasFlowrateAvg = Sum7 / (Num + 1 - bul2)
GasSupVelAvg = Sum8 / (Num + 1 - bul2)
ABBPresureTransmitterAvg = Sum9 / (Num + 1 - bul2)
LowPresureTransmitterAvg = Sum10 / (Num + 1 - bul2)
CollectionTankAvg = Sum11 / (Num + 1 - bul2)
InjectionTankAvg = Sum12 / (Num + 1 - bul2)
InjectionROPAvg = Sum13 / (Num + 1 - bul2)
CollectionROPAvg = Sum14 / (Num + 1 - bul2)
ColeParmerTransmitterAvg = Sum15 / (Num + 1 - bul2)
AnnalusPressureTransmitterAvg = Sum16 / (Num + 1 - bul2)
PipeRPMAvg = Sum17 / (Num + 1 - bul2)
MotorROPAvg = Sum18 / (Num + 1 - bul2)
Range("U" & cvp).Select
Range("U" & cvp).Value = Num
Range("V" & cvp).Select
Range("V" & cvp).Value = TimeAvg
Range("W" & cvp).Select
Range("W" & cvp).Value = HoneywellPressureTransmitterAvg

```

```

Range("X" & cvp).Select
Range("X" & cvp).Value = MudFlowrateAvg
Range("Y" & cvp).Select
Range("Y" & cvp).Value = MudSupVelAvg
Range("Z" & cvp).Select
Range("Z" & cvp).Value = ABBGasFlowRatAvg
Range("AA" & cvp).Select
Range("AA" & cvp).Value = LowGasFolwAvg
Range("AB" & cvp).Select
Range("AB" & cvp).Value = AnnulusGasFlowrateAvg
Range("AC" & cvp).Select
Range("AC" & cvp).Value = GasSupVelAvg
Range("AD" & cvp).Select
Range("AD" & cvp).Value = ABBPressureTransmitterAvg
Range("AE" & cvp).Select
Range("AE" & cvp).Value = LowPressureTransmitterAvg
Range("AF" & cvp).Select
Range("AF" & cvp).Value = CollectionTankAvg
Range("AG" & cvp).Select
Range("AG" & cvp).Value = InjectionTankAvg
Range("AH" & cvp).Select
Range("AH" & cvp).Value = InjectionROPAvg
Range("AI" & cvp).Select
Range("AI" & cvp).Value = CollectionROPAvg
Range("AJ" & cvp).Select
Range("AJ" & cvp).Value = ColeParmerTransmitterAvg
Range("AK" & cvp).Select
Range("AK" & cvp).Value = AnnulusPressureTransmitterAvg
Range("AL" & cvp).Select
Range("AL" & cvp).Value = PipeRPMAvg
Range("AM" & cvp).Select
Range("AM" & cvp).Value = MotorROPAvg
Range("AN" & cvp).Select
Range("AN" & cvp).Value = FlowPatern
bul2 = Num + 1
End If
Next Num
End Sub

```

APPENDIX C

Image processing techniques

C-1 Global thresholding

Global thresholding creates binary images from gray-level ones by turning all pixels below some threshold to zero and all pixels about that threshold to one. In this work, threshold value is arithmetic mean of pixel intensities.

$$g(x, y) = \begin{cases} 1 & \text{if } f(x, y) \geq T \\ 0 & \text{otherwise} \end{cases} \quad T = \frac{1}{m \times n} \sum_{x=1}^m \sum_{y=1}^n f(x, y) \quad (\text{C.1})$$

where m and n denote row and column number of the image, respectively.

C-2 Absolute difference

Absolute difference is used in motion estimation for finding movements in two consecutive frames by taking the absolute value of the difference between each pixel.

$$H(x, y) = | F(x, y) - G(x, y) | \quad (\text{C.2})$$

where H is the output image, and F and G are consecutive input images.

C-3 Background estimation using mean value

The background of an image is estimated by extracting the foreground objects from the background. In this work, the camera is stable and some objects are passing through the pipe irregularly. Therefore, the video is separated into frames, and the background is generated from this frame's mean values of each pixel position.

$$g(x, y) = \frac{1}{q} \sum_{x=1}^m \sum_{y=1}^n \frac{f_1(x, y) + f_2(x, y) + \dots + f_q(x, y)}{q} \quad (\text{C.3})$$

where q is the number of frames, and m and n denote row and column number of the image, respectively.

C-4 enhancing binary image using morphological operations

The morphological operations which are used in this work are; dilation, erosion, opening and closing. Let E be a Euclidean space or an integer grid, a binary image in E , and B a structuring element. The dilation and erosion of A by B are defined by:

- Dilation; $A \oplus B = \{ z \in E \mid (B^S)_z \cap A \neq \emptyset \}$ (C.4)

- Erosion; $A \ominus B = \{ z \in E \mid B_z \subseteq A \}$ (C.5)

where B^S denotes the symmetric of B , that is, $B^S = \{ x \in E \mid -x \in B \}$ (C.6)

where B_z is the translation of B by the vector z , $B_z = \{ b + z \mid b \in B \}$ (C.7)

Opening and closing are operations that are generated by applying dilation and erosion in different combinations.

- Opening; $A \odot B = (A \ominus B) \oplus B$ (C.8)

- Closing; $A \oslash B = (A \oplus B) \ominus B$ (C.9)

where \ominus and \oplus denote erosion and dilation, respectively.

In this work, the dilation operation is used for showing cutting pieces regions in one region. The opening operation is used for noise removal and the closing operation is used for hole filling.

APPENDIX D

A Developed Excel Macro to Determine the Flow Pattern

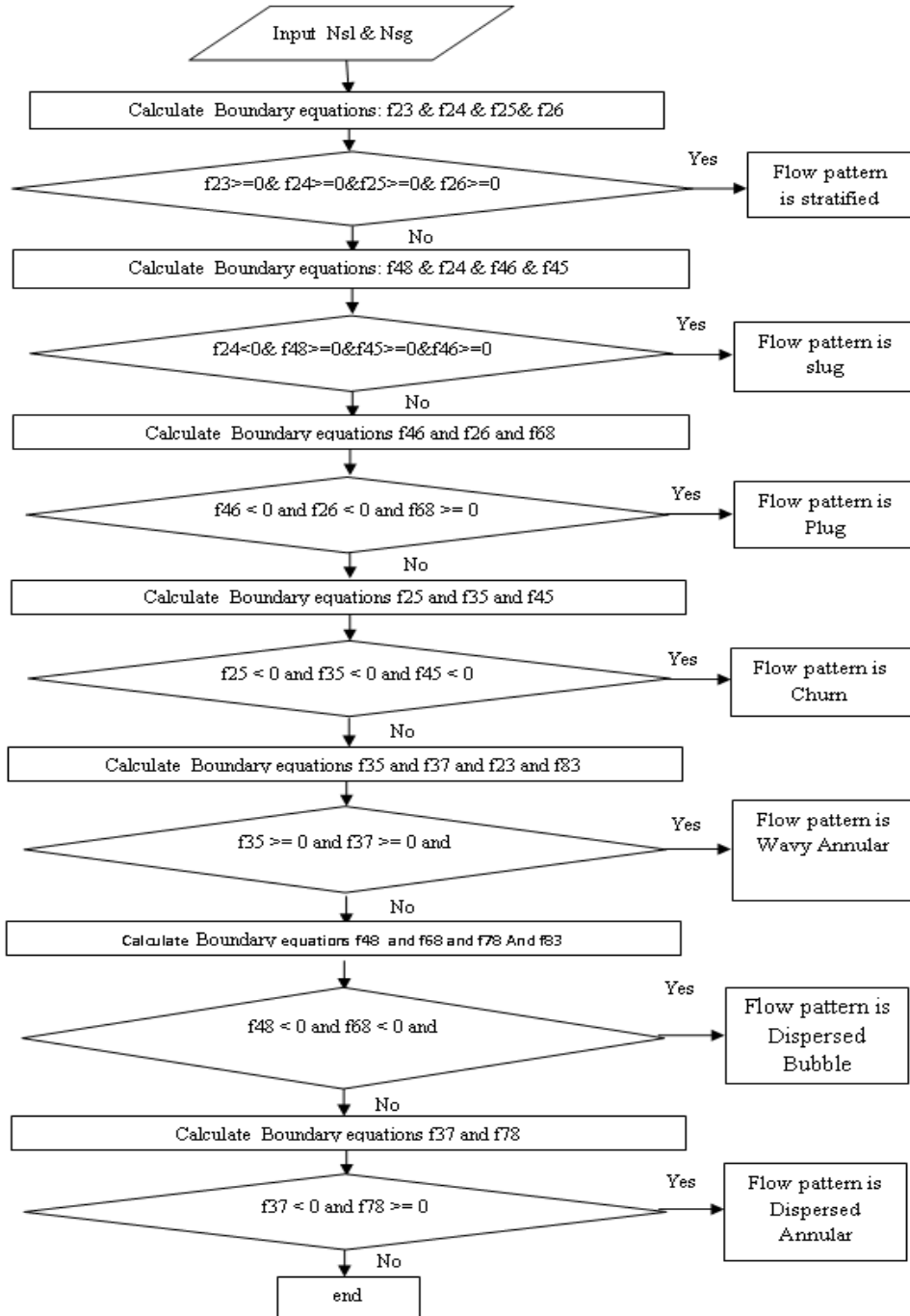


Figure D.1 Flowchart for Flow Pattern Identification in an Annular Section

```

'FlowRegim Macro
' Macro recorded 22/04/2009 by Reza
'
Range("AN2").Select
mug = Range("AN2").Value
Range("AN3").Select
mul = Range("AN3").Value
Range("AN4").Select
deg = Range("AN4").Value
Range("AN5").Select
del = Range("AN5").Value
Range("AN6").Select
dou = Range("AN6").Value
Range("AN7").Select
din = Range("AN7").Value
Range("V2").Select
sayi1 = Range("V2").Value
Range("V4").Select
sayi2 = Range("V4").Value
Dh = dou - din
For i = sayi1 To sayi2
Range("H" & i).Select
VSg = Range("H" & i).Value
Range("D" & i).Select
Vsl = Range("D" & i).Value
Vm = Vsl + VSg
Range("AJ" & i).Select
delp = Range("AJ" & i).Value
Landal = (Vsl / Vm)
Range("P" & i).Select
pa = Range("P" & i).Value
deg1 = deg * (14.7 + pa) / 14.7
dem = del * Landal + deg1 * (1 - Landal)
mum = mul * Landal + mug * (1 - Landal)
Ff = delp * (25.8 * Dh) / (dem * Vm ^ 2)
Range("AK" & i).Select
Range("AK" & i).Value = Ff
NRe = (928 * dem * Vm * Dh) / mum
Range("AL" & i).Select
Range("AL" & i).Value = NRe
NReg = (928 * deg1 * VSg * Dh) / mug
Range("AR" & i).Select
Range("AR" & i).Value = NReg
NRel = (928 * del * Vsl * Dh) / mul
Range("AQ" & i).Select
Range("AQ" & i).Value = NRel
If NReg > 2000 And NRel > 2000 Then

```

```

Range("AP" & i) = Range("AN21")
ElseIf NReg > 2000 And NRel <= 2000 Then
Range("AP" & i) = Range("AN22")
ElseIf NReg <= 2000 And NRel > 2000 Then
Range("AP" & i) = Range("AN23")
ElseIf NReg <= 2000 And NRel <= 2000 Then
Range("AP" & i) = Range("AN24")
End If

```

```

f23 = 0.9667+ 0.0002* NReg + 0.0020* NRe -5.95*10-8* NReg ^ 2 -2.11*10-7* NRe ^ 2
Range("W" & i).Select
Range("W" & i).Value = f23

```

```

f24 = 4.84232 -0.261981 * NReg + 5.32208 * NRe + 0.00392239 * NReg ^ 2 - 6.94573 *
NRe ^ 2
Range("X" & i).Select
Range("X" & i).Value = f24

```

```

f45 = 15.0934 + -0.288117 * NReg + -3.58515 * NRe + 0.0000278835 * NReg ^ 2 +
0.242638 * NRe ^ 2
Range("Y" & i).Select
Range("Y" & i).Value = f45

```

```

f26 = 0.197186 + -0.701564 * NReg + 6.22211 * NRe + 0.142725 * NReg ^ 2 + -7.01371 *
NRe ^ 2
Range("Z" & i).Select
Range("Z" & i).Value = f26

```

```

f37 = 11.03 + -0.0210257 * NReg + -1.69994 * NRe + 0.00000587196 * NReg ^ 2 +
0.0368274 * NRe ^ 2
Range("AA" & i).Select
Range("AA" & i).Value = f37

```

```

f35 = 13.253 + -0.547409 * NReg + -3.59065 * NRe + 0.00417981 * NReg ^ 2 + 0.242194 *
NRe ^ 2
Range("AB" & i).Select
Range("AB" & i).Value = f35

```

```

f46 = -4.64514 + -0.439583 * NReg + 0.90003 * NRe + 0.138802 * NReg ^ 2 + -0.0679863
* NRe ^ 2
Range("AC" & i).Select
Range("AC" & i).Value = f46

```

```

f48 = 498.066 + 0.315844 * NReg + -101.968 * NRe + -0.000224641 * NReg ^ 2 + 5.1682 *
NRe ^ 2
Range("AD" & i).Select
Range("AD" & i).Value = f48

```

```

f68 = 502.711 + 0.755427 * NReg + -102.868 * NRe + -0.139027 * NReg ^ 2 + 5.23619 *
NRe ^ 2
Range("AE" & i).Select

```

Range("AE" & i).Value = f68

$f78 = 485.195 + 0.0775775 * NReg + -100.274 * NRe + 0.00392141 * NReg^2 + 5.13093 * NRe^2$

Range("AF" & i).Select

Range("AF" & i).Value = f78

$f47 = 12.8704 + 0.238266 * NReg + -1.69444 * NRe + -0.00414605 * NReg^2 + 0.037271 * NRe^2$

Range("AG" & i).Select

Range("AG" & i).Value = f47

$f25 = 19.9358 + -0.550098 * NReg + 1.73693 * NRe + 0.00395027 * NReg^2 + -6.70309 * NRe^2$

If f23 >= 0 And f24 >= 0 And f26 >= 0 And f25 >= 0 Then

'stratified Flow Pattern Conditions

Range("S" & i).Select

Range("S" & i) = Range("V8")

Range("T" & i).Select

Range("T" & i) = Range("V8")

Range("U" & i).Select

Range("U" & i) = Range("V15")

Range("AO" & i) = Range("AN13")

Else

For k = 1 To 2

'Slug Flow Pattern Conditions

If f24 < 0 And f47 >= 0 And f48 >= 0 And f46 >= 0 And f45 >= 0 Then

Range("S" & i).Select

Range("S" & i) = Range("V9")

Range("T" & i).Select

Range("T" & i) = Range("V10")

Range("U" & i).Select

Range("U" & i) = Range("V18")

Range("AO" & i) = Range("AN16")

Exit For

'Bubble Flow Pattern Conditions

ElseIf f46 < 0 And f26 < 0 And f68 >= 0 Then

Range("S" & i).Select

Range("S" & i) = Range("V9")

Range("T" & i).Select

Range("T" & i) = Range("V10")

Range("U" & i).Select

Range("U" & i) = Range("V17")

Range("AO" & i) = Range("AN15")

Exit For

'Transition Zone Conditions

ElseIf f25 < 0 And f35 < 0 And f45 < 0 Then

Range("S" & i).Select

Range("S" & i) = Range("V9")

```

Range("T" & i).Select
Range("T" & i) = Range("V10")
Range("U" & i).Select
Range("U" & i) = Range("V16")
Range("AO" & i) = Range("AN14")
Exit For
'Wavy Annular Flow Pattern Conditions
ElseIf f35 >= 0 And f37 >= 0 And f23 < 0 Then
Range("S" & i).Select
Range("S" & i) = Range("V9")
Range("T" & i).Select
Range("T" & i) = Range("V11")
Range("U" & i).Select
Range("U" & i) = Range("V19")
Range("AO" & i) = Range("AN17")
Exit For
'Dispersed Bubble Flow Pattern Conditions
ElseIf f48 < 0 And f68 < 0 And f78 < 0 Then
Range("S" & i).Select
Range("S" & i) = Range("V9")
Range("T" & i).Select
Range("T" & i) = Range("V12")
Range("U" & i).Select
Range("U" & i) = Range("V20")
Range("AO" & i) = Range("AN18")
Exit For
'Dispersed Annular Flow Pattern Conditions
ElseIf f37 < 0 And f47 < 0 And f78 >= 0 Then
Range("S" & i).Select
Range("S" & i) = Range("V9")
Range("T" & i).Select
Range("T" & i) = Range("V12")
Range("U" & i).Select
Range("U" & i) = Range("V21")
Range("AO" & i) = Range("AN19")
Exit For
End If
Next k
End If
Range("AH" & i).Select
If Vsl <= 6.1 Then
Range("AH" & i).Value = (Range("B" & i).Value) / 1.5
Range("AI" & i).Value = (Range("O" & i).Value)
Else
Range("AH" & i).Value = Range("B" & i).Value
Range("AI" & i).Value = (Range("O" & i).Value) / 1.5
End If

```

```
k = Abs(Range("AH" & i).Value - Range("AI" & i).Value)
If k <= 0.001 Then
Range("AJ" & i).Value = (Range("AH" & i).Value + Range("AI" & i).Value) / 2
Else
Range("AJ" & i).Value = Range("AH" & i).Value
End If
Next i
End Sub
```

APPENDIX E

Developed Excel Macro to Estimated Frictional Pressure Drop For Flow in Horizontal Annuli by Using Beggs & Brill Method

```
Private Sub CommandButton1_Click()  
' FlowRegimDeterminator Macro  
' Macro recorded 03/08/2009 by Reza E. Osgouei  
,  
  
Range("V2").Select  
sayi1 = Range("V2").Value  
Range("V4").Select  
sayi2 = Range("V4").Value  
Range("Y1").Select  
rol = Range("Y1").Value  
Range("Y2").Select  
rog = Range("Y2").Value  
Range("Y3").Select  
mul = Range("Y3").Value  
Range("Y4").Select  
mug = Range("Y4").Value  
'Range("Y5").Select  
'zigma = Range("Y5").Value  
Range("Y6").Select  
gr = Range("Y6").Value  
dou = 2.91 / 12  
din = 1.85 / 12  
For i = sayi1 To sayi2  
Range("P" & i).Select  
pa = Range("P" & i).Value  
rog1 = rog * (14.7 + pa) / 14.7  
Range("H" & i).Select  
VSg = Range("H" & i).Value  
Range("D" & i).Select  
Vsl = Range("D" & i).Value  
Vm = Vsl + VSg  
Landa = Vsl / Vm  
Range("AA" & i) = Landa  
NFrm = (0.031056 * Vm ^ 2) / (dou - din)  
Range("AB" & i) = NFrm  
L1 = 316 * Landa ^ (0.302)  
Range("AF" & i) = L1  
L2 = 0.0009252 * Landa ^ (-2.4684)  
Range("AG" & i) = L2
```

```

L3 = 0.1 * Landa ^ (-1.4516)
Range("AH" & i) = L3
L4 = 0.5 * Landa ^ (-6.738)
Range("AI" & i) = L4
If Landa < 0.01 And NFrm < L1 Then
Range("W" & i).Select
Range("W" & i) = Range("V8")
Range("AD" & i) = Range("Y8")
a = 0.98
b = 0.4846
c = 0.0868
d2 = 0
ElseIf Landa >= 0.01 And NFrm < L2 Then
Range("W" & i).Select
Range("W" & i) = Range("V8")
Range("AD" & i) = Range("Y8")
a = 0.98
b = 0.4846
c = 0.0868
d2 = 0
ElseIf Landa >= 0.01 And NFrm <= L3 And NFrm >= L2 Then
Range("W" & i) = Range("V9")
Range("AD" & i) = Range("Y9")
d2 = 1
a = 0.98
b = 0.4846
c = 0.0868
a1 = 0.845
b1 = 0.5351
c1 = 0.0173
ElseIf Landa <= 0.4 And Landa >= 0.01 And NFrm <= L1 And NFrm > L3 Then
Range("W" & i) = Range("V10")
Range("AD" & i) = Range("Y10")
a = 0.845
b = 0.5351
c = 0.0173
d2 = 0
ElseIf Landa >= 0.4 And NFrm <= L4 And NFrm > L3 Then
Range("W" & i).Select
Range("W" & i) = Range("V10")
Range("AD" & i) = Range("Y10")
a = 0.845
b = 0.5351
c = 0.0173
d2 = 0
ElseIf Landa < 0.4 And NFrm >= L1 Then
Range("W" & i).Select

```

```

Range("W" & i) = Range("V11")
Range("AD" & i) = Range("Y11")
a = 1.065
b = 0.5824
c = 0.0609
d2 = 0
ElseIf Landa >= 0.4 And NFrm >= L4 Then
Range("W" & i).Select
Range("W" & i) = Range("V11")
Range("AD" & i) = Range("Y11")
a = 1.065
b = 0.5824
c = 0.0609
d2 = 0
End If
If d2 = 0 Then
HI = (a * Landa ^ b) / NFrm ^ c
Else
HI = ((L3 - NFrm) / (L3 - L2)) * ((a * Landa ^ b) / NFrm ^ c) + (1 - ((L3 - NFrm) /
(L3 - L2))) * ((a1 * Landa ^ b1) / NFrm ^ c1)
End If
Range("AC" & i) = HI
y = Landa / HI ^ 2
y1 = Log(y) / Log(2.718282)
S = (y1 / (-0.0523 + 3.182 * y1 - 0.8725 * (y1) ^ 2 + 0.01853 * (y1) ^ 4))
ftp = Exp(S)
mum = mul * Landa + mug * (1 - Landa)
rom = rol * Landa + rog1 * (1 - Landa)
NRe = 1488 * rom * Vm * (dou - din) / mum
fn = 1 / (2 * Log(NRe / ((4.5223 * Log(NRe)) - 3.8215))) ^ 2
ftp1 = ftp * fn
delp = ((ftp1 * rom * (Vm ^ 2)) / (2 * gr * (dou - din))) / 144
Range("Z" & i) = delp
Next i
End Sub

```

APPENDIX F

Developed Matlab Code to Determine Relationship between Liquid and Gas Superficial Reynolds Number and Experimentally Observed Friction Factor for Current Experimental Data by Using Matlab Statistical Tool Box and Applying Robust Regression

```
load FfNReLG
Ff=FfNReLG(1:407,1);
NReL=FfNReLG(1:407,2);
NReG=FfNReLG(1:407,3);
scatter3(NReL,NReG,Ff,'r')
Xz = [ones(size(NReL,1),1) NReL NReG log(NReL.^2)
log(NReG.^2)];%log(NReL.*NReG)];
alpha = 0.05;
[b,Ibeta,res,Ires]= regress(Ff,Xz); % Removes NaN data
subplot(3,1,1);scatter3(NReL,NReG,Ff,'r','filled');
x1fit = min(NReL):800:max(NReL);
x2fit = min(NReG):4700:max(NReG);
[X1FIT,X2FIT] = meshgrid(x1fit,x2fit);
YFIT = b(1) + b(2)*X1FIT + b(3)*X2FIT + b(4).*log(X1FIT.^2)+
b(5).*log(X2FIT.^2);%+ b(6).*log(X1FIT.*X2FIT) ;
subplot(2,1,1);
meshc(X1FIT,X2FIT,YFIT)
xlabel('Mud Sup. Reynolds Number')
ylabel('Gas Sup. Reynolds Number')
zlabel('Friction Factor')
title(' Linear Regression Model to determine Relationship between Friction Factor
and Mud and Gas Sup. Reynolds Number ')
hold on
scatter3(NReL,NReG,Ff,'r','filled');
Xz=Xz(:,2:5);
[rob,stats] = robustfit(Xz,Ff); % Removes NaN data
hold on
[X12FIT,X22FIT] = meshgrid(x1fit,x2fit);
Y2FIT = rob(1) + rob(2)*X12FIT + rob(3)*X22FIT + rob(4).*log(X12FIT.^2)+
rob(5).*log(X22FIT.^2);%+ b(6).*log(X1FIT.*X2FIT) ;
subplot(2,1,2);
meshc(X12FIT,X22FIT,Y2FIT)
hold on
scatter3(NReL,NReG,Ff,'r','filled');
xlabel('Mud Sup. Reynolds Number')
ylabel('Gas Sup. Reynolds Number')
zlabel('Friction Factor')
title(' Robust Regression Model to determine Relationship between Friction Factor
and Mud and Gas Sup. Reynolds Number')
```

APPENDIX G

Resultant Mix Velocity (Azar 2000)

When drill pipe is rotated, it is necessary to consider the effect of both tangential velocity (V_{θ}), imposed by rotation of inner pipe (Figure G.1) and axial velocity V_z during the calculations.

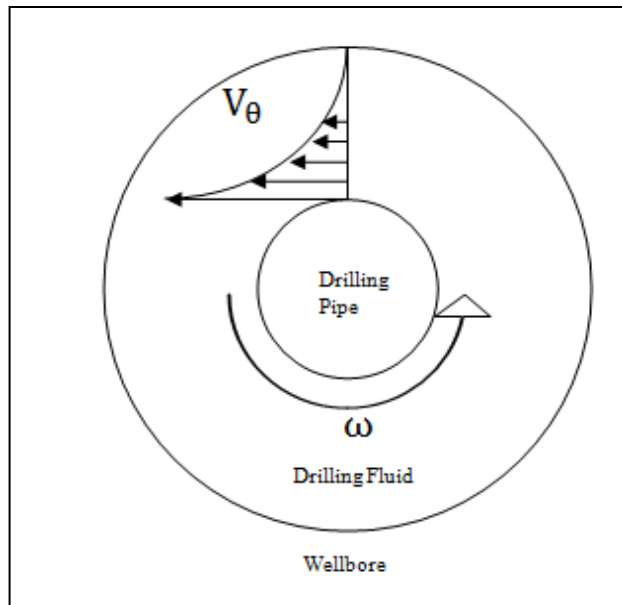


Figure G.1 Tangential Velocity Profile in the Annuli

Based on this component a helical path is described by particle in the fluid as follow:

$$\vec{u}_m = \vec{V}_z + \vec{V}_{\theta} \quad \text{G.1}$$

Axial velocity can be obtained by using the following formulas.

For three phase flow

$$V_z = \frac{4(Q_L + Q_S + Q_G)}{\pi(D_{wh}^2 - D_{dp}^2)} \quad \text{G.2}$$

For two phase flow

$$V_z = \frac{4(Q_L + Q_S)}{\pi(D_{wh}^2 - D_{dp}^2)} \quad G.3$$

In order to determine the tangential velocity component, an annular rotational Couette (Slattery, 1999) flow model was considered.

Therefore the tangential velocity as function of radius is given by:

$$V_\theta = \frac{1}{2} K D_{wh} \omega \left(\frac{2r/D_{wh} - D_{wh}/2r}{K^{-1}/k} \right) \quad G.4$$

Where K is defined by equation G.5, ω is the drilling angular velocity in units of $[t^{-1}]$ and r is any radius in the range $D_{dp}/2 \leq r \leq D_{wh}/2$.

$$K = \frac{D_{dp}}{D_{wh}} \quad G.5$$

An average of these component in annulus area, can be calculated as:

$$\begin{aligned} \bar{V}_\theta &= \frac{\int_{D_{dp}/2}^{D_{wh}/2} \int_0^{2\pi} V_\theta r d\theta dr}{\int_{D_{dp}/2}^{D_{wh}/2} \int_0^{2\pi} r d\theta dr} = \\ &= \frac{\int_{D_{dp}/2}^{D_{wh}/2} \int_0^{2\pi} \left\{ \frac{1}{2} K D_{wh} \omega \left(\frac{2r/D_{wh} - D_{wh}/2r}{K^{-1}/k} \right) \right\} r d\theta dr}{\int_{D_{dp}/2}^{D_{wh}/2} \int_0^{2\pi} r d\theta dr} \quad G.6 \end{aligned}$$

By using Mathematica

$$V_\theta = \frac{K^2 \omega \left[-D_{wh}^2 + D_{dp}^2 + 2D_{wh}^2 (\log D_{wh} - \log D_{dp}) \right]}{(D_{wh}^2 - D_{dp}^2)(1 - K^2)} \quad G.7$$

Finally the resultant average velocity in the upward direction is given by the following equation:

$$\bar{u}_m = \sqrt{\overrightarrow{V}_z^2 + \overrightarrow{V}_\theta^2} \quad \text{G.8}$$

$$\bar{u}_m = \frac{4}{\pi(D_{wh}^2 - D_{dp}^2)} \sqrt{(Q_L + Q_S + Q_G)^2 + \frac{\pi^2 K^2 \omega [-D_{wh}^2 + D_{dp}^2 + 2D_{wh}^2 (\log D_{wh} - \log D_{dp})]}{16(1-K^2)}} \quad \text{G.9}$$

APPENDIX H

Developed Excel Macro to Find Interfacial Friction Factor

Sub Corrolation()

'
' Macro by Reza E.Osgouei 08.06.2010
,

```
Range("x12").Select
ID2 = Range("x12").Value
Range("x13").Select
OD2 = Range("x13").Value
Range("x2").Select
PI2 = Range("x2").Value
Range("x4").Select
Pg2 = Range("x4").Value
Range("x3").Select
Pc2 = Range("x3").Value
Range("x6").Select
UI2 = Range("x6").Value
Range("x5").Select
Ug2 = Range("x5").Value
g = 9.81
Range("x8").Select
alfa1 = Range("x8").Value
Range("x9").Select
Dp2 = Range("x9").Value
Range("x10").Select
h1 = Range("x10").Value
Range("x11").Select
muf = Range("x11").Value
ID = ID2 * 0.0254
OD = OD2 * 0.0254
DP = 0.0019999994
PI = PI2 * 119.826427
Pc = Pc2 * 119.826427
UI = UI2 * 0.001
Db = 0.04 * (OD - ID)
Range("y2").Select
Sayi1 = Range("y2").Value
Range("y4").Select
Sayi2 = Range("y4").Value
For I = Sayi1 To Sayi2
Range("A" & I).Select
QI2 = Range("A" & I).Value
Range("B" & I).Select
ROP = Range("B" & I).Value
```

```

Range("C" & I).Select
RPM = Range("C" & I).Value
Range("d" & I).Select
DP1 = Range("d" & I).Value
DPP = DP1 * 6894.757 / 0.3048
Ql = Ql2 * 6.30902 * 10 ^ (-5)
'Qg2 = Qg1 * 6.30902 * 10 ^ (-5)
'Pa = Pa2 * 6894.757
'FA = Pa2 * (2.448 * (2.91 ^ 2 - 1.86 ^ 2))
'Pa3 = (FA / (2.448 * (OD2 ^ 2 - ID2 ^ 2))) * 6894.757
'Pg = Pg1 * ((14.7 * 6894.757) + Pa) / (14.7 * 6894.757)
'Ug = Ug3 * ((14.7 * 6894.757) + Pa) / (14.7 * 6894.757)
'Qg2 = Qg * ((14.7 * 6894.757) + Pa) / (14.7 * 6894.757)
Qc1 = ((3.14159265358979 / 4) * ROP * ((0.2425) ^ 2)) * 0.12467532647 'flow
rate in gpm
Qc = Qc1 * 6.30902 * 10 ^ (-5)
K = ID / OD
w = RPM * (2 * 3.14159265358979) / 60
y1 = Log(OD) / Log(2.718282)
y2 = Log(ID) / Log(2.718282)
Vt2 = (K ^ 2 * w * (-OD ^ 2 + ID ^ 2 + ((2 * OD ^ 2) * (y1 - y2)))) / ((OD ^ 2 - ID ^
2) * (1 - K ^ 2))
'r = (OD - ID) / 4
'Vt2 = (0.5 * K * OD * w) * (((2 * r) / OD) - (OD / (2 * r))) / (K - (1 / K))
'Vt2 = (0.5 * K * OD * w) * (((2 * r) / OD) - (OD / (2 * r))) / (K - (1 / K))
'SS = (-2 * OD ^ 3 - ID ^ 3 - 6 * OD ^ 2 * ID)
'Vt2 = (K ^ 2 * w * SS) / (24 * (OD ^ 2 - ID ^ 2) * (K ^ 2 - 1))
Vt = Vt2
Vz = 4 * (Ql + Qc) / (3.14159265358979 * (OD ^ 2 - ID ^ 2))
'Vzg11 = (4 * Qg2) / (3.14159265358979 * (OD ^ 2 - ID ^ 2))
Vzc11 = (4 * Qc) / (3.14159265358979 * (OD ^ 2 - ID ^ 2))
Vzf11 = (4 * Ql) / (3.14159265358979 * (OD ^ 2 - ID ^ 2))
If Vzc11 > 0 Then
Vsc = (Vzc11 ^ 2 + Vt ^ 2) ^ (1 / 2)
Else
Vsc = 0
End If
'If Vzg11 > 0 Then
'Vsg = (Vzg11 ^ 2 + Vt ^ 2) ^ (1 / 2)
'Else
'Vsg = 0
'End If
Vsf = (Vzf11 ^ 2 + Vt ^ 2) ^ (1 / 2)
LandaL = Ql / (Qc + Ql)
landaC = Qc / (Qc + Ql)
'landaG = Qg2 / (Qc + Ql + Qg2)
V = (Vz ^ 2 + Vt ^ 2) ^ (1 / 2)

```

*****Determination of Dimentionless group*****

```

Pmix = Pc * landaC + Pl * LandaL
Umix = (1 + 2.5 * landaC * 10.05 + landaC ^ 2 + 0.00273 * Exp(16.6 * landaC)) *
Ul 'Clayton Crowe Book page 4-55
Fr = Vz ^ 2 / (g * (OD - ID))
Nre = Vz * Pmix * (OD - ID) / (Umix)
Nro = Vt * Pmix * (OD - ID) / (Umix)
Range("k" & I).Select
Range("k" & I).Value = Fr
Range("l" & I).Select
Range("l" & I).Value = Nre
Range("m" & I).Select
Range("m" & I).Value = Nro
f12 = 1.89386 + 0.000354136 * Nre + 0.000000722751 * Nro - 0.0000000166456 *
Nre ^ 2 - 0.000000000118935 * Nro ^ 2
Ccm1 = 0.381727813 + 0.01667989 * Fr - 0.0000127 * Nre + 0.000000242 * Nro
Cs = (0.915778389 + 0.055843664 * Fr - 0.0000366 * Nre - 0.00000048 * Nro)
Cc = (-4.5576 * Cs ^ 3 + 4.5898 * Cs ^ 2 - 0.1199 * Cs + 0.0273)
Ccm = -24.074 * Ccm1 ^ 3 + 11.323 * Ccm1 ^ 2 - 0.399 * Ccm1 + 0.0347
Vccal = (1.834892158 + 0.072302258 * Fr - 0.0000432 * Nre - 0.000000947 * Nro)
* Vz11
hbed = (0.891540428 + 0.098857061 * Fr - 0.000037 * Nre - 0.000000751 * Nro) *
OD
A = ((3.14159265358979 * (OD ^ 2 - ID ^ 2)) / 4)
S = 3.14159265358979 * (OD + ID)
Abed = (0.32054387 - 0.062362285 * Fr + 0.0000131 * Nre - 0.000000372 * Nro) *
A
AAct = A - Abed
Range("n" & I).Select
Range("n" & I).Value = Vccal
Range("o" & I).Select
Range("o" & I).Value = Ccm
Range("p" & I).Select
Range("p" & I).Value = Cc
Range("Q" & I).Select
Range("Q" & I).Value = hbed
Range("R" & I).Select
Range("R" & I).Value = Abed
If f12 > 0 Then
Range("ab" & I).Select
Range("ab" & I) = Range("y15")

If Vzc11 > 0 Then

```

```

'X = 1 - (hbed / (OD / 2))
'beta = Atn(-X / Sqr(-X * X + 1)) + 2 * Atn(1)
'X2 = Cos(beta)
If hbed <= (OD / 2) Then
Y = ((OD / 2) - hbed) / (OD / 2)
beta = Atn(-Y / Sqr(-Y * Y + 1)) + 2 * Atn(1)
If hbed <= h1 Then
Ac = (((OD ^ 2) / 4) * beta) - (((OD / 2) * ((OD / 2) - hbed)) * Sin(beta))
Sc = (OD) * beta
Af = A - Ac
Si = OD * Sin(beta)
Sf = S - Sc
Else
hi = hbed - h1
If hi <= (ID / 2) Then
X = ((ID / 2) - hi) / (ID / 2)
alfa = Atn(-X / Sqr(-X * X + 1)) + 2 * Atn(1)
Ac = (((OD ^ 2) / 4) * beta) - (((OD / 2) * ((OD / 2) - hbed)) * Sin(beta)) - (((ID ^ 2) / 4) * alfa) + (((ID / 2) * ((ID / 2) - hi)) * Sin(alfa))
Sc = (OD) * beta + (ID) * alfa
Af = A - Ac
Si = OD * Sin(beta) - ID * Sin(alfa)
Sf = S - Sc
ElseIf f12 <= 0 Then
X = (hi - (ID / 2)) / (ID / 2)
alfa = Atn(-X / Sqr(-X * X + 1)) + 2 * Atn(1)
Ac = (((OD ^ 2) / 4) * beta) - (((OD / 2) * ((OD / 2) - hbed)) * Sin(beta)) - ((3.14159265358979 / 4) * (ID ^ 2)) + (((ID ^ 2) / 4) * alfa) + (((ID / 2) * ((ID / 2) - hi)) * Sin(alfa))
Sc = (OD) * beta + (ID) * (3.14159265358979 - alfa)
Af = A - Ac
Si = OD * Sin(beta) - ID * Sin(3.14159265358979 - alfa)
Sf = S - Sc
End If
End If
Else
Y = -(hbed - (OD / 2)) / (OD / 2)
beta = Atn(-Y / Sqr(-Y * Y + 1)) + 2 * Atn(1)
hi = hbed - h1
If hi >= (ID / 2) Then
X = -(hi - (ID / 2)) / (ID / 2)
alfa = Atn(-X / Sqr(-X * X + 1)) + 2 * Atn(1)
Ac = -(((OD ^ 2) / 4) * beta) + (((OD / 2) * (hbed - (OD / 2))) * Sin(beta)) + ((3.14159265358979 / 4) * (OD ^ 2 - ID ^ 2)) + (((ID ^ 2) / 4) * alfa) + (((ID / 2) * ((ID / 2) - hi)) * Sin(alfa))
Sc = (OD) * (3.14159265358979 - beta) + (ID) * (3.14159265358979 - alfa)
Af = A - Ac

```

```

Si = OD * Sin(3.14159265358979 - beta) - ID * Sin(3.14159265358979 - alfa)
Sf = S - Sc
End If
End If
Dh = (4 * Af / (Sf + Si))
Dc = (4 * Ac / (Sc + Si))

*****
' h1 = 0.008382
' X = 1 - (hbed / (OD / 2))
' beta = Atn(-X / Sqr(-X * X + 1)) + 2 * Atn(1)
' X2 = Cos(beta)
' If ((OD / 2) * X2) < (h1 - ID / 2) Then
' Af = A * (3.14159265358979 - beta) - (OD / 2) * Sin(3.14159265358979 - beta) *
Cos(3.14159265358979 - beta)
' Ac = A - Af
' SS = (Sin(3.14159265358979 - beta))
' Sf = OD * SS
' Sc = S - Sf
' Si = OD * Sin(3.14159265358979 - beta)
' ElseIf ((OD / 2) * X2) > (h1 - ID / 2) And ((OD / 2) * X2) < (h1 + ID / 2) Then
' X1 = (((OD / 2) * Cos(beta) - h1) / (ID / 2))
' alfa = Atn(-X1 / Sqr(-X1 * X1 + 1)) + 2 * Atn(1)
' Ac = (OD / 2) ^ 2 * (beta - Sin(beta) * Cos(beta)) - (ID / 2) ^ 2 * (alfa - Sin(alfa) *
Cos(alfa))
' Af = A - Ac
' Sc = 2 * ((OD / 2) * beta - (ID / 2) * alfa)
' Si = 2 * (OD / 2) * Sin(beta) - 2 * (ID / 2) * Sin(alfa)
' Sf = S - Si
' ElseIf ((OD / 2) * X2) > (h1 + ID / 2) Then
' Ac = (OD / 2) ^ 2 * (beta - Sin(beta) * Cos(beta))
' Af = A - Ac
' Sc = 2 * (OD / 2) * beta
' Si = 2 * (OD / 2) * Sin(beta)
' Sf = S - Sc
' End If
*****

Ccs = Cc - Ccm
Wc = Ccm
Psm = Wc * Pc + (1 - Wc) * Pl
Usm = (1 + 2.5 * Wc + 10.05 * Wc ^ 2 + 0.00273 * Exp(16.6 * Wc)) * Ul 'Clayton
Crowe Book page 4-55
Vzm = (Ql + Qc) / (AAct)
Vmo = (Vzm ^ 2 + Vt ^ 2) ^ (1 / 2)
Vtm = ((Vsc * Pc) + (Vsf * Pl)) / Psm
Psmb = Ccs * Pc + (1 - Ccs) * Pl

```

```

Usmb = (1 + 2.5 * Ccs + 10.05 * Ccs ^ 2 + 0.00273 * Exp(16.6 * Ccs)) * UI
'Clayton Crowe Book page 4-55
Vtmb = ((Vsc * Pc) + (Vsf * Pl)) / Psmb
Else
  Wc = 0
  Psm = Pl
  Usm = UI
  Vtm = V
End If
  Else
  Dh = (OD - ID)
  Dc = ((OD - ID))
  Ccs = Cc - Ccm
  Wc = Ccm
  Psm = Wc * Pc + (1 - Wc) * Pl
  Usm = (1 + 2.5 * Wc + 10.05 * Wc ^ 2 + 0.00273 * Exp(16.6 * Wc)) * UI 'Clayton
  Crowe Book page 4-55
  Vtm = ((Vsc * Pc) + (Vsf * Pl)) / Psm
  Range("ab" & I).Select
  Range("ab" & I) = Range("y16")
End If
  Wm = 1 - Wc - Ccs
' Range("G" & I).Select
' Range("G" & I).Value = hbed
' Range("H" & I).Select
' Range("H" & I).Value = Cc
' Range("I" & I).Select
' Range("I" & I).Value = Psm
' Range("J" & I).Select
' Range("J" & I).Value = Usm
' Range("K" & I).Select
' Range("K" & I).Value = Vtm

*****Determination of Pressure Loss *****
If f12 > 0 Then
  V1 = Vmo 'Vzf11
  Vtm1 = V1 * 3.28
  Psm1 = Psm / 119.826427
  Usm1 = Usm / 0.001
  Nre1 = V1 * Psm * Dh / (Usm)
  y3 = Log(1 / K) / Log(2.718282)
  Fc = (16 * (1 - K) ^ 2) / (((1 - K ^ 4) / (1 - K ^ 2)) - ((1 - K ^ 2) / y3))
  If Nre1 < 2100 Then
    FF = 16 / Nre1
  Else
    'FF1 = 0.0791 * Nre ^ (-0.25) 'Blasius Formula
    A2 = (((4.6 * 10 ^ -5) / (Dh)) / 2.5497) ^ 1.1098 + (7.149 / Nre1) ^ 0.8981
  
```

```

FF = (1 / (-4 * Log((((4.6 * 10 ^ -5) / (Dh)) / 3.7065) - (5.0452 / Nre1) * Log(A2))))
^ 2
FF = 0.046 * Nre1 ^ (-0.2) 'Blasius Formula
End If
V1c = Vsc 'Vzc11
Vtm1 = V1c * 3.28
Psm1 = PI / 119.826427
Usm2 = UI / 0.001
Nre1c = V1c * Psmb * Dc / (Usmb)
y3 = Log(1 / K) / Log(2.718282)
Fc = (16 * (1 - K) ^ 2) / (((1 - K ^ 4) / (1 - K ^ 2)) - ((1 - K ^ 2) / y3))
If Nre1c < 2100 Then
FFc = 16 / Nre1c
Else
'FF1 = 0.0791 * Nre ^ (-0.25) 'Blasius Formula
A1 = (((4.6 * 10 ^ -5) / (Dc)) / 2.5497) ^ 1.1098 + (7.149 / Nre1c) ^ 0.8981
FFc = (1 / (-4 * Log((((4.6 * 10 ^ -5) / (Dc)) / 3.7065) - (5.0452 / Nre1c) *
Log(A1)))) ^ 2
FFc = 0.046 * Nre1c ^ (-0.2) 'Blasius Formula
End If
Tf = 0.5 * FF * Psm * V1 ^ 2
Tc = (0.5 * FFc * Psmb * V1c ^ 2) + (0.5 * (Pc - Pl) * g * (Ac / Sc) * Ccs)
Ti = ((Ac * DPP) + (Tc * Sc)) / (Si)
FFi = (Ti * 2) / (Psm * (V1 - Vsc) ^ 2)
Ti2 = -(Af * DPP) - (Tf * Sf) / (-Si)
FFi2 = (Ti2 * 2) / (Psm * (V1 - Vsc) ^ 2)
ElseIf f12 < 0 Then
V1 = V 'Vzf11
Vtm1 = V1 * 3.28
Psm1 = Psm / 119.826427
Usm1 = Usm / 0.001
Nre1 = V1 * Psm * Dh / (Usm)
y3 = Log(1 / K) / Log(2.718282)
Fc = (16 * (1 - K) ^ 2) / (((1 - K ^ 4) / (1 - K ^ 2)) - ((1 - K ^ 2) / y3))
If Nre1 < 2100 Then
FF = 16 / Nre1
Else
'FF1 = 0.0791 * Nre ^ (-0.25) 'Blasius Formula
A2 = (((4.6 * 10 ^ -5) / (OD - ID)) / 2.5497) ^ 1.1098 + (7.149 / Nre1) ^ 0.8981
FF = (1 / (-4 * Log((((4.6 * 10 ^ -5) / (OD - ID)) / 3.7065) - (5.0452 / Nre1) *
Log(A2)))) ^ 2
FF = 0.046 * Nre1 ^ (-0.2) 'Blasius Formula
End If
'Dpf1 = 2 * (FF * Psm * V1 ^ 2) / (OD - ID)
FFi = DPP * (OD - ID) / (2 * (Psm * V1 ^ 2))
End If
'Dpf = (Dpf1 + 0) * 0.3048 / 6894.757

```

```
Range("s" & I).Select
Range("s" & I).Value = FFi
Range("t" & I).Select
Range("t" & I).Value = Ffi2
'Range("v" & I).Select
'Range("v" & I).Value = DpfF
'Dptt = DpfF
'Range("O" & I).Select
'Range("O" & I).Value = Dptt

Next
End Sub
```

APPENDIX I

Developed Excel Macro to Apply and Verify Developed Mechanistic Model for Gas-Liquid Two Phase Homogeneous Flow in Vertical and Inclined Eccentric annuli to Experimental Data

Sub Button1_Click()

'
' MechanisticModel Macro by Reza E.Osgouei
'

```
Range("U12").Select
ID2 = Range("U12").Value
Range("U13").Select
OD2 = Range("U13").Value
Range("U2").Select
PI2 = Range("U2").Value
Range("U4").Select
Pg2 = Range("U4").Value
Range("U3").Select
Pc2 = Range("U3").Value
Range("U6").Select
UI2 = Range("U6").Value
Range("U5").Select
Ug2 = Range("U5").Value
g = 9.81
Range("U8").Select
alfa = Range("U8").Value
Range("U9").Select
Dp2 = Range("U9").Value
Range("U10").Select
h1 = Range("U10").Value
Range("U11").Select
muf = Range("U11").Value
ID = ID2 * 0.0254
OD = OD2 * 0.0254
Dp = 0.001999994
PI = PI2 * 119.826427
Pc = Pc2 * 119.826427
UI = UI2 * 0.001
Db = 0.04 * (OD - ID)
Range("V2").Select
Sayi1 = Range("V2").Value
Range("V4").Select
Sayi2 = Range("V4").Value
For I = Sayi1 To Sayi2
Range("A" & I).Select
QI2 = Range("A" & I).Value
```

```

Range("B" & I).Select
Qg1 = Range("B" & I).Value
Range("C" & I).Select
ROP = Range("C" & I).Value
Range("D" & I).Select
RPM = Range("D" & I).Value
Range("E" & I).Select
Pa2 = Range("E" & I).Value
Ug3 = Ug2 * 0.001
Pg1 = Pg2 * 119.826427
Ql = Ql2 * 6.30902 * 10 ^ (-5)
Pa = Pa2 * 6894.757
FA = Pa2 * (2.448 * (2.91 ^ 2 - 1.86 ^ 2))
Pa3 = (FA / (2.448 * (OD2 ^ 2 - ID2 ^ 2))) * 6894.757
Pg = Pg1 * ((14.7 * 6894.757) + Pa3) / (14.7 * 6894.757)
Ug = Ug3 * ((14.7 * 6894.757) + Pa3) / (14.7 * 6894.757)
Qg2 = (Qg1 * 6.30902 * 10 ^ (-5) * ((14.7 * 6894.757) + Pa3) / (14.7 * 6894.757))
Qc1 = ((3.14159265358979 / 4) * ROP * ((0.2425) ^ 2)) * 0.12467532647 'flow
rate in gpm
Qc = Qc1 * 6.30902 * 10 ^ (-5)
K = ID / OD
w = RPM * (2 * 3.14159265358979) / 60
y1 = Log(OD) / Log(2.718282)
y2 = Log(ID) / Log(2.718282)
Vt2 = (K ^ 2 * w * (-OD ^ 2 + ID ^ 2 + ((2 * OD ^ 2) * (y1 - y2)))) / ((OD ^ 2 - ID ^
2) * (1 - K ^ 2))
Vt = Vt2
Vz = 4 * (Ql + Qg2 + Qc) / (3.14159265358979 * (OD ^ 2 - ID ^ 2))
Vzg11 = (4 * Qg2) / (3.14159265358979 * (OD ^ 2 - ID ^ 2))
Vzc11 = (4 * Qc) / (3.14159265358979 * (OD ^ 2 - ID ^ 2))
Vzf11 = (4 * Ql) / (3.14159265358979 * (OD ^ 2 - ID ^ 2))
If Vzc11 > 0 Then
Vsc = (Vzc11 ^ 2 + Vt ^ 2) ^ (1 / 2)
Else
Vsc = 0
End If
If Vzg11 > 0 Then
Vsg = (Vzg11 ^ 2 + Vt ^ 2) ^ (1 / 2)
Else
Vsg = 0
End If
Vsf = (Vzf11 ^ 2 + Vt ^ 2) ^ (1 / 2)
LandaL = Ql / (Qc + Ql + Qg2)
landaC = Qc / (Qc + Ql + Qg2)
landaG = Qg2 / (Qc + Ql + Qg2)

V = (Vz ^ 2 + Vt ^ 2) ^ (1 / 2)

```

*****Determination of Gas Void Fraction*****

```

h = h1
Fr = Vzg11 ^ 2 / (g * h * Cos(alfa * 3.14159265358979 / 180))
CD = 0.44
vb = (2 / 3) * (4 * 0.0736 ^ 2 * g / 3 * Pl * Ul) ^ (1 / 5)
rb = CD * vb ^ 2 / (4 * g)
A = (3 * CD / 8)
B = Vzg11 ^ 2 / (g * rb)
A1 = (3 * CD * Pl * Vzg11 ^ 2 * h / (16 * rb))
B1 = 3 * 0.736 / rb
C1 = Pl * g * h / 2
D1 = Pl * Vzg11 ^ 2 / 4
If Vzg11 > 0 Then
fig = 1 / (1 + ((2 * Fr) ^ 0.5))
vbb = 1.18 * ((g * 0.0736 * (Pl - Pg)) / Pl ^ 2) ^ (1 / 4)
Kd = 1 - Exp(-1.1 * (Vzg11 / vbb) ^ 0.5 * ((g * (OD - ID)) ^ 0.5 / Vzg11) ^ (3 / 4))
Kh = 1 - Exp(-0.405 * (Vzg11 / vbb) ^ 0.7 * ((g * h) ^ 0.5 / Vzg11))
Wg = 1 - Kh * Kd * fig
Else
Wg = 0
Pm = Pl
Um = Ul
Vm = Vsf
End If
'Wg = landaG
Wl = 1 - Wg
Pm = Wg * Pg + (1 - Wg) * Pl
Um = Wg * Ug + (1 - Wg) * Ul
Vm = ((Vsg * Pg) + (Vsf * Pl)) / Pm
Range("y" & I).Select
Range("y" & I).Value = Wg
Range("z" & I).Select
Range("z" & I).Value = Wl
Range("H" & I).Select
Range("H" & I).Value = Pm
Range("I" & I).Select
Range("I" & I).Value = Um
Range("J" & I).Select
Range("J" & I).Value = Vm

```

*****Determination of Pressure Loss*****

```

Wgt = Wm * Wg
Wlt = Wm - Wgt
Range("F" & I).Select
Range("F" & I).Value = Wgt
Range("G" & I).Select
Range("G" & I).Value = Wlt

```

```

Range("W" & I).Select
Range("W" & I).Value = landaC
Range("X" & I).Select
Range("X" & I).Value = landaG
DPg1 = g * Cos(alfa * 3.14159265358979 / 180) * Psm
DPg2 = DPg1 * 0.3048 / 6894.757
V1 = Vm
Vtm1 = V1 * 3.28
Psm1 = Pm / 119.826427
Usm1 = Um / 0.001
Qtm = V1 * (3.14159265358979 / 4) * (OD ^ 2 - ID ^ 2)
Nre = 928 * Vtm1 * Psm1 * (OD2 - ID2) / Usm1
y3 = Log(1 / K) / Log(2.718282)
Fc = (16 * (1 - K) ^ 2) / (((1 - K ^ 4) / (1 - K ^ 2)) - ((1 - K ^ 2) / y3))
FF1 = Fc / Nre
If Nre < 2100 Then
FF = Fc / Nre
Else
A = (((4.6 * 10 ^ -5) / (OD - ID)) / 2.5497) ^ 1.1098 + (7.149 / Nre) ^ 0.8981
FF = (1 / (-4 * Log((((4.6 * 10 ^ -5) / (OD - ID)) / 3.7065) - (5.0452 / Nre) *
Log(A)))) ^ 2
FF = 0.0791 * Nre ^ (-0.25) 'Blasius Formula
End If
DpfF = (FF * Psm1 * Vtm1 ^ 2 / (25.8 * (OD2 - ID2)))
Range("P" & I).Select
Range("P" & I).Value = FF
Range("Q" & I).Select
Range("Q" & I).Value = DPg2
Range("R" & I).Select
Range("R" & I).Value = DpfF
Dptt = DpfF + DPg2
Range("S" & I).Select
Range("S" & I).Value = Dptt
Next
End Sub

```

APPENDIX J

Developed Excel Macro to Apply and Verify Developed Mechanistic Model for Cutting-Gas-Liquid Three Phase Homogeneous Flow in Horizontal, Vertical and Inclined Eccentric Annuli to Experimental Data

```
Sub Button1_Click()  
,  
' MechanisticModel Macro by Reza E.Osgouei  
,  
  
Range("U12").Select  
ID2 = Range("U12").Value  
Range("U13").Select  
OD2 = Range("U13").Value  
Range("U2").Select  
PI2 = Range("U2").Value  
Range("U4").Select  
Pg2 = Range("U4").Value  
Range("U3").Select  
Pc2 = Range("U3").Value  
Range("U6").Select  
UI2 = Range("U6").Value  
Range("U5").Select  
Ug2 = Range("U5").Value  
g = 9.81  
Range("U8").Select  
alfa = Range("U8").Value  
Range("U9").Select  
Dp2 = Range("U9").Value  
Range("U10").Select  
h1 = Range("U10").Value  
Range("U11").Select  
muf = Range("U11").Value  
ID = ID2 * 0.0254  
OD = OD2 * 0.0254  
Dp = 0.001999994  
PI = PI2 * 119.826427  
Pc = Pc2 * 119.826427  
UI = UI2 * 0.001  
Db = 0.04 * (OD - ID)  
Range("V2").Select  
Sayi1 = Range("V2").Value  
Range("V4").Select  
Sayi2 = Range("V4").Value  
For I = Sayi1 To Sayi2  
Range("A" & I).Select
```

```

Ql2 = Range("A" & I).Value
Range("B" & I).Select
Qg1 = Range("B" & I).Value
Range("C" & I).Select
ROP = Range("C" & I).Value
Range("D" & I).Select
RPM = Range("D" & I).Value
Range("E" & I).Select
Pa2 = Range("E" & I).Value
Ug3 = Ug2 * 0.001
Pg1 = Pg2 * 119.826427
Ql = Ql2 * 6.30902 * 10 ^ (-5)
Pa = Pa2 * 6894.757
FA = Pa2 * (2.448 * (2.91 ^ 2 - 1.86 ^ 2))
Pa3 = (FA / (2.448 * (OD2 ^ 2 - ID2 ^ 2))) * 6894.757
Pg = Pg1 * ((14.7 * 6894.757) + Pa3) / (14.7 * 6894.757)
Ug = Ug3 * ((14.7 * 6894.757) + Pa3) / (14.7 * 6894.757)
Qg2 = (Qg1 * 6.30902 * 10 ^ (-5) * ((14.7 * 6894.757) + Pa3) / (14.7 * 6894.757))
Qc1 = ((3.14159265358979 / 4) * ROP * ((0.2425) ^ 2)) * 0.12467532647 'flow
rate in gpm
Qc = Qc1 * 6.30902 * 10 ^ (-5)
K = ID / OD
w = RPM * (2 * 3.14159265358979) / 60
y1 = Log(OD) / Log(2.718282)
y2 = Log(ID) / Log(2.718282)
Vt2 = (K ^ 2 * w * (-OD ^ 2 + ID ^ 2 + ((2 * OD ^ 2) * (y1 - y2)))) / ((OD ^ 2 - ID ^
2) * (1 - K ^ 2))
Vt = Vt2
Vz = 4 * (Ql + Qg2 + Qc) / (3.14159265358979 * (OD ^ 2 - ID ^ 2))
Vzg11 = (4 * Qg2) / (3.14159265358979 * (OD ^ 2 - ID ^ 2))
Vzc11 = (4 * Qc) / (3.14159265358979 * (OD ^ 2 - ID ^ 2))
Vzf11 = (4 * Ql) / (3.14159265358979 * (OD ^ 2 - ID ^ 2))
If Vzc11 > 0 Then
Vsc = (Vzc11 ^ 2 + Vt ^ 2) ^ (1 / 2)
Else
Vsc = 0
End If
If Vzg11 > 0 Then
Vsg = (Vzg11 ^ 2 + Vt ^ 2) ^ (1 / 2)
Else
Vsg = 0
End If
Vsf = (Vzf11 ^ 2 + Vt ^ 2) ^ (1 / 2)
LandaL = Ql / (Qc + Ql + Qg2)
landaC = Qc / (Qc + Ql + Qg2)
landaG = Qg2 / (Qc + Ql + Qg2)

```

$$V = (V_z^2 + V_t^2)^{1/2}$$

*****Determination of Gas Void Fraction*****

$$h = h_l$$

$$Fr = V_{zg11}^2 / (g * h * \cos(\alpha * 3.14159265358979 / 180))$$

$$CD = 0.44$$

$$v_b = (2/3) * (4 * 0.0736^2 * g / 3 * \rho_l * U_l)^{1/5}$$

$$r_b = CD * v_b^2 / (4 * g)$$

$$A = (3 * CD / 8)$$

$$B = V_{zg11}^2 / (g * r_b)$$

$$A1 = (3 * CD * \rho_l * V_{zg11}^2 * h / (16 * r_b))$$

$$B1 = 3 * 0.736 / r_b$$

$$C1 = \rho_l * g * h / 2$$

$$D1 = \rho_l * V_{zg11}^2 / 4$$

If $V_{zg11} > 0$ Then

$$fig = 1 / (1 + (2 * Fr^{0.5}))$$

$$v_{bb} = 1.18 * ((g * 0.0736 * (\rho_l - \rho_g)) / \rho_l^2)^{1/4}$$

$$K_d = 1 - \exp(-1.1 * (V_{zg11} / v_{bb})^{0.5} * ((g * (OD - ID))^{0.5} / V_{zg11})^{3/4})$$

$$K_h = 1 - \exp(-0.405 * (V_{zg11} / v_{bb})^{0.7} * ((g * h)^{0.5} / V_{zg11}))$$

$$W_g = 1 - K_h * K_d * fig$$

Else

$$W_g = 0$$

$$P_m = \rho_l$$

$$U_m = U_l$$

$$V_m = V_{sf}$$

End If

Wg= landaG

$$W_l = 1 - W_g$$

$$P_m = W_g * \rho_g + (1 - W_g) * \rho_l$$

$$U_m = W_g * U_g + (1 - W_g) * U_l$$

$$V_{m1} = ((V_{zg11} * \rho_g) + (V_{zf11} * \rho_l)) / P_m$$

$$V_m = (V_{m1}^2 + V_t^2)^{1/2}$$

Range("y" & I).Select

Range("y" & I).Value = Wg

Range("z" & I).Select

Range("z" & I).Value = Wl

Range("H" & I).Select

Range("H" & I).Value = Pm

Range("I" & I).Select

Range("I" & I).Value = Um

Range("J" & I).Select

Range("J" & I).Value = Vm

*****Determination of Particle Void Fraction*****

$$r_p = D_p / 2$$

$$VP = (3.14159265358979 * r_p^3) * (4/3)$$

$$V_a = VP / 2$$

```

Rep = (((Pm) * (Vm) * (Dp)) / Um) * (1 / (1 - 0.36)) 'Ismail Tosun Book page
102
CDp = ((24 / Rep) * (1 + 0.173 * Rep ^ (0.657))) + (0.413 / (1 + (16300 * Rep ^ -
1.09))) 'Ismail Tosun Book page 67
DRD = ((Vt ^ 2 / ((ID / 2) + ((OD - ID) / 2))) - (g * Cos(alfa * 3.14159265358979 /
180)))
Cvpr = -((4 / 3) * (Dp / CDp)) * ((Vt ^ 2 / ((ID / 2) + ((OD - ID) / 2))) + (((Pc - Pm)
/ Pm) * DRD))
Cvpz = -((4 / 3) * (Dp / CDp) * ((Pc - Pm) / Pm)) * (g * Sin(alfa *
3.14159265358979 / 180))
Vsp = (Cvpr ^ 2 + Cvpz ^ 2) ^ 0.25
Vspr = Cvpr / Vsp
Vspz = Cvpz / Vsp
Vrpe = (Vspz ^ 2 + Vspr ^ 2) ^ 0.5
If Vzc11 > 0 Then
If Vspz < 0 Then
Vrp = -Vrpe
Else
Vrp = Vrpe
End If
Wc1 = ((Vrp - Vm - Vsc) / (2 * Vrp)) - (((((Vrp - Vm - Vsc) / (2 * Vrp)) ^ (2)) +
(Vsc / Vrp)) ^ 0.5)
Wc = Wc1
Psm = Wc * Pc + (1 - Wc) * Pm
Usm = (1 + 2.5 * Wc + 10.05 * Wc ^ 2 + 0.00273 * Exp(16.6 * Wc)) * Um 'Clayton
Crowe Book page 4-55
Vtm1 = ((Vzc11 * Pc) + (Vm1 * Pm)) / Psm
Vtm = (Vtm1 ^ 2 + Vt ^ 2) ^ (1 / 2)
Else
Wc = 0
Psm = Pm
Usm = Um
Vtm = Vm
End If
Wm = 1 - Wc
Range("K" & I).Select
Range("K" & I).Value = Wm
Range("L" & I).Select
Range("L" & I).Value = Wc
Range("M" & I).Select
Range("M" & I).Value = Psm
Range("N" & I).Select
Range("N" & I).Value = Usm
Range("O" & I).Select
Range("O" & I).Value = Vtm
'*****Determination of Pressure Loss*****
Wgt = Wm * Wg

```

```

Wlt = Wm - Wgt
Range("F" & I).Select
Range("F" & I).Value = Wgt
Range("G" & I).Select
Range("G" & I).Value = Wlt
Range("W" & I).Select
Range("W" & I).Value = landaC
Range("X" & I).Select
Range("X" & I).Value = landaG
DPg1 = g * Cos(alfa * 3.14159265358979 / 180) * Psm
DPg2 = DPg1 * 0.3048 / 6894.757
V1 = Vtm
Vtm1 = V1 * 3.28
Psm1 = Psm / 119.826427
Usm1 = Usm / 0.001
Qtm = V1 * (3.14159265358979 / 4) * (OD ^ 2 - ID ^ 2)
Nre = 4 * Qtm * Psm / (Usm * 3.14159265358979 * (OD - ID))
y3 = Log(1 / K) / Log(2.718282)
Fc = (16 * (1 - K) ^ 2) / (((1 - K ^ 4) / (1 - K ^ 2)) - ((1 - K ^ 2) / y3))
FF1 = Fc / Nre
If Nre < 2100 Then
FF = 16 / Nre
Else
A = (((4.6 * 10 ^ -5) / (OD - ID)) / 2.5497) ^ 1.1098 + (7.149 / Nre) ^ 0.8981
FF = (1 / (-4 * Log((((4.6 * 10 ^ -5) / (OD - ID)) / 3.7065) - (5.0452 / Nre) *
Log(A)))) ^ 2
End If
Dpf1 = (32 * FF * (Psm) * Qtm ^ 2 / (3.14159265358979 ^ 2 * (OD ^ 5 - ID ^ 5)))
DpfF = (Dpf1 + 0) * 0.3048 / 6894.757
Range("P" & I).Select
Range("P" & I).Value = FF
Range("Q" & I).Select
Range("Q" & I).Value = DPg2
Range("R" & I).Select
Range("R" & I).Value = DpfF
Dptt = DpfF + DPg2
Range("S" & I).Select
Range("S" & I).Value = Dptt
Next
End Sub

```

APPENDIX K

Calculation of Gas, Particle and Liquid Slip Void Fraction into the Three Phase Mixture

Azbel (1981) verified the average fraction of particles in liquid flow by using the definition of the average relative velocity of the solid phase when velocities of the two phases are low and the duct is large enough (no wall effect). He imaged the control plane to pass through the flow perpendicular to the direction of the time-averaged flow velocity vector and he write the volumetric flow rate of solid particles per unit area of this control plane as:(N.1)

$$V_{SC} = \frac{Q_c}{A} = \frac{1}{A \nabla \Gamma} \int_{\nabla \Gamma} \int_A v_p d\Gamma \quad (\text{N.1})$$

Where Q_c is the volumetric flow rate of particles, A is the flow system cross-sectional area, $\nabla \Gamma$ is a period of time substantially greater than the quantity $1/f$ [where f is the frequency of movement of solid particle through the cross section in question], and v_p is the actual velocity of the particles. At a given instant of time the particles do not occupy the whole cross-section of the duct and, in general, a part of every cross section of the duct is occupied by the liquid. Therefore, equations (N.1) must be written in the form of a sum of integrals:

$$V_{SC} = \frac{1}{A \nabla \Gamma} \int_{\nabla \Gamma} \left(\sum_i \int_{A_i} v_p dA \right) d\Gamma \quad (\text{N.2})$$

Where i is the number of particle formations, or groups, in a given cross section at a given instant of time. The ratio:

$$\emptyset = \left(\frac{1}{A} \right) \sum_i A_i \quad (\text{N.3})$$

is defined as the instantaneous value of that fraction of the section of the dispersed flow which is occupied by particle (this section being of thickness dn , where n is

normal to the surface A). The true average velocity of particles in the liquid flow is then:

$$\bar{V}_p = \frac{1}{\nabla\Gamma \sum_i A_i} \int_{\nabla\Gamma} \left(\sum_i \int_{A_i} v_p dA \right) d\Gamma \quad (\text{N.4})$$

and this equation, with equation (N.2), indicates that the true average velocity and superficial velocity of the particles are related by:

$$\bar{V}_p = V_{SC} / \phi \quad (\text{N.5})$$

Now, the ratio of the total mass flow rate of the phases to the product of the cross-sectional area of the channel and the density of the gas- liquid mixture is usually designated as flow velocity of two component flow:

$$V_{stm} = \frac{V_{SC} \rho_c + V_{sm} \rho_{sm}}{\rho_{stm}} \quad (\text{N.6})$$

Where ρ_c and ρ_m are the particle and gas-liquid mixture densities, respectively, and V_{sm} is gas-liquid mixture velocity (see equation 6.94).The average relative velocity of the solid phase is defined by:

$$\bar{v}_{sp} = \bar{V}_m - \bar{V}_p = \frac{V_{sm}}{1-\phi} - \frac{V_{SC}}{\phi} \quad (\text{N.7})$$

And hence

$$\bar{v}_{sp} \phi^2 - (\bar{v}_{sp} - V_{sm} - V_{SC}) \phi - V_{SC} = 0 \quad (\text{N.8})$$

Solving this equation for ϕ , taking into account that when $V_{SC} = 0$:

$$\phi_{avp} = \frac{\bar{v}_{sp} - V_{sm} - V_{SC}}{2\bar{v}_{sp}} - \left[\left(\frac{\bar{v}_{sp} - V_{sm} - V_{SC}}{2\bar{v}_{sp}} \right)^2 + \frac{V_{SC}}{\bar{v}_{sp}} \right]^{1/2} \quad (\text{N.9})$$

CURRICULUM VITAE

REZA ETTEHADI OSGOUEI, PhD



PERSONAL DATA

Date of Birth: September 20, 1976
Place o Birth: TABRIZ-IRAN
Marital Status: Married
Home Address: Sahit Osman Avci M. 72 S. No: 7 D Blok 2 Coksu kent Sit.,
06770 Ankara-Turkey
Work Address: Middle East Technical University, Petroleum & Natural Gas
Engineering Department, 06531 Ankara-Turkey
Telephone:
Office :+90 (312) 210 5690-210 4897
Cellular :+90 (505) 200 8317
Fax: +90 (312) 210 4883
e-mail: e146442@metu.edu.tr , r.ettthadi@gmail.com
Web: <http://www.metu.edu.tr/~e146442/project/>

EDUCATION

2007-2010 Middle East Technical University, Ankara, Turkey

Doctor of Philosophy in Petroleum Engineering, October 2010

Major: Drilling

Cumulative GPA: 3.64 out of 4.0(Honor)

Ph.D. Dissertation: DETERMINATION OF CUTTINGS TRANSPORT
PROPERTIES OF GASIFIED DRILLING FLUIDS

2004-2007 Middle East Technical University, Ankara, Turkey

Master of Science in Petroleum and Natural Gas Engineering

Major: Drilling

Cumulative GPA: 3.79 out of 4.0

M.Sc. Thesis: Determination of optimum drilling parameters using proposed
ROP Model for deviational wells, 2007

1995-1999 SAHAND University of Technology, TABRIZ- IRAN

Bachelor of Science in Mining Engineering

Cumulative GPA: 14.0 out of 20.0

1990-1994 Shahid Kazemzadeh High school, Osku-Iran

Major: Mathematics& Physics

Cumulative GPA: 16.25 out of 20.0

WORK EXPERIENCE

2006-Present Middle East Technical University Petroleum Eng. Department, Ankara, Turkey

Worked as a graduate assistant in METU Petroleum Engineering Department, Drilling Research Projects. Major interests are; underbalanced drilling technology, cuttings transport, directional and horizontal well technology, fluid rheology, wellbore mechanics, software engineering, artificial neural networks. Participated in drilling projects sponsored by several major oil companies such as *STATOIL ASA* as well as the Scientific and Technological Research Council of Turkey.

2008-Present Middle East Technical University Petroleum Eng. Department, Ankara, Turkey

Worked as a tutor of Multiphase flow in pipe course in METU Petroleum Engineering department, Ankara, Turkey

1997 Summer Training Songun Copper Company, Songun, Iran

Conducted experiments on Rock Mechanics in Sungun Copper Company Research Center;

SPECIAL SKILLS AND QUALIFICATIONS

- Computer Skills
 - Operating System* MS Windows, MS DOS
 - Language* C++, Turbo Pascal, Fortran 77, Basic, Matlab 2009a
 - Software* MS Office (Word, Excel, Power Point, Outlook, Access, Front Page), Lab view, Adobe PhotoShop (and similar software), ANSYS, Fluent, Pipe Phase, Statistica, Mathematica
- Ability to work well under pressure, handle multiple tasks and fast learner
- Work well both independently and as a part of a team
- Ability to handle heavy duty

Participated Projects

- *STATOIL ASA – Middle East Technical University (Ozbayoglu E., Saasen A.)*, “Hole Cleaning Performance of Water and Oil Based Muds”, Experimental and Theoretical Work, 2006, No: 4501007879
- *Ozbayoglu M.E.*, “Determination of Cutting Transport Properties of Gasified Drilling Fluids”, METU- Scientific and Technological Research Council of Turkey, June 2008 – June 2010 (still on progress) Project No: 108M106

REFERENCES

- **Dr. Evren Ozbayoglu**, Petroleum Engineering Department, The University of Tulsa
- 800 S Tucker Dr. Tulsa OK 74104, +1 (918) 6071237, evren-ozbayoglu@utulsa.edu & ozevren@metu.edu.tr
- **Dr. Mahmut Parlaktuna**, Middle East Technical university, Petroleum & Natural Gas Eng. Dept., 06531 Ankara – Turkey, +90 (312) 210 2895 mahmut@metu.edu.tr
- **Dr. Mutafa V. Kok**, Middle East Technical university, Petroleum & Natural Gas Eng. Dept., 06531 Ankara – Turkey, +90 (312) 210 4883 kok@metu.edu.tr
- **Dr. Serhat Akin**, Middle East Technical university, Petroleum & Natural Gas Eng. Dept., 06531 Ankara – Turkey, +90 (312) 210 4892 serhat@metu.edu.tr

PUBLICATIONS

- **Osgouei R.E.**, Ozbayoglu *M.E.*, “ Rate of Penetration Estimation Model for Directional and Horizontal Wells ” IPETGAS 07 (The 16th International Petroleum and Natural Gas Congress and Exhibition of Turkey) May 29th-31th 2007 Ankara – Turkey
- **Osgouei R.E.**, Songon M., “A Critical Evaluation for Iranian Natural Gas Resources” Energy Sources Part B. Accepted date: December 01,2008
- **Osgouei R.E.**, Ozbayoglu *M.E.*, “Determination of Cutting Transport Properties of Gasified Drilling Fluids” IPETGAS 09 May 13th-15th 2009Ankara - Turkey
- Ozbayoglu *M.E.*, Ozbayoglu *A.M.*, **Osgouei R.E.**, Yuksel E., “Determination of Cutting Concentration through Horizontal Annular Geometry by using Image Processing Techniques” IPETGAS 09 May 13th-15th 2009Ankara - Turkey
- Ozbayoglu *M.E.*, Ozbayoglu *A.M.*, **Osgouei R.E.**, Yuksel E., “Determination of Liquid Hold up through Horizontal Annular Geometry by using Image Processing Techniques” IPETGAS 09 May 13th-15th 2009Ankara - Turkey
- **Osgouei R.E.**, Ozbayoglu *M.E.* Ozbayoglu *A.M.*, Yuksel E., “ Flow regime identification in gas-liquid flow through horizontal annular geometry” Tracking No: SPE-129123-PP , The 2010 SPE Oil and Gas India Conference and Exhibition (OGIC) 20- 22 January 2010 in Mumbai, India.
- Ozbayoglu *M.E.* ,**Osgouei R.E.**, Ozbayoglu *A.M.*, Yuksel E., “ Hole Cleaning Performance of Gasified Drilling Fluids in Horizontal Well Sections” Tracking No: SPE 131378-PP , The CPS/SPE International Oil & Gas Conference and Exhibition in China held in Beijing, China, 8–10 June 2010.
- Ozbayoglu *M.E.* ,**Osgouei R.E.**, Ozbayoglu *A.M.*, Yuksel E., Estimation of "Very-Difficult-to-Identify" Data for Hole Cleaning, Cuttings Transport and Pressure Drop Estimation in Directional and Horizontal Drilling" 2010 IADC/SPE Asia Pacific Drilling Technology Conference and Exhibition (APDT) - SPE-136304-PP Accepted as Poster/Alternate

HONORS AND ACTIVITIES

Prizes and Awards

- SEP Turkey Section Award of Educational Excellence 10 November 2006
- METU Graduate Courses Performance Award 2007-2008 Academic Year
- The Scientific and Technological Research Council of Turkey PhD Student Research Scholarship, June 2008 – June 2010, Project No: 108M106
- METU International successful PhD students' tuition fee payment exemption scholarship, September 2007-present (International PhD students, who are working 8 hours per week in their departments. The approval of the Department Chairmanship is required for those students.)
- SEP Turkey Section Award of Appreciation Student Paper Contest Graduate Division 24 June 2010

OTHER ACTIVITIES

- SPE Member, 2005-Present

Languages:

- Azeri : Mother Tongue
- English : Advanced Level
- Persian : Advanced Level
- Turkish : Advanced Level
- Arabic : Basic Level